frontiers | Research Topics

Case reports in heart surgery 2022

Edited by
Hendrik Tevaearai Stahel

Published in
Frontiers in Cardiovascular Medicine
Frontiers in Surgery

ISSN 1664-8714
ISBN 978-2-8325-3739-8
DOI 10.3389/978-2-8325-3739-8

About Frontiers

Frontiers is more than just an open access publisher of scholarly articles: it is a pioneering approach to the world of academia, radically improving the way scholarly research is managed. The grand vision of Frontiers is a world where all people have an equal opportunity to seek, share and generate knowledge. Frontiers provides immediate and permanent online open access to all its publications, but this alone is not enough to realize our grand goals.

Frontiers journal series

The Frontiers journal series is a multi-tier and interdisciplinary set of open-access, online journals, promising a paradigm shift from the current review, selection and dissemination processes in academic publishing. All Frontiers journals are driven by researchers for researchers; therefore, they constitute a service to the scholarly community. At the same time, the *Frontiers journal series* operates on a revolutionary invention, the tiered publishing system, initially addressing specific communities of scholars, and gradually climbing up to broader public understanding, thus serving the interests of the lay society, too.

Dedication to quality

Each Frontiers article is a landmark of the highest quality, thanks to genuinely collaborative interactions between authors and review editors, who include some of the world's best academicians. Research must be certified by peers before entering a stream of knowledge that may eventually reach the public - and shape society; therefore, Frontiers only applies the most rigorous and unbiased reviews. Frontiers revolutionizes research publishing by freely delivering the most outstanding research, evaluated with no bias from both the academic and social point of view. By applying the most advanced information technologies, Frontiers is catapulting scholarly publishing into a new generation.

What are Frontiers Research Topics?

Frontiers Research Topics are very popular trademarks of the *Frontiers journals series*: they are collections of at least ten articles, all centered on a particular subject. With their unique mix of varied contributions from Original Research to Review Articles, Frontiers Research Topics unify the most influential researchers, the latest key findings and historical advances in a hot research area.

Find out more on how to host your own Frontiers Research Topic or contribute to one as an author by contacting the Frontiers editorial office: frontiersin.org/about/contact

Case reports in heart surgery: 2022

Topic editor
Hendrik Tevaearai Stahel — University Hospital of Bern, Switzerland

Citation
Stahel, H. T., ed. (2023). *Case reports in heart surgery: 2022*.
Lausanne: Frontiers Media SA. doi: 10.3389/978-2-8325-3739-8

Table of contents

frontiers in Cardiovascular Medicine

CASE REPORT
published: 27 January 2022
doi: 10.3389/fcvm.2022.829328

Case Report: A Young Man With Giant Pericardial Synovial Sarcoma

*Yong Luo[1], Ke Gong[1], Ting Xie[1], Ruilin Liu[1], Hui Guo[1], Lei Wang[1], Zhiping Tan[2], Shi jun Hu[1], Yifeng Yang[1] and Li Xie[1]**

[1] Department of Cardiovascular Surgery, The Second Xiangya Hospital of Central South University, Central South University, Changsha, China, [2] The State Key Laboratory of Medical Genetics, The Clinical Center for Gene Diagnosis and Therapy, The Second Xiangya Hospital of Central South University, Central South University, Changsha, China*

Pericardial synovial sarcomas are sporadic tumors. Herein, we report a case of primary pericardial synovial sarcoma originating from the right pericardium. Missed diagnosis delayed surgical treatment. Eventually, the tumor occupied the almost entire pericardial cavity. The pericardial tumor was surgically removed as soon as possible after admission. In this paper, we aim to provide details that can help further understand the differing symptoms and presentations of pericardial synovial sarcoma and highlight the importance of consideration of this disease in similar cases where the etiology of pericardial effusion is unknown.

Keywords: pericardial synovial sarcomas, pericardium, tumor, treatment, prognosis

OPEN ACCESS

Edited by:
Robert Jeenchen Chen, Stanford University, United States

Reviewed by:
Michael Hofmann, University of Zurich, Switzerland
Paul Philipp Heinisch, German Heart, Germany

****Correspondence:***
Li Xie
xieli55@csu.edu.cn

Specialty section:
This article was submitted to Heart Surgery, a section of the journal Frontiers in Cardiovascular Medicine

Received: *05 December 2021*
Accepted: *03 January 2022*
Published: *27 January 2022*

Citation:
Luo Y, Gong K, Xie T, Liu R, Guo H, Wang L, Tan Z, Hu Sj, Yang Y and Xie L (2022) Case Report: A Young Man With Giant Pericardial Synovial Sarcoma. Front. Cardiovasc. Med. 9:829328. doi: 10.3389/fcvm.2022.829328

INTRODUCTION

Pericardial synovial sarcoma (PSS) is a rare malignant tumor. Thus far, only a few cases of PSS have been reported. Synovial sarcoma (SS) is also reported in some uncommon sites such as the pleura, heart, kidney, lung, prostate, liver, gastrointestinal tract, and peripheral nerves. The diagnosis of SS in these unusual locations is challenging and requires additional diagnostic procedures such as immunohistochemistry, electron microscopy, and molecular genetic techniques for confirmation of the diagnosis. The case cardiac tamponade presented as the initial symptom, but no obvious evidence supported the diagnosis of pericardial synovial sarcoma. After 5 months, the anterior mediastinal tumor was found using transthoracic echocardiography. Non-random occurrence of t(x;18) was consistently found in SS. In some cases, the only cytogenetic abnormality noted is the t(X;18), suggesting that this is a key molecular event in tumor development (1). The survival rate of patients with primary cardiac sarcoma is poor, and most patients die within a few months after the diagnosis is confirmed. However, because of the rarity of PSS, it is difficult to determine the prognostic factors; however, diagnosis at a young age, lack of complicated chromosome abnormalities, and tumor originating from the pericardium appear to be factors pointing to good prognosis (2).

CASE REPORT

A 19-year-old man was referred to our hospital for the first time because of chest tightness and dyspnea. Chest echocardiography and computed tomography (CT) revealed a large amount of pericardial effusion, pleural effusion, left lung swelling, and right lower lung swelling (**Figure 1A**). The patient was subjected to pericardiocentesis and drainage; the drained fluid was sent for pathological examination. The pathology report revealed a lack of tumor cells (**Figure 2A**); acid-fast staining of the sample was also not positive for *Mycobacterium tuberculosis* (**Figure 2B**). The

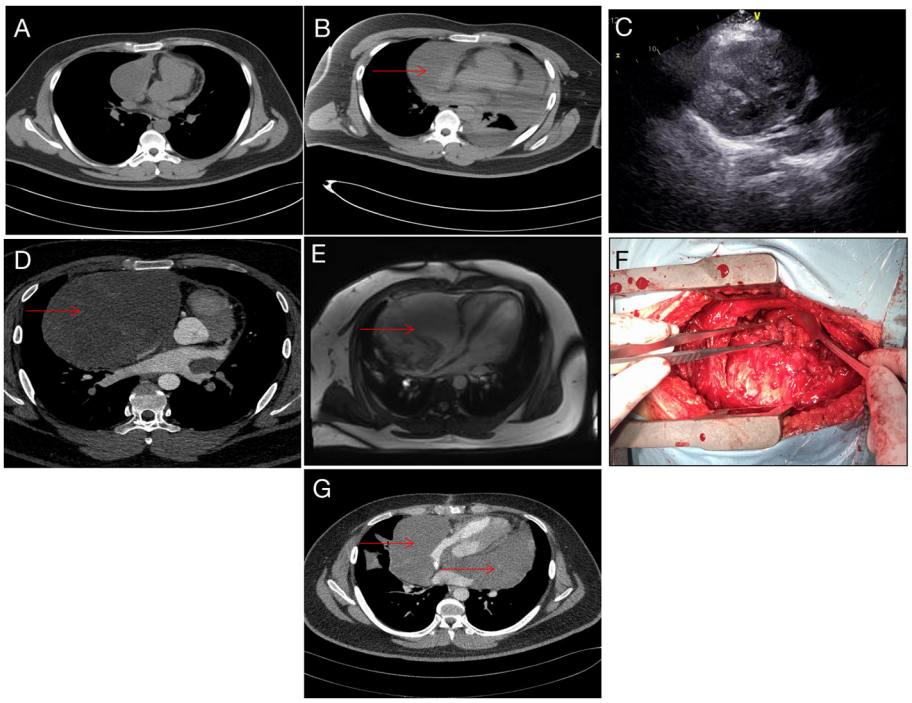

FIGURE 1 | Imaging data. **(A)** CT image taken during the first admission. **(B)** After pericardiocentesis, CT indicating a suspicious mass (red arrow). **(C)** Echocardiography showing pericardial space-occupying lesions. **(D)** Reexamination after 5 months showed obvious space occupation (red arrow). **(E)** Preoperative magnetic resonance imaging, right pericardium, showing a cystic mass (red arrow). **(F)** During the operation, the tumor filled the pericardial cavity. **(G)** Tumor recurrence noted 5 months after operation (red arrow).

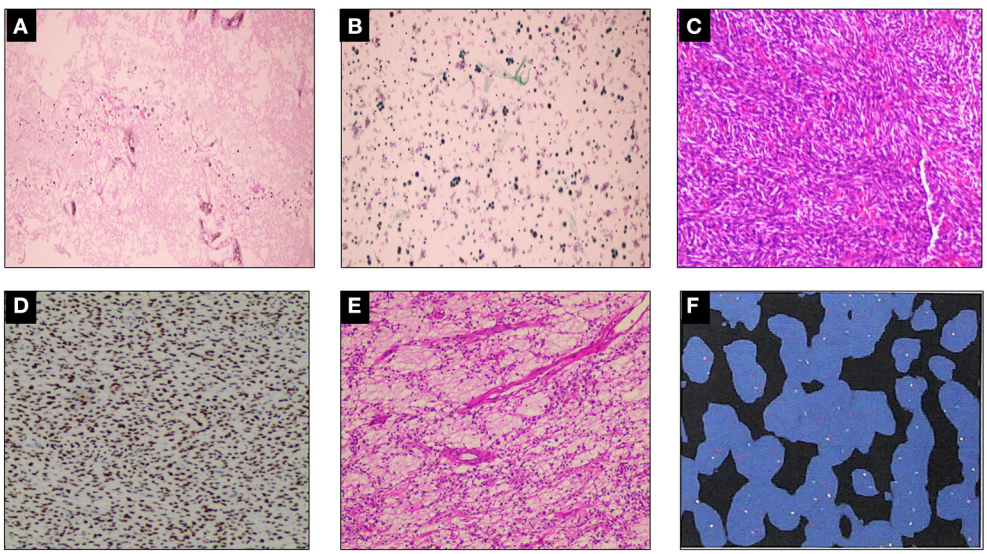

FIGURE 2 | Histopathological examination. **(A)** A small number of mesothelial cells and lymphocytes were found in the pleural effusion, but no malignant tumor cells were found. **(B)** Tissue cells, lymphocytes, and no malignant tumor cells could be found in the left pleural effusion. *Mycobacterium tuberculosis* was found to be negative by acid-fast staining (–). **(C–E)** Damaged tissue of pericardial tumor, which measured 20 × 17 × 5 cm, with some gelatinous areas. Mesenchymal tissue-derived tumors, with dense spindle cell areas and edema areas, combined with immunohistochemistry, do not rule out SS. Immunohistochemistry results: CK (–), EMA (focal +), TLEL (+), CD34 (–), S100 (–), CD99 (partial +), Bcl-2 (+), Ki67 (hot spot 25% +), WT-1 (–), Desmin (–), SMA (–), Vim (+), calponin (partial +), INI-1 (–), ERG (–), p53 (30% weak +), HMB45 (–), FLI-1 (–). **(F)** Fluorescence *in situ* hybridization (FISH) showing rearrangement of the SS18 gene, indicating positive result.

patient was also subjected to bone marrow puncture; however, the biopsy sample did not show any positive results. Following pericardiocentesis and treatment aimed at providing symptomatic relief, his pleural effusion and pericardial effusion were absorbed (**Figure 1B**). He was then discharged after symptom improvement. Therefore, some special manifestations of patients have been ignored. Although a mediastinal mass was noted in the first CT images, the pathological examination and related auxiliary examinations of pericardial effusion did not discover any positive results (**Figure 1B**). Five months later, the patient was re-examined at the local hospital and was found to have a pericardial mass through echocardiography and chest CT.

Then the patient had seen a doctor again for further treatment. Echocardiography, CT, and nuclear magnetic resonance imaging (MRI) at our hospital indicated that the right anterior mediastinum mass had compressed the right heart (**Figure 1C**) and the aortic root; it measured 15.3 × 11.7 × 15.1 cm (**Figures 1D,E**). He had no family history relevant to cardiac complaints. Following relevant preoperative examinations, he underwent mass resection *via* a median sternum incision. The size of the mass was about 20 × 15 × 19 cm (**Figure 1F**). The mass was found to completely cover the right atrium, superior and inferior vena cava, ascending aorta, and part of the pulmonary artery; it also partly covered the anterior wall of the right ventricle. After the operation, pathological examination (**Figures 2C–E**); furthermore, an SS18 gene test was done (**Figure 2F**). It was found that the SS18 gene was broken, so the result was positive, suggesting SS. A postoperative echocardiography performed 2 months after discharge demonstrated a heterogeneous hypoechoic lump in the pericardium; thus, tumor recurrence was considered. After 2 months of treatment with traditional Chinese medicine, he was referred to our hospital again. CT angiography revealed a more significant layer of cystic consolidation on the left margin of the heart that measured about 12 × 6.9 cm (left), 11.5×5.6 cm (right) (**Figure 1G**). Thus, following discussion with the patient, chemotherapy was initiated. The patient is currently undergoing chemotherapy with regimen at the oncology department of our hospital.

DISCUSSION

The incidence of heart tumors is quite hidden, and most of them are caused by accidentally discovered cardiac lumps. These occasional phenomena often means thrombus or neoplasms, which usually occur in specific clinical environments (3). The incidence rate of cardiac tumors ranges from 0.001 to 0.03%. The overwhelming majority of these tumors are benign, and only about one-fourth are malignant. PSS is an even rarer form of cardiac tumors. As of 2018, only 36 cases have been reported in the literature; thus, limited data prevent further understanding of this condition (4). However, this lesion undoubtedly predicts a dismal prognosis (5).

SS is an uncommon malignant tumor mainly seen in children and adolescents; its 10-year overall survival rate is about 0–20% (6, 7). The name SS is possibly indicative of its origin in synovial tissue. It has a biphasic appearance on histology and is divided into two different subtypes: spindle and epithelial cell subtypes. However, no epithelioid differentiation was found in tumor tissues, neither were epithelial markers, such as IHC staining of cytokeratin, observed. Therefore, the real origin of SS remains unknown. The characteristic chromosomal abnormality of SS is t(X;18) (p11.2; q11.2). This has a sensitivity of about 90–100%, strongly suggesting its direct involvement in certain aspects of the occurrence and progression of this cancer (1, 8). Even in our case, the diagnosis of SS was proven following a positive result of the SS18 genetic testing.

The morbidity rate of young people with PSS is relatively high, and the most common site of the disease is in the pericardium (9). Even in our case, the tumor originated from the pericardium. The clinical symptoms of the disease are non-specific, with dyspnea and chest pain being the most common presenting symptoms. The patient described herein presented with chest tightness, dyspnea, and fatigue before admission. There was a large amount of pericardial effusion noted in the early stage. According to a new study conducted in China, the most common causes of pericardial effusion were found to be malignant tumors and tuberculosis (10). However, in our case, pericardiocentesis and etiological examination of the pleural effusion did not support the diagnosis of malignant pleural effusion. This could be possible because malignant tumor cells may not be present in 25% of the cases of malignant pericardial effusion (10). Therefore, despite the absence of malignant cells in the pericardial effusion, the possibility of malignant pleural effusion should not be completely ruled out.

The reason for the initially missed diagnosis in our case was the absence of tumor cells and related markers in the pleural fluid. Besides, the patient's symptoms improved significantly after symptomatic treatment. However, the initial beginning stage of the tumor can be seen on the CT performed initially. After 5 months, the tumor had grown up, leading to aggravation of the patient's condition. It was visible on echocardiography and compressed the right heart and the root of the great artery.

As regards the treatment of PSS, on the one hand, due to the invasiveness and expansibility of the tumor, it is generally impossible to remove the tumor completely. On the other hand, there is no systemic study on this topic due to extremely low incidence of the disease; thus, no optimal treatment strategy has yet been proposed. Besides surgical resection, radiotherapy and chemotherapy are also used; this, however, depends on the clinician's discretion and the patient's condition. In general, surgical resection should be performed as soon as possible once the tumor diagnosis is confirmed, especially when the possibility of malignancy is high. Resection can be performed based on the preoperative MRI evaluation, with the premise of negative margin. Because positive margin is an independent risk factor for cardiac tumors, we recommend MRI before surgery to evaluate the degree of disease and assess whether it can be resected on the premise of negative margin. If this is not possible, second-line radiotherapy and chemotherapy can be considered; evaluation can then be performed and resection undertaken after the tumor has shrunk in size until it can be resected with a negative margin (11). Reports of successful

total artificial heart transplantation have been published, and this can also be a solution (12). Although patients with PSS have a low probability of lung metastasis, according to the evaluation by Lee et al., metastatic resection is a good choice for metastatic SS (13). In a recent study, a comparative result of the treatment of primary cardiac sarcoma was reported. Although some authors found no improvement in survival rate compared with traditional surgical treatment (14, 15). However, other authors have found that many patients survive longer after transplantation (16). The patient described herein also considered heart transplantation but considered chemotherapy first due to the lack of donors.

As regards prognosis, a recent statistical study showed that the 2-year survival rate following complete surgical resection of PSS was 75.2% (± 9.7 SE), while that following incomplete resection was 55.0% (± 11.5SE) (Log-Rank test: $P = 0.029$). The survival rate at 12 months was 96.5% (±3.8 SE) in patients treated with chemoradiotherapy (CRT), while it was 21.9% (±10.8 SE) in those not treated with CRT (Log-Rank test: $P \leq 0.0001$) (17). Thus, it was concluded that advanced age and absence of CRT were significantly associated with reduced survival, while total tumor resection was associated with remarkably improved survival. Furthermore, the clinical outcomes of patients receiving postoperative adjuvant chemotherapy was good, and adjuvant chemotherapy was found to be associated with significantly prolonged survival (18–22). Putnam et al. showed that radiotherapy alone seemed to have little impact on prognosis (23). The age of patients with PSS was also shown to be a strong prognostic indicator in this study. In a large meta-analysis of 1,268 patients with SS, Sultan et al. found that younger patients had better outcomes than older patients; (24) this finding was also confirmed by other authors (25–27). The patient in our report was 19 years old; thus, this young age is indicative of a favorable prognosis. After surgical resection, the patient relapsed 2 months later and was transferred to the Department of Oncology for chemotherapy.

CONCLUSION

Herein, we describe a case of a patient with PSS. The missed diagnosis highlights the necessity and difficulty of differential diagnosis in patients with such tumors. Histopathology is key to the diagnosis of PSS. In our case, no abnormality in the pericardial effusion was noted, and our patient presented with atypical clinical symptoms. Although primary PSS is not common, when the etiological diagnosis of pericardial effusion is unknown, further tests need to be carried out to help rule out or confirm the diagnosis of PSS.

DATA AVAILABILITY STATEMENT

The raw data supporting the conclusions of this article will be made available by the authors, without undue reservation.

ETHICS STATEMENT

Written informed consent was obtained from the individual(s) for the publication of any potentially identifiable images or data included in this article.

AUTHOR CONTRIBUTIONS

YL, ZT, and LX contributed to conception and design of the study. YL completed the data collection and wrote the first draft of the manuscript. YL, KG, TX, HG, RL, SH, and LW wrote sections of the manuscript. All authors contributed to manuscript revision, read, and approved the submitted version.

FUNDING

This study was supported by the National Science Foundation for Young Scientists of China (8150020951) and the Natural Science Foundation for Young Scientists of Hunan Province (2016JJ4099).

REFERENCES

1. Sandberg AA, Bridge JA. Updates on the cytogenetics and molecular genetics of bone and soft tissue tumors. *Synovial sarcoma Cancer Genet Cytogenet.* (2002) 133:1–23. doi: 10.1016/s0165-4608(01)00626-4
2. Varma T, Adegboyega P. Primary cardiac synovial sarcoma. *Arch Pathol Lab Med.* (2012) 136:454–8. doi: 10.5858/arpa.2011-0008-RS
3. Bruce CJ. Cardiac tumours: diagnosis and management. *Heart.* (2011) 97:151–60. doi: 10.1136/hrt.2009.186320
4. Duran-Moreno J, Kampoli K, Kapetanakis EI, Mademli M, Koufopouos N, et al. Pericardial synovial sarcoma: case report, literature review and pooled analysis. *In Vivo.* (2019) 33:1531–8. doi: 10.21873/invivo.11633
5. Ouarrak S, El Ouali Z, Elkebir A, Moumna K, Karkouri M, Azzouzi L, et al. Diagnostic approach to a cardiac mass: a case report of misdiagnosed cardiac synovial sarcoma. *Eur Heart J Case Rep.* (2021) 5:ytab039. doi: 10.1093/ehjcr/ytab039
6. Boulmay B, Cooper G, Reith JD, Marsh R. Primary cardiac synovial sarcoma: a case report and brief review of the literature. *Sarcoma.* (2007) 2007:94797. doi: 10.1155/2007/94797
7. Coli A, Chiariello GA, Novello M, Colizzi C, Massetti M. Treatment of cardiac synovial sarcoma: experience of two cases. *J Cardiothorac Surg.* (2018) 13:84. doi: 10.1186/s13019-018-0771-0
8. Kawai A, Woodruff J, Healey JH, Brennan MF, Antonescu CR, Ladanyi M. SYT-SSX gene fusion as a determinant of morphology and prognosis in synovial sarcoma. *N Engl J Med.* (1998) 338:153–60. doi: 10.1056/NEJM199801153380303
9. Coindre JM. New WHO classification of tumours of soft tissue and bone. *Ann Pathol.* (2012) 32 Supplement:S115–6. doi: 10.1016/j.annpat.2012.07.006
10. Ma W, Liu J, Yeng Z, Chen S, Zheng Y, Ye S, et al. Causes of moderate to large pericardial effusion requiring pericardiocentesis in 140 Han Chinese patients. *Herz.* (2012) 37:183–7. doi: 10.1007/s00059-011-3428-5
11. Kim MP, Correa AM, Blackmon S, Quiroga-Garza G, Weilbaecher D, Bruckner B. et al. Outcomes after right-side heart sarcoma resection. *Ann Thorac Surg.* (2011) 91:770–6. doi: 10.1016/j.athoracsur.2010.09.079
12. Bruckner BA, Abu Saleh WK, Al Jabbari O, Copeland JG, Estep JD, Loebe M. Total artificial heart implantation after excision of right ventricular angiosarcoma. *Tex Heart Inst J.* (2016) 43:252–4. doi: 10.14503/THIJ-15-5131

13. Lee K, Chul Kang M, Lee HW, Park JH, Baek HJ, Cho SJ, et al. Pulmonary metastasectomy in adult patients with synovial sarcoma: a single-center experience. *Korean J Thorac Cardiovasc Surg.* (2016) 49:451–5. doi: 10.5090/kjtcs.2016.49.6.451
14. Michler RE, Goldstein DJ. Treatment of cardiac tumors by orthotopic cardiac transplantation. *Semin Oncol.* (1997) 24:534–9
15. Jiménez Mazuecos JM, Manso RF, Cubero JS, Ramos JT, Oteo Dominiguez JF. Rivera LAP Is heart transplantation for primary cardiac sarcoma a useful therapeutic option? *Rev Esp Cardiol.* (2003) 56:408–11. doi: 10.1016/s0300-8932(03)76886-9
16. Gowdamarajan A, Michler RE. Therapy for primary cardiac tumors: is there a role for heart transplantation? *Curr Opin Cardiol.* (2000) 15:121–5. doi: 10.1097/00001573-200003000-00010
17. Coli A, Cassano A, Novello M, Ranelletti FO, Lauriola L. Primary cardiac synovial sarcoma: a review correlating outcomes with surgery and adjuvant therapy. *J Card Surg.* (2019) 34:1321–7. doi: 10.1111/jocs.14214
18. Kim CH, Dancer JY, Coffey D, Zhai QJ, Reardon M, Ayala AG, et al. Clinicopathologic study of 24 patients with primary cardiac sarcomas: a 10-year single institution experience. *Hum Pathol.* (2008) 39:933–8. doi: 10.1016/j.humpath.2007.12.018
19. Look Hong NJ, Pandalai PK, Hornick JL, Shekar PS, Harmon DC, Chen YL, et al. Cardiac angiosarcoma management and outcomes: 20-year single-institution experience. *Ann Surg Oncol.* (2012) 19:2707–15. doi: 10.1245/s10434-012-2334-2
20. Mayer F, Aebert H, Rudert M, Konigsrainer A, Horger M, Kanz L, et al. Primary malignant sarcomas of the heart and great vessels in adult patients—a single-center experience. *Oncologist.* (2007) 12:1134–42. doi: 10.1634/theoncologist.12-9-1134
21. Eckstein R, Gössner W, Rienmüller R. Primary malignant fibrous histiocytoma of the left atrium. Surgical and chemotherapeutic management. *Br Heart J.* (1984) 52:354–7. doi: 10.1136/hrt.52.3.354
22. Aboud A, Farha K, Hsieh WC, Brasch F, Esminger S, Gummert J, et al. Prognostic factors for long-term survival after surgical resection of primary cardiac sarcoma. *Thorac Cardiovasc Surg.* (2019) 67:665–71. doi: 10.1055/s-0039-1692409
23. Putnam JB Jr., Sweeney MS, Colon R, Lanza LA, Frazier OH, Cooley DA. Primary cardiac sarcomas. *Ann Thorac Surg.* (1991) 51:906–10. doi: 10.1016/0003-4975(91)91003-e
24. Sultan I, Rodriguez-Galindo C, Saab R, Yasir S, Casanova M, Ferrari A. Comparing children and adults with synovial sarcoma in the Surveillance, Epidemiology, and End Results Program, 1983 to 2005: an analysis of 1268 patients. *Cancer.* (2009) 115:3537–47. doi: 10.1002/cncr.24424
25. Bergh P, Meis-Kindblom JM, Gherlinzoni F, Berlin O, Bacchini P, Bertoni F, et al. Synovial sarcoma: identification of low and high risk groups. *Cancer.* (1999) 85:2596–607. doi: 10.1002/(sici)1097-0142(19990615)85:12<2596::aid-cncr16>3.0.co;2-k
26. Spurrell EL, Fisher C, Thomas JM, Judson IR. Prognostic factors in advanced synovial sarcoma: an analysis of 104 patients treated at the Royal Marsden Hospital. *Ann Oncol.* (2005) 16:437–44. doi: 10.1093/annonc/mdi082
27. Vlenterie M, Ho VKY, Kaal SEJ, Vlenterie R, Haas R, van der Graaf WTA. Age as an independent prognostic factor for survival of localised synovial sarcoma patients. *Br J Cancer.* (2015) 113:1602–6. doi: 10.1038/bjc.2015.375

Conflict of Interest: The authors declare that the research was conducted in the absence of any commercial or financial relationships that could be construed as a potential conflict of interest.

Publisher's Note: All claims expressed in this article are solely those of the authors and do not necessarily represent those of their affiliated organizations, or those of the publisher, the editors and the reviewers. Any product that may be evaluated in this article, or claim that may be made by its manufacturer, is not guaranteed or endorsed by the publisher.

frontiers | Frontiers in Cardiovascular Medicine

CASE REPORT
published: 25 May 2022
doi: 10.3389/fcvm.2022.839590

Case Report: Successful Concomitant Pulmonary Thromboendarterectomy and Carotid Endarterectomy

Zhan Liu[1,2†], Xiaopeng Liu[2†], Xia Zheng[2], Fan Lin[2], Guang Sun[2], Zhidong Ye[2], Yanan Zhen[2‡] and Peng Liu[1,2*‡]*

[1] Peking University China-Japan Friendship School of Clinical Medicine, Beijing, China, [2] Department of Cardiovascular Surgery, China-Japan Friendship Hospital, Beijing, China

Pulmonary thromboendarterectomy is the treatment of choice for chronic thromboembolic pulmonary hypertension. Pulmonary thromboendarterectomy concomitant with additional cardiac procedures was reported as safe and feasible. However, the treatment strategy for chronic thromboembolic pulmonary hypertension patients with severe carotid stenosis is still not clear. We describe a case of successful concomitant pulmonary thromboendarterectomy and carotid endarterectomy.

Keywords: pulmonary thromboendarterectomy (PTE), carotid endarterectomy (CEA), chronic thromboembolic pulmonary hypertension (CTEPH), cerebral protection, carotid stenosis

OPEN ACCESS

Edited by:
Marcin Kurzyna, Medical Center of Postgraduate Medication, Poland

Reviewed by:
Szymon Darocha, European Health Center Otwock, Poland
Bao Liu, Peking Union Medical College Hospital (CAMS), China

***Correspondence:**
Yanan Zhen
jamario@163.com
Peng Liu
pengliu5417@163.com

†These authors have contributed equally to this work and share first authorship
‡These authors have contributed equally to this work and share last authorship

Specialty section:
This article was submitted to Heart Surgery, a section of the journal Frontiers in Cardiovascular Medicine

Received: *20 December 2021*
Accepted: *25 April 2022*
Published: *25 May 2022*

Citation:
Liu Z, Liu X, Zheng X, Lin F, Sun G, Ye Z, Zhen Y and Liu P (2022) Case Report: Successful Concomitant Pulmonary Thromboendarterectomy and Carotid Endarterectomy. Front. Cardiovasc. Med. 9:839590. doi: 10.3389/fcvm.2022.839590

INTRODUCTION

Chronic thromboembolic pulmonary hypertension (CTEPH) is classified as Group 4 pulmonary hypertension (1) and characterized pathologically by organized thromboembolic material and altered vascular remodeling (2). Pulmonary thromboendarterectomy (PTE) is the treatment of choice for CTEPH and potentially curative (3). For CTEPH patients with other cardiac issues, studies have shown that PTE concomitant with additional cardiac procedures, such as defect repair, valvuloplasty, and even heart transplantation, is safe and feasible (4–6). There are some other diseases that may pose a serious threat to patients if left untreated. One of them is carotid artery stenosis. Since PTE surgery is conducted under deep hypothermic circulatory arrest (DHCA), severe carotid artery stenosis can cause irreversible damage to the brain. To date, the treatment strategy for CTEPH patients with severe carotid stenosis is still not clear. We describe a case of a CTEPH patient with severe carotid stenosis who underwent successful concomitant PTE and carotid endarterectomy (CEA).

CASE DESCRIPTION

A 63-year-old male was transferred to our hospital for progressive shortness of breath. Seven months prior to referral, the patient was diagnosed with pulmonary embolism in a local hospital and treated with thrombolysis (alteplase, 100 mg) and anticoagulation (low molecular weight heparin, 100 U/kg, q12h) therapy, and then oral rivaroxaban (10 mg, bid) and bosentan (125 mg, bid) after discharge. However, his clinical condition failed to improve. He was admitted to our hospital and finally diagnosed with CTEPH. The patient did not have any other previous history.

Transthoracic echocardiography examination showed enlargement of his right heart; the diameter of the right atrium and ventricle was 42 and 48 mm, respectively. Mild to moderate tricuspid regurgitation was detected. Doppler ultrasonography estimated a pulmonary artery systolic pressure of 76 mmHg. The ventilation/perfusion lung scan revealed the presence of mismatched perfusion defects. Pulmonary computed tomography angiography demonstrated filling defects located in the main trunk of the right pulmonary artery and in most lobar and segmental branches of bilateral pulmonary arteries (**Figure 1A**). Subsequent right heart catheterization (RHC) examination showed severe pulmonary hypertension, with a mean pulmonary pressure (mPAP) of 55 mmHg and pulmonary vascular resistance (PVR) of 1,296 dyn·s·cm^{-5}. Moreover, angiography showed severe stenosis of the right internal carotid artery, while the left carotid artery was patent (**Figure 1B**). An ultrasound showed no evidence of deep venous thrombosis of the lower extremities. The NT-proBNP plasma level was as high as 1,251 pg/mL.

After discussion by a multidisciplinary team, we decided to perform concomitant procedures of CEA and PTE. We informed the patient and his family of the different treatments and related risks, and they grace approval for concomitant PTE and CEA treatment. After general anesthesia, we first treated the carotid disease with a standard eversion CEA procedure. An oblique longitudinal incision along the anterior edge of the right sternocleidomastoid muscle was made. After systemic heparinization, the common, internal, and external carotid arteries were controlled. The proximal part of the right internal carotid artery was transected, and eversion CEA was performed. The total carotid artery clamp time was 16 min. The internal carotid artery was anastomosed using a 6-0 Prolene suture. Since the PTE procedure was conducted under systemic heparinization and cardiopulmonary bypass, we decided to leave the neck incision opened to prevent hematoma. Pulmonary arteries were exposed through a median sternotomy. Cardiopulmonary bypass was established by ascending aortic and bicaval cannulation. After system cooling to 20 °C, PTE was performed under DHCA. After 3 circulatory arrests, the old thrombus and fibrotic intima were entirely removed (**Figure 2**). The total circulation arrest time was 57 min, the total CPB time was 315 min, the aortic cross-clamp time was 135 min, and the total operation time was 780 min.

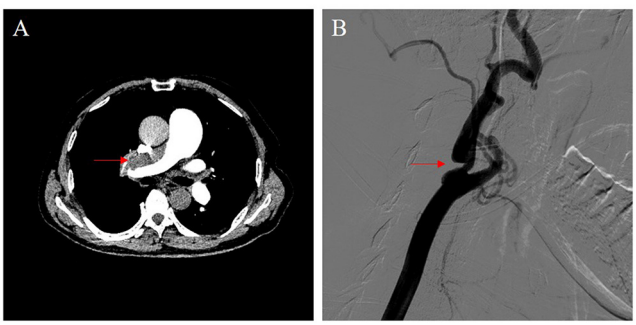

FIGURE 1 | Imaging data. **(A)** Pulmonary computed tomography angiography demonstrated a filling defect located in the main trunk of the right pulmonary artery (red arrow). **(B)** Carotid artery angiography showed severe stenosis of the right internal carotid artery (red arrow).

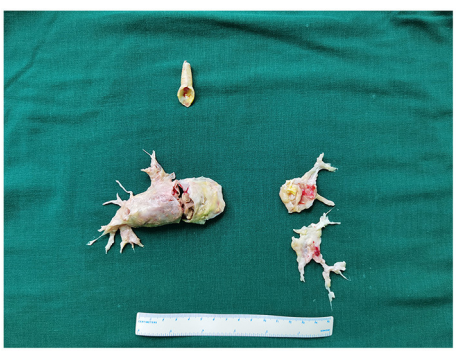

FIGURE 2 | The old thrombus and fibrotic intima were entirely removed.

After surgery, mannitol was administered for 3 days and the mean arterial pressure of the patient was controlled at 70–75 mmHg. All these treatment strategies were aimed at preventing cerebral overperfusion and bleeding. The patient recovered uneventfully in the intensive care unit (ICU). The mechanical ventilation time was 113 h, and the ICU length of stay was 6 days. A Swan-Ganz catheter was placed intraoperatively after tracheal intubation was discontinued to measure the postoperative mPAP and PVR. At this time, no narcotics were used and only low-dose phenylephrine (1 μg/kg/min) was administered to control the cardiac index. The postoperative mPAP decreased to 18 mmHg, and the PVR was 200 dyn·s·cm^{-5}. The patient was discharged 21 days postoperatively without any complications. During the 5-month follow-up, the patient recovered well without any obvious symptoms. The reviewed RHC examination showed that the mPAP and PVR were 15 mmHg and 136 dyn·s·cm^{-5}, respectively. Furthermore, the 6-min walk distance increased from 275 m preoperatively to 435 m postoperatively, and the New York Heart Association functional class improved from grade III to grade I (**Table 1**). The ultrasound revealed patency of the bilateral carotid arteries. The detailed timeline of the clinical course of this patient is displayed in **Table 2**.

DISCUSSION

PTE is the treatment of choice for CTEPH and is potentially curative (3). The international registry of incident cases of CTEPH reported a 3-year survival of 90% in those who underwent surgery and 70% in those who did not undergo surgery (7). Clinical guidelines recommend that PTE should be offered to all surgical candidates with CTEPH (2, 8). The evaluation of potential surgical patients mainly includes the evaluation of technical operability and the assessment of the potential risks and benefits of surgery (3). With advances in surgical experience and imaging, PTE could be performed

TABLE 1 | The baseline and follow-up parameters of the patient.

Parameters	Baseline	Follow-up
Transthoracic echocardiography		
Diameter of RA (mm)	42	32
Diameter of RV (mm)	48	29
Right heart catheterization		
mPAP (mmHg)	55	15
PVR (dyn·s·cm^{-5})	1,251	136
6-min walk distance (m)	275	435
NYHA functional class	III	I

RA, right atrium; RV, right ventricle; mPAP, mean pulmonary pressure; PVR, pulmonary vascular resistance; NYHA, New York Heart Association.

TABLE 2 | Detail timeline of clinical course of the patient.

5/4/2018	The patient suffered from progressive shortness of breath.
11/28/2020	The patient was diagnosed with pulmonary embolism in a local hospital and treated with thrombolysis (alteplase, 100 mg) and anticoagulation (low molecular weight heparin, 100 U/kg, q12h) therapy, and then oral rivaroxaban (10 mg, bid) and bosentan (125 mg, bid) after discharge.
6/22/2021	The patient was transferred to our hospital and diagnosed with chronic thromboembolic pulmonary hypertension.
6/25/2021	The preoperative angiography showed severe stenosis of the right internal carotid artery.
6/29/2021	After discussion by a multidisciplinary team, we decided to perform concomitant procedures of carotid endarterectomy (CEA) and PTE.
7/1/2021	Concomitant CEA and PTE was performed successfully.
7/22/2021	The patient was discharged 21 days postoperatively without any complications.
7/22/2021 to present	During the 5-month follow-up, the patient recovered well without any obvious symptoms. Significant improvements were found in hemodynamics, exercise capacity, and functional status during follow-up.

successfully in patients with distal disease (9). On the other hand, the presence of comorbid conditions, with the exception of those that are terminal or end-stage, does not represent an absolute contraindication to PTE (3).

Studies have shown that PTE concomitant with additional cardiac procedures, even heart transplantation, is safe and feasible (4–6). However, the treatment strategy for CTEPH patients with severe carotid stenosis is not clear. Neurological injury is one of the most common perioperative complications of PTE and is associated with cerebral ischemia resulting from DHCA (10). The presence of severe carotid artery stenosis could dramatically increase the risk of perioperative neurological injury. Therefore, carotid stenosis should be resolved before cardiac arrest. After discussion by a multidisciplinary team composed of cardiovascular surgeons, PH physicians, radiologists, anesthesiologists, and perfusionists, we decided to perform concomitant PTE and CEA procedures. One important reason that our team thought concomitant procedures could be feasible was that the postoperative management principles of CEA and PTE are consistent; that is, dehydration and control of cardiac output (or blood pressure). Mannitol (125 mg q12h) was administered, and the cardiac index was controlled at 2.0 to 2.5 L/min/m^2 after surgery. Therefore, the risk of hyperperfusion after CEA may be lower. The patient recovered uneventfully with significant improvements in symptoms and hemodynamics. During a 5-month follow-up, the patient recovered well without any symptoms of neurological injury. Furthermore, significant improvements were found in hemodynamics, exercise capacity, and functional status during follow-up.

Another option for this patient is staged surgery. To minimize the risk of neurological injury, carotid stenosis should be treated first. Unfortunately, it is difficult for the patient to tolerate CEA surgery under general anesthesia. If pulmonary artery obstruction is left untreated, the patient may not be able to wean from the ventilator after CEA surgery. Furthermore, surgical stimulation may aggravate heart failure and even lead to pulmonary hypertensive crisis. Carotid artery stenting is also feasible for this patient and can be performed under local anesthesia. However, at least 3 months of dual antiplatelet therapy is required after stent implantation, which prolongs the time until PTE surgery and increases the risk of heart failure and death in the patient.

In conclusion, our case demonstrates the first successful concomitant PTE and CEA surgery reported in the literature. For CTEPH patients with severe carotid artery stenosis, concomitant PTE and CEA may be safe and effective. Adequate preoperative evolution by an experienced multidisciplinary team is necessary.

DATA AVAILABILITY STATEMENT

The raw data supporting the conclusions of this article will be made available by the authors, without undue reservation.

ETHICS STATEMENT

The studies involving human participants were reviewed and approved by the Ethics Committee of the China-Japan Friendship Hospital. The patients/participants provided their written informed consent to participate in this study.

AUTHOR CONTRIBUTIONS

ZL and XL wrote the manuscript. XZ, FL, GS, and ZY were involved in data collection and validation. YZ and PL contributed to conceptualization and revised the manuscript. All authors have read and approved the final manuscript.

REFERENCES

1. Simonneau G, Montani D, Celermajer DS, Denton CP, Gatzoulis MA, Krowka M, et al. Haemodynamic definitions and updated clinical classification of pulmonary hypertension. *Eur Respir J.* (2019) 53:1801913. doi: 10.1183/13993003.01913-2018
2. Kim NH, Delcroix M, Jais X, Madani MM, Matsubara H, Mayer E, et al. Chronic thromboembolic pulmonary hypertension. *Eur Respir J.* (2019) 53:1801915. doi: 10.1183/13993003.01915-2018
3. Papamatheakis DG, Poch DS, Fernandes TM, Kerr KM, Kim NH, Fedullo PF. Chronic thromboembolic pulmonary hypertension: JACC focus seminar. *J Am Coll Cardiol.* (2020) 76:2155–69. doi: 10.1016/j.jacc.2020.08.074
4. Erdem H, Korun O, Yanartaş M, Taş S, Erden B, Yerlikhan O, et al. Outcomes of pulmonary endarterectomy operation concomitant with cardiac procedures. *Thorac Cardiovasc Surg.* (2021) 69:279–83. doi: 10.1055/s-0040-1710580
5. Vaca-Cartagena BF, Lee CY, Tran HA, Fernandes T, Kim NH, Pretorius V. Successful concomitant pulmonary thromboendarterectomy and heart transplant. *Ann Thorac Surg.* (2021) 111:e421–3. doi: 10.1016/j.athoracsur.2020.09.065
6. Qin X, Liang W, Wu Z. A rare case of cardiac mass complicated with chronic thromboembolic pulmonary hypertension. *J Card Surg.* (2020) 35:3567–8. doi: 10.1111/jocs.15031
7. Delcroix M, Lang I, Pepke-Zaba J, Jansa P, D'Armini AM, Snijder R, et al. Long-term outcome of patients with chronic thromboembolic pulmonary hypertension: results from an international prospective registry. *Circulation.* (2016) 133:859–71. doi: 10.1161/CIRCULATIONAHA.115.016522
8. Galiè N, Humbert M, Vachiery JL, Gibbs S, Lang I, Torbicki A, et al. 2015 ESC/ERS Guidelines for the diagnosis and treatment of pulmonary hypertension: the joint task force for the diagnosis and treatment of pulmonary hypertension of the European society of cardiology (ESC) and the European Respiratory Society (ERS): Endorsed by: Association for European Paediatric and Congenital Cardiology (AEPC), International Society for Heart and Lung Transplantation (ISHLT). *Eur Respir J.* (2015) 46:903–75. doi: 10.1183/13993003.01032-2015
9. D'Armini AM, Morsolini M, Mattiucci G, Grazioli V, Pin M, Valentini A, et al. Pulmonary endarterectomy for distal chronic thromboembolic pulmonary hypertension. *J Thorac Cardiovasc Surg.* (2014) 148:1005–11. doi: 10.1016/j.jtcvs.2014.06.052
10. Kratzert WB, Boyd EK, Saggar R, Channick R. Critical care of patients after pulmonary thromboendarterectomy. *J Cardiothorac Vasc Anesth.* (2019) 33:3110–26. doi: 10.1053/j.jvca.2019.03.005

Conflict of Interest: The authors declare that the research was conducted in the absence of any commercial or financial relationships that could be construed as a potential conflict of interest.

frontiers | Frontiers in Cardiovascular Medicine

CASE REPORT
published: 07 July 2022
doi: 10.3389/fcvm.2022.900803

Case Report: Anomalous Origin of the Right Coronary Artery From the Left Sinus of Valsalva With Aortic Dissection: New Myocardial Ischemia Mechanism

Zhongshang Xie[1,2], *Junlin Zou*[2,3], *Hong Zhu*[1,2*†] *and Haisong Bu*[1,2*†]

[1] Department of Cardiovascular Surgery, Xiangya Hospital, Central South University, Changsha, China, [2] National Clinical Research Center for Geriatric Disorders, Xiangya Hospital, Central South University, Changsha, China, [3] Department of Cardiology, Xiangya Hospital, Central South University, Changsha, China

The aortic anomaly of the right coronary artery (AAORCA) originating from the left aortic sinus (LCS) is a rare malformation that may result in sudden cardiac death (SCD), which may be due to the dilated aorta-pulmonary artery affecting the blood supply of the coronary artery. However, there are still some disputes about the treatment of the AAORCA. Herein, we present a rare case of AAORCA from the LCS with aortic dissection (AD). Considering the risk of dissection rupture and SCD, an emergency surgery of aortic replacement and coronary anomaly correction was performed successfully for the patient. This report illustrated that AAORCA complicated with acute AD (AAD) is lethal and may promote the occurrence of coronary ischemia or sudden death by a new "double-kill" mechanism that myocardial ischemia was based on the extent of a fixed and a dynamic component like slit-like ostium, proximal narrowing, acute take-off angle and intramural course with the elliptic vessel shape. There is no doubt that surgery is the best treatment option for the AAORCA with AAD.

Keywords: the anomalous aortic origin of the right coronary artery, left sinus, aortic dissection, coronary blood flow, mechanism

OPEN ACCESS

Edited by:
Cuntao Yu,
Chinese Academy of Medical Sciences and Peking Union Medical College, China

Reviewed by:
Maruti Haranal,
U N Mehta Institute of Cardiology and Research, India
Cristina Aurigemma,
Agostino Gemelli University Polyclinic (IRCCS), Italy

***Correspondence:**
Haisong Bu
buhaisong@csu.edu.cn
Hong Zhu
doczhu2014@csu.edu.cn

†These authors have contributed equally to this work

Specialty section:
This article was submitted to Heart Surgery, a section of the journal Frontiers in Cardiovascular Medicine

Received: *21 March 2022*
Accepted: *13 June 2022*
Published: *07 July 2022*

Citation:
Xie Z, Zou J, Zhu H and Bu H (2022) Case Report: Anomalous Origin of the Right Coronary Artery From the Left Sinus of Valsalva With Aortic Dissection: New Myocardial Ischemia Mechanism. Front. Cardiovasc. Med. 9:900803. doi: 10.3389/fcvm.2022.900803

INTRODUCTION

The aortic anomaly of the right coronary artery (AAORCA) originating from the left aortic sinus (LCS) is a rare malformation, which has the possibility of sudden cardiac death (SCD) due to coronary artery ischemia. However, there are still some disputes about the treatment of the AAORCA (1, 2). Although most variants of AAORCA are benign, the challenge for clinicians is to recognize, which may attribute to the possibility of SCD, especially in the presence of strenuous exercise (3). Its mechanism has been attributed to the dilated aorta-pulmonary artery affecting the blood supply of the coronary artery (3, 4). Meanwhile, acute aortic dissection (AAD) is lethal and may promote the occurrence of SCD by a similar mechanism (5).

CASE PRESENTATION

A 54-year-old female was admitted urgently again because of sudden chest and back pain. At her first admission in June 2020, due to chronic atypical chest pain with paroxysmal syncope without any history, she was diagnosed with AAORCA and slight coronary stenosis (**Figures 1A,B**; **Supplementary Video 1**) after trans-radial coronary angiography and recovered after 2-week symptomatic treatment with medicine. At this time, no positive signs were found except a blood pressure of 162/90 mmHg at resting conditions and a slight diastolic murmur. An electrocardiogram (ECG) showed the mild ST-segment depression and cardiac troponin I was 0.17 ng/ml. Transthoracic echocardiography showed a Stanford type A aortic dissection (AD) with the widening from the aortic sinus to the thoracic aorta, avulsion injury at the opening of the right coronary artery (RCA), and the RCA originated from the left coronary sinus (LCS) (**Figures 2A,B**). Total aorta plus coronary CTA clarified the Stanford type A AD involving from the aortic root to the abdominal aorta, while left and right coronary arteries originated from the LCS (**Figures 3A–C**; **Supplementary Video 2**). The RCA was abnormally distributed and walked between the aorta-pulmonary artery (**Figure 3D**; **Supplementary Video 3**).

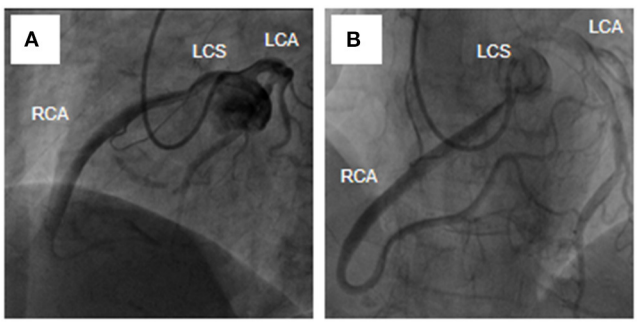

FIGURE 1 | Transradia coronary angiography showed AAORCA **(A,B)**. AAORCA, the anomalous aortic origin of the right coronary artery; RCA, right coronary artery; LCS, left coronary sinus; LCA, left coronary artery.

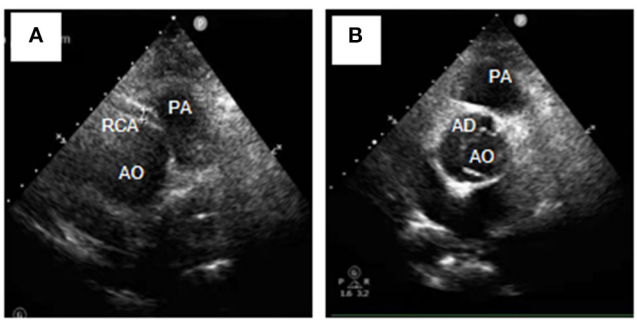

FIGURE 2 | Transthoracic echocardiography (Short-axis view at the great artery) revealed Stanford type A aortic dissection **(A)**, avulsion of the RCA, and the RCA originating from the left coronary sinus **(B)**. RCA, right coronary artery; AD, aortic dissection; AO, aortic; PA, pulmonary artery.

Considering the risk of dissection rupture and SCD, an emergency surgery of aortic replacement and coronary anomaly correction was performed successfully for the patient. The AAORCA with AAD was identified and the aortic valves and LCS were still normal. We repaired the AAD with ascending aorta and total arch replacement combined with stent-graft elephant trunk technique, and corrected AAORCA with a right coronary artery bypass grafting. Postoperatively, the patient recovered well with medicine therapy including aspirin and clopidogrel, and was discharged on the 9th day after the operation. The patient is well now and has no limitations in daily activities at her 4-month follow-up visit.

DISCUSSION AND CONCLUSIONS

The AAORCA is usually recognized when patients present with symptoms or are incidentally diagnosed, and its prevalence is between 0.008 and 0.32% of the population, which is considered to be due to differences in the definitions, imaging methods used and patient groups studied (3, 6). When RCA originates from the contralateral sinus and abnormally distributes between the aorta-pulmonary artery, there is the possibility of sudden cardiac death, which may be due to the dilated artery affecting the blood supply of the coronary artery (3, 4). However, the interarterial course between the aorta-pulmonary artery may only represents a surrogate for ischemia-associated anatomical

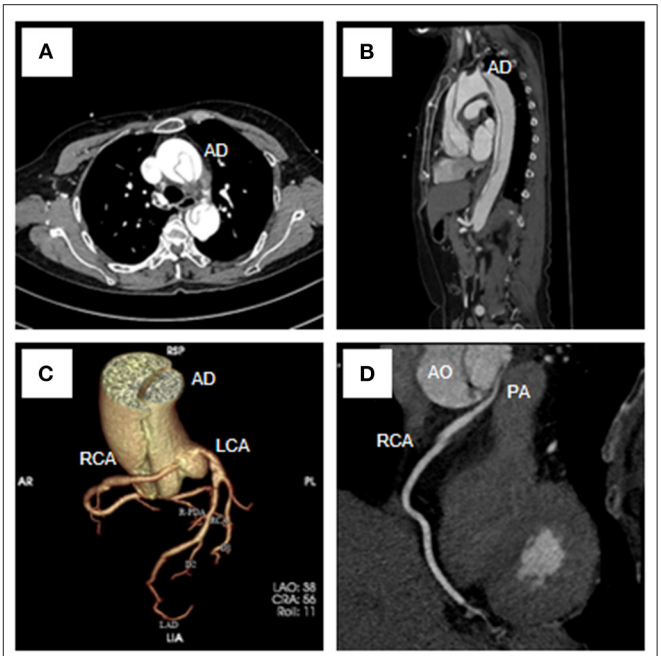

FIGURE 3 | Total aorta plus coronary computed tomography angiogram showed the Stanford type A aortic dissection **(A–C)**, the RCA originated from the LCS **(C,D)** and coursed between the aorta and the pulmonary artery **(D)**. RCA, right coronary artery; LCA, left coronary artery; AD, aortic dissection; AO, aortic; PA, pulmonary artery.

high-risk features like slit-like ostium, acute take-off angle, proximal narrowing (also referred to as hypoplasia) with elliptic vessel shape and intramural course, which referred to a two-tier concept for the pathomechanisms of ischemia in AAORCA. In this concept, the occurrence of ischemia is based on the extent of a fixed (anatomic high-risk features of slit-like ostium and proximal narrowing) and a dynamic (acute take-off angle, intramural course with the elliptic vessel shape) component (7). In our case, the patient's first hospitalization in June 2020 may be due to myocardial ischemia caused by a fixed component like proximal narrowing similar to classic coronary lesions. However, the patient with AAORCA suffered from an AAD in this emergency admission. AAD is a life-threatening disease that demands urgent surgery. The proximal aortic lesion of the AAD not only increased the risk of rupture but also increased the risk of myocardial infarction. About 2% of all AAD patients have an acute myocardial infarction (AMI), which may be attributed to the exogenous compression of the enlarged pseudolumen on the opening of the coronary artery or the obstruction of the intimal valve (4). Meanwhile, the AAD increased the risk of myocardial infarction in patients with AAORCA by slit-like ostium, proximal narrowing, acute take-off angle and intramural course with the elliptic vessel shape.

Although echocardiographic diagnosis has been described to diagnose AAORCA (6), cardiac catheterization and angiocardiography are still considered the gold criterion diagnostic strategy. Recently, coronary CTA has gradually been used to differentiate and diagnose AAORCA. CTA is a non-invasive diagnostic aid, which can accurately show the origin and distribution of the coronary artery, evaluate and describe its anatomical relationship with surrounding structures (8). Hence, the non-invasive detection method is widely considered and selected to describe the anatomical structure of the coronary artery.

All patients with AAORCA, especially combined with AAD, should be treated with emergency surgery. The dilated aorta compressed the RCA located between the aorta-pulmonary artery and was considered to be the cause of AMI. The enlargement of the sinus of Valsalva in AD also possibly led to acute myocardial infarction. Therefore, patients with AAORCA from the contralateral sinus of Valsalva complicated with AAD should be intervened early, especially in high-risk patients (hypertension or Marfan syndrome) with AAD (3). Meanwhile, AAD with multiple arterial malformations may be a new syndrome caused by a certain gene or chromosome similar to Down syndrome or Marfan syndrome (9). Moreover, the coronary anomaly may be a risk for aortic dissection with possible hemodynamic abnormalities in the aortic root and increase the difficulty of aortic root replacement (10). However, for AAD patients with coronary artery abnormalities, we recommend the use of coronary CTA for clear diagnosis to avoid the risk of dissection rupture. Taken together, this report illustrated that patients with AAORCA from the contralateral sinus of Valsalva complicated with AAD may result in AMI by the new "double-kill" mechanism that myocardial ischemia was based on the extent of a fixed and a dynamic component like slit-like ostium, proximal narrowing, acute take-off angle and intramural course with the elliptic vessel shape.

DATA AVAILABILITY STATEMENT

The original contributions presented in the study are included in the article/**Supplementary Material**, further inquiries can be directed to the corresponding author/s.

ETHICS STATEMENT

The studies involving human participants were reviewed and approved by the Ethics Committee of Xiangya Hospital of Central South University, Changsha, China. The patients/participants provided their written informed consent to participate in this study. Written informed consent was obtained from the individual(s) for the publication of any potentially identifiable images or data included in this article.

AUTHOR CONTRIBUTIONS

ZX, HZ, and HB prepared and wrote the main manuscript. JZ, HZ, and HB prepared figures and supplementary videos. HB and ZX collected, checked, and analyzed the data. All authors have read and approved the final manuscript and agreed to be accountable for the content of the work.

FUNDING

This work was supported by the Natural Science Foundation of Hunan (2022JJ40765) and the Natural Science Foundation of Changsha City, China (kq2202366).

ACKNOWLEDGMENTS

We thank the patient for participating in this study.

SUPPLEMENTARY MATERIAL

The Supplementary Material for this article can be found online at: https://www.frontiersin.org/articles/10.3389/fcvm.2022.900803/full#supplementary-material

Supplementary Video 1 | Transradia coronary angiography showed AAORCA.

Supplementary Video 2 | The computed tomography angiogram showed the RCA originated from the LCS.

Supplementary Video 3 | The computed tomography angiogram showed the RCA abnormally distributed and walked between the aorta-pulmonary artery.

REFERENCES

1. Jegatheeswaran A, Brothers JA. Anomalous aortic origin of a coronary artery: learning from the past to make advances in the future. *Curr Opin Pediatr*. (2021) 33:482–8. doi: 10.1097/MOP.0000000000001056
2. Jiang MX, Blackstone EH, Karamlou T, Ghobrial J, Brinza EK, Haupt MJ, et al. Anomalous aortic origin of a coronary artery in adults. *Ann Thorac Surg*. (2021) 112:1299–305. doi: 10.1016/j.athoracsur.2020.06.153
3. Machii Y, Shimada N, Okamoto T, Tanaka M. A case of right ventricular infarction due to acute type A aortic dissection with anomalous aortic origin of the right coronary artery from the left sinus of Valsalva. *J Card Surg*. (2021) 36:4776–8. doi: 10.1111/jocs.16024
4. Tessitore A, Caiffa T, Bobbo M, D'Agata Mottolese B, Barbi E, Chicco D. Anomalous aortic origin of coronary artery: for a challenging diagnosis, a transthoracic echocardiogram is recommended. *Acta Paediatr*. (2022) 111:265–8. doi: 10.1111/apa.16160
5. Tang L, Hu XQ, Zhou SH. Acute stanford type A aortic dissection mimicking acute myocardial infarction: a hidden catastrophe which should prompt greater vigilance. *Acta Cardiol Sin*. (2014) 30:493–6.
6. Cheezum MK, Liberthson RR, Shah NR, Villines TC, O'Gara PT, Landzberg MJ, et al. Anomalous aortic origin of a coronary artery from the inappropriate sinus of valsalva. *J Am Coll Cardiol*. (2017) 69:1592–608. doi: 10.1016/j.jacc.2017.01.031
7. Bigler MR, Ashraf A, Seiler C, Praz F, Ueki Y, Windecker S, et al. Hemodynamic relevance of anomalous coronary arteries originating from the opposite sinus of valsalva-in search of the evidence. *Front Cardiovasc Med*. (2021) 7:591326. doi: 10.3389/fcvm.2020.591326
8. Bu H, Gong X. Image diagnosis: an anomalous origin of right pulmonary artery from the ascending aorta. *J Cardiovasc Comput Tomogr*. (2020) 14:e37–9. doi: 10.1016/j.jcct.2018.12.053
9. Wanamaker KM, Amadi CC, Mueller JS, Moraca RJ. Incidence of aortic arch anomalies in patients with thoracic aortic dissections. *J Card Surg*. (2013) 28:151–4. doi: 10.1111/jocs.12072
10. Tran D, Ghoreishi M, Taylor B, Kaczorowski DJ. Neomedia aortic root repair for type A aortic dissection despite anomalous right coronary artery. *Ann Thorac Surg*. (2020) 110:e513–5. doi: 10.1016/j.athoracsur.2020.04.023

Conflict of Interest: The authors declare that the research was conducted in the absence of any commercial or financial relationships that could be construed as a potential conflict of interest.

frontiers | Frontiers in Cardiovascular Medicine

CASE REPORT
published: 22 July 2022
doi: 10.3389/fcvm.2022.926527

A Rare Ultra-Long-Term Complication of Occluder Recanalization Due to Spontaneous Perforation of Polyvinyl Alcohol Membrane of Atrial Septal Defect Occluder: A Case Report and Review of the Literature

*Kun Xiang, Huanwei Zhuang, Qin Wu, Mi Tang, Jinfu Yang and Chengming Fan**

Department of Cardiovascular Surgery, The Second Xiangya Hospital, Central South University, Changsha, China

OPEN ACCESS

Edited by:
Hendrik Tevaearai Stahel, Bern University Hospital, Switzerland

Reviewed by:
Christopher Learn, Mass General Brigham, United States
Ömer Faruk Çiçek, Selcuk University, Turkey

***Correspondence:**
Chengming Fan
fanchengming@csu.edu.cn

Specialty section:
This article was submitted to Heart Surgery, a section of the journal Frontiers in Cardiovascular Medicine

Received: *22 April 2022*
Accepted: *14 June 2022*
Published: *22 July 2022*

Citation:
Xiang K, Zhuang H, Wu Q, Tang M, Yang J and Fan C (2022) A Rare Ultra-Long-Term Complication of Occluder Recanalization Due to Spontaneous Perforation of Polyvinyl Alcohol Membrane of Atrial Septal Defect Occluder: A Case Report and Review of the Literature. Front. Cardiovasc. Med. 9:926527. doi: 10.3389/fcvm.2022.926527

Percutaneous closure of atrial septal defect (ASD) has emerged as a feasible alternative strategy to surgical repair in many cardiac centers worldwide. Occluder recanalization due to device failure is a rare and severe complication that often occurs within weeks to years after ASD closure. We reported a rare ultra-long-term complication of occluder recanalization due to delayed spontaneous perforation of polyvinyl alcohol (PVA) membrane of ASD occluder after 18 years of ASD closure. Surgical removal of the faulty device and reconstruction of the atrial septum with a bovine pericardial patch was performed. The patient was discharged and recovered uneventfully without syncope or residual shunt. The cause of this rare complication of spontaneous PVA membrane perforation of the occluder has not been fully detected. To our knowledge, this is the first report about PVA membrane perforation of an occluder that occurred soon after ASD closure.

Keywords: atrial septal defect, closure, occluder recanalization, ultra-long-term complication, surgery

BACKGROUND

Atrial septal defect (ASD) is one of the most common congenital heart diseases in children, accounting for 7–10% of all congenital heart diseases (1). Percutaneous closure of ASD has emerged as a viable alternative to surgery when feasible in the case of favorable anatomy (2–4). The technique of catheter intervention for the treatment of ASD and patent foramen ovale was pioneered by King and Mills in 1975, which led to the invention of various devices from the late 1980s to the mid-1990s (5). The mushroom umbrella occluder (Huayi Shengjie Co., Ltd., Beijing, China) is made of two disc frames woven by a nitinol wire mesh and has a mushroom-shaped hole structure with self-expanding properties. The two discs and the waist are covered with medical polymer PVA membrane film to enhance the occlusion effect. PVA is a water-soluble polymer, which becomes insoluble for medical applications with formaldehyde or glutaraldehyde cross-links (6). The PVA membranes have a long history of permanent implantation in the medical field (2–4, 7). However, the complications of spontaneous perforation of the PVA membrane have been observed with ASD

occluders made by both domestic and foreign manufacturers. Neither the previous surgeons nor the manufacturers could explain the mechanism of the PVA membrane disappearance. To date, the reports of long-term complications of occluder recanalization due to spontaneous PVA membrane perforation are extremely rare (8). Herein, we reported a 40-year-old woman with an ultra-long-term complication of massive left-to-right shunt due to spontaneous PVA membrane perforation of the occluder after 18 years of ASD closure.

CASE REPORT

A 40-year-old female with sudden syncope was referred to our department. She has an 18-year history of percutaneous ASD (30 mm in diameter) closure with a 40-mm mushroom umbrella occluder (Huayi Shengjie Co., Ltd., Beijing, China). The surgical result was satisfactory, and no residual shunt was seen. Regular re-examination 3 years after the operation showed no abnormality. Two cesarean sections after 4 and 7 years of percutaneous ASD closure and a hysteromyoma surgery after 13

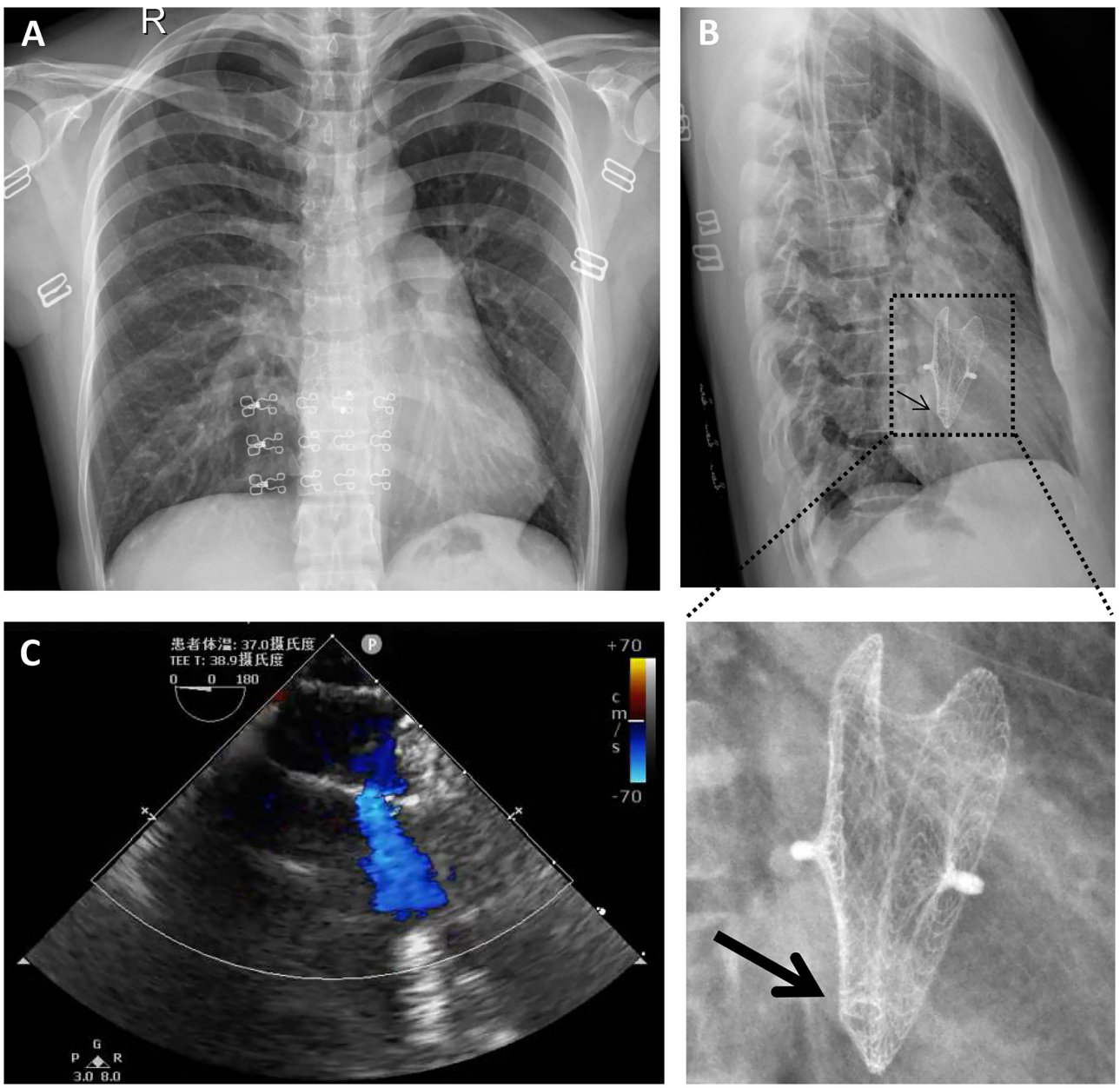

FIGURE 1 | Chest radiography **(A,B)** and transthoracic echocardiography **(C)** preoperatively indicated that most parts of the closure were deformed, especially the left atrial side [**(B)**, arrow]; a significant multi-bundle left-to-right shunt through the device and a small adhesion on the occluder was detected **(C)**.

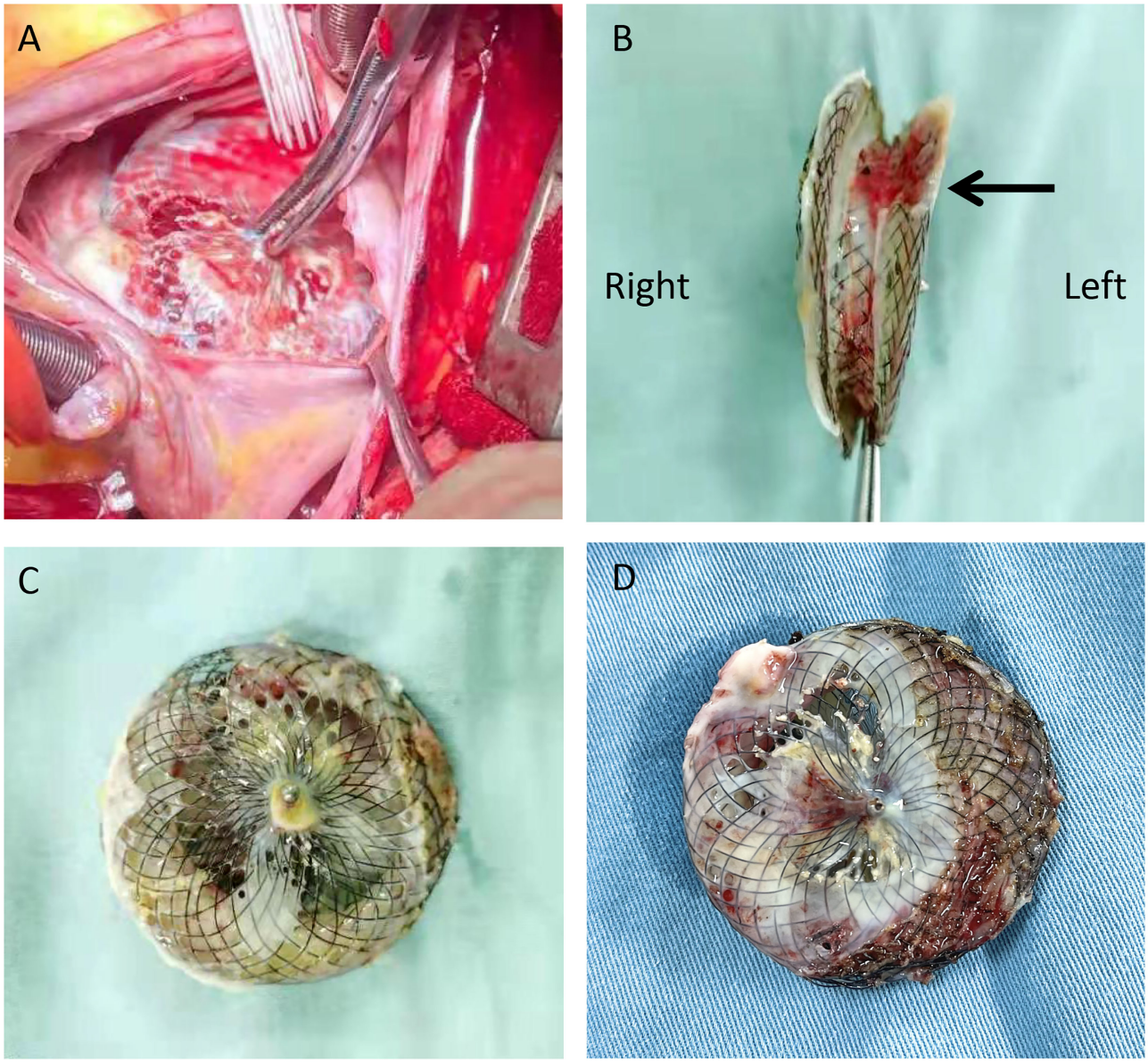

FIGURE 2 | Intraoperative view of the procedure: After opening the right atrium, a deformed occluder was found in the atrial septum **(A)**; the left side of the occluder was damaged more obvious than the right [**(B)**, arrow]; The PVA membranes showed multiple perforations and were partly dissolved, and the diameter of the largest void was around 10 mm **(C,D)**.

years of percutaneous ASD closure had been done. Transthoracic echocardiography and electrocardiogram during these three hospitalizations showed no abnormality. The patient in our case has not been followed up and had not undergone transthoracic echocardiography for the last 5 years. In the past 3 months, the patient had two episodes of sudden syncope, one was induced by exercise, and another had no obvious incentive, accompanied by sweating and pale complexion, which was relieved spontaneously in about 5 min. She denied chest pain, chest tightness, shortness of breathing, and palpitations. On physical examination, a soft blowing murmur was heard in the second and third costal margin of the left margin of the sternum. There were no other notable clinical findings during a physical examination and no medical, family, or psychosocial history including genetic information about cardiovascular disease. X-rays (**Figures 1A,B**) showed that most parts of the closure were deformed, especially the left atrial side (**Figure 1B**, arrow) and that the nitinol frame of the occluder was not displaced and there was no evidence of a frame fracture. The electrocardiogram demonstrated sinus rhythm and an incomplete right bundle branch block. Transthoracic echocardiography revealed a recurrent significant multi-bundle left-to-right shunt through the device and small adhesions were visible on the occluder (**Figure 1C**). Moreover, the enlarged right heart chambers and mild mitral valve regurgitation

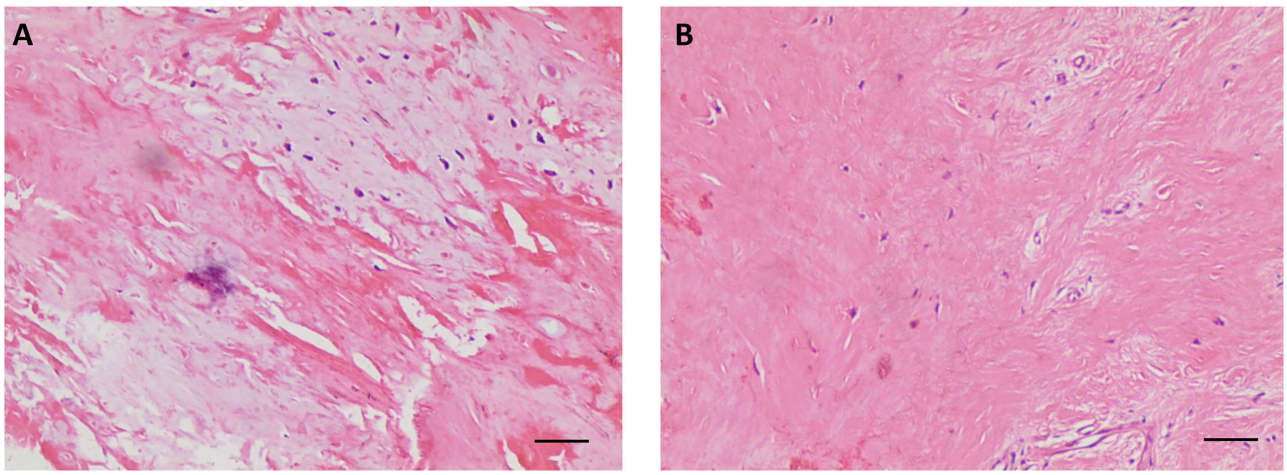

FIGURE 3 | Postoperative histological examination with hematoxylin-eosin staining showing the proliferation of fibrous collagenous tissue **(A,B)**. (100×, scale bar = 50 μm).

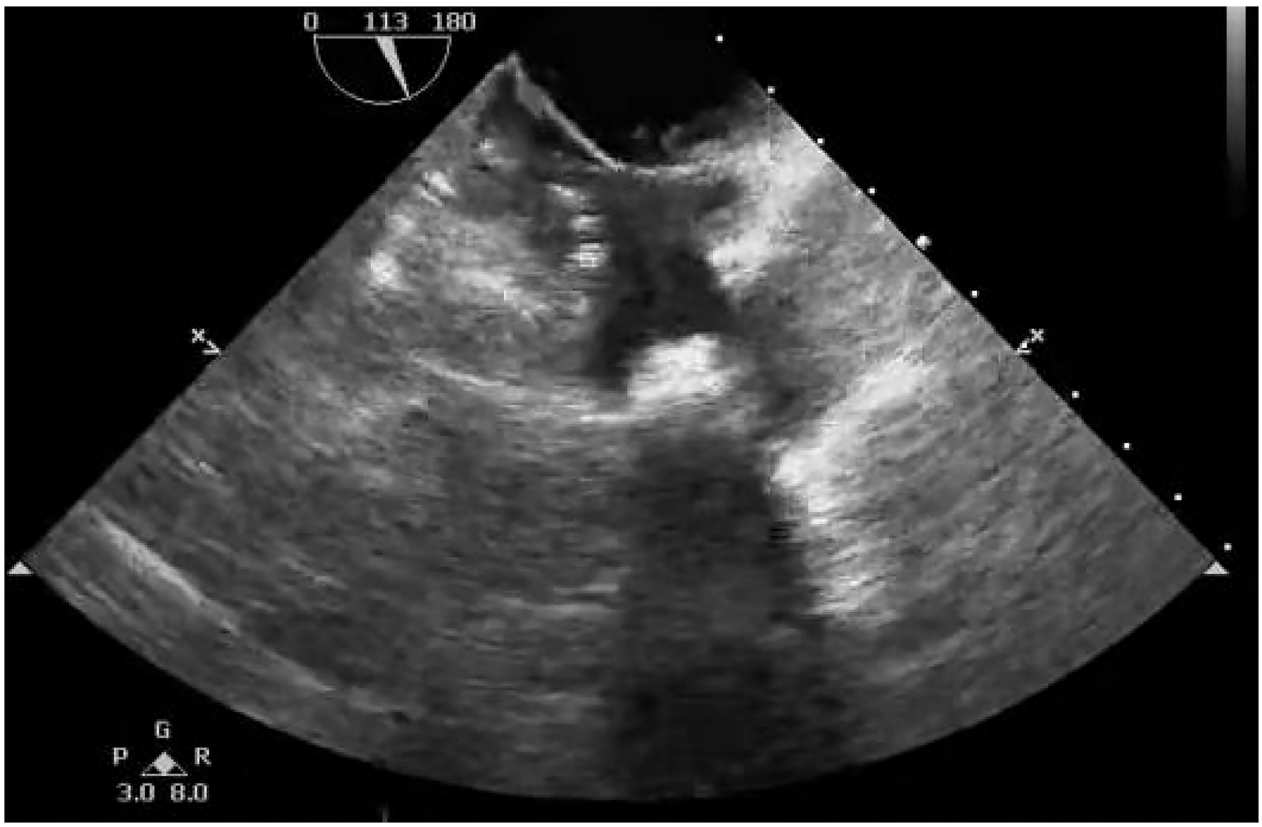

FIGURE 4 | Postoperative transthoracic echocardiography showing that no residual shunt through the atrial septum was detected.

were detected. The patient was eventually diagnosed with a late-onset residual shunt of transcatheter device occlusion of ASD (occluder recanalization).

Considering the multiple perforations of the occluder with an unusual irregular surface of the discs (**Figure 1B**), and after a careful discussion with the patient and her family, an open heart surgery was scheduled and performed. A standard median sternotomy incision was performed. The aorta was then cannulated, followed by separate cannulas placed in the superior vena cava and inferior vena cava. After full heparinization,

TABLE 1 | Summary of reported cases of polyvinyl alcohol membrane perforation of atrial septal occluders.

First author (year)	Patient age/sex	Device type	Device size	Occluder recanalization after procedure	Symptom	Management	References
Bozyel (2)	54/F	Cardia Ultrasept septal occluder	30 mm	2 years	No	Surgical device removal and Gore-Tex patch repair	(2)
Labombarda (3)	20/F	Ultrasept II ASD occluder device	20 mm	1 months	Recurrent dyspnea	Surgical device removal and Gore-Tex patch repair	(3)
Ramoglu (4)	4/M	Cardia Ultrasept II ASD occluder	20 mm	1 week	NA	Surgical device removal and Gore-Tex patch repair	(4)
Aubry et al. (7)	77/M	ASD Ultrasept II closure device	24 mm	4 months	No	Surgical device removal and Gore-Tex patch repair	(7)
Aubry et al. (7)	41/F	ASD Ultrasept II closure device	32 mm	3 months	No	Surgical device removal and Gore-Tex patch repair	(7)
Ten Freyhaus (8)	72/M	Atrial septal defect occluder system	NA	8 years	Worsening dyspnea on exertion	Surgical device removal and bovine pericardial patch repair	(8)
Chamie et al. (9)	28/F	Ultrasept^{TM} II CARDIA ASD occluder	20 mm	3 months	Easy tiredness and fatigue on exertion	Device-in-device technique	(9)
Chamie et al. (9)	33/F	Ultrasept^{TM} II CARDIA ASD occluder	16 mm	4 months	NA	Device-in-device technique	(9)
Chamie et al. (9)	49/F	Ultrasept^{TM} II CARDIA ASD occluder	16 mm	6 months	NA	Device-in-device technique	(9)
Chamie et al. (9)	17/F	Ultrasept^{TM} II CARDIA ASD occluder	14 mm	3 months	NA	Device-in-device technique	(9)
Bartel (29)	62/F	ATRIASEPT II device	24 mm	6 weeks	No	Surgical device removal and patch repair	(29)
Bartel (29)	42/F	ATRIASEPT II device	20 mm	5 weeks	No	Surgical device removal and patch repair	(29)
Kitamura (30)	20/M	Amplatzer septal occluder	NA	3 years	NA (infective endocarditis)	Surgical device removal and bovine pericardial patch repair	(30)
Weryński (31)	9/M	Cardia Ultrasept occluder	20 mm	4 years	NA	Surgical device removal and bovine pericardial patch repair	(31)
Weryński (31)	6/F	Cardia Ultrasept occluder	20 mm	3 years	NA	Surgical device removal and bovine pericardial patch repair	(31)
Aguiar Rosa (32)	39/F	Ultrasept ASD Occluder	22 mm	2 years	NA	Device-in-device technique	(32)
Bhattacharyya et al. (38)	69/M	Cardia Ultrasept septal occluder	28 mm	10 months	Several transient neurological events	Covering the damaged membrane with another occlusion device	(38)

NA, Note available; M, Male; F, Female.

cardiopulmonary bypass (CPB) was routinely applied. The aorta was cross-clamped, and a cold cardioplegic solution (Del Nido) was instilled *via* the aortic root to arrest the heart. After the right atrium was opened, the initialized tissue of the failed occluder was sufficiently freed, the occluder was then released and completely removed, and a bovine pericardial patch was used to reconstruct the atrial septum. During the operation, most parts of the closure were deformed (**Figure 2**), especially the left atrial side closed to the edge of the pulmonary vein, which resulted in the possible cause of late-onset residual shunt. The PVA membranes showed multiple perforations and were partly dissolved, the diameter of the largest void was around 10 mm, and the left atrial side of the occluder was damaged more obvious than the right (**Figure 2B**, arrow). No thrombus and other vegetations were seen. Furthermore, according to the pathology report (**Figure 3**), the surface of the occluder has not been fully epithelialized, instead, there was an extensive proliferation of fibrous collagenous tissue. This may have been due to the constant flow of blood. The implanted device did not show evidence of infection, and the bacterial cultures were negative. Finally, the patient recovered uneventfully without recurrent syncope and residual shunt (**Figure 4**).

DISCUSSION

Percutaneous closure of ASD has emerged as a feasible alternative to surgical repair due to its shorter recovery and less invasiveness in the late 1990s and has even become the treatment of choice in many heart centers worldwide (9, 10). It is well-known

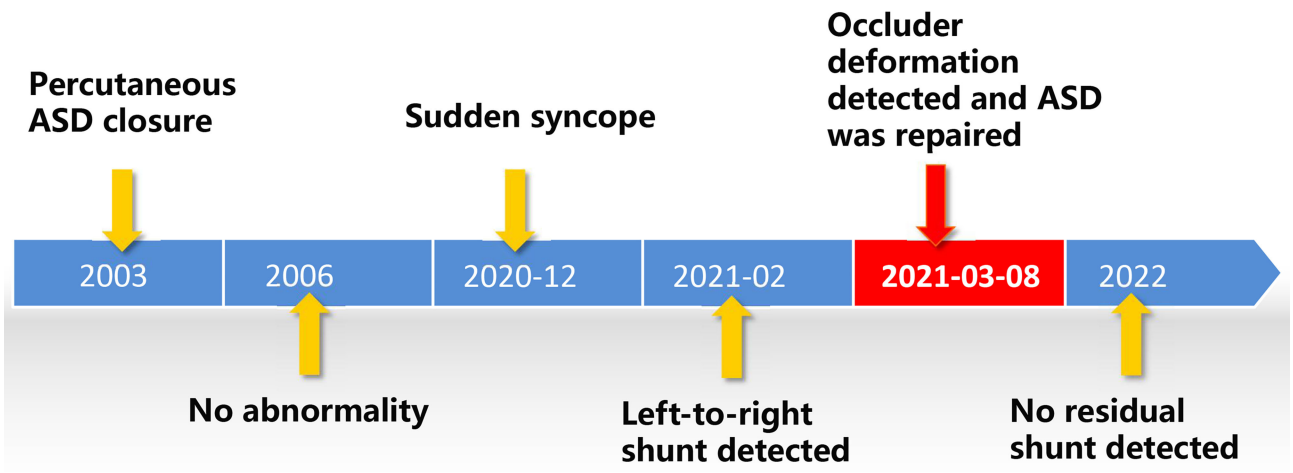

FIGURE 5 | A figure showcasing a timeline with relevant data from the presented case.

that percutaneous ASD closure also has potential short-term problems, such as occluder displacement and dislodgement (11, 12), residual shunt, arrhythmia (13), occluder device failure (14), occluder abrasion (15), bleeding or thromboembolism (16), air embolism (17), hemolysis (18), pericardial effusion or cardiac tamponade (15), mitral regurgitation (19), headache or migraine, etc. There are also some interventional complications, such as anesthesia accident, wound infection, arteriovenous fistula, and so on. With the development of medical equipment and technology, percutaneous ASD closure is known to have satisfactory short-term outcomes and complication rates. However, an important consideration for percutaneous ASD closure is the long-term and ultra-long-term complications that have emerged after its widespread adoption. Some of these, including cardiac erosion (15, 20–23), infective endocarditis (24, 25), and thromboembolism (26, 27), carry unignored morbidity and mortality (4, 28). We report a case of spontaneous perforation of the PVA membrane observed after 18 years in a patient treated with a 40-mm mushroom umbrella occlude (Huayi Shengjie Co., Ltd., Beijing, China). Similar cases have been previously reported in many versions of the PVA membrane-covered ASD occluder (29–31) (**Table 1**). However, to our knowledge, this is the first report about the PVA membrane perforation of occluder occurring at the latest time after ASD closure.

The PVA is a synthetic polymer widely used in medical devices due to its good biocompatibility, chemical resistance, low adsorption to proteins, non-toxicity, and adhesion (6, 9, 32). Although the application of this material in ASD occluders has been generally successful, some cases of spontaneous disintegration and perforation of the PVA membrane have been described (**Table 1**). Neither the previous surgeons nor the manufacturers could explain the mechanism of the PVA membrane disappearance. It may be due to the incomplete endothelialization of the occluder, poor occluder placement, long-term medications, underlying immunocompromise, syndromic comorbidities, or metabolic disorders (2, 28, 32). Undoubtedly, more detailed and comprehensive follow-up data were needed to answer that question. In our patient, there was no evidence of an early and mid-term residual shunt due to device failure, but we cannot speculate on the specific cause of long-term device perforation. Similar complications of occluder recanalization due to dissolution of the PVA membrane has previously been reported as early as 1 week and as late as 8 years after implantation (4, 8). We report a case of spontaneous perforation of the PVA membrane of the occluder 18 years after surgery, so there should be no direct relationship between this complication and the time of device implantation. In our case, we did not find any evidence of infection, long-term medications, or systemic disease, so it is speculated that this may be the cause of PVA membrane degradation of the occluder, external force damage, or long-term endothelialization insufficiency. Another possible reason may be that the size of the occluder was too large, which make the endothelial tissue unsuitable for migration, and the endothelialization coverage was poor. Although complete endothelialization of ASD devices was thought to occur 3–6 months after device implantation, late incomplete endothelialization has been described based on animal and human studies (33–36). It can be seen from the disassembled occluder that the left atrial side near the edge of the pulmonary veins was more seriously damaged than the right. In addition, mitral valve regurgitation and long-term pulmonary venous blood flow scouring lead to damage of the PVA membrane of the occluder, followed by chronic dissolution. After some adverse events, the manufacturer announced the development of a new device in hopes of ameliorating this complication by adding a Gore-Tex patch between two metal disc pieces (3). The new device was proved to be safe and feasible. This conclusion was drawn from a study of 30 Mexican patients after ASD closure without occluder recanalization due to the PVA membrane perforation at follow-up for 6 (range: 1–15) months (37). However, the conclusion was only based on early follow-up data.

The patient in the presentation first experienced syncope 18 years after ASD closure, but device perforation may have occurred months or years earlier. A timeline with relevant data from the presented case was shown in **Figure 5**. Patients with device failure were mostly asymptomatic but may also present with progressive dyspnea, fatigue, or stroke (3, 9, 38). It has been reported that occluder failure often induces some long-term complications after ASD closure, such as thrombosis on the surface of the occluder, thromboembolism, infective endocarditis, cardiac erosion, nickel hypersensitivity, and valve damage (8, 24, 25, 28). In most reported cases of occluder recanalization, surgical removal of the faulty device and repair with a patch were preferred (2). With the development of medical equipment and technology, covering the damaged membrane with a second device with intervention is considered a viable alternative to surgery when feasible in case of favorable anatomy (9, 32, 38). This should be done at a heart center with comprehensive imaging interventional equipment and experienced interventional cardiac surgeons.

CONCLUSION

In conclusion, for the first time, we report a rare case of severe left-to-right shunt due to spontaneous perforation of the PVA membrane of ASD occluder 18 years after ASD closure. The cause of the rare serious complication of occluder recanalization due to the PVA membrane perforation has not been clearly explained. Surgeons and manufacturers should be aware of this potential ultra-long-term complication that cannot be ignored, and they should conduct long-term systematic follow-up examinations for all patients implanted with occluder devices to reduce the potential losses of the patient while obtaining comprehensive clinical data to guide the optimization of devices and technologies.

DATA AVAILABILITY STATEMENT

The raw data supporting the conclusions of this article will be made available by the authors, without undue reservation.

ETHICS STATEMENT

The studies involving human participants were reviewed and approved by the Ethics Committee of the Second Xiangya Hospital of Central South University. The patients/participants provided their written informed consent to participate in this study.

AUTHOR CONTRIBUTIONS

KX drafted the manuscript. CF designed the study. HZ, QW, MT, CF, and JY revised the manuscript. KX, MT, and QW were responsible for the collection of data or analysis. All authors read and approved the final manuscript.

FUNDING

This work was supported by the Key Project of Science and Technology of Hunan Province (No. 2020SK53420 to JY).

REFERENCES

1. Feltes TF, Bacha E, Beekman RH, Cheatham JP, Feinstein JA, Gomes AS, et al. et al. Indications for cardiac catheterization and intervention in pediatric cardiac disease: a scientific statement from the American Heart Association. *Circulation*. (2011) 123:2607–52. doi: 10.1161/CIR.0b013e31821b1f10
2. Bozyel S, Sahin T, Dervis E, Aktas M, Saskin H, A. massive left-to-right shunt due to delayed spontaneous perforation of polyvinyl alcohol membrane of atrial septal occluder. *Turk Kardiyol Dern Ars*. (2017) 45:541–4. doi: 10.5543/tkda.2017.04640
3. Labombarda F, Roule V, Beygui F. Delayed spontaneous perforation of polyvinyl alcohol membrane-Covered atrial septal defect closure devices. *Catheter Cardiovasc Interv*. (2017) 89:E141–4. doi: 10.1002/ccd.26704
4. Ramoglu MG, Ucar T, Tutar E. Early malfunction of polyvinyl alcohol membrane of septal occluder. *Catheter Cardiovasc Interv*. (2016) 87:E151–153. doi: 10.1002/ccd.26057
5. King TD, Thompson SL, Steiner C, Mills NL. Secundum atrial septal defect. Nonoperative closure during cardiac catheterization. *JAMA*. (1976) 235:2506–9. doi: 10.1001/jama.1976.03260490024013
6. Alexandre N, Ribeiro J, Gartner A, Pereira T, Amorim I, Fragoso J, et al. Biocompatibility and hemocompatibility of polyvinyl alcohol hydrogel used for vascular grafting—In vitro and in vivo studies. *J Biomed Mater Res A*. (2014) 102:4262–75. doi: 10.1002/jbm.a.35098
7. Aubry P, Brochet E, du Fretay XH, Bouton-Brochet S, Ibrahim H, Arrault X, et al. Early malfunction of polyvinyl alcohol membrane-covered atrial septal defect closure devices. *Circ Cardiovasc Interv*. (2014) 7:721–2. doi: 10.1161/CIRCINTERVENTIONS.114.001429
8. Ten Freyhaus H, Rosenkranz S, Sudkamp M, Hopp HW. Dysfunction of an atrial septal defect occluder 8 years after implantation. *J Interv Cardiol*. (2006) 19:163–5. doi: 10.1111/j.1540-8183.2006.00124.x
9. Chamie F, Maia J, Giuliano LC. Device-in-device: A transcatheter alternative to surgical explantation of a failing atrial septal defect intracardiac prosthesis. *Catheter Cardiovasc Interv*. (2016) 88:239–43. doi: 10.1002/ccd.26456
10. Masura J, Gavora P, Formanek A, Hijazi ZM. Transcatheter closure of secundum atrial septal defects using the new self-centering amplatzer septal occluder: initial human experience. *Cathet Cardiovasc Diagn*. (1997) 42:388–93.
11. Boysan E, Cicek OF, Cicek MC, Hamurcu Z, Gurkahraman S. Surgical removal of an atrial septal occluder device embolized to the main pulmonary artery. *Tex Heart Inst J*. (2014) 41:91–3. doi: 10.14503/THIJ-12-3003
12. Truong QA, Gupta V, Bezerra HG, Okada DR, Rogers IS, Holmvang G, et al. Images in cardiovascular medicine. The traveling amplatzer: rare complication of percutaneous atrial septal occluder device embolism. *Circulation*. (2008) 118:e93–96. doi: 10.1161/CIRCULATIONAHA.108.765586
13. Agarwal S, Bajaj NS, Kumbhani DJ, Tuzcu EM, Kapadia SR. Meta-analysis of transcatheter closure versus medical therapy for patent foramen ovale in prevention of recurrent neurological events after presumed paradoxical embolism. *JACC Cardiovasc Interv*. (2012) 5:777–89. doi: 10.1016/j.jcin.2012.02.021
14. Qureshi AM, Mumtaz MA, Latson LA. Partial prolapse of a HELEX device associated with early frame fracture and mitral valve perforation. *Catheter Cardiovasc Interv*. (2009) 74:777–82. doi: 10.1002/ccd.22081
15. Divekar A, Gaamangwe T, Shaikh N, Raabe M, Ducas J. Cardiac perforation after device closure of atrial septal defects with the Amplatzer septal occluder. *J Am Coll Cardiol*. (2005) 45:1213–8. doi: 10.1016/j.jacc.2004.12.072

16. Abaci A, Unlu S, Alsancak Y, Kaya U, Sezenoz B. Short and long term complications of device closure of atrial septal defect and patent foramen ovale: meta-analysis of 28,142 patients from 203 studies. *Catheter Cardiovasc Interv.* (2013) 82:1123–38. doi: 10.1002/ccd.24875
17. Alkashkari W, Albugami S, Hijazi ZM. Current practice in atrial septal defect occlusion in children and adults. *Expert Rev Cardiovasc Ther.* (2020) 18:315–29. doi: 10.1080/14779072.2020.1767595
18. Yu M, Shan X, Bai Y, Qin Y, Zhao X. Percutaneous closure of a large atrial septal defect presenting with acute severe hemolysis. *Clin Res Cardiol.* (2019) 108:828–30. doi: 10.1007/s00392-019-01431-z
19. Dialetto G, Covino FE, Scognamiglio G, Della Corte A, Manduca S, Iacono C, Calabro R, Cotrufo M. A rare complication of atrial septal occluders: diagnosis by transthoracic echocardiography. *J Am Soc Echocardiogr.* (2006) 19:836 e835–838. doi: 10.1016/j.echo.2006.01.027
20. Maimon MS, Ratnapalan S, Do A, Kirsh JA, Wilson GJ, Benson LN. Cardiac perforation 6 weeks after percutaneous atrial septal defect repair using an Amplatzer septal occluder. *Pediatrics.* (2006) 118:e1572–75. doi: 10.1542/peds.2005-0825
21. Vitanova K, Cleuziou J, Vogt M, Nobauer C, Schreiber C, Lange R, et al. Delayed perforation of a transcatheter patent foramen ovale occluder 10 years after implantation. *Ann Thorac Surg.* (2015) 99:700–1. doi: 10.1016/j.athoracsur.2014.04.117
22. Mendirichaga R, Smairat RA, Sancassani R. Late tissue erosion after transcatheter closure of an atrial septal defect. *Catheter Cardiovasc Interv.* (2017) 89:502–4. doi: 10.1002/ccd.26277
23. Crawford GB, Brindis RG, Krucoff MW, Mansalis BP, Carroll JD. Percutaneous atrial septal occluder devices and cardiac erosion: a review of the literature. *Catheter Cardiovasc Interv.* (2012) 80:157–67. doi: 10.1002/ccd.24347
24. Amedro P, Soulatges C, Fraisse A. Infective endocarditis after device closure of atrial septal defects: case report and review of the literature. *Catheter Cardiovasc Interv.* (2017) 89:324–34. doi: 10.1002/ccd.26784
25. Nguyen AK, Palafox BA, Starr JP, Gates RN, Berdjis F. Endocarditis and incomplete endothelialization 12 years after amplatzer septal occluder deployment. *Tex Heart Inst J.* (2016) 43:227–31. doi: 10.14503/THIJ-14-4949
26. Fernando RR, Koranne KP, Barker CM, AMPLATZER. Septal Occluder failure resulting in paradoxical cerebral embolism. *Tex Heart Inst J.* (2012) 39:647–52.
27. Kalayci B, Kalayci S. Right atrial ball thrombus associated with atrial septal occluder device: A late complication of transcatheter atrial septal defect closure. *Anatol J Cardiol.* (2017) 18:E9. doi: 10.14744/AnatolJCardiol.2017.8012
28. Prabhu NK, Turek JW, Andersen ND. Commentary: Don't leave patients to their own devices: consider long-term complications after percutaneous atrial septal defect closure. *JTCVS Tech.* (2021) 7:242–3. doi: 10.1016/j.xjtc.2021.02.015
29. Bartel T, Bonaros N, Muller S. Device failure weeks to months after transcatheter closure of secundum type atrial septal defects. *Hearts.* (2010) 96:1603. doi: 10.1136/hrt.2009.185942
30. Kitamura H, Yamamoto M, Kagase A. Mobile vegetations on a poorly endothelialized atrial septal defect closure device. *JTCVS Tech.* (2021) 7:240–1. doi: 10.1016/j.xjtc.2021.01.010
31. Werynski P, Sabiniewicz R. Unexpected long-term complications of atrial septal defects closure. *Postepy Kardiol Interwencyjnej.* (2020) 16:514–5. doi: 10.5114/aic.2020.101782
32. Aguiar Rosa S, Ferreira F, de Sousa L, Fiarresga A, Martins JD, Galrinho A, et al. Successful percutaneous closure of a residual atrial septal defect due to device failure. *Rev Port Cardiol.* (2017) 36:475 e471–5 e473. doi: 10.1016/j.repc.2016.09.020
33. Lock JE, Rome JJ, Davis R, Van Praagh S, Perry SB, Van Praagh R, et al. Transcatheter closure of atrial septal defects. *Exp Stud Circ.* (1989) 79:1091–9. doi: 10.1161/01.CIR.79.5.1091
34. Chen F, Zhao X, Zheng X, Chen S, Xu R, Qin Y. Incomplete endothelialization and late dislocation after implantation of an Amplatzer septal occluder device. *Circulation.* (2011) 124:e188–9. doi: 10.1161/CIRCULATIONAHA.110.991836
35. Sigler M, Jux C, Ewert P. Histopathological workup of an Amplatzer atrial septal defect occluder after surgical removal. *Pediatr Cardiol.* (2006) 27:775–6. doi: 10.1007/s00246-006-1413-1
36. Sigler M, Kriebel T, Wilson N. Histological confirmation of complete endothelialisation of a surgically removed Amplatzer ASD occluder. *Heart.* (2006) 92:1723. doi: 10.1136/hrt.2006.091256
37. Mijangos-Vazquez R, Garcia-Montes AJ, Soto-Lopez EM, Guarner-Lans V, Zabal C. Atrial septal defect closure with the new Cardia Ultrasept II device with interposed Goretex patch: Mexican experience—has the perforation of Ivalon's membrane been solved? *Cardiol Young.* (2018) 28:709–14. doi: 10.1017/S1047951118000100
38. Bhattacharyya S, Ilsley CD, Baltabaeva A. Disintegration of polyvinyl alcohol membrane covering atrial septal defect closure device. *Eur Heart J Cardiovasc Imag.* (2015) 16:1153. doi: 10.1093/ehjci/jev163

Conflict of Interest: The authors declare that the research was conducted in the absence of any commercial or financial relationships that could be construed as a potential conflict of interest.

Publisher's Note: All claims expressed in this article are solely those of the authors and do not necessarily represent those of their affiliated organizations, or those of the publisher, the editors and the reviewers. Any product that may be evaluated in this article, or claim that may be made by its manufacturer, is not guaranteed or endorsed by the publisher.

frontiers | Frontiers in Cardiovascular Medicine

TYPE Case Report
PUBLISHED 16 August 2022
DOI 10.3389/fcvm.2022.950829

OPEN ACCESS

EDITED BY
Hendrik Tevaearai Stahel,
Bern University Hospital, Switzerland

REVIEWED BY
Hidetoshi Masumoto,
RIKEN Center for Biosystems Dynamics Research (BDR), Japan
Philippe Menasché,
Assistance Publique - Hôpitaux de Paris, France

*CORRESPONDENCE
Shigeru Miyagawa
miya-p@surg1.med.osaka-u.ac.jp

SPECIALTY SECTION
This article was submitted to Heart Surgery, a section of the journal Frontiers in Cardiovascular Medicine

RECEIVED 23 May 2022
ACCEPTED 02 August 2022
PUBLISHED 16 August 2022

CITATION
Miyagawa S, Kainuma S, Kawamura T, Suzuki K, Ito Y, Iseoka H, Ito E, Takeda M, Sasai M, Mochizuki-Oda N, Shimamoto T, Nitta Y, Dohi H, Watabe T, Sakata Y, Toda K and Sawa Y (2022) Case report: Transplantation of human induced pluripotent stem cell-derived cardiomyocyte patches for ischemic cardiomyopathy. *Front. Cardiovasc. Med.* 9:950829. doi: 10.3389/fcvm.2022.950829

Case report: Transplantation of human induced pluripotent stem cell-derived cardiomyocyte patches for ischemic cardiomyopathy

Shigeru Miyagawa[1]*, Satoshi Kainuma[1], Takuji Kawamura[1], Kota Suzuki[1], Yoshito Ito[1], Hiroko Iseoka[1], Emiko Ito[1], Maki Takeda[1], Masao Sasai[1], Noriko Mochizuki-Oda[1], Tomomi Shimamoto[1], Yukako Nitta[1], Hiromi Dohi[2], Tadashi Watabe[3], Yasushi Sakata[4], Koichi Toda[1] and Yoshiki Sawa[1]

[1]Department of Cardiovascular Surgery, Osaka University Graduate School of Medicine, Suita, Japan, [2]Center for iPS Cell Research and Application, Kyoto University, Kyoto, Japan, [3]Department of Nuclear Medicine and Tracer Kinetics, Osaka University Graduate School of Medicine, Suita, Japan, [4]Department of Cardiology, Osaka University Graduate School of Medicine, Suita, Japan

Despite major therapeutic advances, heart failure, as a non-communicable disease, remains a life-threatening disorder, with 26 million patients worldwide, causing more deaths than cancer. Therefore, novel strategies for the treatment of heart failure continue to be an important clinical need. Based on preclinical studies, allogenic human induced pluripotent stem cell-derived cardiomyocyte (hiPSC-CM) patches have been proposed as a potential therapeutic candidate for heart failure. We report the implantation of allogeneic hiPSC-CM patches in a patient with ischemic cardiomyopathy (ClinicalTrials.gov, #jRCT2053190081). The patches were produced under clinical-grade conditions and displayed cardiogenic phenotypes and safety *in vivo* (severe immunodeficient mice) without any genetic mutations in cancer-related genes. The patches were then implanted via thoracotomy into the left ventricle epicardium of the patient under immunosuppressive agents. Positron emission tomography and computed tomography confirmed the potential efficacy and did not detect tumorigenesis in either the heart or other organs. The clinical symptoms improved 6 months after surgery, without any major adverse events, suggesting that the patches were well-tolerated. Furthermore, changes in the wall motion in the transplanted site were recovered, suggesting a favorable prognosis and the potential tolerance to exercise. This study is the first report of a successful transplant of hiPSC-CMs for severe ischemic cardiomyopathy.

KEYWORDS

human induced pluripotent stem cell-derived cardiomyocyte, ischemic cardiomyopathy, transplantation, regenerative therapy, clinical trial

Introduction

Severe heart failure is a lethal disease with high mortality, and patients' quality of life is significantly reduced despite the development of medical treatments (1). When severe heart failure is reversible, drug treatment is prioritized; however, at the irreversible stage, a left ventricular assist device (LVAD) or heart transplantation is considered to be the first-line therapy. Heart transplantation is an extremely effective treatment for heart failure that can prolong life expectancy. However, a shortage of donors worldwide is a major drawback, and securing donors is expected to be increasingly challenging in the future (2). For LVAD, destination therapy or bridge-to-transplant is performed; however, complications such as infections and cerebral thrombosis are major problems (3). Therefore, there is a need for the development of new treatments that can replace artificial hearts and heart transplants for irreversible stages of heart failure and therapies that prevent the progression of heart failure toward the irreversible stage. Considering these challenges, the expectations for regenerative medicine are increasing.

In recent years, although cytokine-based angiogenesis treatment using somatic stem cells for heart failure has been performed, it is considered that angiogenesis-induced activation in the hibernating myocardium does not provide sufficient clinical effects in cases of severe cardiomyopathy wherein a large number of functional cardiomyocytes have been lost. In such cases, it is necessary to generate cardiomyocytes externally, transplant them into the failing heart, and electrically and functionally integrate them with the recipient heart.

The generation of a large number of new cardiomyocytes, followed by their integration within recipient hearts, is a promising treatment for severely damaged myocardia with few cardiomyocytes. Recently, induced pluripotent stem cells (iPSCs) have been developed from human somatic cells. iPSCs have the property of being able to differentiate into cells of all body organs and are expected to be a source of cell therapy for various diseases (4, 5). Basic research studies have demonstrated that iPSCs can differentiate into cardiomyocytes as single cells or myocardial tissues (6–10). These iPSC-derived cardiomyocytes beat spontaneously and produce and release cytokines that induce angiogenesis. Thus, it is conceivable that iPSCs may be used to achieve cardiomyogenesis to form cardiomyocytes that can mechanically contract and repair myocardial tissue via paracrine angiogenic factors.

Here, we report the case of a 51-year-old male patient with ischemic cardiomyopathy who had already received maximum anti-heart failure medications such as digitalis, diuretics, angiotensin-converting-enzyme (ACE) inhibitors, angiotensin receptor blockers, beta-blockers, anti-aldosterone drugs, and oral cardiotonic. He was successfully treated with clinical-grade human induced pluripotent stem cell-derived cardiomyocyte (hiPSC-CM) patches with typical cardiogenic phenotypic properties in a first-in-human clinical trial.

Case description

A 51-year-old male patient was repeatedly admitted to the hospital owing to severe heart failure due to ischemic cardiomyopathy (Figure 1A). In 2019, he suffered an acute myocardial infarction and was treated via percutaneous coronary intervention (PCI) targeting the three major coronary arteries. Six months after treatment, he complained of chest pain. A second acute myocardial infarction episode was diagnosed; PCI was introduced via intra-aortic balloon pumping (IABP), and percutaneous cardiopulmonary support was administered due to ventricular fibrillation. However, his condition worsened, and catecholamine and Impella® were then used as therapeutic agents. Although catecholamine treatment and circulatory support could eventually be withdrawn on day 21 after the second attack (Figure 1A), the heart failure persisted (New York Heart Association [NYHA] classification = III). Ultrasonography revealed severe asynergy throughout the wall of the left ventricle (LV) (ejection fraction [EF] = 30%). Positron emission tomography (PET) further revealed ischemia in the middle-apex (anterior wall) and the base-apex (posterior-lateral wall); an infarcted area in the inferior wall was observed despite the absence of significant stenosis in all coronary arteries. The patient was then treated with anti-heart failure medications (maximum dosages), such as beta-blockers, ACE inhibitors, and diuretics. Finally, hiPSC-CM transplantation was considered a therapeutic option.

The regenerative treatment protocol (Japan Registry of Clinical Trials, https://jrct.niph.go.jp/en-latest-detail/jRCT2053190081, Figure 1B) using allogeneic iPSC-CM patches was approved by the institutional review boards of Osaka University (#199006-A) and the Ministry of Health, Labor, and Welfare, Japan (#2019-143). The transplantation procedure was performed after obtaining written informed

Abbreviations: 4DCT, four-dimensional computed tomography; CGH, comparative genomic hybridization; CiRA, Center for iPS Cell Research and Application, Kyoto University; CNV, copy number variation; Cx, circumflex coronary artery; cTNT, cardiac Troponin T; ESS, end-systolic wall stress; FDG-PET, fluorodeoxyglucose-positron emission tomography; H&E, hematoxylin and eosin; hiPSC-CM, human induced pluripotent stem cell-derived cardiomyocyte; IABP, intra-aortic balloon pumping; LAD, left anterior descending coronary artery; LV, left ventricle; LVESVI, left ventricle end-systolic volume index; MBF, myocardial blood flow; MCB, master cell bank; NOG, NOD/Shi-scid, IL-2R γnull; NYHA, New York Heart Association classification; PCI, percutaneous coronary intervention; peak VO_2, peak oxygen uptake; PET, positron emission tomography; RCA, right coronary artery.

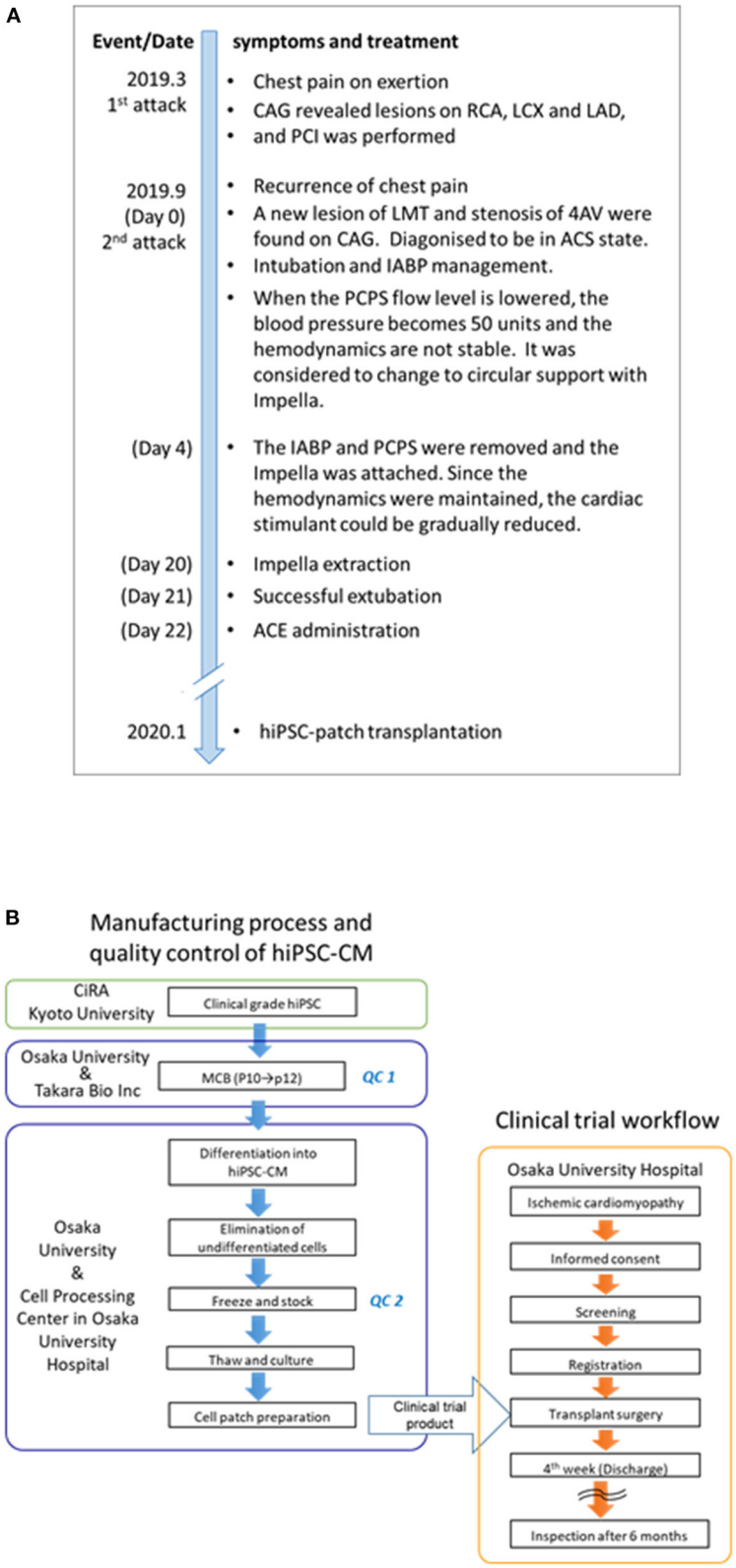

FIGURE 1
Timeline of symptoms and treatment and the clinical trial flowchart of the human induced pluripotent stem (iPS) cell-derived cardiomyocyte (hiPSC-CM) patches. **(A)** The date in parentheses indicates the number of days since the first attack. The patient underwent anti-heart failure medications (maximum dosages), such as beta-blockers, ACE inhibitors, and diuretics, before transplantation. In the first 3 months after

(Continued)

FIGURE 1
transplantation, the patient received immunosuppressant drugs, including steroids, tacrolimus hydrate, and mycophenolic acid (mofetil); thereafter, these drugs were discontinued. Notably, no medications were introduced/stopped post transplantation. **(B)** The clinical trial flowchart of hiPSC-CM patches. Clinical-grade iPS cells were established and procured from CiRA (Kyoto University). The hiPSC-CM patches were manufactured in the cell processing center in Osaka University Hospital using the MCB cells generated in the Center for Gene and Cell Processing of Takara Bio Inc. (Kusatsu, Japan). The following quality inspections were performed during the manufacturing process: QC1: Quality check of the MCB (7). The detailed procedure of the generation of MCB is described elsewhere (7). QC2: viability, purity of cardiomyocytes, sterility, mycoplasma testing, and endotoxin testing (Supplementary Table 1). CAG, coronary angiography; RCA, right coronary artery; LCX, left circumflex coronary artery branch; LAD, left anterior descending coronary artery; PCI, percutaneous coronary intervention; LMT, left main coronary trunk; AV, atrioventricular node branch; ACS, acute coronary syndrome; IABP, intra-aortic balloon pumping; PCPS, percutaneous cardiopulmonary support; and ACE, angiotensin-converting enzyme; iPS, induced pluripotent stem; hiPSC-CM, human induced pluripotent stem cell-derived cardiomyocyte; MCB, master cell bank.

consent from the patient and his family. The study was conducted in accordance with the principles of the Declaration of Helsinki.

Properties of hiPSC-CM patches used for transplantation

The methods for hiPSC culture, cardiomyogenic differentiation, purification, and cell patch preparation as well as details regarding the *in vivo* tumorigenicity assay are described in the Supplementary Methods. The detailed characterization of the hiPSCs and the master cell bank (MCB) are presented elsewhere (7) and in the Supplementary Data (Supplementary Figure 1 and Supplementary Table 1), respectively. The hiPSC-CM patch used in this clinical trial was prepared by a method that cleared the tumorigenicity denial test earlier (7). The hiPSC-CM cells used passed all quality inspections, as shown in Supplementary Table 1.

Measurement of cardiac function

Regional myocardial displacement was assessed using four-dimensional computed tomography (4DCT), as described in the Supplementary Methods. The methods for evaluating end-systolic wall stress (ESS), tumor formation, and myocardial blood flow (MBF), including the acquisition of PET/computed tomography (CT) imaging, are also described in Supplementary Methods.

Clinical trial

We prepared three allogeneic iPSC-CM patches (3.3×10^7 cells/patch) that were successfully transplanted into the epicardium of the LV anterior and lateral walls (Figure 2A) through the fourth intercostal space under IABP support; no other surgical procedures, including coronary artery bypass grafting, were performed. The IABP support was withdrawn the day after surgery, and the catecholamine infusion was discontinued 8 days post transplantation. During the first 3 months after transplantation, the patient received immunosuppressant drugs, including prednisolone, tacrolimus, and mycophenolate mofetil; thereafter, these drugs were discontinued (Supplementary Figure 2). The patient underwent standard rehabilitation after surgery. Arrhythmia was constantly monitored with a 24-h electrocardiogram (ECG) monitor, and Holter ECG was also measured at the required timing to check for arrhythmias. The cardiac function and myocardial blood perfusion were measured using cardiac CT, wall stress measurements, and MBF PET. Tumorigenesis (safety) was investigated via fluorodeoxyglucose-PET (FDG-PET).

The patient was extubated the day after surgery, stayed in the ICU for 3 days, including the day of surgery, and was discharged 1 month after surgery. He underwent standard rehabilitation after surgery.

We did not detect any complications, including arrhythmias, tumor formation, or immunosuppression-related severe adverse events. Importantly, the patients' symptoms improved from NYHA III to II at 6 months and 1 year after transplantation (Supplementary Table 2). Enhanced CT demonstrated that the LV end-systolic volume index (LVESVI) increased after transplantation (Supplementary Table 2) but was substantially decreased 1 year after transplantation. Peak VO2 improved at 6 months and 1 year after transplantation without cardiac rehabilitation (Supplementary Table 2).

Myocardial displacement was determined based on the regional myocardial wall motion in each region using a dedicated workstation comprising 320 cardiac CT images. This analysis revealed that the moving distance, especially in the transplantation area, improved significantly at 6 months and 1 year after transplantation (Figure 2B and Supplemental Movies), indicating that the myocardium under the transplanted sheets greatly benefited from the angiogenesis mediated by cytokine-paracrine effects. The LV global wall stress, especially that in the LV anterior and lateral walls that received the allogeneic iPSC-CM patches, was reduced after surgery (Figure 3), suggesting the possible attenuation of cardiac fibrosis and the prolongation of survival.

According to the ^{13}N-ammonia PET images (Figure 4A), the MBF at rest was left anterior descending (LAD) 0.85, circumflex

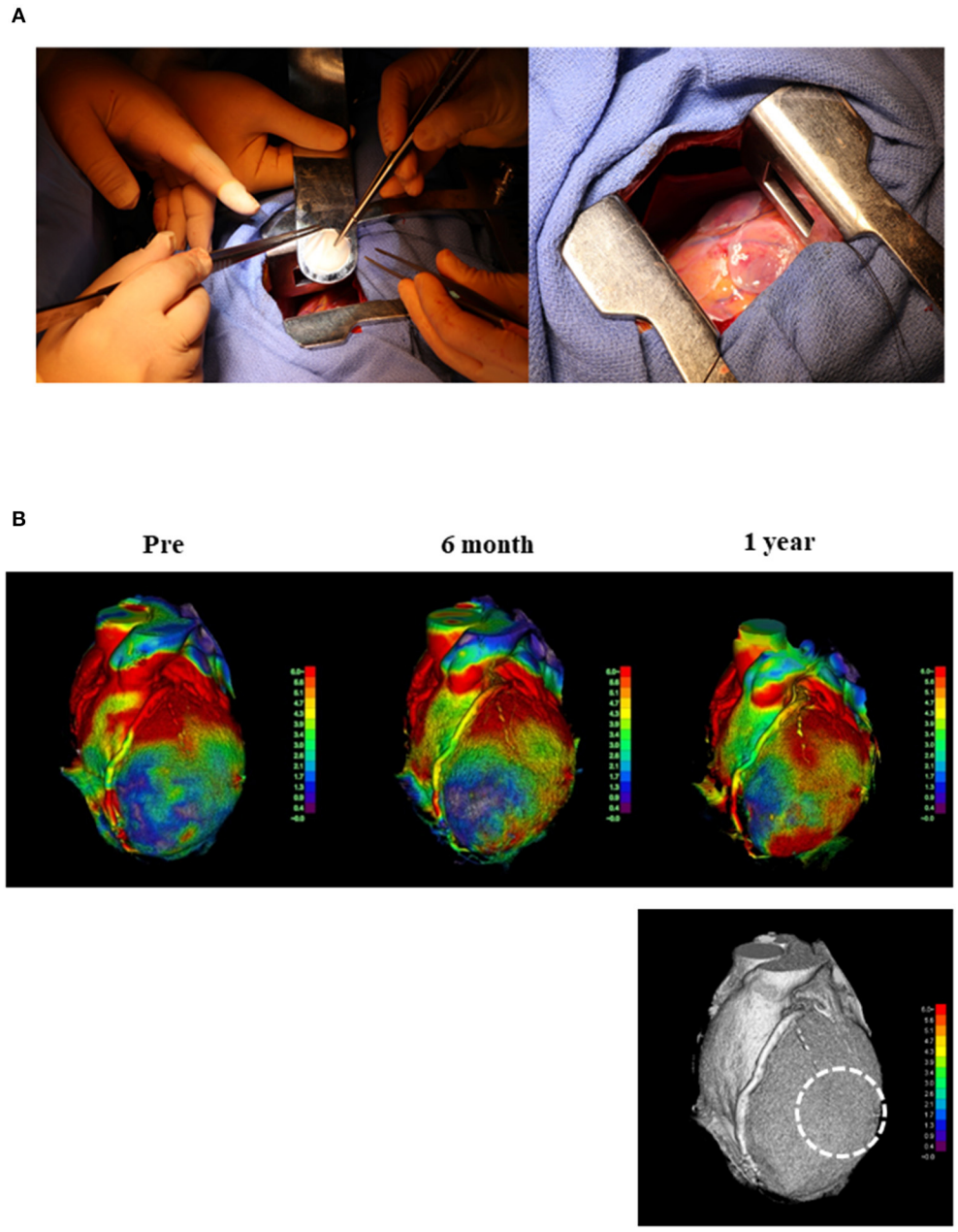

FIGURE 2
Transplantation of hiPSC-CM and cardiac moving pattern before and after surgery. **(A)** First transplantation of hiPSC-CM patches onto the heart surface of a patient with severe cardiomyopathy. Left: hiPSC-CM patch was transplanted into the epicardium of the anterior and lateral walls of the LV through the fourth intercostal space under IABP support. Right: Three patches were transplanted into the epicardium of the LV anterior and lateral walls. **(B)** The moving pattern observed via four-dimensional CT. Colors were set so that red indicated a good dynamic area; the darker the color, the lower the movement. The images show the moving pattern in chronological order of the heart at pre-implantation (pre), 6 months, and 1 year after implantation. The dotted line in the bottom figure shows the area where the patches were attached. hiPSC-CM, human induced pluripotent stem cell-derived cardiomyocyte; LV, left ventricle; IABP, intra-aortic balloon pumping; CT, computed tomography.

coronary artery (Cx) 0.69, and right coronary artery (RCA) 0.66 ml/g/min at 6 months after transplantation (Figure 4B). However, 1 year after transplantation, the MBF at rest showed a slight decline (LAD 0.65; Cx 0.54; RCA 0.50 ml/g/min) (Figure 4B). The MBF under stress was LAD 1.80, Cx 1.58, and RCA 1.49 ml/g/min at 6 months after transplantation but improved 1 year after transplantation (LAD 3.19; Cx 2.93; RCA 3.17 ml/g/min) (Figure 4B). Moreover, from 6 months

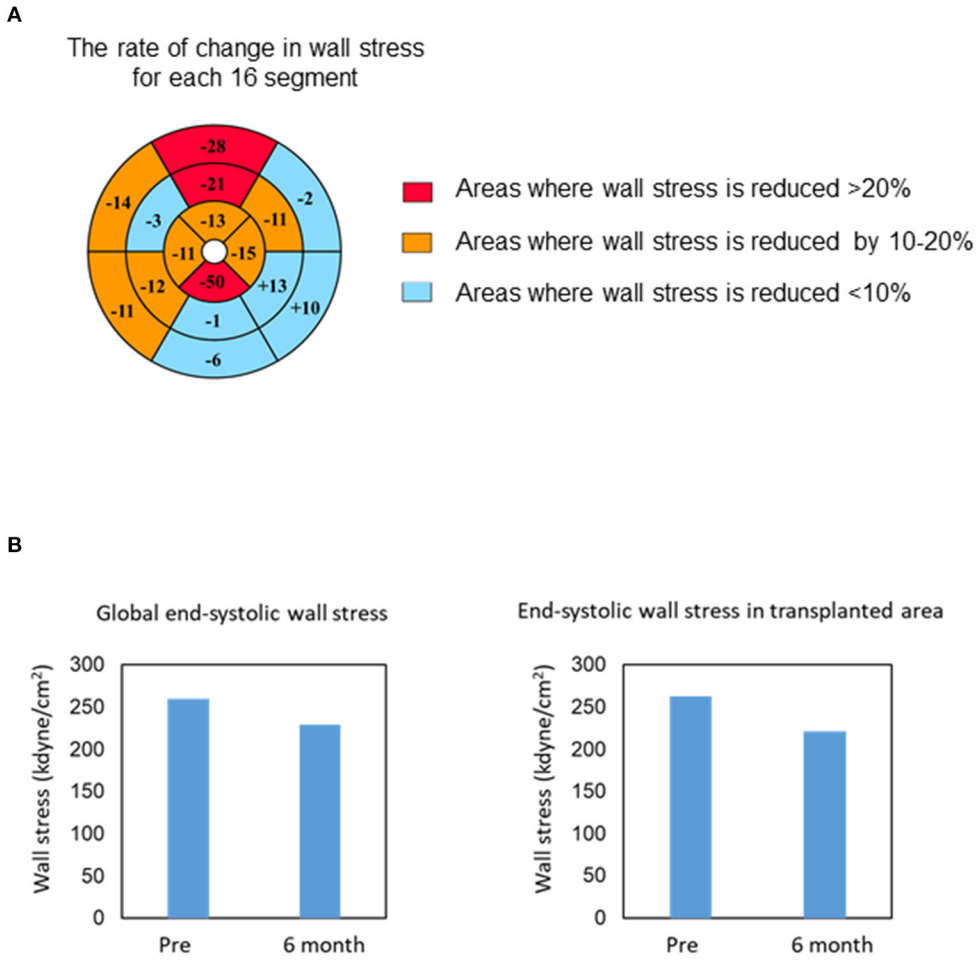

FIGURE 3
Changes in end-systolic wall stress. **(A)** Bull's-eye grid showing the changes in end-systolic wall stress before and 6 months after surgery, calculated by computed tomography. Red and orange highlight the areas of reduction in wall stress by over 20 and 10–20%, respectively. Light blue highlights the remaining areas. **(B)** Change in the global (left) and regional (transplanted area, right) end-systolic wall stress 6 months after transplantation.

to 1 year after transplantation, the coronary flow reserves in the whole myocardium greatly improved from 2.16 to 5.30, and the coronary flow reserves in all segmental regions of LV were also dramatically ameliorated (6 months vs. 1 year: LAD 2.12 vs. 4.90; Cx 2.27 vs. 5.40; RCA 2.21 vs. 6.47) (Figure 4C). Furthermore, changes in LV wall motion in the transplanted site were quite dramatic comparing the values at rest with those under stress conditions (Supplemental Movies), and the coronary flow reserve values were similar to those in healthy individuals. Overall, this result suggests a favorable prognosis and the potential tolerance to exercise. Notably, no medications were introduced or stopped post transplantation. Consistent with the potential tumorigenic safety reported in the preclinical study, the FDG-PET analysis revealed no tumorigenesis after transplantation (Supplementary Figure 3).

Discussion

Here, we report the first-in-human trial of clinical-grade hiPSC-CM patches to treat ischemic cardiomyopathy in a patient and describe its potential efficacy and safety. Shiba et al. (11) reported that arrhythmias markedly increased in the early phase after transplantation of hiPSC-CMs using a needle. By contrast, we did not detect lethal arrhythmias or tumorigenesis after transplantation in the clinical case. Moreover, our preclinical data (7) also revealed that the clinical-grade hiPSC-CM patches are non-tumorigenic and non-arrhythmogenic and might be a safe methodology to deliver cardiac cells. Therefore, we assume that the reported arrhythmias did not occur due to transplantation of cardiomyocytes, but rather due to the cell introduction method, particularly due to the needle injection;

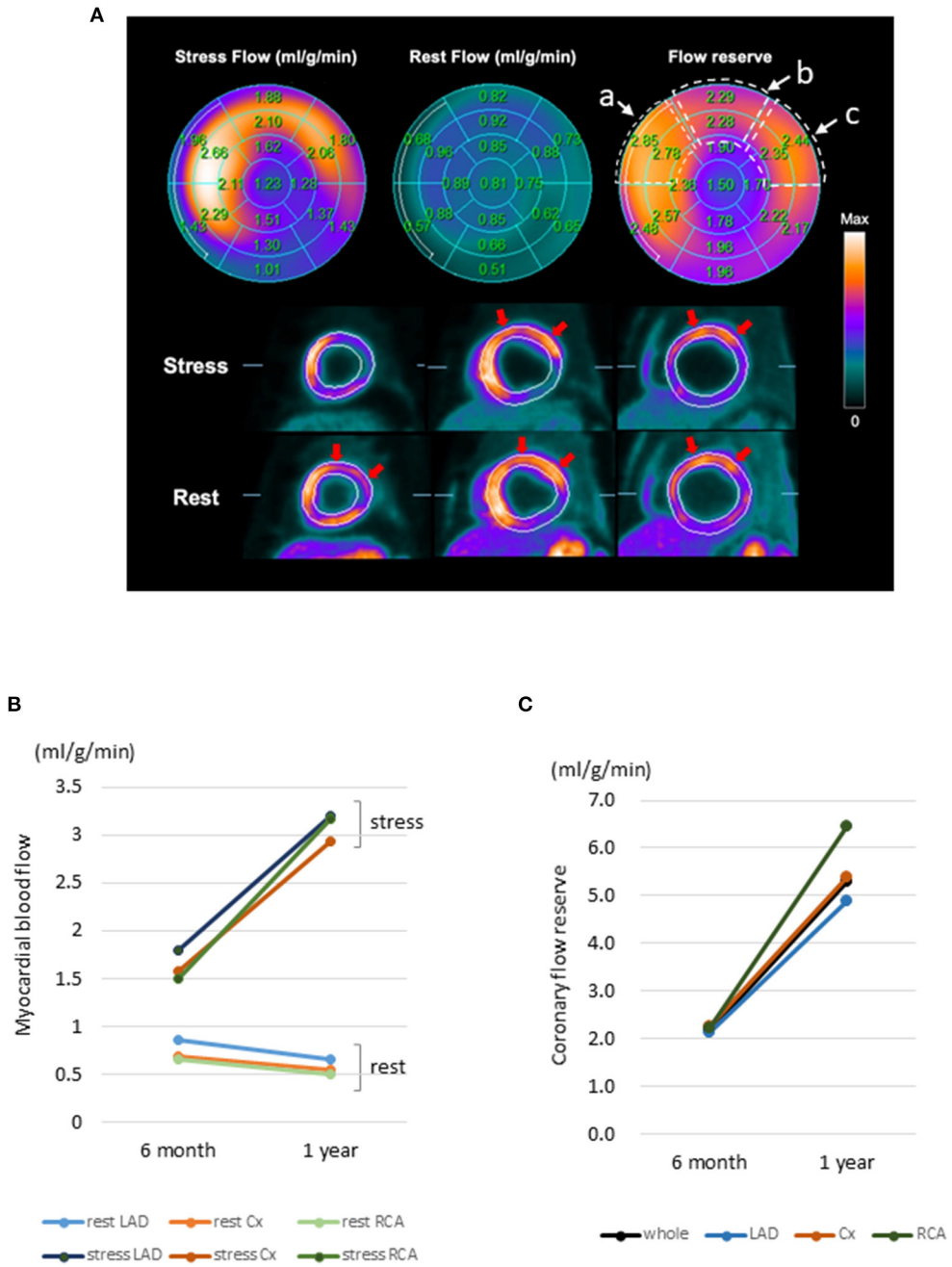

FIGURE 4
^{13}N-ammonia PET images of myocardial blood flow at rest and during stress after hiPSC-CM sheet implantation. **(A)** Color-coded polar maps with superimposed 17-segment bull's-eye grids with blood flow quantitated under stress and at rest, as well as flow reserve values, are shown in each segment (upper figures). Myocardial blood flow images (short axis) are shown in the lower figures. Red arrows indicate preserved myocardial flow reserves in the anteroseptal to lateral segments. The areas surrounded by the dotted line in the flow reserve figure show a: anteroseptal, b: anterior, and c: anterolateral regions, and the average values of the two area parts were calculated. **(B)** Change in myocardial blood flow. Myocardial blood flow in the segmental regions LAD, Cx, and RCA at rest and under stress. **(C)** Change in myocardial flow reserve. Myocardial flow reserve in the whole and each segmental region at 6 months and 1 year after hiPSC-CM patch transplantation. ^{13}N-ammonia PET, ^{13}N-ammonia positron emission tomography; hiPSC-CM, human induced pluripotent stem cell-derived cardiomyocyte; LAD, left anterior descending coronary artery; Cx, circumflex coronary artery; RCA, Right coronary artery.

nonetheless, further clinical evaluations are needed for safety assurance (11, 12).

The major question in the context of hiPSC-CM patches is whether the transplanted cardiac tissues may be electrically integrated within the recipient's heart, i.e., whether they can undergo "cardiomyogenesis" in a damaged heart with few functional cardiomyocytes. Transplanted cardiomyocyte patches can reportedly undergo contraction/relaxation (13) or repeated electrical potential activation (14) in the recipient heart in a synchronous fashion. The cardiogenic properties (both histological and functional) of cardiomyocyte patches were also demonstrated in our preclinical study (7) (Supplementary Figure 1). Importantly, in the preclinical study, we observed that the transplanted cardiac tissues facilitated functional recovery; however, the extent of the mechanical contribution of the transplanted cardiomyocytes to the contractile force of the diseased heart needs further investigation.

The functional recovery may also depend on angiogenesis, which positively impacts the hibernating myocardium (15, 16). In particular, the generation of new functional blood vessels, as we detected in the preclinical experiments (7), may be sufficient to allow effective perfusion of blood to hibernating myocytes and improve the coronary flow reserve in damaged hearts. Based on the *in vitro* cytokine expression profile, the angiopoietin family may have a role in the maturation of blood vessels (7). The decrease in the resistance of the peripheral coronary arteries (7) may contribute to the improvement of the global coronary flow reserve in the ischemic myocardial tissue and may lead to tolerance to exercise.

In this study, PET detected improved LV wall motion upon transplantation of the patches, especially under stress, accompanied with ameliorated coronary flow reserve, suggesting a potential improvement in exercise tolerance. Furthermore, our PET study revealed that MBF at rest gradually decreased, suggesting that the myocardium could function under low blood flow at rest. The damaged myocardium showed time-dependent recovery after transplantation.

In this clinical trial, we suspended the administration of immunosuppressant drugs 3 months after transplantation. Notably, we could not clearly elucidate whether transplanted patches survived in the human heart. However, we speculate that the changes in cardiac function, as well as the preserved coronary flow reserve, were mainly dependent on the angiogenic action, which was sufficient to achieve the clinical needs in the treatment of severe heart failure. Further research is warranted to increase the effectiveness of hiPSC transplantation therapy. For instance, a method of monitoring cell survival after transplantation, a detailed analysis of the immune response and immune control mechanism to establish a more appropriate immunosuppressive agent administration routine, and attempts to co-transplant hiPSCs with other types of cells (17) or tissues (18) to enhance cardiomyogenesis should be considered.

Data availability statement

The original contributions presented in the study are included in the article/Supplementary material. Further inquiries can be directed to the corresponding author.

Ethics statement

The studies involving human participants were reviewed and approved by the Institutional Review Boards of Osaka University (#199006-A) and the Ministry of Health, Labor, and Welfare, Japan (#2019-143). The patients/participants provided their written informed consent to participate in this study.

Author contributions

SM: project planning, experimental design, clinical studies, data analysis, and manuscript writing. SK, TK, YSak, and KT: conducting clinical studies. KS, YI, and TW: clinical data collection and analysis. HI, EI, and MT: preparation and quality control of clinical trial products. MS: coordinating the clinical trial. NM-O: editing of manuscript drafts. TS and YN: coordinating clinical trials. HD: providing clinical-grade cells. YSaw: design and supervision of the entire project. All authors contributed to the article and approved the submitted version.

Funding

This study was funded by Japan Agency for Medical Research and Development (AMED) under the Grant Numbers JP20bm0204003, JP17bk0104044, JP19bk0104002, and JP20bk0104110.

Acknowledgments

We thank the staff of the Department of Cardiovascular Surgery and the Department of Frontier Regenerative Medicine for manufacturing clinical trial products. We also thank the clinical staff in our institution for patient care and data collection.

Conflict of interest

The authors declare that the research was conducted in the absence of any commercial or financial relationships that could be construed as a potential conflict of interest.

Publisher's note

Supplementary material

The Supplementary Material for this article can be found online at: https://www.frontiersin.org/articles/10.3389/fcvm.2022.950829/full#supplementary-material

SUPPLEMENTARY FIGURE 1
Characteristic properties of hiPSC-CM patch.

SUPPLEMENTARY FIGURE 2
Dose of immunosuppressants, the trough value of tacrolimus, and biomarker levels of renal and liver function.

SUPPLEMENTARY FIGURE 3
FDG-PET imaging at 6 months after transplantation of hiPSC-CM patch.

SUPPLEMENTARY TABLE 1
Quality test of hiPSC-CMs.

SUPPLEMENTARY TABLE 2
Changes in cardiac function, exercise tolerance, and heart failure classification after transplant surgery.

SUPPLEMENTARY VIDEO 1
4DCT movie at 6 months after transplantation.

SUPPLEMENTARY VIDEO 2
4DCT movie at 1 year after transplantation.

References

1. Cohn JN. Continue what we are doing to treat HF, but do it better. *Nat Rev Cardiol.* (2014) 11:69–70. doi: 10.1038/nrcardio.2013.212

2. Longnus SL, Mathys V, Dornbierer M, Dick F, Carrel TP, Tevaearai HT. Heart transplantation with donation after circulatory determination of death. *Nat Rev Cardiol.* (2014) 11:354–63. doi: 10.1038/nrcardio.2014.45

3. Abraham WT, Smith SA. Devices in the management of advanced, chronic heart failure. *Nat Rev Cardiol.* (2013) 10:98–110. doi: 10.1038/nrcardio.2012.178

4. Takahashi K, Yamanaka S. Induction of pluripotent stem cells from mouse embryonic and adult fibroblast cultures by defined factors. *Cell.* (2006) 126:663–76. doi: 10.1016/j.cell.2006.07.024

5. Takahashi K, Tanabe K, Ohnuki M, Narita M, Ichisaka T, Tomoda K, et al. Induction of pluripotent stem cells from adult human fibroblasts by defined factors. *Cell.* (2007) 131:861–72. doi: 10.1016/j.cell.2007.11.019

6. Kawamura M, Miyagawa S, Miki K, Saito A, Fukushima S, Higuchi T, et al. Feasibility, safety, and therapeutic efficacy of human induced pluripotent stem cell-derived cardiomyocyte sheets in a porcine ischemic cardiomyopathy model. *Circulation.* (2012) 126:S29–37. doi: 10.1161/CIRCULATIONAHA.111.084343

7. Miyagawa S, Kawamura T, Ito E, Takeda M, Iseoka H, Yokoyama J, et al. Evaluation of the efficacy and safety of a clinical grade human induced pluripotent stem cell-derived cardiomyocyte patch: a pre-clinical study. *bioRxiv [Preprint].* (2021). doi: 10.1101/2021.04.07.438744

8. Nakagawa M, Taniguchi Y, Senda S, Takizawa N, Ichisaka T, Asano K, et al. A novel efficient feeder-free culture system for the derivation of human induced pluripotent stem cells. *Sci Rep.* (2014) 4:3594. doi: 10.1038/srep03594

9. Ito E, Miyagawa S, Yoshida Y, Sawa Y. Efficient method to dissociate induced pluripotent stem cell-derived cardiomyocyte aggregates into single cells. *Methods Mol Biol.* (2021) 2320:29–33. doi: 10.1007/978-1-0716-1484-6_4

10. Ito E, Miyagawa S, Takeda M, Kawamura A, Harada A, Iseoka H, et al. Tumorigenicity assay essential for facilitating safety studies of hiPSC-derived cardiomyocytes for clinical application. *Sci Rep.* (2019) 9:1881. doi: 10.1038/s41598-018-38325-5

11. Shiba Y, Gomibuchi T, Seto T, Wada Y, Ichimura H, Tanaka Y, et al. Allogeneic transplantation of iPS cell-derived cardiomyocytes regenerates primate hearts. *Nature.* (2016) 538:388–91. doi: 10.1038/nature19815

12. Patila T, Miyagawa S, Imanishi Y, Fukushima S, Siltanen A, Mervaala E, et al. Comparison of arrhythmogenicity and proinflammatory activity induced by intramyocardial or epicardial myoblast sheet delivery in a rat model of ischemic heart failure. *PLoS ONE.* (2015) 10:e0123963. doi: 10.1371/journal.pone.0123963

13. Higuchi T, Miyagawa S, Pearson JT, Fukushima S, Saito A, Tsuchimochi H, et al. Functional and electrical integration of induced pluripotent stem cell-derived cardiomyocytes in a myocardial infarction rat heart. *Cell Transplant.* (2015) 24:2479–89. doi: 10.3727/096368914X685799

14. Iseoka H, Miyagawa S, Fukushima S, Saito A, Masuda S, Yajima S, et al. Pivotal role of non-cardiomyocytes in electromechanical and therapeutic potential of induced pluripotent stem cell-derived engineered cardiac tissue. *Tissue Eng Part A.* (2018) 24:287–300. doi: 10.1089/ten.tea.2016.0535

15. Bolli R, Marbán E. Molecular and cellular mechanisms of myocardial stunning. *Physiol Rev.* (1999) 79:609–34. doi: 10.1152/physrev.1999.79.2.609

16. Fallavollita JA, Perry BJ, Canty JM Jr. ^{18}F-2-deoxyglucose deposition and regional flow in pigs with chronically dysfunctional myocardium. Evidence for transmural variations in chronic hibernating myocardium. *Circulation.* (1997) 95:1900–9. doi: 10.1161/01.CIR.95.7.1900

17. Yoshida S, Miyagawa S, Toyofuku T, Fukushima S, Kawamura T, Kawamura A, et al. Syngeneic mesenchymal stem cells reduce immune rejection after induced pluripotent stem cell-derived allogeneic cardiomyocyte transplantation. *Sci Rep.* (2020) 10:4593. doi: 10.1038/s41598-020-58126-z

18. Kawamura M, Miyagawa S, Fukushima S, Saito A, Miki K, Ito E, et al. Enhanced survival of transplanted human induced pluripotent stem cell-derived cardiomyocytes by the combination of cell sheets with the pedicled omental flap technique in a porcine heart. *Circulation.* (2013) 128:S87–94. doi: 10.1161/CIRCULATIONAHA.112.000366

frontiers | Frontiers in Cardiovascular Medicine

TYPE Case Report
PUBLISHED 23 August 2022
DOI 10.3389/fcvm.2022.928265

OPEN ACCESS

EDITED BY
Hendrik Tevaearai Stahel,
Bern University Hospital, Switzerland

REVIEWED BY
Giacomo Bianchi,
Toscana Gabriele Monasterio Foundation, Italy
Paul Philipp Heinisch,
Congenital and Pediatric Heart Surgery, Germany

*CORRESPONDENCE
Daxing Liu
13639222003@163.com

†These authors have contributed equally to this work

SPECIALTY SECTION
This article was submitted to Heart Surgery, a section of the journal Frontiers in Cardiovascular Medicine

RECEIVED 25 April 2022
ACCEPTED 02 August 2022
PUBLISHED 23 August 2022

CITATION
Zhang D, Wei S, Tao W, Liao Y, Xiao R and Liu D (2022) Case report: Traumatic ventricular aneurysm combining tricuspid valve avulsion in a child: Diagnostic findings and treatment protocols.
Front. Cardiovasc. Med. 9:928265.
doi: 10.3389/fcvm.2022.928265

Case report: Traumatic ventricular aneurysm combining tricuspid valve avulsion in a child: Diagnostic findings and treatment protocols

Dengshen Zhang[1†], Shan Wei[1†], Wenhong Tao[2], Yuanfeng Liao[1], Ruihan Xiao[1] and Daxing Liu[1*]

[1]Department of Cardiovascular Surgery, Affiliated Hospital of Zunyi Medical University, Zunyi, China, [2]Department of Ultrasonography, Affiliated Hospital of Zunyi Medical University, Zunyi, China

This case report is an extremely rare case of a traumatic left ventricular aneurysm in a 3-year-old child who also had tricuspid valve avulsion due to blunt trauma. The diagnostic findings and treatment protocols are discussed to provide a clinical reference.

KEYWORDS

traumatic tricuspid regurgitation, aneurysmoplasty, blunt cardiac injury, acquired left ventricular aneurysm, cardiac surgery

Introduction

The left ventricular aneurysm can be categorized as congenital or acquired. The congenital left ventricular aneurysm is a dysplastic heart malformation thataffects approximately 0.04% of the population (1). The most common cause of acquired ventricular aneurysms is myocardial infarction, which can also occur in cardiomyopathy, myocarditis, complications of a cardiovascular procedure, and blunt trauma (2). The most uncommon type is a traumatic ventricular aneurysm. In this work, we report a rare case of left ventricular aneurysm associated with tricuspid valve avulsion in a 3-year-old boy after a road traffic accident. Our initial findings were a femur fracture and tricuspid valve avulsion. After 6 months transthoracic echocardiography revealed a giant ventricular aneurysm. Following that, the patient underwent ventricular aneurysmectomy, ventricular aneurysmosurgery, and tricuspid valvuloplasty with successful clinical outcomes.

Case presentation

A 3-year-old child was admitted to our department with blunt injuries from a road traffic accident. Following the crash, he remained conscious while crying and was taken to our the emergency department of our hospital. The child felt considerable pain when pressure was applied to his right thigh during the physical examination without revealing any further abnormalities. Radiographs of his extremities showed

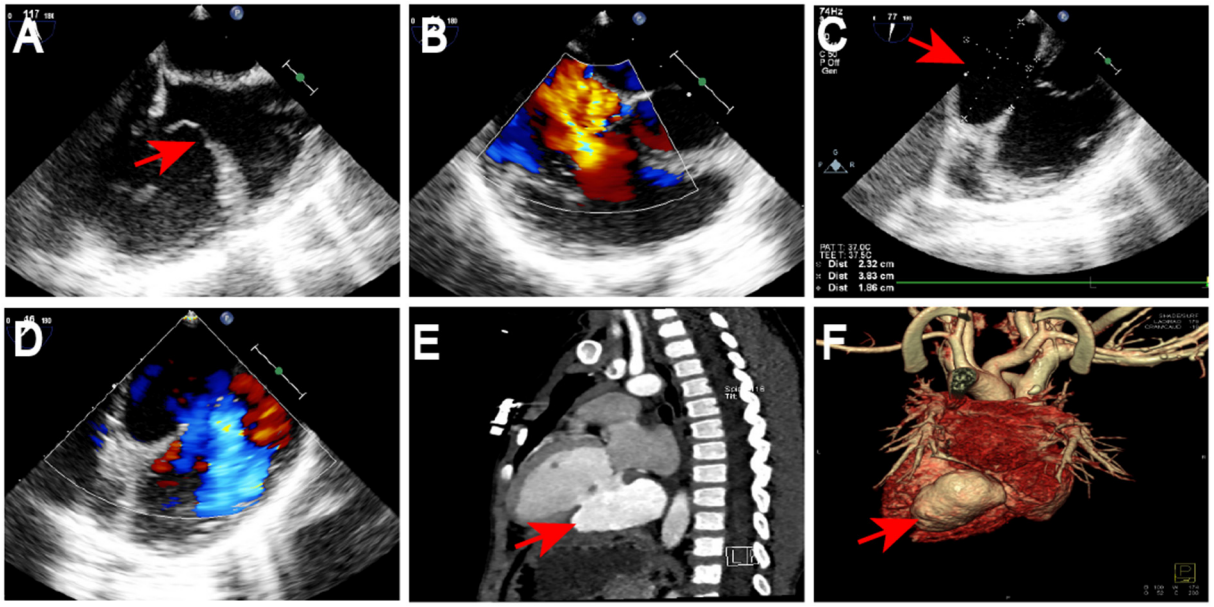

FIGURE 1
Preoperative echocardiography and computed tomography results. Anterior tricuspid leaflet prolapse was observed by TTE (red arrow; **A**). Tricuspid prolapse resulted in moderate tricuspid regurgitation **(B)**. TTE revealed avulsion of anterior tricuspid leaflet resulting in moderate tricuspid regurgitation, a 23 mm × 38 mm giant aneurysm with a 19-mm diameter of the neck in the LVPW (red arrow; **C**) and visible blood flow into the aneurysm **(D)**. CT scan and reconstruction confirmed a massive ventricular aneurysm in the LVPW (red arrow; **E,F**). TTE, Transthoracic Echocardiography; LVPW, left ventricular posterior wall; CT, computed tomography.

a fractured right femur, and chest X-rays showed that the lungs were normal. An electrocardiogram (ECG) revealed low and flat T waves in leads III, aVF, and V1. Laboratory examination indicateda slight elevation in troponin to 21 ng/mL. Using transthoracic echocardiography (TTE), anterior tricuspid leaflet prolapse was observed because it is the first-line diagnostic tool for evaluating the tricuspid valve (Figure 1A). This tricuspid prolapse resulted in moderate tricuspid regurgitation (Figure 1B). The fracture was treated with a plaster cast in the Surgery department. The patient was then referred to our department for further treatment and was discharged after 1 week.

After 6 months, ECG revealed continuous abnormal Q waves in leads III and aVF during normal myocardial enzymes. TTE revealed avulsion of anterior tricuspid leaflet resulting in moderate tricuspid regurgitation, a 23 × 38 mm giant aneurysm with a 19-mm diameter of the neck in the left ventricular posterior wall (LVPW) (Figure 1C), and visible blood flow into the aneurysm (Figure 1D). Computed tomography (CT) scan and reconstruction confirmed a massive ventricular aneurysm in LVPW (Figures 1E,F). Finally, the patient was scheduled for surgery.

During surgery, after sternotomy and the pericardium being incised, we found that the aneurysmal portion of the left ventricle was thinned and was greatly expanded (Figure 2A), and there was no pericardial adhesion. The myocardial layers were continuous, the aneurysm well had sharply defined edges (Figure 2A). After being surgically incised, the bovine pericardium was used to close the aneurysm's neck (Figures 2B,C). Felt pads were then employed to close the epicardium over the patch (Figure 2D), resulting in a detour formed around the posterior descending artery (Figures 2E,F). The third strip of the felt pad reinforced the "sandwich" structure (Figure 2F). A right atriotomy was performed to repair the anterior leaflet of the tricuspid valves with a 5 mm tear. 5.0 Prolene suture lines were utilized to sew the rupture, and valvuloplasty of the anterior tricuspid leaflet was performed (Figures 2G–I). 5.0 Prolene suture was used to figure-of-eight suture on the junction between the anterior annulus and the posterior annulus, and the junction between posterior annulus and septum annulus. Testing with saline solution injection and intraoperative esophageal echocardiography showed no tricuspid regurgitation (Figures 2I, 3A) and revealed no residual shunt for LVPW (Figure 3B). Histological examination demonstrated massive fibrous tissue in the aneurysm wall,myocardial fiber disappears is replaced by hyperplained fibrous tissue, fibrous connective tissue increases, and glass -like changes in local fiber tissue (uniform consistency, no structure and translucent protein accumulation) (Figure 4, ×200), consistent with trauma-induced aneurysms.

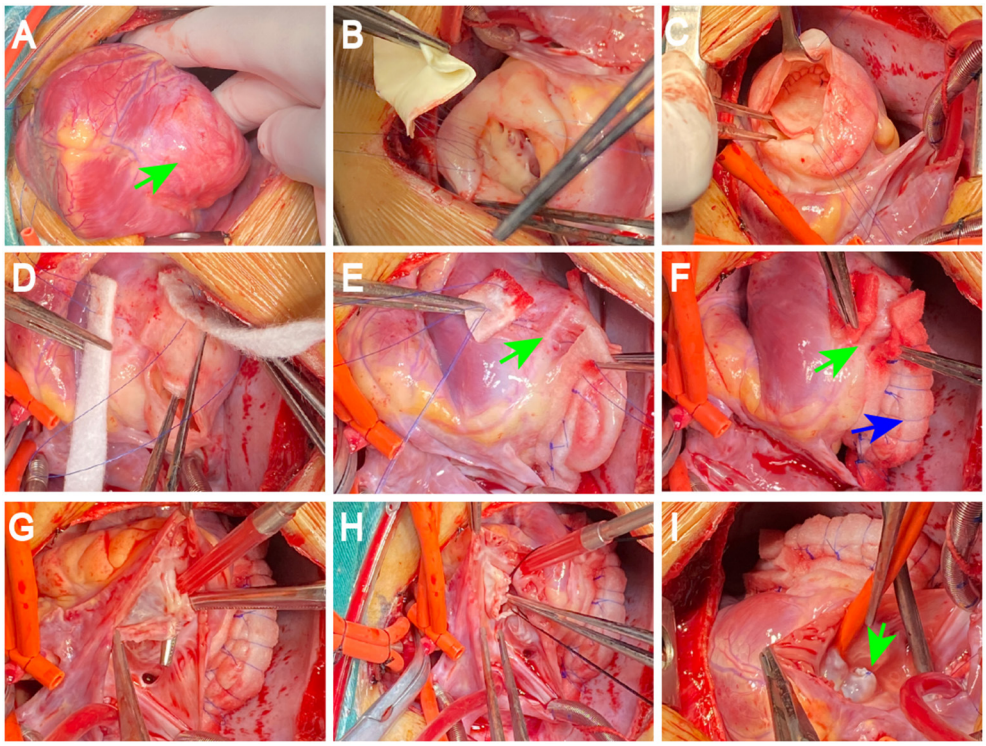

FIGURE 2
Surgical procedure. The aneurysmal portion of the left ventricle was thinned and was significantly expansive, the aneurysm well has sharply defined edges (blue arrow; **A**). The bovine pericardium was used to close the aneurysm's neck after being surgically incised **(B,C)**. Felt pads were used to close the epicardium over the patch **(D)**, resulting in a detour formed around the posterior descending artery (PDA) and PDA was well protected in a "sandwich" (green arrow; **E,F**). The third strip of the felt pad reinforced the "sandwich" structure (blue arrow; **F**). 5.0 Prolene suture lines were used to sew the rupture, valvuloplasty of the anterior tricuspid leaflet was performed **(G,H)**. Testing with saline solution injection showed no tricuspid regurgitation (green arrow; **I**). PDA: the posterior descending artery.

The sketch of ventricular aneurysmorrhaphy and tricuspid valvuloplasty was provided (Supplementary Figures S1, S2). The postoperative CT scan and reconstruction revealed successful surgery (Figures 3C,D). One week after surgery, the patient was discharged, and follow-up care was provided in the outpatient setting. Finally, the child recovered well and was followed up for 12 months.

Discussion

The case reported here has the following two notable features. Initially, the patient presented with only an anterior tricuspid leaflet avulsion on an ECG following blunt chest injury, but 6 months later he developed a massive ventricular aneurysm. A second observation was that the posterior left ventricle branch was well protected in the process of ventricular aneurysmectomy and aneurysmorrhaphy in a "sandwich" structure. In addition, the third strip of the felt pad was added to reinforce the "sandwich" structure.

The left ventricular aneurysm can be congenital or acquired, while both types present as a nodular structure protruding out of the cardiac chamber with regional ventricular wall expansion and thinning. A congenital ventricular aneurysm is a highly rare dysplastic heart malformation reported in around 0.04% of the population and is characterized by aberrant wall motion abnormality and large variations in size. Acongenital ventricular aneurysm is mainly presented in the neonatal period, and is generally accompanied by other congenital malformations, such as ventricular septal defect, atrial septal defect, tricuspid atresia, and tetralogy of Fallot (1). The acquired ventricular aneurysm is the most common in myocardial infarction, and it is also seen in cases such as cardiomyopathy (3), sarcoidosis (4), myocarditis (5), cardiovascular procedure complications (6), and blunt trauma. Traumatic ventricular aneurysms are extremely rare among them. The traumatic ventricular aneurysm has been reported in children under 2 9 years old (7–9). In these cases, blunt injuries were involved, such as chest injuries from vehicle crashes and falls from height. Several studies have reported that acquired traumatic ventricular aneurysms can be accompanied by ventricular septal perforation and hemopericardium.

Early findings in the present case included low T waves in leads III, aVF, V1, elevation in troponin, moderate tricuspid

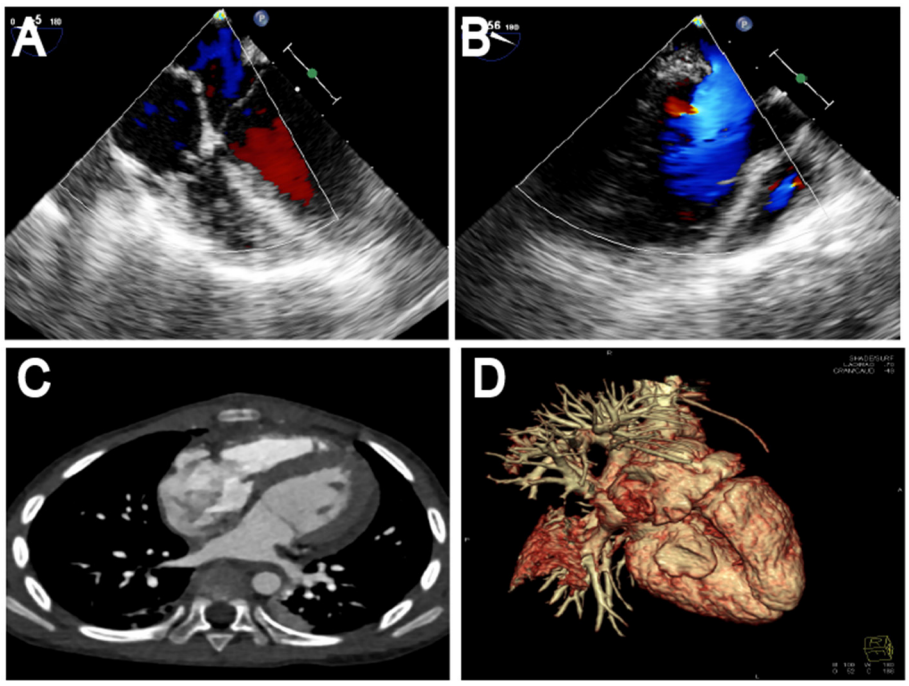

FIGURE 3
Follow-up. It showed no tricuspid regurgitation by intraoperative esophageal echocardiography showed no tricuspid regurgitation **(A)** and revealed no residual shunt for LVPW **(B)**. The postoperative CT scan and reconstruction revealed successful surgery **(C,D)**. LVPW, left ventricular posterior wall; CT, computed tomography.

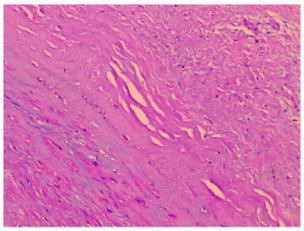

FIGURE 4
Histological examination. Histological examination revealed massive fibrous tissue in the aneurysm wall (Figure ×200).

regurgitation, and no evidence of ventricular aneurysms. After 6 months of injury, continuous abnormal Q waves in leads III and aVF were demonstrated on ECG while myocardial enzymes were normal. Furthermore, TTE identified a massive aneurysm located in the left ventricle. This suggests that in pediatric cases suffering from a blunt chest injury, especially those experiencing cardiac injury such as complex valvular injury, the possibility of ventricular aneurysm should be considered.

An untreated large ventricular aneurysm carries a high risk of rupture and embolization. Due to the childbeing young and having a poor prognosis, conservative treatment arrangements were made to address the initial finding of tricuspid regurgitation. Surgery was performed after 6 months for the diagnosed sizeable ventricular aneurysm. The timing of surgery for traumatic ventricular aneurysms remains undetermined because of its rarity and lack of evidence regarding its management. In the present case, the ventricular aneurysm boundary and the scar wereformed after 6 months of injury, which may facilitatethe surgical procedure.

Traumatic tricuspid insufficiency is an uncommon complication of blunt cardiac injury (9). In avoidance of delayed right ventricular deterioration, early identification and surgical treatment of this disease are significant. A previous case of a 9-year-old boy exhibiting traumatic ventricular aneurysm combined with tricuspid insufficiency due to rupture of papillary muscles was eventually treated by valve replacement (10). For the present 3-year-old child presenting with femur fracture and tricuspid leaflet avulsion, valvuloplasty was performed with a satisfactory outcome at a 1-year follow-up.

Surgery for ventricular aneurysms requires protection for the major coronary branches, as the deformation and tamponade of the coronary postoperatively can cause malignant arrhythmia and death (11). As observed in this case, the ventricular aneurysm was located in the posterior wall close to the branches of the left ventricle. Resection was performed, and a bovine pericardium was used. Meanwhile, the pericardium

was closed over the patch using two strips of felt pads (~0.8 × 4 cm) to form a "sandwich" structure with the left strip broken to avoid pressure on the posterior branch artery. Furthermore, the third strip of the felt pad was used to reinforce the "sandwich" structure to prevent hemorrhage, which is the first case using this way (a third strip) that has never been reported.

Summary

We reported an extremely rare case of traumatic left ventricular aneurysm combining tricuspid valve avulsion following blunt injury. We present confirmed diagnosis, ventricular aneurysmorrhaphy, and tricuspid valvuloplasty with a successful clinical outcome. It suggests that in pediatric cases suffering from a blunt chest injury, especially experiencing a cardiac injury, a ventricular aneurysm may be considered and coronary arterial branches should be well protected in ventricular aneurysmectomy in a "sandwich."

Data availability statement

The original contributions presented in the study are included in the article/Supplementary material, further inquiries can be directed to the corresponding author.

Ethics statement

Ethical review and approval was not required for the study on human participants in accordance with the local legislation and institutional requirements. Written informed consent to participate in this study was provided by the participants' legal guardian/next of kin. Written informed consent was obtained from the minor(s)' legal guardian/next of kin for the publication of any potentially identifiable images or data included in this article.

Author contributions

DZ and SW performed the data analyses and wrote the manuscript. WT contributed to provided and analyzed intraoperative and postoperative cardiac ultrasound images required for the study. RX and YL contributed significantly to analysis and manuscript preparation. DL helped perform the analysis with constructive discussions. All authors contributed to the article and approved the submitted version.

Funding

This work was supported by the National Natural Science Foundation of China (Grant No. 82160060) and Guizhou Provincial Science and Technology Projects ZK [2022] YB669 and ZK [2022] YB652.

Acknowledgments

We thank our patient, who permitted us to publish this case report.

Conflict of interest

The authors declare that the research was conducted in the absence of any commercial or financial relationships that could be construed as a potential conflict of interest.

Publisher's note

Supplementary material

The Supplementary Material for this article can be found online at: https://www.frontiersin.org/articles/10.3389/fcvm.2022.928265/full#supplementary-material

References

1. Ohlow MA, von Korn H, Lauer B. Characteristics and outcome of congenital left ventricular aneurysm and diverticulum: analysis of 809 cases published since 1816. *Int J Cardiol.* (2015) 185:34–45. doi: 10.1016/j.ijcard.2015.03.050

2. Bisoyi S, Dash AK, Nayak D, Sahoo S, Mohapatra R. Left ventricular pseudoaneurysm versus aneurysm a diagnosis dilemma. *Ann Card Anaesth.* (2016) 19:169–72. doi: 10.4103/0971-9784.173042

3. Rowin EJ, Maron BJ, Haas TS, Garberich RF, Wang W, Link MS, et al. Hypertrophic cardiomyopathy with left ventricular apical aneurysm: implications for risk stratification and management. *J Am Coll Cardiol.* (2017) 69:761–773. 4. doi: 10.1016/j.jacc.2016.11.063

4. Jmeian A, Thawabi M, Goldfarb I, Shamoon F. Left ventricular aneurysm and ventricular tachycardia as initial presentation of cardiac

sarcoidosis. *N Am J Med Sci.* (2015) 7:114–8. doi: 10.4103/1947-2714.153923

5. Chiyoya M, Fukuda I, Sasaki S, Okumura K. Direct ablation and excision of myocardial scar in post-myocarditis ventricular aneurysm. *Interact Cardiovasc Thorac Surg.* (2020) 30:316–18. doi: 10.1093/icvts/ivz258

6. Zhang X. Atypical takotsubo cardiomyopathy with persistent left ventricular aneurysm after cardiac surgery. *Heart Surg Forum.* (2021) 24:E442–4. doi: 10.1532/hsf.3705

7. Vossler JD, Fontes A, Moza R, Menon SC, Wong VL, Husain SA. Traumatic left ventricular aneurysm and ventricular septal defect in a child. *World J Pediatr Congenit Heart Surg.* (2021) 13:116–9. doi: 10.1177/21501351211038838

8. Brock MA, Co-Vu J, Bleiweis MS, Reyes K, Shih RS. Left ventricular aneurysm following blunt-force trauma in a child. *CASE (Phila).* (2018) 3:39–42. doi: 10.1016/j.case.2018.08.002

9. Eranki A, Villanueva C, Wilson-Smith A, Seah P. Traumatic tricuspid valve regurgitation: a two case series. *Trauma Case Rep.* (2021) 37:100593. doi: 10.1016/j.tcr.2021.100593

10. Veeragandham RS, Backer CL, Mavroudis C, Wilson AD. Traumatic left ventricular aneurysm and tricuspid insufficiency in a child. *Ann Thorac Surg.* (1998) 66:247–8. doi: 10.1016/S0003-4975(98)00380-4

11. Sartipy U, Löfving A, Albåge A, Lindblom D. Surgery for ventricular tachycardia and left ventricular aneurysm provides arrhythmia control. *Scand Cardiovasc J.* (2008) 42:226–32. doi: 10.1080/14017430802005240

frontiers | Frontiers in Cardiovascular Medicine

TYPE Case Report
PUBLISHED 13 September 2022
DOI 10.3389/fcvm.2022.988271

OPEN ACCESS

EDITED BY
Hendrik Tevaearai Stahel,
Bern University Hospital, Switzerland

REVIEWED BY
Maruti Haranal,
U N Mehta Institute of Cardiology and Research, India
Lilia Oreto,
Mediterranean Pediatric Cardiology Center, Italy

*CORRESPONDENCE
Long Song
longs@csu.edu.cn

SPECIALTY SECTION
This article was submitted to Heart Surgery, a section of the journal Frontiers in Cardiovascular Medicine

RECEIVED 07 July 2022
ACCEPTED 10 August 2022
PUBLISHED 13 September 2022

CITATION
Huang S, Wang S, Tang Z, Dai Y and Song L (2022) Case report: Right ventricular outflow tract obstruction caused by multicomponent mesenchymal tumor.
Front. Cardiovasc. Med. 9:988271.
doi: 10.3389/fcvm.2022.988271

Case report: Right ventricular outflow tract obstruction caused by multicomponent mesenchymal tumor

Shengyuan Huang[1], Shiye Wang[2], Zhixiang Tang[3], Yinghuan Dai[4] and Long Song[1]*

[1]Department of Cardiovascular Surgery, The Second Xiangya Hospital, Central South University, Changsha, China, [2]Clinical Nursing Teaching and Research Section, Operation Room, The Second Xiangya Hospital, Central South University, Changsha, China, [3]Department of Cardiovascular Surgery, The Second Hospital of Hebei Medical University, Shijiazhuang, China, [4]Department of Pathology, The Second Xiangya Hospital, Central South University, Changsha, China

Right ventricular outflow tract obstruction (RVOTO) is a cause of hemodynamic instability that can lead to right ventricular dysfunction. Cardiac tumors located in the right ventricle or surrounding structures can cause RVOTO. Herein, we present a rare case of a 21-year-old male with palpitations due to RVOTO caused by a cardiac multicomponent mesenchymal tumor. The tumor was localized in the right ventricular outflow tract, resulting in right side heart enlargement, tricuspid regurgitation, and RVOTO. Hence, tumor resection was performed. The patient was in a stable condition and discharged home on the 6th post-operative day. However, histopathological examination of the tumor specimen suggested a three-component mesenchymal tumor containing mucinous components, formed blood vessels, and fibrous tissue, which is like an atypical capillary hemangioma. After seven years of follow-up, the patient had no right heart enlargement, tricuspid regurgitation, and tumor recurrence. We believe surgical treatment is effective, and this case will provide a reference for clinicians to treat and evaluate the prognosis of similar three-component mesenchymal cardiac tumor cases in the future.

KEYWORDS

case report, right ventricular outflow tract obstruction (RVOTO), cardiac tumor, histopathology, hemangioma

Introduction

The large autopsy series revealed that the incidence of primary cardiac tumors was 0.02%, of which 75% were benign, 25% were malignant, and myxoma accounted for 50–70% (1). But the incidence of tumor metastasis to the heart is much higher than that of the primary tumor, and researchers found that 10% of patients with tumors had cardiac metastases in an autopsy study (1). Cardiac tumors can alter hemodynamics, and when the tumor localizes in the right ventricle or surrounding structures, it may cause obstruction of the right ventricular outflow tract (RVOTO). In this case, the maximum systolic pressure difference between the right ventricle and the pulmonary

artery is greater than 25 mmHg (2), and there can be many dangerous pathophysiological changes, such as right side heart enlargement, cardiac dysfunction, arrhythmias, and embolisms. Extracardiac tumor metastasis accounts for 13.7% of the total causes of RVOTO, and myxoma accounts for 6.9%, the two most common tumor-related causes (3). However, other tumor types that cause RVOTO are extremely rare. Here we report a RVOTO caused by a rare cardiac three-component mesenchymal tumor in a patient with right side heart enlargement and tricuspid regurgitation.

Case presentation

A 21-year-old man was admitted to our hospital with a 6-day history of palpitations without chest pain, fever, and headache. The patient had a 4 years smoking history with an average of 12 cigarettes per day. There were no other significant findings in medical history or family history. Physical examination showed that body temperature was 36.1°C, pulse was 81 bpm, blood pressure was 125/75 mmHg at resting conditions, and the cardiac border was slightly enlarged on percussion. A grade 3/6 systolic murmur was heard in the third left intercostal space. Except for elevated total bilirubin (29.8 μmol/L, reference value: 5.1–17.1μmol/L) and direct bilirubin (7.5 μmol/L, reference value: 1–6.0 μmol/L), other laboratory tests revealed no specific abnormalities.

Electrocardiogram suggested sinus rhythm with sharpened T waves. No notable abnormalities were found following chest X-ray examination. Echocardiography showed enlargement of the right atrium (50 mm), right ventricle (46 mm), and right ventricular outflow tract (31 mm) in diameter. Left atrium, left ventricle, and aorta were normal in diameter with a left ventricular ejection fraction of 74%. However, a hyperechoic space occupying mass with clear boundary (approximately 36 × 30 mm in size) was found in the right ventricle near the outflow tract (Figures 1A–C). The mass was connected to the anterior wall of the right ventricle by a pedicle and oscillated with the cardiac cycle. The tricuspid valve opened well but could not close properly, and Color Doppler Flow Imaging (CDFI) showed regurgitation under the tricuspid valve. Affected by the mass, the blood flow in the right ventricular outflow tract accelerated to 3.8 m/s, and the pressure difference (PG) across the pulmonary valve increased to 58 mmHg. Computed tomography angiography (CTA) also showed that the right atrium and right ventricle were enlarged, and a round filling defect of about 3.5*4.2*2.2 cm was seen in the right ventricular outflow tract (Figures 1D–F). Its density was roughly equivalent to that of the myocardium with clear boundaries.

Based on the above data, we diagnosed the patient with right ventricular tumor, RVOTO, and tricuspid regurgitation. To relieve the patient's obstruction and prevent potentially dangerous complications, we decided to perform surgery after fully assessing the patient's condition.

The surgical team performed right ventricular tumor resection. A standard median sternotomy incision was made. After pericardiotomy, the right atrium and right ventricle were found to be enlarged. After systemic heparinization, cardiopulmonary bypass was established. The surgery was performed on beating heart without aortic cross clamping. A right ventricular outflow tract incision was made, and a pedunculated tumor was found in the anterior wall of the right ventricle, with a diameter of about 3.5*2.5 cm (Figure 2A). The tricuspid annulus was enlarged, with mild to moderate regurgitation. The pedunculated tumor was completely excised. The incision was then sutured, heparin neutralized with protamine, and the patient was carefully transferred to the intensive care unit.

Interestingly, histopathological examination of the surgically excised specimen suggested that it was not a common myxoma, but a three-component mesenchymal tumor containing mucus, blood vessels, and fibers. The specimen was a pale-yellow pedunculated ball with a texture close to myocardial tissue, and the cut surface had a "fish-meat" like texture (Figure 2B). Low magnification of Hematoxylin-Eosin (HE) stained section shows numerous formed blood vessels against a background of fibrous tissue (Figure 2C). At high magnification, fibrous components, formed blood vessels, and mucus components were also observed (Figures 2D–F). The results indicated that the cells were positive for F8, CD34, and CD31, but negative for Ki-67, CD99, myogenin, desmin, SMA, bcl-2, and alcian blue.

The patient recovered without palpitations and other complications and was discharged on the 6th post-operative day with a recommendation for follow-up. After 7 years of follow-up, no tumor recurrence was found on echocardiography (Figure 3 and Supplementary materials). The diameter of the right atrium decreased from 50 to 35 mm, the right ventricle from 46 to 34 mm, the RVOT from 31 to 25 mm, and the PG across the pulmonary valve to 4 mmHg. The tricuspid valve functioned normally, and no regurgitation was seen.

Discussion

Here, we present a 21-year-old male patient with palpitations whose echocardiography revealed a hyperechoic space occupying mass in RVOT. The differential diagnosis in the presence of RVOT mass in young individuals is tumor, thrombosis, embolism, infection, foreign bodies etc. If the patient has a history of atrial fibrillation or abnormal hypercoagulability, it should be considered as thrombosis. History of fractures or prolonged immobilization after surgery in young patients can also lead to thrombosis of the lower extremities, and the thrombus may fall off into the right ventricle. If the patient has a history of long-term fever,

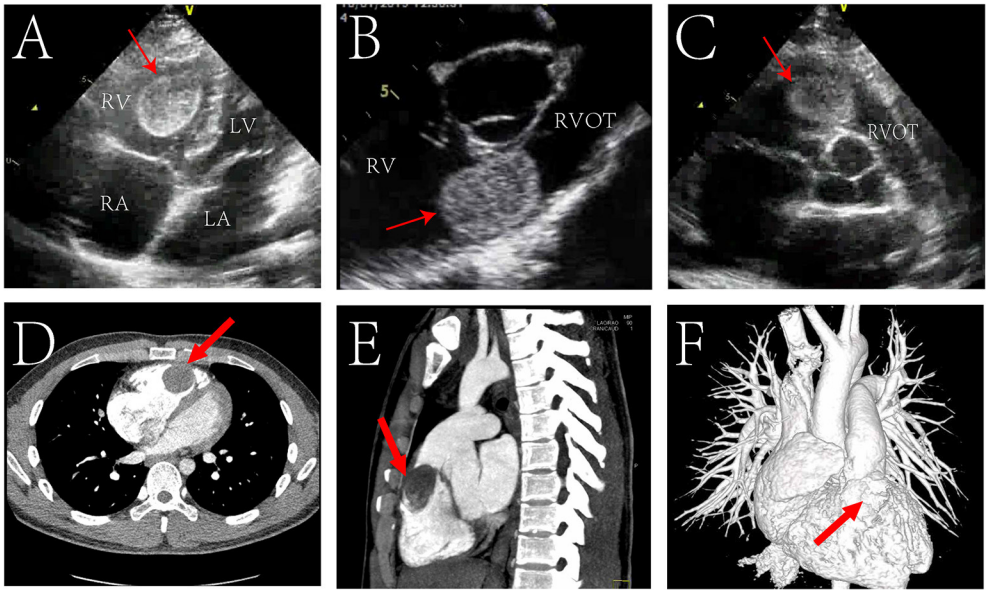

FIGURE 1
Echocardiogram pre-operatively showing a mass (red arrow) located in the in the right ventricular outflow tract (RVOT) in transthoracic four chamber cross section **(A)**, transthoracic short axis section of aorta **(B)**, transesophageal short axis section of aorta **(C)**. Preoperative cardiac Computed Tomography (CT) showed a mass (red arrow) in the RVOT in transverse view **(D)**, sagittal view **(E)**; CT angiography (CTA) showed a filling defect (red arrow) in the right ventricular outflow tract **(F)**. RV, right ventricle; LV, left ventricle; RA, right atrium; LA, left atrium.

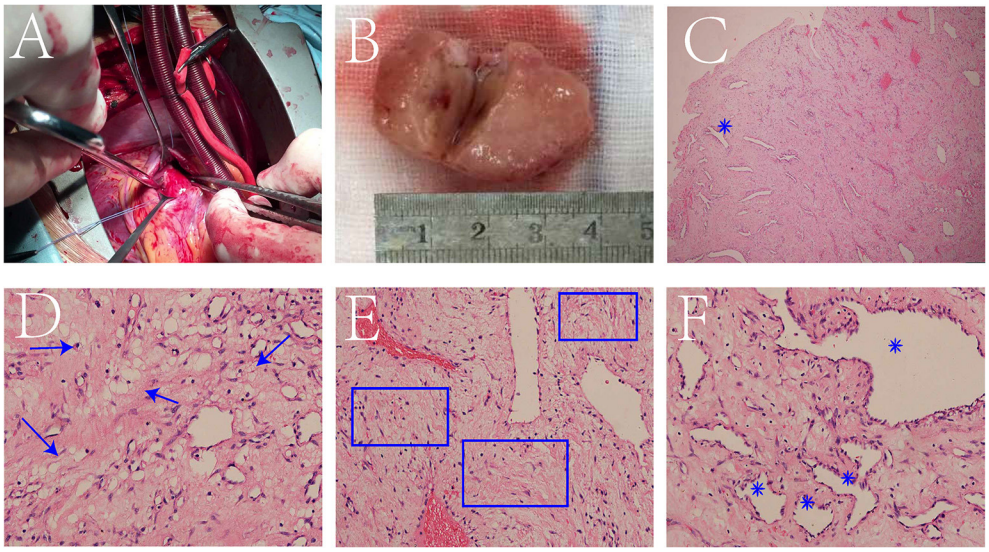

FIGURE 2
A tumor was found in the anterior wall of the right ventricle **(A)**. The specimen is a pale-yellow pedunculated ball with a texture close to myocardial tissue, and the cut surface with the "fish flesh" like texture **(B)**. Low magnification of the hematoxylin-eosin (HE) stained section showed numerous blood vessels formed (blue star) against a background of fibrous tissue **(C)**. At high magnification, mucus components (blue arrow) **(D)**, fibrous components (blue box) **(E)** and formed blood vessels (blue star) **(F)** were observed.

antibiotic use, fatigue, and weight loss, the mass may be an intracardiac vegetation due to infective endocarditis. Intracardiac foreign bodies are also possible if there is a history of venous catheterization or other surgical procedures. In our case, the mass was solitary with clear boundaries, and the patient had no history of fever, atrial fibrillation, or fracture and postoperative histopathology confirmed that it was a benign cardiac tumor.

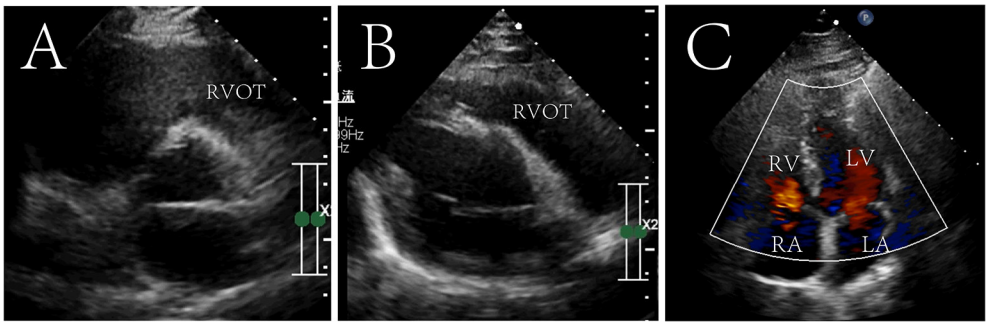

FIGURE 3
Seven-year postoperative echocardiography in transthoracic aortic short-axis views **(A)**, right ventricular outflow tract view **(B)** and four chamber cross section view **(C)**. The tumor did not recur and the right ventricular outflow tract was not obstructed. Right ventricular outflow tract, RVOT; RV, right ventricle; LV, left ventricle; RA, right atrium; LA, left atrium.

Difficulties arose in the histopathological typing of the specimens in this case. The mucinous background in HE sections can easily lead to the diagnosis of myxoma. Myxomas are typically soft and gelatinous, or hard and calcified (4). In this case, the density of the tumor tissue in the CT scan was roughly equal to that of the myocardium. The excised specimen was spheroid with a yellowish pedicle, and the cut surface had a "fish-meat" like texture. Large amount of differentiated and mature vascular components was seen in the HE section, all of which indicated that the tumor was not myxoma, but closer to the diagnosis of hemangioma.

However, this case cannot be classified as a pure hemangioma either. According to the 2015 WHO classification guidelines for cardiac and pericardial tumors, hemangioma can be classified as capillary hemangioma, cavernous hemangioma, arteriovenous malformation and intramuscular hemangioma (4). A typical HE section of a capillary hemangioma shows thin and tortuous capillaries under high magnification microscopy (5). Cavernous hemangiomas are aggregates of dilated, packed, thin-walled capillaries filled with blood cells (5, 6). The pathological images of our patient are different from the images of various types of hemangiomas in the above literature. The specimen from our case was found to have a mucinous component and many mature blood vessels in a fibrotic background under high magnification. Pathologists at our hospital spent a long time to make a diagnosis. They believed it was a multicomponent tumor of mesenchymal origin with a predominantly vascular component containing mucus and fibers. Of the four hemangiomas, it was more similar to capillary hemangioma, but had more mucous and fibrous components than typical capillary hemangiomas. Actually, there was a similar case, a family of hyperkeratotic papules reported by Dr. Peterson in 1982 (7). Histopathological examination of the biopsy showed neovascularization with mucin like change in a background of fibrosis, and a diagnosis of "myxovascular fibromas" was made. Since our patient's tumor was dominated by hemangioma components, borrowing the nomenclature "myxovascular fibromas", we thought that this patient might be called "myxofibrous hemangioma". However, in the existing classification system, the final histopathological diagnosis of this case was atypical capillary hemangioma with mucinous, fibrous components.

Although HE sections suggest that the tumor has a low degree of malignancy, whether it will recur is still a question, because there are no reports of an associated recurrence rate for the multicomponent mesenchymal tumor such as our case. Cardiac myxoma recurrence after surgery is about 5%, atypical cases are more likely to recur (8), and the cumulative recurrence rate is higher in younger patients (13%) (9). A review of 200 cases of cardiac hemangioma found recurrence in 3 patients and one manifested angiosarcoma at the site of hemangioma (10). A study reported that the recurrence rate of cardiac Fibroelastoma was 12.2% (11). Now the question is, do multicomponent tumors increase recurrence rates? Fortunately, our patient at 7-years follow-up showed no tumor recurrence and the heart was functioning normally.

Different tumor types and tumor location in right ventricle can cause RVOTO. We reviewed the literature on RVOTO caused by cardiac tumors reported in the past decade (Table 1). In terms of tumor types, the literature reported primary tumors such as fibroma (12), leiomyoma (13), hemangioma (17), rhabdomyoma (20), and metastatic cardiac tumor from sigmoid colon cancer (16), testicular tumor (15), neuroendocrine tumor (25) etc. Interestingly, tumors not located in the right ventricle can also cause obstruction, such as tumors located in the right atrium, interventricular septum, and anterior mediastinum (24, 32, 33).

Similar case of capillary hemangioma has been reported by Shekarkhar et al. (17). Their case was a 41-year-old man who complained of chest pain and fatigue. Ultrasound showed normal size right heart, tricuspid regurgitation, and a 1.6*1.8 cm mass located in the RVOT at the base of the septum. They

TABLE 1 Cases of RVOTO due to cardiac tumors reported in the past decade.

Year of publication	Age	Tumor type	Location	References
2012	6 months	Primary fibroma	Right ventricle	(12)
2012	7 months	Primary cardiac leiomyoma	Ventricular septum	(13)
2012	70 years	Malignant fibrous histiocytoma	RVOT	(14)
2012	42 years	Testicular tumor metastasis	Right ventricle	(15)
2013	70 years	Sigmoid colon cancer metastasis	Right ventricle	(16)
2014	41 years	Cardiac capillary hemangioma	Right ventricle	(17)
2014	24 years	Primary leiomyoma	Right ventricle	(18)
2016	62 years	Renal cell carcinoma metastasis or tumor thrombus	Right ventricle	(19)
2016	6 months	Rhabdomyoma	Right ventricle	(20)
2017	5 months	Rhabdomyoma	RVOT, pulmonary valve annulus	(21)
2018	46 years	Yolk sac tumors metastasis	Right ventricle	(22)
2018	67 years	Metastatic adenocarcinoma	Right ventricle and pulmonary artery	(23)
2018	15 months	Primary fibroma	Right-sided interventricular septal	(24)
2018	68 years	Metastatic neuroendocrine tumor	Right ventricle	(25)
2019	9 days	Teratoma	Right ventricle	(26)
2020	60 years	Neuroendocrine carcinoma metastasis	Right ventricle	(27)
2020	42 years	Primary undifferentiated spindle cell sarcoma	Right ventricle, pulmonary trunk	(28)
2021	54 years	AIDS-associated primary cardiac lymphoma	Right atrium and ventricle	(29)
2021	44 years	Myxoma	Right ventricle	(30)
2021	5 years	Cardiac inflammatory myofibroblastic tumor	Pulmonary valve, extending into the main pulmonary artery	(31)

also removed the tumor, and pathological examination under the high magnification microscope found neoformed vessels filled with blood. Compared to their case, our patient did not show symptoms of chest pain and fatigue, the right heart was significantly enlarged, and the tumor was located in the anterior wall of the right ventricle. And there was no recurrence after many years of follow-up, and the tricuspid regurgitation also disappeared.

Notably, the surgical team had difficulty deciding whether to perform surgery for tricuspid regurgitation (TR) in this patient. The patient had a marked enlargement of the right atrium, dilated tricuspid annulus to 37 mm, and mild TR on Echocardiography, which were suggestive of surgical intervention. However, after consulting the European Society of Cardiology (ESC) guidelines of 2012 (34), it was found that tricuspid valve surgery is a class IIa recommendation for patients with secondary TR when annulus is larger than 40 mm. In addition, considering that the tricuspid valve was not invaded by the tumor and the left heart function was normal, we speculated that the TR would disappear after hemodynamic correction. Therefore, we did not perform tricuspid valve surgery, and 7 years later the TR disappeared which confirmed our conjecture. This suggests that when such patients have TR, if the valve annulus does not exceed 40 mm, the tumor does not invade the tricuspid valve, and the left heart function is normal, TR may disappear spontaneously without tricuspid valve surgery.

In conclusion, we report a rare case of cardiac tumor induced RVOTO in a patient with right atrial and ventricular enlargement and tricuspid regurgitation. More interestingly, histopathological examination of the tumor revealed it was a three-component mesenchymal tumor with mucinous components and formed blood vessels in a fibrotic background. In the existing WHO classification of cardiac tumors, it is more like an atypical capillary hemangioma. Resection of the tumor relieved symptoms and there was no recurrence after 7 years. We case can be a reference for clinicians to treat similar three-component mesenchymal cardiac tumor cases in the future.

Data availability statement

The original contributions presented in the study are included in the article/Supplementary material, further inquiries can be directed to the corresponding author/s.

Ethics statement

The studies involving human participants were reviewed and approved by Ethics Committee of the Second Xiangya Hospital of Central South University, Changsha, China. The patients/participants provided their written informed consent to participate in this study. Written informed consent was obtained from the individual(s) for the publication of any potentially identifiable images or data included in this article.

Author contributions

SH drafted the manuscript. LS designed the study and were responsible for the collection of data or analysis. SW, ZT, and YD analyzed the data and revised the manuscript. All authors read and approved the final manuscript.

Funding

This work was supported by the Natural Science Foundation of Hunan Province (Grant No. 2021JJ30951) and Clinical Technology Innovation Guide Project of Hunan Province (Grant No. 2020SK53421).

Conflict of interest

The authors declare that the research was conducted in the absence of any commercial or financial relationships that could be construed as a potential conflict of interest.

Publisher's note

All claims expressed in this article are solely those of the authors and do not necessarily represent those of their affiliated organizations, or those of the publisher, the editors and the reviewers. Any product that may be evaluated in this article, or claim that may be made by its manufacturer, is not guaranteed or endorsed by the publisher.

Supplementary material

The Supplementary Material for this article can be found online at: https://www.frontiersin.org/articles/10.3389/fcvm.2022.988271/full#supplementary-material

References

1. Hoffmeier A, Sindermann JR, Scheld HH, Martens S. Cardiac tumors–diagnosis and surgical treatment. *Dtsch Arztebl Int.* (2014) 111:205–11. doi: 10.3238/arztebl.2014.0205

2. Therrien J, Dore A, Gersony W, Iserin L, Liberthson R, Meijboom F, et al. CCS Consensus Conference 2001 update: recommendations for the management of adults with congenital heart disease. *Part I Can J Cardiol.* (2001) 17:940–59.

3. Zeng YH, Calderone A, Rousseau-Saine N, Elmi-Sarabi M, Jarry S, Couture J, et al. Right ventricular outflow tract obstruction in adults: a systematic review and meta-analysis. *CJC Open.* (2021) 3:1153–68. doi: 10.1016/j.cjco.2021.03.011

4. Burke A, Tavora F. The 2015 WHO classification of tumors of the heart and pericardium. *J Thorac Oncol.* (2016) 11:441–52. doi: 10.1016/j.jtho.2015.11.009

5. Anbardar MH, Soleimani N, Mohammadzadeh S. Two cases of cardiac hemangioma in different anatomical locations presenting with chest pain and palpitation. *Clin Case Rep.* (2022) 10:e05495. doi: 10.1002/ccr3.5495

6. Zhou X, Song L, Feng X, Han X. Giant cavernous hemangioma of the right ventricle. *Eur J Cardiothorac Surg.* (2022). doi: 10.1093/ejcts/ezac317. [Epub ahead of print].

7. Peterson JL, Read SI, Rodman OG. Familial myxovascular fibromas. *J Am Acad Dermatol.* (1982) 6:470–2. doi: 10.1016/S0190-9622(82)80362-9

8. Samanidis G, Khoury M, Balanika M, Perrea DN. Current challenges in the diagnosis and treatment of cardiac myxoma. *Kardiol Pol.* (2020) 78:269–77. doi: 10.33963/KP.15254

9. Elbardissi AW, Dearani JA, Daly RC, Mullany CJ, Orszulak TA, Puga FJ, et al. Survival after resection of primary cardiac tumors: a 48-year experience. *Circulation.* (2008) 118:S7–15. doi: 10.1161/CIRCULATIONAHA.107.783126

10. Li W, Teng P, Xu H, Ma L, Ni Y. Cardiac hemangioma: a comprehensive analysis of 200 cases. *Ann Thorac Surg.* (2015) 99:2246–52. doi: 10.1016/j.athoracsur.2015.02.064

11. Sorour AA, Kurmann RD, El-Am EA, Bois MC, Scott CG, Lee AT, et al. Recurrence of pathologically proven papillary fibroelastoma. *Ann Thorac Surg.* (2022) 113:1208–14. doi: 10.1016/j.athoracsur.2021.03.114

12. Horovitz A, van Geldorp IE, Roubertie F, Thambo JB. Large right ventricular fibroma in a 6-month-old infant. *Pediatr Cardiol.* (2012) 33:1458–60. doi: 10.1007/s00246-012-0390-9

13. Melo IS, Belo F, Gouveia R, Anjos R. Primary cardiac leiomyoma of the ventricular septum: a rare form of pediatric intracardiac tumor. *Pediatr Cardiol.* (2012) 33:649–51. doi: 10.1007/s00246-012-0161-7

14. Tamenishi A, Matsumura Y, Okamoto H. Malignant fibrous histiocytoma originating from right ventricular outflow tract. *Asian Cardiovasc Thorac Ann.* (2012) 20:702–4. doi: 10.1177/0218492312440806

15. Vieira MS, Meireles A, Gomes C, Antunes N, Sá I, Cabral S, et al. The importance of multimodality cardiac imaging: Echocardiography and cardiovascular magnetic resonance imaging contributions to the diagnosis and management of a right ventricular mass. *J Cardiol Cases.* (2012) 6:e109–11. doi: 10.1016/j.jccase.2012.06.005

16. Sudo Y, Enomoto Y. Surgical management of metastatic colon cancer causing obstruction of the right ventricular outflow tract. *Kyobu Geka.* (2013) 66:907–10.

17. Shekarkhar S, Shekarkhar G, Foroughinia M, Javanmard E. Cardiac capillary hemangioma in a patient with atypical chest pain and normal ECG. *J Cardiol Cases.* (2014) 10:16–8. doi: 10.1016/j.jccase.2014.03.010

18. Song L, Wang L, Huang WC, Zhou XM, Hu JG, Liu LM, et al. Primary leiomyoma: a rare space occupying lesion in the right ventricle. *Ann Thorac Surg.* (2014) 97:324–6. doi: 10.1016/j.athoracsur.2013.05.097

19. Kim HY, Baek SH, Yoon JU, Lee DH, Byeon GJ, Ahn JH, et al. Cardiac arrest during radical nephrectomy due to a mass in the right ventricular outflow tract. *J Clin Anesth.* (2016) 33:156–9. doi: 10.1016/j.jclinane.2016.02.041

20. Lefort B, Lothion J, Arid JM, Tabareau-Delalande F, Nassimi A, Neville P, et al. Unusual Outcome of a Right Ventricular Rhabdomyoma in an Infant. *World J Pediatr Congenit Heart Surg.* (2016) 7:397–9. doi: 10.1177/2150135115593133

21. Han X, Song H, Zhou L, Jiang C. Surgical resection of right ventricular rhabdomyoma under the guidance of transesophageal echocardiography on a beating heart. *J Thorac Dis.* (2017) 9:E215–e218. doi: 10.21037/jtd.2017.02.63

22. Isom N, Rali AS, Damjanov I, Hubbard K, Grigsby J, Gupta K, et al. Right ventricular heart failure from a cardiac yolk sac tumor. *Am J Case Rep.* (2018) 19:229–33. doi: 10.12659/AJCR.907639

23. Karabag T, Arslan C, Yakisan T, Vatan A, Sak D. Metastatic adenocarcinoma involving the right ventricle and pulmonary artery leading to right heart failure: case report. *São Paulo Med J.* (2018) 136:262–5. doi: 10.1590/1516-3180.2016.0351280117

24. Picarelli D, Leone R, Surraco JL, Fernandez N, Antelo M, Grela C, et al. Complete Resection of a Right-Sided Interventricular Septal Fibroma. *World J Pediatr Congenit Heart Surg.* (2018) 9:242–3. doi: 10.1177/2150135117747830

25. Sood A, Chiadika SM, Everett JM, Au J, Rowe J. Right ventricular outflow obstruction due to metastatic neuroendocrine tumor. *Cureus.* (2018) 10:e3261. doi: 10.7759/cureus.3261

26. Farid Y, Chebli L, Seghers V, Dewals W, Sanoussi A, Wauthy P, et al. Obstructive teratoma in the right ventricle of a newborn: a case report. *J Cardiothorac Surg.* (2019) 14:55. doi: 10.1186/s13019-019-0874-2

27. Fabregat-Andrés Ó, Jacas-Osborn V, Margarit J, Valverde-Navarro AA. Successful surgery of neuroendocrine carcinoma infiltrating right ventricle and pulmonary artery. *J Card Surg.* (2020) 35:2802–3. doi: 10.1111/jocs.14701

28. Kwon J, Kwon K. Primary undifferentiated spindle cell sarcoma obstructing the right ventricular outflow tract. *J Cardiothorac Surg.* (2020) 15:71. doi: 10.1186/s13019-020-01129-8

29. Fuseya H, Yoshimura T, Tsutsumi M, Nakaya Y, Horiuchi M, Yoshida M, et al. Extracorporeal Membrane Oxygenation with rituximab-combined chemotherapy in AIDS-associated primary cardiac lymphoma: A case report. *Clin Case Rep.* (2021) 9:e04704. doi: 10.1002/ccr3.4704

30. Lu C, Yang P, Hu J. Giant right ventricular myxoma presenting as right heart failure with systemic congestion: a rare case report. *BMC Surg.* (2021) 21:64. doi: 10.1186/s12893-020-00977-4

31. Yildiz K, Genc HZ, Kir M, Unal N, Oto O, Paytoncu S, et al. Cardiac inflammatory myofibroblastic tumor causing pulmonary artery obstruction: a rare case report. *J Pediatr Hematol Oncol.* (2021) 43:e903–6. doi: 10.1097/MPH.0000000000002000

32. Agarwala BN, Thomas LE, Waldman JD. Acquired pulmonary stenosis: ultrasonographic diagnosis. *Pediatr Cardiol.* (1995) 16:179–81. doi: 10.1007/BF00794190

33. Fernando Val-Bernal J, Hernández-Nieto E. and Symptomatic intracavitary (noninvasive) cardiac metastasis from low grade endometrial stromal sarcoma of the uterus. *Pathol Res Pract.* (1999) 195:717–22. doi: 10.1016/S0344-0338(99)80067-3

34. Vahanian A, Alfieri O, Andreotti F, Antunes MJ, Barón-Esquivias G, Baumgartner H, et al. Guidelines on the management of valvular heart disease (version 2012). *Eur Heart J.* (2012) 33:2451–96. doi: 10.1093/eurheartj/ehs109

frontiers | Frontiers in Cardiovascular Medicine

TYPE Case Report
PUBLISHED 04 October 2022
DOI 10.3389/fcvm.2022.986904

OPEN ACCESS

EDITED BY
Hendrik Tevaearai Stahel,
Bern University Hospital, Switzerland

REVIEWED BY
Filippo Rapetto,
University Hospitals Bristol NHS Foundation Trust, United Kingdom
Roberto Spina,
Gosford Hospital, Australia

*CORRESPONDENCE
Songsong Wu
fjslwss@163.com

†These authors have contributed equally to this work and share first authorship

SPECIALTY SECTION
This article was submitted to Heart Surgery, a section of the journal Frontiers in Cardiovascular Medicine

RECEIVED 05 July 2022
ACCEPTED 06 September 2022
PUBLISHED 04 October 2022

CITATION
Zhao Y, Lin Y, Hong Z, Lai B, Lian L, Chen L, Xie Q, Zhou X and Wu S (2022) Minimally invasive repair of iatrogenic right ventricular perforation guided by bedside contrast-enhanced ultrasound: A case report and literature review.
Front. Cardiovasc. Med. 9:986904.
doi: 10.3389/fcvm.2022.986904

Minimally invasive repair of iatrogenic right ventricular perforation guided by bedside contrast-enhanced ultrasound: A case report and literature review

Yanchun Zhao[1†], Yucheng Lin[2†], Zhiliang Hong[1], Baochun Lai[1], Lianghua Lian[3], Lin Chen[3], Qi Xie[3], Xiaofen Zhou[3] and Songsong Wu[1*]

[1]Department of Ultrasonography, Fujian Provincial Hospital, Shengli Clinical Medical College of Fujian Medical University, Fuzhou, China, [2]Department of Ultrasonography, Affliated Fuzhou First Hospital of Fujian Medical University, Shengli Clinical Medical College of Fujian Medical University, Fuzhou, China, [3]Department of Cardiology, Fujian Provincial Hospital, Shengli Clinical Medical College of Fujian Medical University, Fuzhou, China

This case report involves a 93-year-old female patient with atrioventricular block and suffered right ventricular free wall perforation during installation of Micra Leadless Pacemaker (MLP). Pericardial tamponade occurred shortly, and we adopted pericardial catheter drainage as the primary emergency treatment. Considering the patient's physical conditions and leveraging the special treatment facilitates of the Intensive Care Unit (ICU), we tried a new emergency treatment approach. After putting the patient under intravenous anesthesia (no cardiac arrest), we made a small intercostal incision and performed bedside minimally invasive repair of right ventricular free wall perforation. It should be noted that ultrasound played a key role in pinpointing the breach and intraoperative guidance. We first used contrast-enhanced ultrasound (CEUS) to locate the breach. Then guided by bedside ultrasound, we accessed the perforation with the minimum incision size (5 cm). Our experience in this case may serve as a good reference in the emergency treatment for right ventricular free wall perforation.

KEYWORDS

cardiac perforation, leadless pacemaker, pericardial tamponade, bedside ultrasound, case report

Introduction

Implantation of permanent cardiac pacemaker is an effective treatment modality for bradyarrhythmia. MLP implantation, featuring short procedure and no pocket, has proven to be a safe and reasonable substitute for traditional transvenous pacemaker for senile patients (1). Since the MLP delivery system has a relatively large inner

diameter, there is certain incidence (c. 4%) of serious adverse events. The most commonly seen and severe complication is cardiac perforation (2). Clinical manifestations vary according to the location, aperture size and the patient's blood coagulation state, and may include chest pain, dyspnea and/or tamponade. Dynamic monitoring of pericardial effusion and accurate location of the breach are perquisites for determining subsequent treatment. Transthoracic echocardiography is first choice in this regard. Most small perforations on the myocardial wall will close naturally during heart beating. Generally speaking, evidence of hemodynamic instability and pericardial tamponade are decisive criteria for emergency clinical intervention. Left ventricular perforation can rapidly lead to severe hemodynamic damage. In this scenario, emergency open surgery is the only viable salvage option. Conversely, right ventricular lesions may be stabilized without open surgery (3), and there have been reports on successful closure of right ventricular perforations with glue and devices (4, 5). Only a handful of previous reports mentioned the value of contrast-enhanced ultrasound (CEUS) in locating myocardial perforation, while no report has been made on bedside minimally invasive repair of cardiac perforation through a small intercostal incision. Our report is the first to describe a new approach for successful bedside repair of an iatrogenic right ventricular perforation with the help of CEUS.

Case presentation

The patient is a 93-year-old woman with post-activity chest tightness and shortness of breath for 6 months. She was hospitalized after experiencing worsened symptoms for 10 days. 24-hour ambulatory electrocardiograph confirmed the diagnosis of third-degree atrioventricular block and second-degree type II atrioventricular block. The patient has a history of hypertension, hypertensive heart disease and coronary artery disease. When hospitalized, her blood pressure was 150/70 mmHg, her heart rate was 48 beats per minute, and her cardiac function was class II by NYHA criteria. No obvious abnormalities were found in her physical tests, serologic test and other biochemical tests.

After clinical evaluation, we proposed implanting a MLP (Medtronic, USA) to mitigate clinical symptoms. The procedure, conducted in the interventional catheterization laboratory, was as follows: After local anesthesia, the patient's left femoral vein was punctured to place the sheath catheter, and temporary pacing electrode was placed in the apex of right ventricle. The pacing started well at a frequency of 60 beats per minute. The patient's right femoral vein was punctured and fed with a stiffened guidewire, while the transfer sheath and delivery system carrying the Micra were delivered into the middle of the right atrium successively, then the delivery system bent across the tricuspid valve to the right ventricular septum (Figure 1A). During the procedure, however, the patient became irritable and her blood pressure dropped to 98/70 mmHg. Metabolic acidosis ensued. Clinical presentations indicated high probability of cardiac perforation in the patient. Therefore, the procedure was terminated.

A multidisciplinary consultation was immediately requested. A medium dose of pericardial fluid and heart compression (Figure 1B) were identified with a Mindray M8 portable color Doppler ultrasound diagnostic instrument and a C5-1 probe (frequency: 2–5 MHz). For emergency treatment, a 12F pigtail catheter (Lingjie, Guangzhou, China) was inserted, with the guidance of ultrasound, to drain the pericardial effusion (Figure 1C). However, conventional ultrasound failed to locate the breach. After orotracheal intubation, autologous blood transfusion, blood transfusion and related medication, the patient's blood pressure temporarily recovered (145/60 mmHg), and she was immediately transferred to the ICU.

After pericardial tamponade was mitigated, the patient was injected 2 ml SonoVue (Bracco Suisse SA) with a 20 G cannula needle through the median cubital vein. Eight seconds later, microsphere contrast agent spilled into pericardial cavity through right ventricular free wall and concentrated locally (Figure 1D; Supplementary Video 1). Notably, this breach was small (inner diameter: c. 4 mm), while the outside of the perforated ventricular wall was surrounded by pericardial tissue and thrombus.

About 30 min after the breach was located, the patient once again fell into a comma, and her blood pressure dropped to 37/32 mmHg. Considering that the patient was too old to undergo open-heart surgery and there was not enough time to transfer her to the operation room, the cardiac surgeon and the ultrasound interventionalist devised a minimally invasive surgical plan for conducting bedside repair of the perforation. That is to put the patient under intravenous anesthesia (rocuronium, propofol, and remifentanil), and directly access the breach through a small intercostal incision. An ultrasonic probe was used for transverse scanning of the fourth and fifth intercostal space in the precordial region. After the breach in the right ventricular wall was located, the probe was rotated by 90 degrees to mark the breach on both the transverse and longitudinal views by pressing with a blunt instrument. The corresponding body surface position was the fourth intercostal space in the precordial region. After routine disinfection, the cardiac surgeon made 2.5 cm incisions leftward and rightward from the anchor point, and then incised the skin, subcutaneous tissue, pericardium and pleura, so as to access the breach in the right ventricular free wall. The perforation was about 6 mm in diameter, larger than that shown by CEUS, while the pericardial and myocardial tissues were brittle. Five stitches of 3-0 prolene with spacers were used to intermittently close the perforation (Figure 1E; Supplementary Video 2). When there was no more

Abbreviations: MLP, Micra Leadless Pacemaker; CEUS, contrast-enhanced ultrasound.

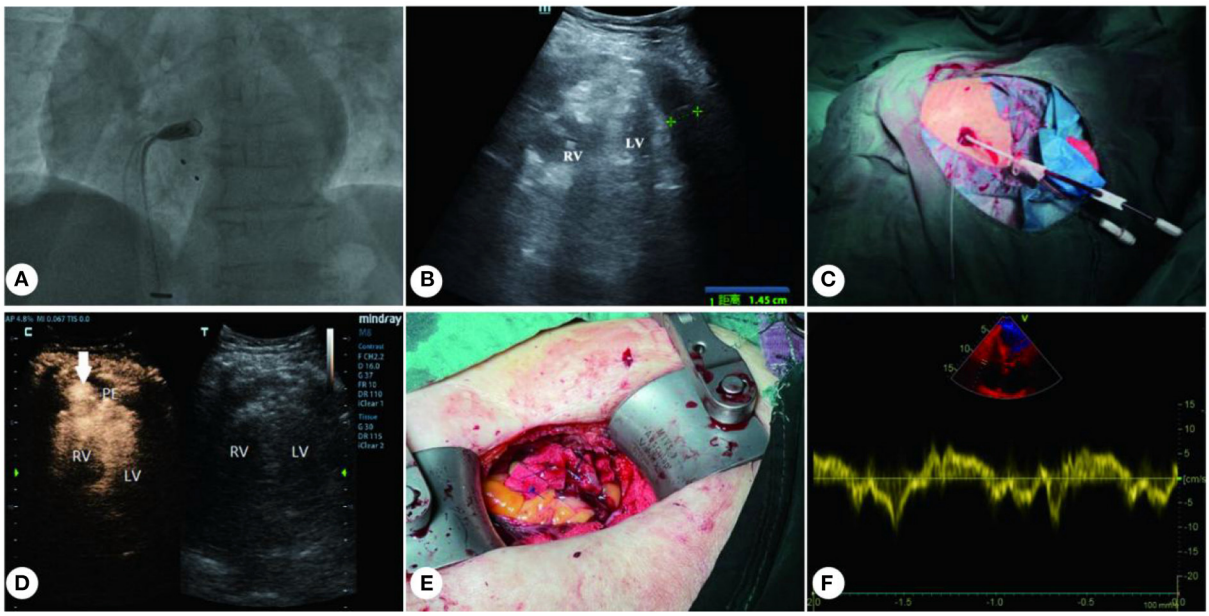

FIGURE 1
Treatment for iatrogenic right ventricular perforation. **(A)** Delivery system carrying the MLP to right ventricle. **(B)** Medium-volume effusion in the pericardial cavity. **(C)** 12F pigtail catheter placed (under ultrasound guidance) into the pericardial cavity. **(D)** CEUS shows right ventricular free wall perforation (with arrow indication). **(E)** 3-0 prolene with spacers were used to close the RV perforation. **(F)** Recovery of cardiac function after surgery. RV, right ventricle; LV, left ventricle; PE, pericardial effusion.

active bleeding, the pericardial blood clot was cleared and the incisions were routinely sutured. The original 12F drainage catheter was retained, and the patient's blood pressure gradually recovered during the procedure.

Two hours after the procedure, the patient's vitals recovered to HR 80 bpm, R 26 bpm, BP 88/37 mmHg, SPO2 100%, and she was successfully resuscitated. Two days after the surgery, transthoracic echocardiography results showed that the patient's cardiac function was restored, with left ventricular ejection fraction at 50% (Figure 1F). After being observed for 10 days to ensure hemodynamic stability, the patient underwent permanent transvenous pacemaker implantation (Medtronic, Minneapolis, Minnesota). Two weeks after the implantation, the patient recovered well and was discharged from the hospital.

Discussion

This case report provides a new emergency treatment—minimally invasive repair of right ventricular free wall perforation with the help of bedside ultrasound. While treating a senile patient with an iatrogenic right anterior ventricular wall perforation, we used CEUS to pinpoint the breach and performed a successful ultrasound-guided bedside repair through a small intercostal incision (Figure 2).

The probability of cardiac perforation or pericardial tamponade during MLP implantation is 1.6% (1). Giudici et al. (6) have successfully used the strategy of temporary-permanent pacemaker in MLP implantation, which is applicable to severely ill patients with underlying diseases and poor prognoses, and can reduce complications. Our placement plan also followed this strategy, but cardiac perforation occurred anyway. We suspect that the perforation resulted from the sheath catheter touching the fragile myocardium during the delivery of the Micra. Research findings show that female, low BMI, history of myocardial infarction and/or pulmonary diseases are significant factors that may cause cardiac perforation during MLP implantation (7). The patient herein is a senile woman with several underlying diseases; her conditions are a key factor causing cardiac perforation.

Bedside ultrasound plays a key role in early detection of pericardial effusion and pericardial tamponade. However, conventional ultrasound often fails to pinpoint the breach since the perforation is of a small inner diameter. Our case proved that CEUS has additional diagnostic value in this regard. Mittle et al. (8) also reported that CEUS can better diagnose cardiac rupture. Immediate intervention should be performed if spillage of contrast agent into the pericardial cavity or evidence of pseudoaneurysm is detected. Other cases also proved that focused transesophageal echocardiography (TEE) is a safe and efficient means for diagnosing an iatrogenic cardiac perforation in the posterior lateral free wall (9). It should be emphasized that not all cases of myocardial rupture will present spillage of

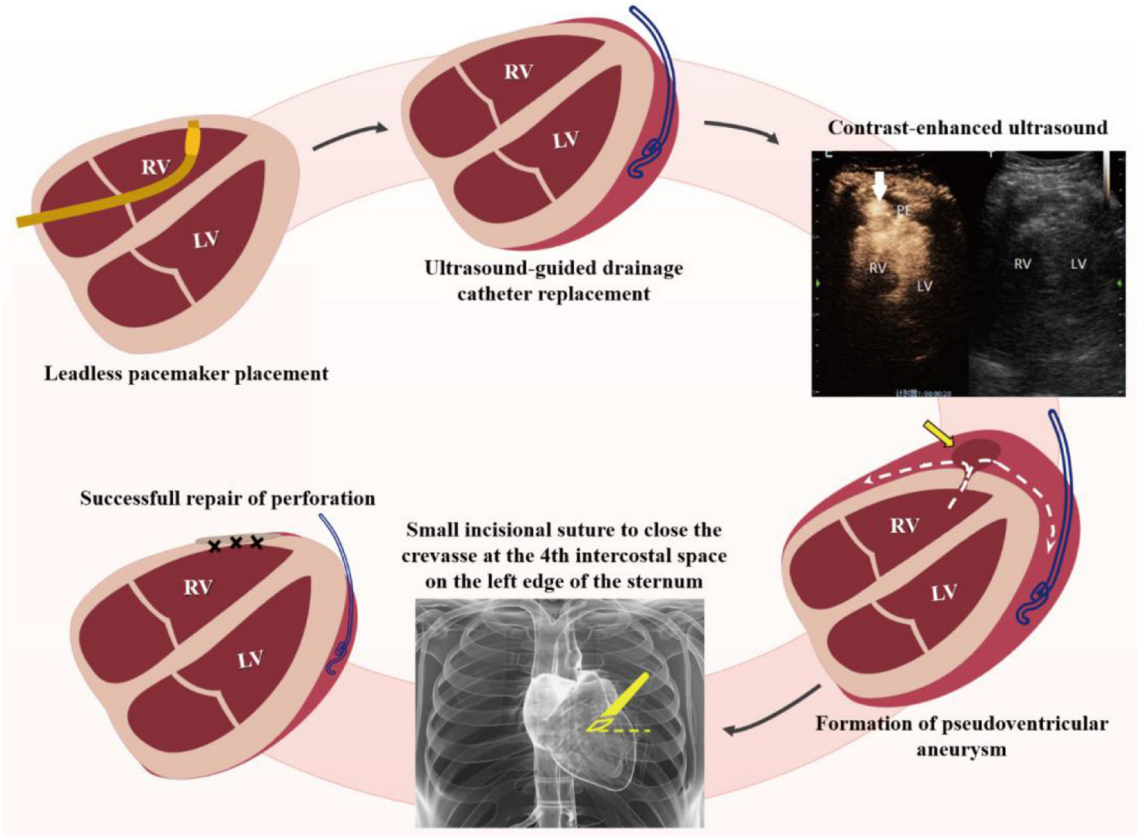

FIGURE 2
Schematic diagram of treatment for iatrogenic right ventricular perforation. RV, right ventricle; LV, left ventricle; PE, pericardial effusion.

ventricular contrast agent into the pericardial space, as some cases may present a local filling defect due to obstruction of the rupture site by thrombus (8).

Bedside pericardiocentesis is an essential procedure for emergency care, while ultrasound can play a key role in preventing myocardial re-injury. For right ventricular perforation, interventional procedure can be implemented to close the breach when the patient is hemodynamically stable (10). Such a procedure requires that the catheterization laboratory is equipped with corresponding hardware and expertise (4, 5). Thoracotomy for repair of cardiac perforation in the presence of life-threatening complications is an effective therapy (3). However, such a procedure is not applicable to some patients, due to the high risks of thoracotomy, advanced age and underlying diseases. Take our case for example. Sudden recurrence of pericardial tamponade left no time for transferring the patient to the operating room or the interventional catheterization laboratory. In this context, emergency bedside surgery was a new and daring attempt.

To the best of our knowledge, we reported the first case of a senile patient undergoing successful CEUS-guided bedside minimally invasive repair of an iatrogenic ventricular wall perforation through a small intercostal incision. With no need for sternotomy and temporary cardiac arrest, the patient was only under intravenous anesthesia. Guided by bedside ultrasound, we accessed the breach through a transverse incision along the intercostal space. Such a procedure, featuring smaller surgical trauma, can serve as an alternative of bedside emergency treatment. The three key factors of the successful procedure are: (1) CEUS can help pinpoint the perforation and evaluate its severity; (2) The breach was close to the thoracic wall, allowing ultrasound-guided direct access through a small intercostal incision; and (3) The breach was small, and the intraoperative blood extravasation was slow as a result of weakened heart beating, which made bedside procedure viable. Our experience in this case may serve as a good reference in the emergency treatment for right ventricular free wall perforation.

Conclusion

To sum up, bedside ultrasound plays a key role in the diagnosis of and treatment for cardiac perforation, while CEUS can enhance diagnosis of small perforations on the

myocardial wall. For right ventricular free wall perforation in life-threatening emergencies, bedside ultrasound-guided small-incision surgical repair is an alternative emergency treatment modality, which helps avoid unnecessary cardiac surgery with sternotomy.

Data availability statement

The original contributions presented in the study are included in the article/Supplementary material, further inquiries can be directed to the corresponding author/s.

Ethical statement

This study, involving a human participant, has been reviewed and approved by Fujian Provincial Hospital. The participant has provided her written informed consent to participate in this study. Written informed consent was obtained from the individual for the publication of any and all images or data included in this report.

Author contributions

YZ followed the patients and wrote the paper. SW, BL, LL, LC, QX, and XZ participated in the treatment of patients. YL contributed in picture editor. All authors contributed to the article and approved the submitted version.

Funding

This study was funded by a grant (grant number: 2020J011090) from the Natural Science Foundation of Fujian Province.

Acknowledgments

All authors herein are grateful to Fujian Provincial Hospital for its support.

Conflict of interest

The authors declare that the research was conducted in the absence of any commercial or financial relationships that could be construed as a potential conflict of interest.

Publisher's note

Supplementary material

The Supplementary Material for this article can be found online at: https://www.frontiersin.org/articles/10.3389/fcvm.2022.986904/full#supplementary-material

SUPPLEMENTARY VIDEO 1
Contrast-enhanced ultrasound (CEUS) of ventricular wall perforation.

SUPPLEMENTARY VIDEO 2
Minimally invasive repair of cardiac perforation.

References

1. Pagan E, Gabriels J, Khodak A, Chang D, Beldner S, Epstein LM, et al. Safety of leadless pacemaker implantation in the very elderly. *Heart Rhythm.* (2020) 17:2023–8. doi: 10.1016/j.hrthm.2020.05.022

2. Chan KH, McGrady M, Wilcox I. A leadless intracardiac transcatheter pacing system. *N Engl J Med.* (2016) 374:2604. doi: 10.1056/NEJMc1604852

3. Provaznik Z, Holzamer A, Camboni D, Rupprecht L, Resch M, Wittmann S, et al. Perforation of myocardial wall and great vessels after cardiovascular interventions-a 5-year analysis. *J Thorac Dis.* (2017) 9:5288–94. doi: 10.21037/jtd.2017.10.113

4. Zipse MM, Messenger JC, Carroll JD, Seres T. Percutaneous repair of right ventricular perforation with Amplatzer septal defect occlusion device. *Eur Heart J.* (2018) 39:817. doi: 10.1093/eurheartj/ehw514

5. Saxena A, Karmakar S, Narang R. Successful percutaneous device closure of right ventricular perforation during pericardiocentesis. *JACC Cardiovasc Interv.* (2016) 9:e221–2. doi: 10.1016/j.jcin.2016.09.031

6. Giudici M, Shantha G, Rasmussen T. Temporary-permanent pacemakers - why they should be in your toolbox. Circulation. (2017) 136:A18226. doi: 10.1161/circ.136.suppl_1.18226

7. Kirkfeldt RE, Johansen JB, Nohr EA, Jørgensen OD, Nielsen JC. Complications after cardiac implantable electronic device implantations: an analysis of a complete, nationwide cohort in Denmark. *Eur Heart J.* (2014) 35:1186–94. doi: 10.1093/eurheartj/eht511

8. Mittle S, Makaryus AN, Mangion J. Role of contrast echocardiography in the assessment of myocardial rupture. *Echocardiography.* (2003) 20:77–81. doi: 10.1046/j.1540-8175.2003.00012.x

9. Yeoh CB, Fischer GW, Tollinche LE. Focused transesophageal echocardiography for bedside diagnosis of iatrogenic cardiac perforation: a case report. *A A Pract.* (2019) 13:407–8. doi: 10.1213/XAA.0000000000001077

10. Petrov I, Dimitrov C. Closing of a right ventricle perforation with a vascular closure device. *Catheter Cardiovasc Interv.* (2009) 74:247–50. doi: 10.1002/ccd.21997

frontiers | Frontiers in Cardiovascular Medicine

TYPE Case Report
PUBLISHED 21 October 2022
DOI 10.3389/fcvm.2022.1023501

OPEN ACCESS

EDITED BY
Hendrik Tevaearai Stahel,
Bern University Hospital, Switzerland

REVIEWED BY
Randolph Wong,
Prince of Wales Hospital, China
Maruti Haranal,
U N Mehta Institute of Cardiology and Research, India

*CORRESPONDENCE
Huiming Guo
guohuiming@gdph.org.cn

SPECIALTY SECTION
This article was submitted to Heart Surgery, a section of the journal Frontiers in Cardiovascular Medicine

RECEIVED 19 August 2022
ACCEPTED 23 September 2022
PUBLISHED 21 October 2022

CITATION
Tan T, Liu H, Ma J, Liu J, Yuan H and Guo H (2022) Case report: Total thoracoscopic repair of sinus of Valsalva aneurysm combined with ventricular septal defect. *Front. Cardiovasc. Med.* 9:1023501. doi: 10.3389/fcvm.2022.1023501

Case report: Total thoracoscopic repair of sinus of Valsalva aneurysm combined with ventricular septal defect

Tong Tan[1,2], Haozhong Liu[1,2], Jianrui Ma[1,2], Jian Liu[1], Haiyun Yuan[1] and Huiming Guo[1]*

[1]Department of Cardiovascular Surgery, Guangdong Provincial Key Laboratory of South China Structural Heart Disease, Guangdong Cardiovascular Institute, Guangdong Provincial People's Hospital, Guangdong Academy of Medical Sciences, Guangzhou, China, [2]Shantou University Medical College, Shantou, China

The sinus of Valsalva aneurysm (SVA) is a rare cardiac anomaly. It can develop into the heart failure if it ruptures, which requires early intervention. However, such congenital anomalies are usually treated using a median sternotomy approach. Here, we report a rare case of SVA combined with a ventricular septal defect in which the patient underwent patch repair of the defects under a total thoracoscopy approach. She was discharged uneventfully and showed no residual shunt or aortic regurgitation postoperatively or at the 12-month follow-up. The total thoracoscopic approach for SVA repair is technically feasible.

KEYWORDS

Valsalva aneurysm, ventricular septal defect, total thoracoscopic surgery, transaortic approach, congenital heart surgery

Introduction

A sinus of Valsalva aneurysm (SVA) is an abnormal bulge located between the aortic valve annulus and the sinotubular junction that does not belong to any coronary sinuses. It is a rare cardiac anomaly occurring in less than 1% of the cases (1). It is predominant in males (4:1) and most common in young Asian individuals (2, 3). The natural history of SVA has been suggested to contribute to a deficiency of the elastic fibers between the aortic media and the annulus fibrosis layer (4). The sinus of origin most commonly involves the right coronary, followed by the non-coronary and the left coronary. Most unruptured SVAs are asymptomatic, depending on the degree of left to right shunt and associated lesions, but SVA rupturing into the ventricular system may cause acute onset symptoms and even heart failure in severe cases. Since the first successful surgery of SVA was reported by Lillehei et al. (5), the safety and efficiency of thoracotomy surgery to repair SVA has been demonstrated in numerous studies (2, 5, 6).

We performed repair of the shunts under total thoracoscopy for a patient diagnosed with SVA combined with the ventricular septal defect (VSD).

Case presentation

A 48-year-old female visited our clinic with complaints of dyspnea for 4 months. On arrival, her vital signs were stable, including a body temperature of 36.1°C, a heart rate of 96 beats/min, a respiratory rate of 20 breaths/min, and a blood pressure of 121/67 mmHg. Jugular vein distension or limb edema was absent. A continuous third-degree heart murmur was noted over the left sternal border. She was diagnosed with SVA at the age of 15. However, she was asymptomatic until 6 years ago, when she experienced occasional shortness of breath and fatigue. Surgery was recommended, but she accepted medical therapy for fear of cardiac surgery. Four months prior to her presentation, her symptoms were exacerbated, and she developed dyspnea. Transthoracic echocardiography (TTE) showed a 10.6 mm × 9.6 mm dilated SVA with a ruptured right coronary sinus into the right ventricular outflow tract (RVOT) (**Figure 1A**). The diameter of the aortocardial shunt was approximately 5.0 mm, and turbulent blood flow was observed from the aorta to the RVOT with a peak flow velocity of 4.9 m/s and a pressure gradient of 96 mmHg. The aortic regurgitation was traced, but the aortic valve anatomy and function were normal. The atria and ventricles remained normal in size. The ejection fraction of the left ventricle was 64%. No defects involving the atrial septum or the ventricular septum, endocarditis, or severe valvular regurgitation were noted on TTE. However, transesophageal echocardiography (TEE) revealed a small infundibular VSD with no other congenital pathology.

The patient provided written and fully informed consent, and she underwent surgical repair through a totally thoracoscopic approach. After insertion of a double-lumen tracheal intubation under general anesthesia, the patient was placed in the supine position with the right chest elevated by 15 degrees (**Figure 2A**). Cannulation will be carried out through the femoral artery and vein. A soft tissue retractor was inserted into the working port established in the third intercostal space lateral to the right midclavicular line (**Figure 2B**). The assistant port was made in the third intercostal space in the anterior axillary line, where the thoracoscope, an aortic cross-clamp and a left ventricle vent catheter were placed (**Figure 2A**). Cardiopulmonary bypass and moderate systemic hypothermia were initiated. The ascending aorta was cross-clamped and then transected. Antegrade perfusion of histidine–tryptophan–ketoglutarate cardioplegia solution was infused directly into the coronary ostia. In total, two or three retraction sutures were placed over the transected aorta to achieve full exposure of the aortic root (**Figure 2C**). An infundibular VSD was detected with its superior border connected to the right coronary valve of the aortic valve. The SVA originating in the right coronary sinus was also found, from which an aorto-right ventricular fistula was created. The VSD and the SVA were repaired with two separate bovine pericardial patches with interrupted 4–0 monofilament sutures and reinforced at the edge with Gore-Tex pledgetted sutures (**Supplementary Video 1**). The effect of patch repair was evaluated by saline injection, and postoperative TEE confirmed that no interventricular or aorto-right ventricular shunt flow existed. The cardiopulmonary bypass time (CPB) was 127 min, and the aortic cross-clamp (ACC) time was 88 min. The patient stayed in the ICU for 1 day and was discharged uneventfully 5 days postoperatively. At the 12-month follow-up, TTE demonstrated no residual shunt or valve regurgitation (**Figure 1B**).

Discussion

The SVA can be either ruptured or non-ruptured. Non-ruptured SVA is usually asymptomatic, while ruptured SVA presents with symptoms of ventricular overload, such as dyspnea and decreased activity tolerance. The symptoms of ruptured SVA might be delayed due to good tolerance of the right heart. Patients with ruptured SVAs usually express themselves at an average age of 34 (ranging from 11 to 67 years old) (7). For ruptured SVAs, Sakakibara and Konno first proposed a classification system to distinguish their site of origin and rupture (8). However, it only includes SVAs originating from the right coronary sinus (Types I to III), non-coronary (Type IV) and protruding into the right ventricle and right atrium. Xin-Jin et al. proposed a modified Sakakibara classification system with five types that is simpler and more practical for clinical use, according to the site of SVA rupture (9).

Although SVA is rare, it is frequently associated with other congenital cardiac anomalies, such as VSD, aortic regurgitation, and tetralogy of Fallot (10–12). The combined VSD could be a membranous, perimembranous, supracristal or muscular type, and the supracristal type is the principal type associated with ruptured SVA (13). However, VSD could be missed preoperatively by TTE, as in our case. Some case reports contributed to the aortocardiac shunt overlapping with the VSD shunt, which might also occur in our case. Other reasons included either the large aneurysmal sacs embedded into the VSD or the shunt flow across the VSD reduced by high right ventricular pressure (14–16). Therefore, TEE, three-D echocardiogram, CT or MRI are recommended modalities to improve the early detection rate of VSD and the accuracy of diagnosis (16, 17).

Ruptured SVAs require early surgical repair, and excellent long-term outcomes have been reported (18). Apart from the traditional open surgical approach, including aortotomy, right atriotomy, and right ventriculotomy, the minimally invasive

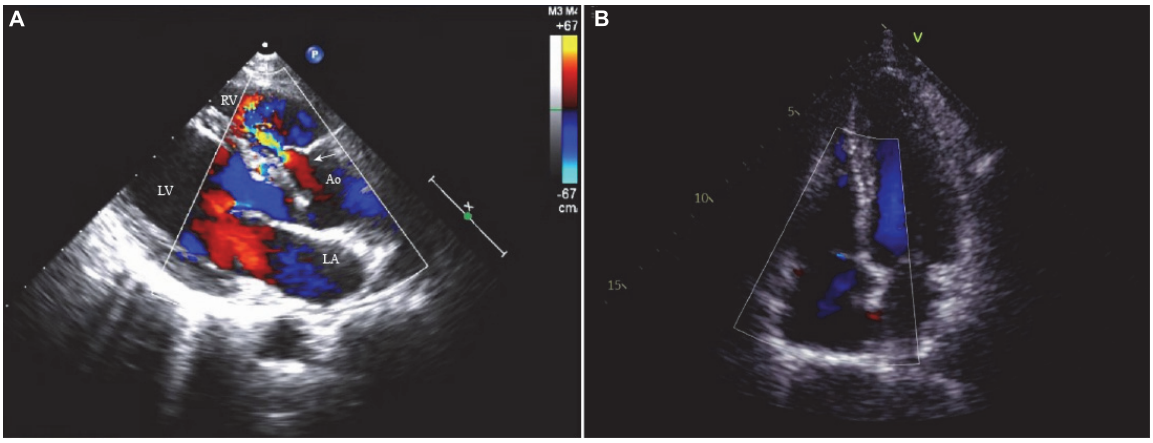

FIGURE 1
(A) The two-dimensional echocardiogram showed a 10.6 mm × 9.6 mm ruptured sinus of Valsalva aneurysm (right coronary sinus) and a 5.0 mm aortocardiac shunt (*white arrow*). **(B)** No residual shunt or valve regurgitation noted on the postoperative echocardiogram. LA, left atrium; LV, left ventricle; RV, right ventricle; Ao, aorta.

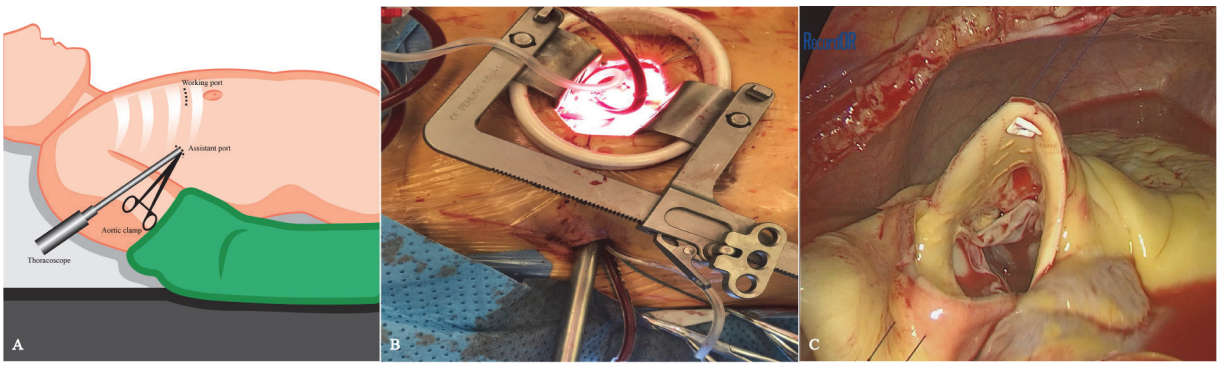

FIGURE 2
Schematic diagram of the thoracoscopic procedure. **(A)** The patient was positioned in a supine position with the right chest elevated by 15 degrees. The working port was placed at the third intercostal space on the mid-clavicular line, while the thoracoscopic port was made in the third intercostal space at the level of the anterior axillary line. **(B)** Thoracoscopic approach view. **(C)** To fully expose the aortic root, two or three retraction sutures were placed over the transected aorta.

surgical approach has become increasingly preferred. In our case, the patient was satisfied with the minimal invasiveness and cosmetic results of total thoracoscopy. In addition, the incidence of SVA is higher in young to middle-aged adults; the total thoracoscopic approach has a better chance of reoperation than median sternotomy. The total thoracoscopic technique has been reported and effectively used for some congenital cardiac diseases, such as VSD and atrial septal defect (19, 20). Fukumoto et al. (21) reported a case of aorto-right ventricular fistula using 3D endoscopy. To the best of our knowledge, our case is the first reported case of total thoracoscopic repair of SVA combined with VSD. Our approach was similar to the thoracoscopic aortic valve replacement at our center. The endoscope provides a good view of the right coronary cusp and non-coronary cusp while exposing the infundibular VSD well (**Figures 3A,B**). In some cases, the SVA was associated with cardiovascular lesions, fistula opening to the right atrium, and even severe RVOT obstruction (22–24). Note such complex cardiac anomalies require more detailed surgical exploration and more manipulation instead of simple repair with patch through transaortic approach. We carefully evaluated preoperative imaging data (especially TEE) and applied this approach for excellent exposure of the aneurysm and the VSD that were easily targeted. Such an approach is technically feasible, as we successfully repaired both the SVA and VSD with patches without residual shunts or aortic regurgitation noted postoperatively (**Figures 3C,D**) or at the 12-month follow-up. The CPB and ACC times were comparable to those of the conventional approach, and our patient made an expedient recovery and was discharged uneventfully. We also have extensive experience with aortic

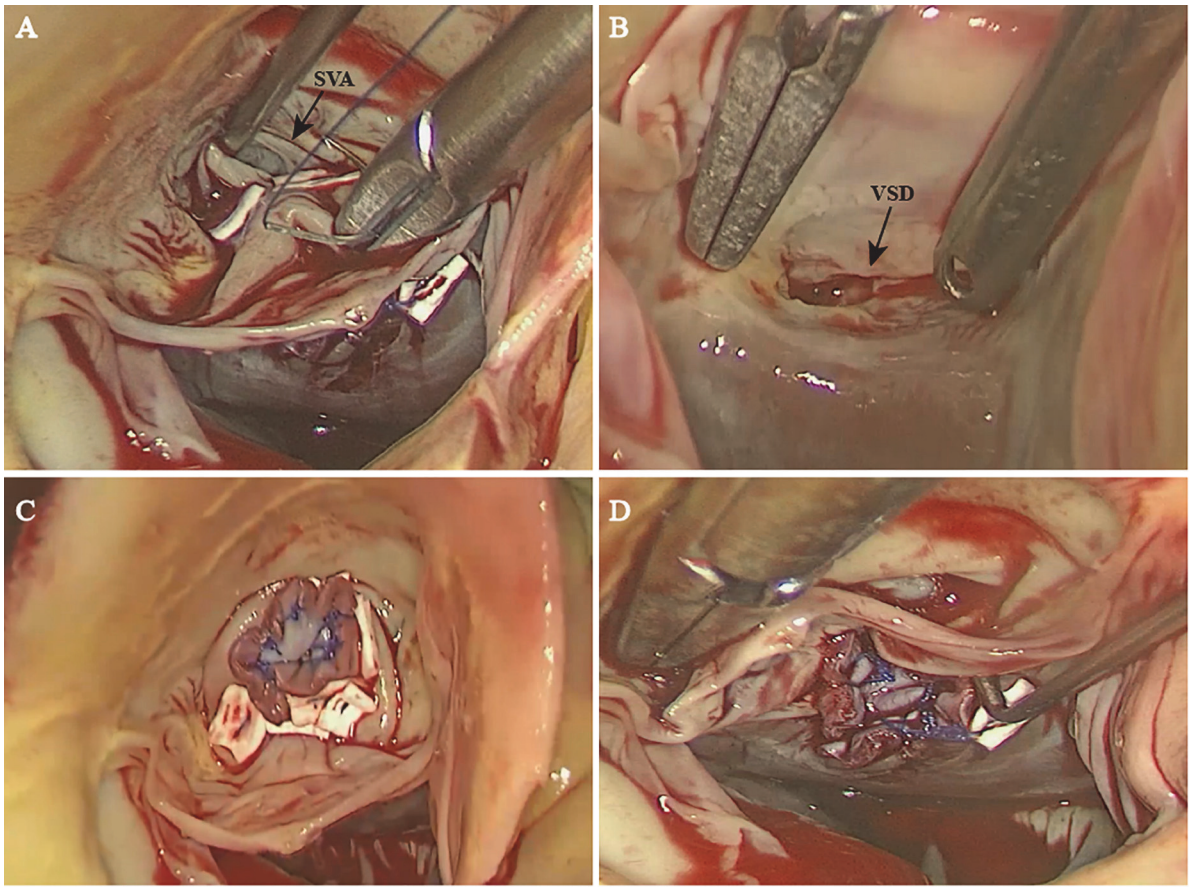

FIGURE 3
The sinus of Valsalva with a ruptured right coronary sinus **(A)** and the ventricular septal defect **(B)** were exposed well through the endoscope. The sinus of Valsalva aneurysm **(C)** and the ventricular septal defect **(D)** were successfully repaired with a patch. SVA, sinus of Valsalva aneurysm; VSD, ventricular septal defect.

valve surgery; therefore, aortic valvuloplasty or aortic valve replacement could be performed under endoscopy if necessary.

In conclusion, total thoracoscopic repair of selected SVAs combined with VSD is a minimally invasive procedure with a clear visual field of the orifice of the fistula. Such an approach is technically feasible and has excellent outcomes.

Data availability statement

The original contributions presented in the study are included in the article/**Supplementary material**, further inquiries can be directed to the corresponding author.

Ethics statement

This study was performed in accordance with the Declaration of Helsinki and approved by the Ethics Committee of Guangdong Provincial People's Hospital, Guangdong Academy of Medical Sciences (No. KY-Q-2022-223-01). The patients/participants provided their written informed consent to participate in this study. Written informed consent was obtained from the individual(s) for the publication of any potentially identifiable images or data included in this article.

Author contributions

TT and HL contributed to study design, data acquisition, and manuscript drafting. JM, JL, HY, and HG contributed greatly to the revision of the manuscript. HG approved the submission of the final version. All authors contributed to the article and approved the submitted version.

Funding

This study was supported by grants from Cardiovascular Special Project of Guangdong Provincial People's Hospital

(2020XXG010), Guangdong Provincial Clinical Research Center for Cardiovascular Disease (2020B1111170011), Science and Technology Program of Guangzhou (202201010768), and also supported by Guangdong special funds for science and technology innovation strategy, China (Stability support for scientific research institutions affiliated to Guangdong Province-GDCI 2021).

Conflict of interest

The authors declare that the research was conducted in the absence of any commercial or financial relationships that could be construed as a potential conflict of interest.

Publisher's note

Supplementary material

The Supplementary Material for this article can be found online at: https://www.frontiersin.org/articles/10.3389/fcvm.2022.1023501/full#supplementary-material

References

1. Takach TJ, Reul GJ, Duncan JM, Cooley DA, Livesay JJ, Ott DA, et al. Sinus of Valsalva aneurysm or fistula: management and outcome. *Ann Thorac Surg.* (1999) 68:1573–7. doi: 10.1016/s0003-4975(99)01045-0

2. Lee JH, Yang JH, Park PW, Song J, Huh J, Kang IS, et al. Surgical repair of a sinus of Valsalva aneurysm: a 22-year single-center experience. *Thorac Cardiovasc Surg.* (2021) 69:26–33. doi: 10.1055/s-0039-1692660

3. Scagliotti D, Fisher EA, Deal BJ, Gordon D, Chomka EV, Brundage BH. Congenital aneurysm of the left sinus of Valsalva with an aortopulmonary tunnel. *J Am Coll Cardiol.* (1986) 7:443–5. doi: 10.1016/s0735-1097(86)80520-4

4. Bass D, Tivakaran VS. *Sinus Of Valsalva Aneurysm*. Treasure Island, FL: StatPearls (2022).

5. Lillehei CW, Stanley P, Varco RL. Surgical treatment of ruptured aneurysms of the sinus of Valsalva. *Ann Surg.* (1957) 146:459–72. doi: 10.1097/00000658-195709000-00014

6. Jaswal V, Kumar V, Thingnam SKS, Puri GD. Surgical repair of ruptured sinus of Valsalva aneurysm: 13-year single center experience. *J Card Surg.* (2021) 36:1264–9. doi: 10.1111/jocs.15358

7. Perloff JK. Congenital heart disease in adults. A new cardiovascular subspecialty. *Circulation.* (1991) 84:1881–90. doi: 10.1161/01.cir.84.5.1881

8. Sakakibara S, Konno S. Congenital aneurysm of the sinus of Valsalva. Anatomy and classificati on. *Am Heart J.* (1962) 63:405–24. doi: 10.1016/0002-8703(62)90287-9

9. Xin-Jin L, Xuan L, Bo P, Hong-Wei G, Wei W, Shou-Jun L, et al. Modified Sakakibara classification system for ruptured sinus of Valsalva aneurysm. *J Thorac Cardiovasc Surg.* (2013) 146:874–8. doi: 10.1016/j.jtcvs.2012.12.059

10. Sarikaya S, Adademir T, Elibol A, Buyukbayrak F, Onk A, Kirali K. Surgery for ruptured sinus of Valsalva aneurysm: 25-year experience with 55 patients. *Eur J Cardiothorac Surg.* (2013) 43:591–6. doi: 10.1093/ejcts/ezs450

11. Hartlage GR, Consolini MA, Pernetz MA, Williams BR III, Clements SD, Chen EP, et al. Bad company: supracristal VSD presenting with ruptured sinus of valsalva aneurysm. a case presentation with echocardiographic depiction and an analysis of contemporary literature. *Echocardiography.* (2015) 32:575–83. doi: 10.1111/echo.12718

12. Togashi K, Paez FJG, Sheu RD. Sinus of Valsalva aneurysm rupture associated with a ventricular septal defect: the importance of multi-angle assessment by intraoperative transesophageal echocardiography. *J Cardiothorac Vasc Anesth.* (2020) 34:3376–81. doi: 10.1053/j.jvca.2020.07.028

13. Ishii M, Masuoka H, Emi Y, Mori T, Ito M, Nakano T. Ruptured aneurysm of the sinus of valsalva coexisting with a ventricul ar septal defect and single coronary artery. *Circ J.* (2003) 67:470–2. doi: 10.1253/circj.67.470

14. Sarhan HHT, Shawky AH, Anilkumar S, Elmaghraby A, Sivadasan PC, Omar AS, et al. Association of ruptured sinus of Valsalva aneurysm and congenital ventricular septal defect: a case series. *Eur Heart J Case Rep.* (2021) 5:ytab233. doi: 10.1093/ehjcr/ytab233

15. Jin Y, Han XM, Wang HS, Wang ZW, Fang MH, Yu Y, et al. Coexisting ventricular septal defect affects the features of ruptured sinus of Valsalva aneurysms. *Saudi Med J.* (2017) 38:257–61. doi: 10.15537/smj.2017.3.15842

16. Gurgun C, Ozerkan F, Akin M. Ruptured aneurysm of sinus of valsalva with ventricular septal defect: the role of transesophageal echocardiography in diagnosis. *Int J Cardiol.* (2000) 74:95–6. doi: 10.1016/s0167-5273(00)00261-8

17. Masaki N, Iwatsuka R, Nagahori W, Ohno M, Arakawa T, Suzuki M, et al. Three-dimensional echocardiography could distinguish a ventricular sep tal defect adjacent to asymptomatic ruptured sinus of valsalva aneurysm. *J Cardiol.* (2008) 51:139–43. doi: 10.1016/j.jjcc.2008.01.007

18. van Son JA, Danielson GK, Schaff HV, Orszulak TA, Edwards WD, Seward JB. Long-term outcome of surgical repair of ruptured sinus of Valsalva aneurysm. *Circulation.* (1994) 90(5 Pt. 2):II20–9.

19. Zhou K, Yang L, He BC, Ke YJ, Yang YC, Yan Q, et al. Total thoracoscopic repair of ventricular septal defect: a single-center experience. *J Card Surg.* (2021) 36:2213–8. doi: 10.1111/jocs.15504

20. Ma ZS, Dong MF, Yin QY, Feng ZY, Wang LX. Totally thoracoscopic closure for atrial septal defect on perfused beating hearts. *Eur J Cardiothorac Surg.* (2012) 41:1316–9. doi: 10.1093/ejcts/ezr193

21. Fukumoto Y, Hosoba S, Goto Y, Ito T. Totally 3D-endoscopic patch closure of aorto-right ventricular fistula. *JTCVS Tech.* (2020) 3:47–9. doi: 10.1016/j.xjtc.2020.06.010

22. Qiu J, Xie E, Wang Y, Wang W, Yu C, Luo X. Surgical interventions are effective for treating unruptured sinus of Valsalva aneurysms. *Front Cardiovasc Med.* (2021) 8:707147. doi: 10.3389/fcvm.2021.707147

23. Doost A, Craig JA, Soh SY. Acute rupture of a sinus of Valsalva aneurysm into the right atrium: a case report and a narrative review. *BMC Cardiovasc Disord.* (2020) 20:84. doi: 10.1186/s12872-020-01383-7

24. Abu Saleh WK, Lin CH, Reardon MJ, Ramlawi B. Right ventricular outflow tract obstruction caused by isolated sinus of Valsalva aneurysm. *Tex Heart Inst J.* (2016) 43:357–9. doi: 10.14503/THIJ-15-5407

frontiers | Frontiers in Cardiovascular Medicine

TYPE Case Report
PUBLISHED 03 November 2022
DOI 10.3389/fcvm.2022.1001073

OPEN ACCESS

EDITED BY
Hendrik Tevaearai Stahel,
Bern University Hospital, Switzerland

REVIEWED BY
Şami Akbulut,
İnönü University, Turkey
Yener Aydin,
Atatürk University, Turkey

*CORRESPONDENCE
Yingqiang Guo
drguoyq@hotmail.com

†These authors have contributed equally to this work and share first authorship

SPECIALTY SECTION
This article was submitted to Heart Surgery, a section of the journal Frontiers in Cardiovascular Medicine

RECEIVED 22 July 2022
ACCEPTED 23 September 2022
PUBLISHED 03 November 2022

CITATION
Liu L, Wu B, Li M and Guo Y (2022) Case report: Right atrium-inferior vena cava bypass in a patient with unusual cardiac cystic echinococcosis. *Front. Cardiovasc. Med.* 9:1001073. doi: 10.3389/fcvm.2022.1001073

Case report: Right atrium-inferior vena cava bypass in a patient with unusual cardiac cystic echinococcosis

Lulu Liu†, Binggang Wu†, Mei Li and Yingqiang Guo*

Department of Cardiovascular Surgery, West China Hospital, Sichuan University, Chengdu, China

Cardiovascular hydatid disease is caused by parasitic infection of *Echinococcus granulosus*, which could be asymptomatic or life-threatening depending on lesion site, granuloma size, and disease progression. Diagnosis and treatment of cardiac echinococcosis should be under comprehensive consideration. In this case, we reported a successful right atrium-inferior vena cava bypass surgery in a 31-year-old female with unresectable right atrial echinococcosis and inferior vena cava obstruction.

KEYWORDS

hydatid disease, cardiac echinococcosis, right atrium mass, inferior vena cava obstruction, vascular bypass graft

Introduction

Hydatid disease is caused by *Echinococcus* species, which remains to be a common and severe public health problem in husbandry areas. Cystic echinococcosis is responsible for 95% of human hydatid cases. Humans are accidental hosts and are usually infected by ingesting parasitic ova (1). Cardiac involvement is uncommon for hydatid disease, which is usually found in the liver and lungs. Most of the patients are asymptomatic and the discovery of cardiac echinococcosis is often incidental. However, cardiac hydatid disease might lead to severe complications, including severe allergic reaction resulting from intracardiac rupture of hydatid cyst and sudden death caused by pulmonary embolism or acute valvular obstruction (2). Although there is no official guideline for the treatment of cardiac hydatid disease, surgical R0 resection associated with albendazole-based chemotherapy is usually preferred (3). For the patients whose cardiac lesion could not achieve R0 resection, the perioperative management and clinical outcome remain to be a tough problem. We reported a case in which palliative vascular bypass surgery was performed on a patient with unresectable right-atrium echinococcosis.

Case presentation

Case description

A 31-year-old female patient was admitted to the hospital with repeated hemoptysis and dyspnea on exertion for 3 years. In addition, a fever reaching 39°C and watery diarrhea had occurred 4 days before admission. Long-term residence history in an endemic area of echinococcosis was confirmed on admission. On physical examination, the patient presented with persistent tachycardia of 102 beats per minute. Besides, the cardiac murmur was not found during auscultation of the heart. Peripheral blood test demonstrated concurrent moderate anemia with the hemoglobin (Hb) of 85 g/L and eosinophilia with the eosinophil percentage (EO%) of 10.6%. The hepatic function test showed elevation in total bilirubin (TBIL, 32.1 μmol/L) and direct bilirubin (DBIL, 16.4 μmol/L), while alanine transaminase (ALT) and aspartate transaminase (AST) remained normal. Furthermore, detection of the echinococcosis granulosus IgG was positive. Preoperative transthoracic echocardiography (TTE) revealed a 24 mm × 50 mm immobile mass extending from the inferior vena cava (IVC) into the right atrium. There was no clear boundary between the epicardium and the mass (**Figure 1A**). Computed tomography angiogram (CTA) and magnetic resonance imaging (MRI) confirmed the mass, while multiple lesions were also found in the left lung and the brain (**Figures 1B–E** and **Supplementary Video 1**). In addition, the azygos vein dilated significantly as a compensatory sign of IVC obstruction (**Figure 1F**). Transbronchoscopic lung biopsy demonstrated that the pathological diagnosis of the left lung lesion was granulomatous inflammation resulting from echinococcosis infection.

Diagnostic assessment

After 4-week therapy with albendazole (400 mg, three times per day), cardiac surgery was performed to relieve obstruction of IVC. The pericardium was opened following a median sternotomy and the extracorporeal circulation was established by cannulation of the right femoral artery, right femoral vein

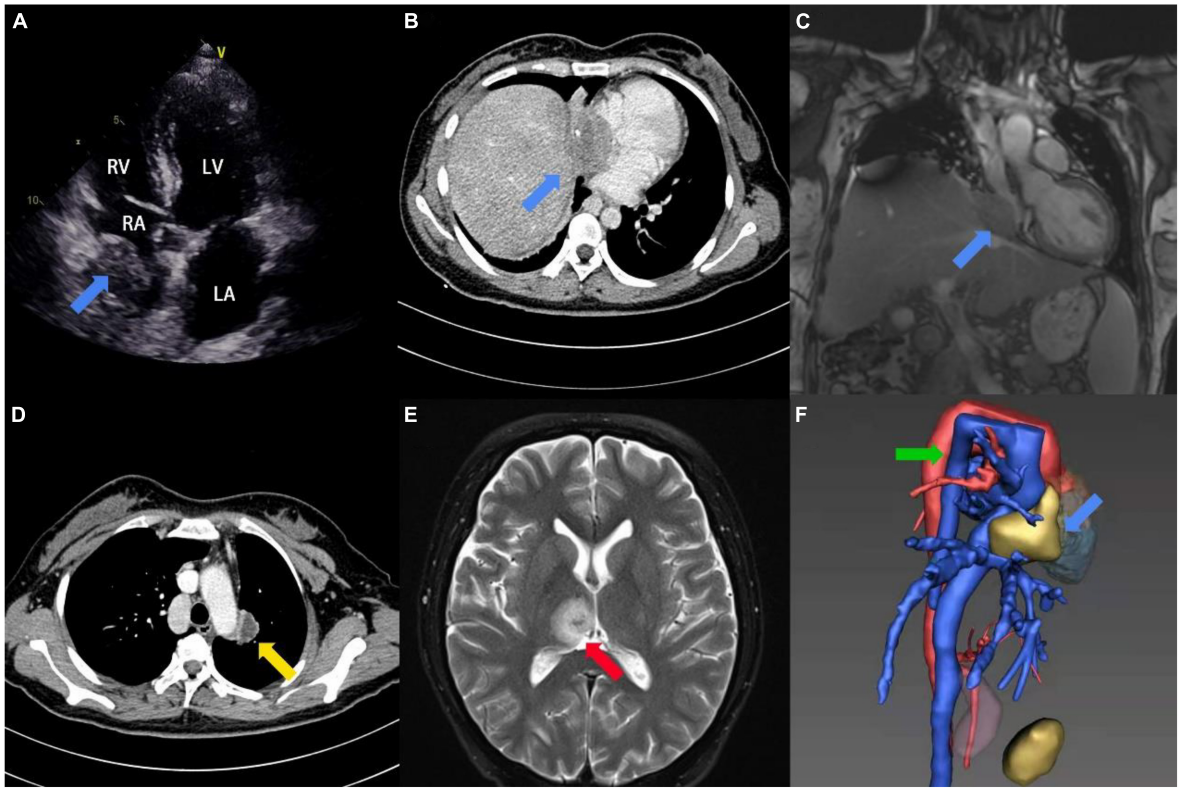

FIGURE 1
Image findings. **(A)** Preoperative 2D-TTE four-chamber view showed an irregular mass (blue arrow) within the right atrium. **(B)** Preoperative CTA showed a mass with slight calcification (blue arrow) within the right atrium and IVC. **(C)** Preoperative MRI showed a hypointense mass (blue arrow) at the junction of the right atrium and IVC on coronary-reconstruction view. **(D)** Preoperative CTA showed a lesion with slight enhancement in the left lung (yellow arrow). **(E)** Preoperative MRI showed an oval hypertense lesion (red arrow) within the brain on T2-weighted image. **(F)** 3D-reconstruction view of preoperative CTA showed the cardiac mass (blue arrow) and enlarged azygos vein (green arrow).

and superior vena cava (SVC). Then antegrade cardioplegic perfusion was performed and a right atriotomy was applied to expose the mass. A piece of 24 mm × 50 mm gray hard tissue was found within the right atrium, which invaded outward to form tight adhesions with the pericardium, right phrenic nerve, right lower lung, and diaphragm. The mass also invaded downward and resulted in severe obstruction of the IVC. The intracavitary portion of the mass and part of the right atrium wall were removed for test and the diagnosis of intraoperative frozen section examination was granulomatous inflammation. Complete resection of the mass was evaluated to be impossible after rigorous discussion among cardiovascular surgeons, cardiologists, and infectiologists, therefore the IVC was fully exposed with the assistance of the right-sided thoracotomy and a right atrium-IVC bypass was performed. One side of a 20 mm polytetrafluoroethylene vascular graft (W. L. Gore & Associates, Inc., USA) was connected to the right atrial appendage by end-to-side anastomosis and another side was connected to the IVC with end-to-side anastomosis, which was just lower than the level of the second porta hepatis (Figure 2A). Bovine pericardial

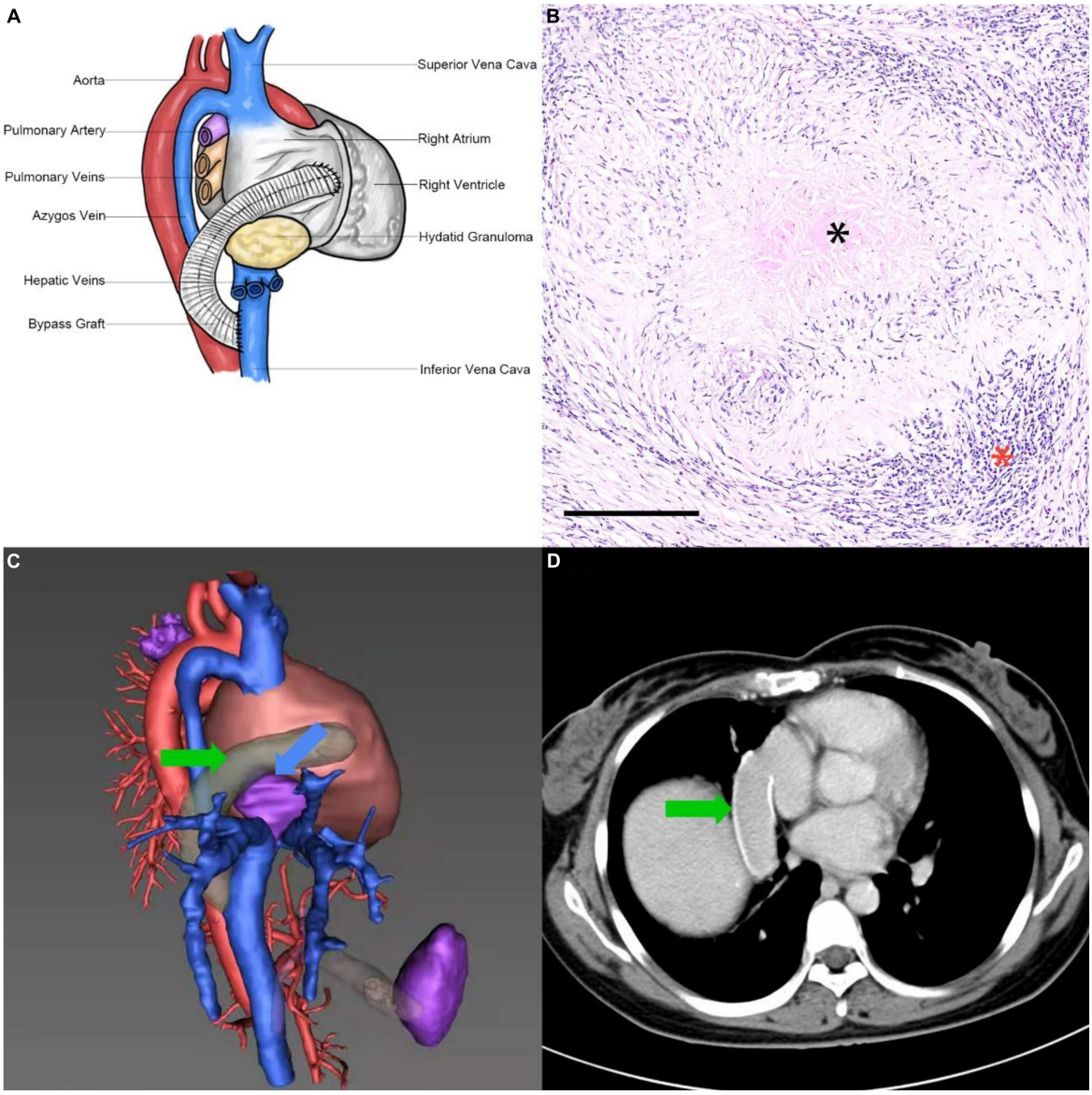

FIGURE 2
Surgical technique and postoperative findings. **(A)** Illustration of the right atrium-IVC bypass. **(B)** Postoperative pathological analysis showed the existence of cysticercosis (black asterisk), aggregation of eosinophils and proliferation of epithelioid cells (red asterisk). H/E 10×. The black bar indicates 250 μm. **(C)** 3D-reconstruction view of postoperative CTA on 5-year follow-up showed the cardiac mass without enlargement (blue arrow) and vascular graft (green arrow). **(D)** Postoperative CTA on 5-year follow-up showed the vascular graft remained patent (green arrow).

patch was used to repair the defect of right atrium. The patient went through an uncomplicated postoperative period in the intensive care unit (ICU) and proceeded to continuous anti-parasitic therapy with albendazole (400 mg, twice per day) for maintenance treatment after the operation. In addition, anti-coagulation therapy was not administrated. The postoperative pathological analysis confirmed the diagnosis of echinococcosis granulosus (**Figure 2B**). The patient was discharged from the hospital 30 days after the surgery and remained in good condition of cardiac function and hepatic function at the time of the 5-year follow-up. The TTE and CTA revealed that the vascular graft remained patent and there was no enlargement in the mass (**Figures 2C,D**). Moreover, no thrombo-hemorrhage event, anaphylactic reaction, new lesion or other complication was found during the 5-year follow-up.

Table timeline

Day 0

- A 31-year-old female was admitted into the department of cardiovascular surgery due to repeated hemoptysis and dyspnea on exertion.
- Physical examination revealed persistent tachycardia.

Laboratory test evidenced moderate anemia, eosinophilia, bilirubinemia, and positive echinococcosis granulosus IgG.

Day 1

- Transthoracic echocardiogram revealed an immobile mass in the right atrium.

Day 2

- Computed tomography angiogram and magnetic resonance imaging confirmed the inferior vena cava obstruction and multiple lesions in the left lung and the brain.

Day 7

- Transbronchoscopic lung biopsy demonstrated the left pulmonary lesion was hydatid granuloma.

Day 8

- Albendazole was prescribed prior to the cardiovascular surgery.

Week 4

- Right atrium-inferior vena cava bypass surgery was performed.
- Histological confirmation of cardiac hydatid granuloma.

Year 5

- Follow-up Doppler echocardiography and computed tomography angiogram demonstrated patent vascular graft and no mass progression.
- Patient was asymptomatic. Cardiac function and hepatic function returned to normal.

Discussion

Hydatid disease is classified as a parasitic infection resulting from the larvae of *Echinococcus granulosus* and most of the patients had a residence history in pastoral areas. The most common source of transmission is the domestic dog and the major route of infection transmission is intaking food and water containing the ova of the parasite (4). Cardiac involvement of hydatidosis is rare in humans, which accounts for 0.2–2% of all cases, while most common lesions occur in the liver (50–70%) and lung (20–30%). Among the heart involvement cases, the left ventricle is the dominant susceptible area (55–60%), followed by the right ventricle (10–20%), interventricular septum (5–9%), left atrium (8%), pulmonary arteries (7–8%), pericardium (5%), and right atrium (3–4%) (5). Thus, involvement of the right atrium is extremely rare in human cases.

Depending on the growth rate, mass volume and lesion site, cardiac hydatid disease could be asymptomatic or life-threatening. Most of the patients have no symptoms due to the slow growth of the granuloma. However, about 10% of the patients might have variable complications, including pericarditis, pericardial effusion, anaphylactic reaction, systemic embolism, pulmonary embolism, and myocardial infarction (6). In this case, the hydatidosis invaded the right atrium, leading to severe obstruction of the IVC and symptoms like Budd-Chiari syndrome, which was uncommon among cardiac-involved cases.

Diagnosis of hydatid disease relies on imaging examination and pathological analysis. The TTE, CTA, and MRI are sensitive in detecting lesion sites and involving the extent of cardiac hydatidosis. Multiple lesions in the liver, lung and other parts of the body might assist in the diagnosis of cardiac hydatidosis (7). Confirmation of cardiac echinococcosis depends on postoperative pathological examination, of which the major signs include the presence of cysticercosis, aggregation of eosinophils and proliferation of epithelioid cells. Seropositive echinococcosis granulosus IgG in enzyme-linked immunosorbent assay might also help diagnose cardiac echinococcosis.

Surgical treatment and medicinal therapy were the two major components of the management of hydatid disease (8). Surgical removal of echinococcosis granuloma with cardiopulmonary bypass under cardioplegic arrest is the optimal choice for cardiac hydatid disease. However, hydatid granuloma tends to grow subendocardially and form tight adhesion with adjacent structures (7). In our case, the cardiac mass invaded the right atrium, IVC, pericardium, right lower lung and diaphragm, which resulted in obstruction of IVC and could not be resected completely. Under this circumstance, the right atrium-IVC bypass surgery might be a feasible option to restore venous circulation. Chemotherapy with albendazole is equally important in treating cardiac echinococcosis. It is recommended to use prophylactic chemotherapy a few weeks prior to the cardiac operation and continued after the surgery to inhibit the growth of hydatid granuloma and reduce the risks of recurrence (9). Chemotherapy with albendazole plus praziquantel could be used as adjunctive treatment to surgery (1).

Conclusion

Right atrium echinococcosis is extremely rare and could possibly cause IVC obstruction. Chemotherapy associated with right atrium-IVC bypass surgery might be a feasible treatment when hydatid granuloma could not be removed completely.

Data availability statement

The original contributions presented in this study are included in the article/**Supplementary material**, further inquiries can be directed to the corresponding author.

Ethics statement

The studies involving human participants were reviewed and approved by the West China Hospital Ethics Committees and Institutional Review Board, Sichuan, China. The patients/participants provided their written informed consent to participate in this study. Written informed consent was obtained from the individual(s) for the publication of any potentially identifiable images or data included in this article.

Author contributions

LL and BW: conception and design, data analysis, and interpretation. YG: administrative support. LL, BW, and ML: collection and assembly of data. All authors wrote the manuscript and approved the final manuscript.

Funding

This work was funded by the 1.3.5 project for disciplines of excellence, West China Hospital, Sichuan University.

Conflict of interest

The authors declare that the research was conducted in the absence of any commercial or financial relationships that could be construed as a potential conflict of interest.

Publisher's note

All claims expressed in this article are solely those of the authors and do not necessarily represent those of their affiliated organizations, or those of the publisher, the editors and the reviewers. Any product that may be evaluated in this article, or claim that may be made by its manufacturer, is not guaranteed or endorsed by the publisher.

Supplementary material

The Supplementary Material for this article can be found online at: https://www.frontiersin.org/articles/10.3389/fcvm.2022.1001073/full#supplementary-material

SUPPLEMENTARY VIDEO 1
Preoperative magnetic resonance imaging showed a 24 mm × 50 mm mass existing at the junction of the right atrium and IVC.

References

1. Nazligul Y, Kucukazman M, Akbulut S. Role of chemotherapeutic agents in the management of cystic echinococcosis. *Int Surg.* (2015) 100:112–4. doi: 10.9738/INTSURG-D-14-00068.1

2. Nunes MC, Guimarães Júnior MH, Diamantino AC, Gelape CL, Ferrari TC. Cardiac manifestations of parasitic diseases. *Heart (Br Cardiac Soc).* (2017) 103:651–8. doi: 10.1136/heartjnl-2016-309870

3. Kahlfuß S, Flieger RR, Roepke TK, Yilmaz K. Diagnosis and treatment of cardiac echinococcosis. *Heart (Br Cardiac Soc).* (2016) 102:1348–53. doi: 10.1136/heartjnl-2016-309350

4. Gormus N, Yeniterzi M, Telli HH, Solak H. The clinical and surgical features of right-sided intracardiac masses due to echinococcosis. *Heart Vessels.* (2004) 19:121–4. doi: 10.1007/s00380-003-0732-x

5. Tasdemir K, Akcali Y, Gunebakmaz O, Kaya MG, Mavili E, Sarli B, et al. Surgical approach to the management of cardiovascular echinococcosis. *J Cardiac Surg.* (2009) 24:281–4. doi: 10.1111/j.1540-8191.2008.00727.x

6. Aydoğdu T, Sahin N, Ulusan V, Gürpinar F, Türkay C, Bayezid O. Right atrial hydatid cyst associated with multiple organ involvement: case report. *J Thoracic Cardiovasc Surg.* (2001) 121:1009–11. doi: 10.1067/mtc.2001.112628

7. Dursun M, Terzibasioglu E, Yilmaz R, Cekrezi B, Olgar S, Nisli K, et al. Cardiac hydatid disease: CT and Mri findings. *AJR Am J Roentgenol.* (2008) 190:226–32. doi: 10.2214/AJR.07.2035

8. Eris C, Akbulut S, Yildiz MK, Abuoglu H, Odabasi M, Ozkan E, et al. Surgical approach to splenic hydatid cyst: single center experience. *Int Surg.* (2013) 98:346–53. doi: 10.9738/INTSURG-D-13-00138.1

9. Yan F, Huo Q, Abudureheman M, Qiao J, Ma S, Wen H. Surgical treatment and outcome of cardiac cystic echinococcosis. *Eur J Cardio Thoracic Surg Off J Eur Assoc Cardio Thoracic Surg.* (2015) 47:1053–8. doi: 10.1093/ejcts/ezu323

frontiers | Frontiers in Cardiovascular Medicine

TYPE Case Report
PUBLISHED 09 December 2022
DOI 10.3389/fcvm.2022.1061665

OPEN ACCESS

EDITED BY
Hendrik Tevaearai Stahel,
Bern University Hospital, Switzerland

REVIEWED BY
Hiroki Teragawa,
JR Hiroshima Hospital, Japan
Chengming Fan,
The Second Xiangya Hospital, Central South University, China

*CORRESPONDENCE
Ilkhom K. Zugurov
ilxom160594@gmail.com

SPECIALTY SECTION
This article was submitted to Heart Surgery, a section of the journal Frontiers in Cardiovascular Medicine

RECEIVED 18 October 2022
ACCEPTED 18 November 2022
PUBLISHED 09 December 2022

CITATION
Zugurov IK, Osadchii AM, Simakova MA, Moiseeva OM and Gordeev ML (2022) Surgical treatment of chronic thromboembolic pulmonary hypertension in combination with a left anterior descending artery myocardial bridge: A case report.
Front. Cardiovasc. Med. 9:1061665.
doi: 10.3389/fcvm.2022.1061665

Surgical treatment of chronic thromboembolic pulmonary hypertension in combination with a left anterior descending artery myocardial bridge: A case report

Ilkhom K. Zugurov[1]*, Aleksei M. Osadchii[1], Maria A. Simakova[2], Olga M. Moiseeva[2] and Mikhail L. Gordeev[1]

[1]Department of Cardiac Surgery, Almazov National Medical Research Centre, St. Petersburg, Russia, [2]Department of Non-Coronary Heart Diseases, Almazov National Medical Research Centre, St. Petersburg, Russia

Pulmonary thromboendarterectomy is a potentially curative option for most patients with chronic thromboembolic pulmonary hypertension (CTEPH). However, a special group of patients with CTEPH requires simultaneous cardiac procedures. We report a rare case of successful surgical treatment of a CTEPH patient with a left anterior descending artery myocardial bridge. Despite the complexity of performing pulmonary thromboendarterectomy (PTE), the issue concerning the method of revascularization of the artery in the case of the left anterior descending artery myocardial bridge is controversial. PTE and supracoronary myotomy were performed. In our case, the optimal surgery method for the left anterior descending artery myocardial bridge was chosen intraoperatively based on the depth and length of the myocardial bridge. The patient's significant functional improvement after surgery and hemodynamic normalization were confirmed at the follow-up assessment. This case demonstrates rare but potentially dangerous pathologies that can be treated with minimal adverse effects.

KEYWORDS

chronic thromboembolic pulmonary hypertension, left anterior descending artery myocardial bridge, supracoronary myotomy, deep hypothermic circulatory arrest, pulmonary thromboendarterectomy

Introduction

Pulmonary thromboendarterectomy (PTE) is the gold standard for chronic thromboembolic pulmonary hypertension (CTEPH) patients' treatment; however, in some cases, combined heart surgery is required, which increases the intervention risk (1). The left anterior descending artery myocardial bridge (LAD-MB) is difficult to derive, and treatment options are still being discussed (2). LAD-MB management depends on the functional significance of coronary artery damage;

however, its assessment is difficult in conditions of high pulmonary hypertension (2). The clinical case presented the experience of simultaneous pulmonary thrombendarterectomy and supra-arterial myotomy.

Case report

A 36-year-old man was referred to the Almazov National Medical Research Centre with a history of progressive heart failure (NYHA III functional class), chest pain, and the presence of severe pulmonary hypertension (PH) according to a transthoracic echocardiographic evaluation (TTE). The patient had a documented history of acute pulmonary embolism with a delayed diagnosis and initiation of anticoagulant therapy. TTE showed right atrial and right ventricle dilatation with preserved right ventricle function, left ventricle size, and function, and the estimated pulmonary artery systolic pressure was 120 mmHg (Table 1). Chest dual-energy CT-angiography and pulmonary angiography confirmed CTEPH (level II according to San Diego pulmonary endarterectomy disease levels) (Figures 1a,b). Right heart catheterization (RHC) defined precapillary PH: mean pulmonary artery pressure (PAP) of 59 mmHg, a pulmonary capillary wedge pressure (PCWP) of 13 mmHg, and a pulmonary vascular resistance of 7,98 Wood units. Riociguat treatment was started. Thrombophilia markers were tested, and antiphospholipid antibody syndrome was revealed as the main CTEPH risk factor. There were no data in favor of systemic lupus erythematosus or other systemic connective tissue diseases. Due to chest pain, selective coronary angiography was performed, and the LAD-MB was revealed. The length of the LAD-MD was ∼25 mm, with left anterior descending artery stenosis in the systole reaching 70% (Figures 2a,c, arrowhead).

Considering confirmed CTEPH with a level II lesion (San Diego classification of pulmonary endarterectomy disease levels) and a significant myocardial bridge of the left anterior descending artery, a pulmonary thromboendarterectomy in combination with a supracoronary myotomy was performed. Intraoperative revision showed LAD-MB lying at a depth of 4–5 mm for 20–22 mm (Figure 3), suggesting that a supra-arterial myotomy may be performed while the patient was being warmed up. Total surgery time was 330 min, and deep hypothermic circulatory arrest (DHCA) time was 73 min (four sessions were carried out). At the end of the operation, the mean pulmonary pressure had decreased by 65% and was 25 mmHg. The full view of endarterectomized tissues is shown in Figure 4.

The postoperative period was characterized by moderate cardiovascular and respiratory insufficiency without signs of reperfusion edema. The patient was extubated 22 h after the surgery. The intensive care unit treatment lasted 45 h without requiring PAH-targeted therapy. The patient was discharged on the 12th day after surgery with much dyspnea regression. Only vitamin K antagonists' treatment was prescribed.

The patient's health significantly improved and had no dyspnea at 8 months of follow-up. Selective pulmonary angiography demonstrated preserved blood flow over all pulmonary fields. No stenosis and occlusion of segmental branches were visible (Figures 1c,d). Coronary angiography found no local stenosis of the LAD artery (Figures 2c,d). The control RHC showed normalization of pulmonary hemodynamics with a reduced mean pulmonary artery pressure of 22 mmHg and an RVR of 1.7 WU (Table 2).

In our case, the final diagnosis was chronic thromboembolic pulmonary hypertension with the third functional class according to the WHO classification of PH, CHD, and LAD-MB, with up to 70% stenosis in the systole. The surgical treatment was sternotomy, pulmonary endarterectomy, and simultaneous supracoronary myotomy of the LAD-MB.

TABLE 1 Echocardiography parameters.

Indicator	Before surgery	Post-surgery (7 days)	Post-surgery (8 months)
RV (parasternal long axis size) (mm)	32	30	28
RV (four-chamber basal size) (mm)	52	48	36
TAPSE (mm)	17		24
PA pressure (systolic) (mmHg)	120	30	40
Tricuspid insufficiency (grade)	1	1	1
IVS/PW (mm)	14/11	13/11	10/9
EDS/ESS LV (mm)	48/30	47/32	48/32
EDV/ESV LV (ml)	108/34	100/40	107/41
EF (%)	68	60	64
LA (mm)	36	37	42

EDS, the end-diastolic size of the left ventricle; EDV, end-diastolic volume of the left ventricle; EF, ejection fraction of the left ventricle; ESV, the end-systolic volume of the left ventricle; ESS, the end-systolic size of the left ventricle; IVS, interventricular septum; LA, left atrium; PW, left ventricle posterior wall; RA, right atrium; RV, right ventricle; and TAPSE, tricuspid annular plane systolic excursion.

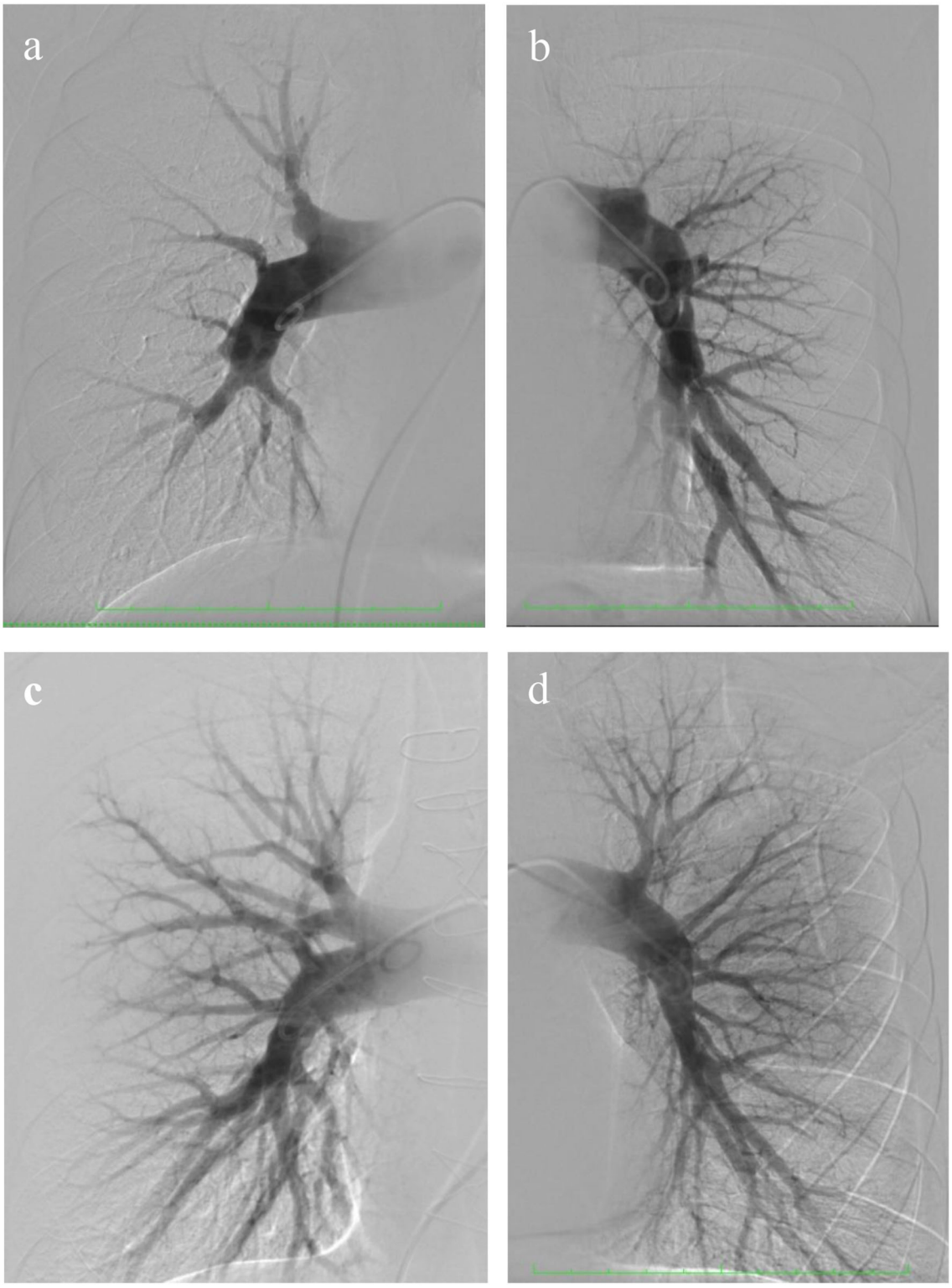

FIGURE 1
Pre- and post-operative selective pulmonary angiography. **(a)** Selective pulmonary angiography of the *right pulmonary* arteries identified: eccentric and extended stenoses in the segmental arteries A 1, 2, 4, 5, 6, 7, 8, and occlusion of A 3, 9, 10; **(b)** *left pulmonary artery:* occlusion of the upper lobe branch, roughness of the contours of the lower lobe branch, and eccentric and extended stenoses in the segmental arteries of the lingual segment and lower lobe; **(c,d)** selective pulmonary angiography after surgery.

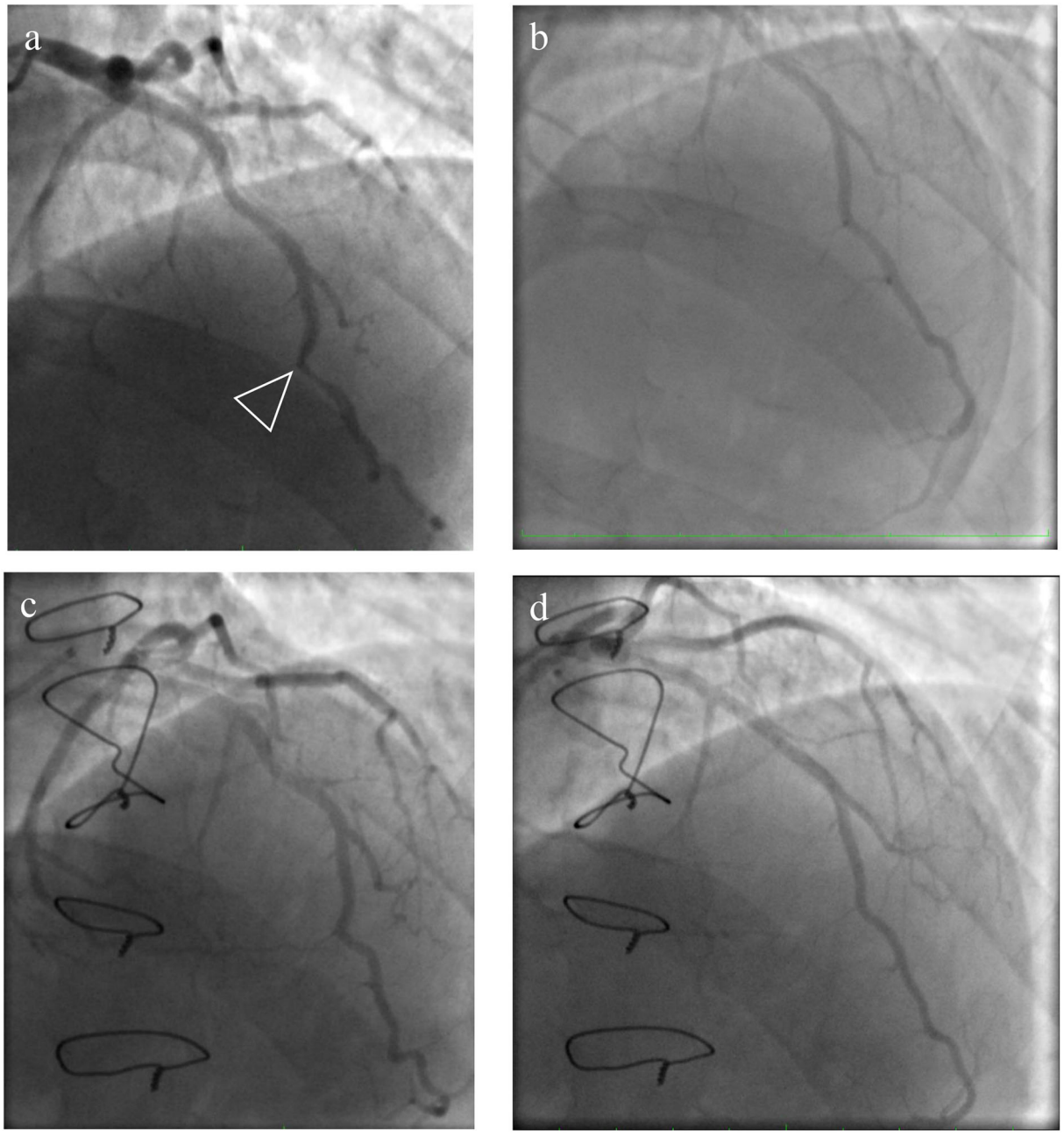

FIGURE 2
Pre- and post-operative view of coronary angiography. **(a)** An intramyocardially located section of the left anterior descending artery (LAD) in the middle third with stenosis in the systole up to 60–70%; **(c)** the systolic phase of the LAD-MB after the surgery; **(b,d)** the diastolic phase of the LAD-MB before and after the operation.

Discussion

This clinical case is a good example of a complicated course in PE. One of the well-known risk factors is the delay in PE diagnosis and, consequently, the late appointment of anticoagulants (more than 2 months from the PE clinic in our case). This factor is crucial for incomplete thrombi recanalization and their fibrosis transformation. Antiphospholipid syndrome is the second obvious CTEPH risk factor in this patient. Modern scientific research aims to discover new CTEPH formation predictors and study its pathogenesis. Such

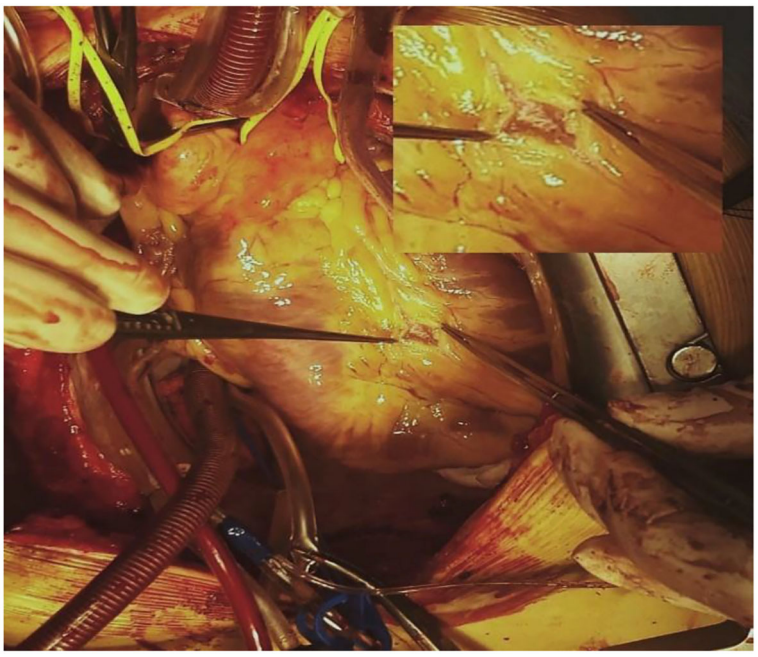

FIGURE 3
Intraoperative view of LAD-MB. The left anterior descending artery myocardial bridge lies at a depth of 4–5 mm with a length of 20–22 mm. LAD-MB was located on the border of the middle and distal thirds of the artery.

studies are important for optimizing the management of PE survivors.

Besides, our case demonstrates the complexity of the LAD-MB functional significance assessment in patients with CTEPH. Due to chest pain is a common complaint in such patients, it can be difficult to distinguish it from angina pectoris. It should be noted that stress echocardiography performance was limited by high pulmonary hypertension because the patient even could not perform any daily life activities. The pharmacological test to clarify the LAD-MB significance was limited by the riociguate treatment (adverse drug interactions). Additionally, nitroglycerin intracoronary administration for LAD-MB severity evaluation can sometimes increase artery narrowing in the bridge segment and vasodilate adjacent non-bridged coronary segments with myocardial ischemia occurrence (3).

In addition, Maeda and his colleagues observed the prevalence of plaque formation proximal to the bridged segment (4). Some reports showed that damaged segments stay free of plaques, likely due to the systolic compression of those segments, with subsequent improved lymphatic drainage and decreased lipid accumulation in those segments. Plaque formation in the artery upstream of the bridged segment has been frequently reported, especially after intravascular ultrasonography, which helped detect lesions not previously detected by angiography (5). This can be explained by endothelial injury associated with flow disturbances and wall shear stress at that proximal segment. Progression of proximal plaque formation is thought to increase with age, as evidenced in the study by Maeda and colleagues (4). Their study population was composed of patients aged 11–20 years, with a plaque burden of almost 19%, lower than that reported in adults (34%). Nonetheless, the presence of plaque in this young adult patient cohort with myocardial bridges is an important and concerning finding that may warrant a more aggressive approach in these cases.

Thereby LAD-MB potentially can be associated with acute coronary symptoms or with atherosclerotic disease progression. It is unknown whether patients with asymptomatic myocardial bridges should be medically treated or whether they should be exercise restricted for acute coronary event prevention. Further evaluation of myocardial bridges natural history may be necessary for these patients care and the adverse events occurance decrease (6).

A number of studies show that safe LAD-MB surgery can be considered if the narrowed segment of the artery lies at a depth of no more than 5 mm and a length of no more than 25 mm (7, 8). In our case, when assessing the narrowed segment intraoperatively, it was revealed that the bridge lies at a depth of 4–5 mm with a length of

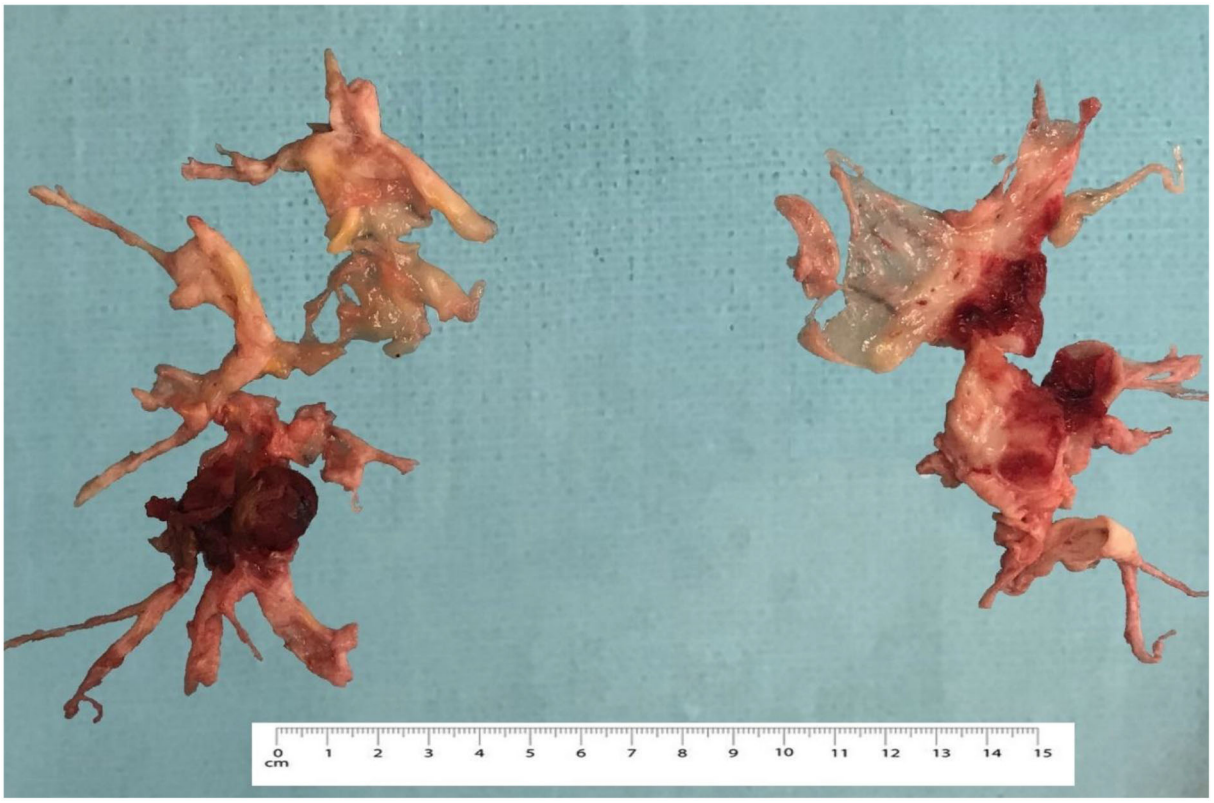

FIGURE 4
Intraoperative view of endarterectomized tissues.

TABLE 2 Right heart catheterization parameters.

Indicator	Before surgery	Post-surgery (1 day)	Post-surgery (8 months)
Blood pressure (systolic/diastolic) (mmHg)	124/89	110/60	127/70
Pulmonary pressure (systolic/diastolic/mean) (mmHg)	102/31/59	31/10/20	32/10/22
PCWP (mmHg)	13	11	10
RAP (mmHg)	15	10	12
CO (per L/min)	5,76	5,9	7,1
CI (per L/min/m^2)	2,45	2,5	3,02
PVR (Wood units)	7,98	2,0	1,7

CI, cardiac index; CO, cardiac output; PCWP, pulmonary capillary wedge pressure; PVR, pulmonary vascular resistance; and RAP, right atrium pressure.

20–22 mm. LAD-MB was located on the border of the middle and distal thirds of the artery. Furthermore, there was no artery narrowing in the LAD-MB segment in the diastole phase during coronary angiography before the operation.

All of the above arguments, combined with the procedure's technical feasibility, led us to decide on a combined cardiac surgery intervention for this CTEPH patient.

Conclusion

Operable patients with CTEPH requiring combined heart surgery represent a special group with an increased risk of perioperative complications. The current case suggests that PTE combined with LAD-MB surgery is associated with acceptable perioperative morbidity and mortality rates and improved hemodynamic and functional status in the patient.

Data availability statement

The original contributions presented in the study are included in the article/supplementary material, further inquiries can be directed to the corresponding authors.

Ethics statement

The studies involving human participants were reviewed and approved by Extract No. 0801-21 from the protocol of the meeting of the Ethics Committee of the Almazov National Medical Research Center No. 01–21 dated January 18, 2021. The patients/participants provided their written informed consent to participate in this study.

Author contributions

All authors listed have made a substantial, direct, and intellectual contribution to the work and approved it for publication.

Funding

This work was financially supported by a Russian Science Foundation Grant (No. 22-25-20132, https://rscf.ru/project/22-25-20132/).

Conflict of interest

The authors declare that the research was conducted in the absence of any commercial or financial relationships that could be construed as a potential conflict of interest.

Publisher's note

All claims expressed in this article are solely those of the authors and do not necessarily represent those of their affiliated organizations, or those of the publisher, the editors and the reviewers. Any product that may be evaluated in this article, or claim that may be made by its manufacturer, is not guaranteed or endorsed by the publisher.

References

1. Thistlethwaite PA, Auger WR, Madani MM, Pradhan S, Kapelanski DP, et al. Pulmonary thromboendarterectomy combined with other cardiac operations: indications, surgical approach, and outcome. *Ann Thorac Surg.* (2001) 72:13–7; discussion 17–9. doi: 10.1016/S0003-4975(01)02686-8

2. Tarantini G, Migliore F, Cademartiri F, Fraccaro C, Iliceto S. Left anterior descending artery myocardial bridging: a clinical approach. *J Am Coll Cardiol.* (2016) 68:2887–99. doi: 10.1016/j.jacc.2016.09.973

3. Hongo Y, Tada H, Ito K, Yasumura Y, Miyatake K, Yamagishi M. Augmentation of vessel squeezing at the coronary-myocardial bridge by nitroglycerin: a study by quantitative coronary angiography and intravascular ultrasound. *Am Heart J.* (1999) 138:345–50. doi: 10.1016/S0002-8703(99)70123-7

4. Maeda K, Schnittger I, Murphy DJ, Tremmel JA, Boyd JH, Peng L, et al. Surgical unroofing of hemodynamically significant myocardial bridges in a pediatric population. *J Thorac Cardiovasc Surg.* (2018) 156:1618–26. doi: 10.1016/j.jtcvs.2018.01.081

5. Corban MT, Hung OY, Eshtehardi P, Rasoul-Arzrumly E, McDaniel M, Mekonnen G, et al. Myocardial bridging: contemporary understanding of pathophysiology with implications for diagnostic and therapeutic strategies. *J Am Coll Cardiol.* (2014) 63:2346–55. doi: 10.1016/j.jacc.2014.01.049

6. Alsoufi B. Do not miss the bridge. *J Thorac Cardiovasc Surg.* (2018) 156:1627–8. doi: 10.1016/j.jtcvs.2018.02.082

7. Wu QY, Xu ZH. Surgical treatment of myocardial bridging: report of 31 cases. *Chin Med J (Eng).* (2007) 120:1689–93. doi: 10.1097/00029330-200710010-00009

8. Huang XH, Wang SY, Xu JP, Song YH, Sun HS, Tang Y, et al. Surgical outcome and clinical follow-up in patients with symptomatic myocardial bridging. *Chin Med J (Eng).* (2007) 120:1563–6. doi: 10.1097/00029330-200709020-00001

frontiers | Frontiers in Cardiovascular Medicine

TYPE Case Report
PUBLISHED 13 December 2022
DOI 10.3389/fcvm.2022.1086457

OPEN ACCESS

EDITED BY
Hendrik Tevaearai Stahel,
Bern University Hospital, Switzerland

REVIEWED BY
Bastianus De Mol,
Amsterdam University Medical Center, Netherlands
Johannes Blumenstein,
St.-Johannes-Hospital Dortmund, Germany

*CORRESPONDENCE
Haibo Zhang
zhanghb2318@163.com

SPECIALTY SECTION
This article was submitted to Heart Surgery, a section of the journal Frontiers in Cardiovascular Medicine

RECEIVED 01 November 2022
ACCEPTED 28 November 2022
PUBLISHED 13 December 2022

CITATION
Zhou J, Li Y and Zhang H (2022) Case report: Transapical transcatheter double valve-in-valve replacement of degenerated aortic and mitral bioprosthetic valves with limited radiopaque landmarks. *Front. Cardiovasc. Med.* 9:1086457. doi: 10.3389/fcvm.2022.1086457

Case report: Transapical transcatheter double valve-in-valve replacement of degenerated aortic and mitral bioprosthetic valves with limited radiopaque landmarks

Jiawei Zhou, Yuehuan Li and Haibo Zhang*

Department of Cardiac Surgery, Beijing Anzhen Hospital, Capital Medical University, Beijing, China

A 67-year-old male patient who had undergone double valve replacement 11 years before presented with severe dyspnea to our department. The bioprosthetic aortic and mitral valves have failed. Because of the high risk of redo surgery. We perform a simultaneous transapical transcatheter valve-in-valve replacement of degenerated aortic and mitral bioprosthetic valves with limited radiopaque landmarks using the second-generation self-expanding J-valve. The post-operative course was stable and the patient was discharged on post-operative day eight.

KEYWORDS

transapical, double valve-in-valve replacement, J-valve, TVI-transcatheter valve implantation, structural valve deterioration

Introduction

With the increasing use of bioprosthetic valves, structural valve deterioration has become a major challenge for long-term prognosis. Valve-in-valve (VIV) is a minimally invasive and effective treatment for valve failure (1). VIV has been described in aortic, mitral, tricuspid and pulmonary positions, but it is usually performed on a single valve (2). Here we report a case of transapical double VIV replacement in a patient with severe mitral and aortic bioprosthetic valve regurgitation.

Case presentation

The 67-year-old male patient had undergone double valve replacement for rheumatic valvular disease in 2011 with a 21-mm Medtronic Mosaic bioprosthesis (Medtronic, Inc, Minneapolis, MN, USA) in the aortic position and a 27-mm Medtronic Mosaic bioprosthesis (Medtronic, Inc, Minneapolis, MN, USA) in the mitral position. The patient underwent permanent pacemaker implantation due to a third-degree

atrioventricular block. The patient was referred to our department recently, presenting with New York Heart Association (NYHA) grade IV dyspnea. Diuretic therapy is not effective. The patient also had a medical history of chronic lung disease and coronary atherosclerotic heart disease.

Transthoracic echocardiography revealed moderate bioprosthetic mitral valve stenosis (valvular orifice area of 1.8 cm^2) with severe mitral valve regurgitation (regurgitant area of 16.2 cm^2) and concurrent severe bioprosthetic aortic valve regurgitation, severe tricuspid regurgitation (regurgitant area of 18.8 cm^2). Furthermore, the left ventricular end-diastolic diameter was 63 mm with a normal ejection fraction of 58%. Computed tomography angiography of the coronary artery showed a 50–60% stenosis in the middle segment of the anterior descending artery. The left ventricular outflow tract was calculated with 609 mm^2 (**Figure 1A**). Aorto-mitral angle was steep with 67° (**Figure 1B**). Left coronary ostium height is 12.8 mm, right coronary ostium height is 14.3 mm. The frailty screening scale was four points. The preoperative logistic EuroSCORE II for redo surgery in this patient was calculated with 19.02%. Considering preoperative EuroSCORE II, the redo surgery and the extensive experience with transapical transcatheter aortic valve replacement (TAVR) procedures at our institution, the decision was made to perform a simultaneous transapical VIV procedure in the mitral and aortic positions.

The procedure was performed in a hybrid operating room. The chest was entered in the fifth intercostal space through a small left anterolateral incision. Two pledged purse-string sutures were placed at the apex. The annulus of the Medtronic Mosaic aortic and mitral bioprosthesis was not visualized on fluoroscopy (**Figure 2A**). After the apical puncture, a soft guide-wire and then a super stiff guide-wire were used to cross the bioprosthetic valve and into the aorta. The J-valve delivery device was inserted. Then, a 21-mm J-valve (Jiecheng Medical Technology, Suzhou, China) was deployed in the aortic position. Transesophageal echocardiography revealed massive perivalvular leakage. Therefore, a second 21-mm J-valve was implanted in the aortic position. A total of 20 mm Atlas gold post-dilatation was used for post-dilatation in the aortic position (**Figure 2B**). Thereafter the super stiff guidewire was placed in the left atrium through the mitral bioprosthetic valve. The J-valve was reversely loaded on the delivery system (**Figure 2C**). A 25-mm J-valve was deployed under rapid pacing in the mitral position. After that, a 25 mm Newman balloon was used for post-dilation. A post-operative fluoroscopic image with both aortic and mitral VIV replacements in place was taken (**Figure 2D**).

Post-procedural echocardiography could detect neither paravalvular leakage nor aortic or mitral regurgitation. Three-dimensional transesophageal echocardiography showed a good shape of the mitral transcatheter heart valve (**Figure 3**). Echocardiography showing a mitral valve area of 1.7 cm^2 and mitral valve mean gradient of 3 mm Hg and a transaortic gradient valve mean gradient of 13 mm Hg. The post-operative course was uneventful and without complication. The patient was discharged on post-operative day eight. After 2 months of follow-up, the patient's NYHA class improved to grade 2.

Discussion

Patients with bioprosthetic valves may contribute a higher incidence of subsequent repeat valve replacement in the future for structural deterioration. Although redo surgery is the current standard of care, this carries a significant risk of mortality (3). VIV could potentially be considered as viable alternatives in inoperable or high risks patients. Some patients may need underwent simultaneous double VIV procedures for the failed bioprosthetic valves. In this case, we present the simultaneous transcatheter transapical VIV for both failed bioprosthetic mitral and aortic valves with severe regurgitation using the J-Valve.

J-valve is a second-generation self-expanding transcatheter heart valve designed for transapical TAVR. It has been also proven effective and safe in transapical mitral VIV implantation (4). The transapical approach provides coaxial alignment and therefore reduces the risk of valve migration and left ventricular outflow tract obstruction. Bauernschmitt et al reported on the first transcatheter double valve replacement into native valves from transapical access (5). D'Onofrio et al believe that it should be considered the first access choice in these cases (2). However, Savoj et al reported one case of transcatheter double VIV replacement of the aortic and mitral bioprosthetic valve *via* the femoral artery (6).

There are several difficulties in this case. First, the double VIV at one puncture point of the heart apex, the spatial structure of the two biological valves may interact with each other. Second, the annulus of the patient's original biological valve was not visualized on fluoroscopy. It can only be done under the guidance of three-dimensional ultrasound. Third, regurgitation was predominant in the aortic and mitral biological valves of the patient.

Regarding the order of deployment in double VIV, D'Onofrio et al suggested that aortic valve deployment should be done first in this procedure (2). There are several reasons for this order. There is an immediate afterload reduction and consequently better hemodynamic conditions for the mitral procedure after the aortic valve is implanted. Less risk of deployed mitral valve displacement or aortic valve malposition. In our case, we used the same sequence.

The VIV reports in the United States and Europe are mostly balloon-expandable valves (Sapien 3) (7). The Sapien 3 is anchored by radial support force, which is prone to displacement and paravalvular leakage after the operation. J-valve is a short stent valve, and its specific three locators design enables it to be firmly anchored in the failed valve. The three U-shape graspers of the J-valve are one-to-one buckled

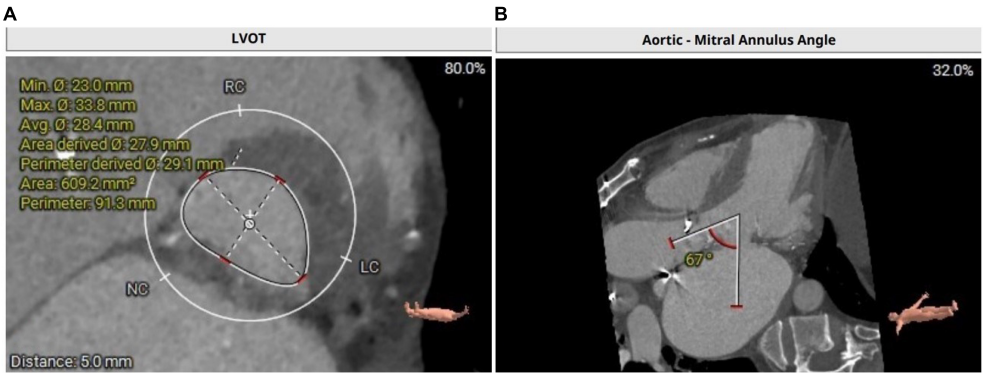

FIGURE 1
(A) Calculation of left ventricular outflow tract with an area of 609.2 mm^2. **(B)** CT depicting a steep aorto-mitral annulus angle with 67°.

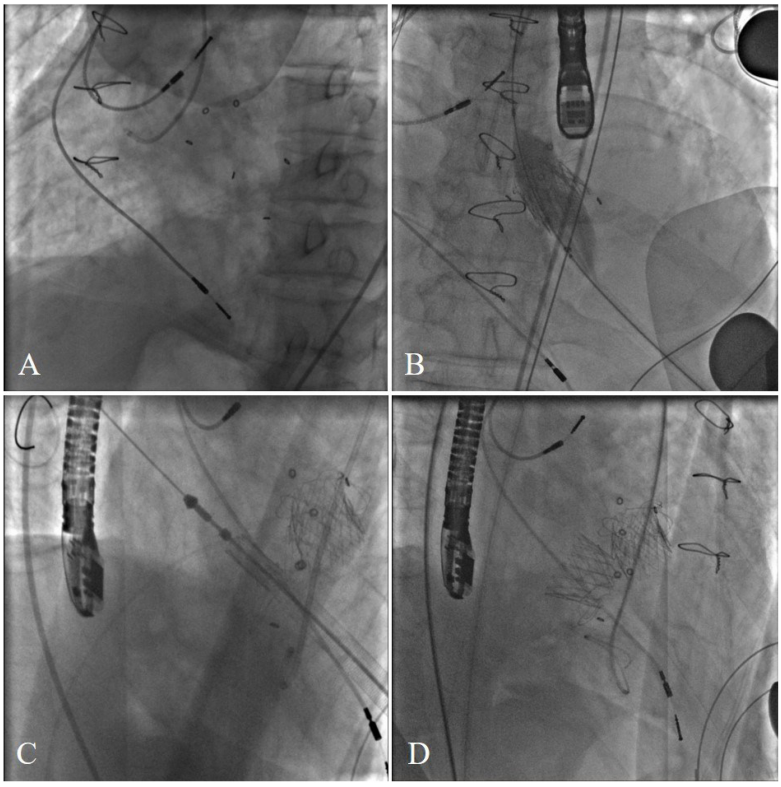

FIGURE 2
(A) The annulus of the Medtronic Mosaic aortic and mitral bioprosthesis was not visualized on fluoroscopy. **(B)** A total of 20 mm Atlas gold post-dilatation was used for post-dilatation in the aortic position. **(C)** Transcatheter bioprosthetic mitral valve implantation. **(D)** Final cardiac fluoroscopy showing both valves deployed and seated well.

with the three bioprosthetic valve struts to avoid displacement to the left ventricle or left atrium. The self-expanding nitinol stent minimizes the risk of paravalvular leakage. The large left ventricular outflow tract area and short stent J-valve were used in this patient to reduce the risk of left ventricular outflow tract obstruction. Another advantage of J-valve is coronary protection. The positioning key of the J-valve can prevent the aortic bioprosthetic valve leaflet from getting closer to the coronary orifice and avoid coronary occlusion. In addition, the price of J-valve is much cheaper than Sapien 3.

Paravalvular leakage was significantly reduced after the second J-valve was released in the aortic position. The first J-valve did not fully expand after release. At the same time, due to the prior aortic bioprosthetic valves with limited

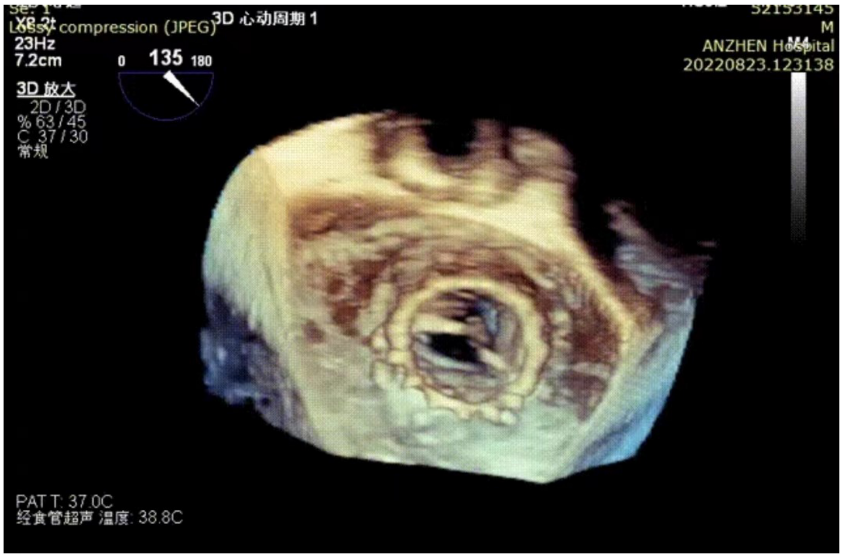

FIGURE 3
Three-dimensional transesophageal echocardiography reconstruction showing the mitral transcatheter heart valve.

radiopaque landmarks, the coaxiality of the released valve and the original biological valve is not ideal, resulting in paravalvular leakage. In this patient, we did not concurrently manage severe tricuspid regurgitation. We expected that the reduction in mitral regurgitation, combined with the use of diuretics, would reduce tricuspid regurgitation. Follow-up echocardiography did show a significant reduction in tricuspid regurgitation.

In conclusion, our case report shows the feasibility and efficacy of a double VIV procedure in the failed mitral and aortic bioprosthetic valve with a self-expanding valve *via* a transapical approach.

Data availability statement

The original contributions presented in this study are included in the article/**Supplementary material**, further inquiries can be directed to the corresponding author.

Ethics statement

Written informed consent was obtained from the individual(s) for the publication of any potentially identifiable images or data included in this article.

Author contributions

JZ and YL contributed to composing the manuscript. JZ collected the patient's data. YL and HZ revised the manuscript. All authors contributed to the article and approved the submitted version.

Funding

This study was funded by the National Key R&D Program of China (2020YFC2008105).

Conflict of interest

The authors declare that the research was conducted in the absence of any commercial or financial relationships that could be construed as a potential conflict of interest.

Publisher's note

All claims expressed in this article are solely those of the authors and do not necessarily represent those of their affiliated organizations, or those of the publisher, the editors and the reviewers. Any product that may be evaluated in this article, or claim that may be made by its manufacturer, is not guaranteed or endorsed by the publisher.

Supplementary material

The Supplementary Material for this article can be found online at: https://www.frontiersin.org/articles/10.3389/fcvm.2022.1086457/full#supplementary-material

References

1. Whisenant B, Kapadia S, Eleid M, Kodali S, McCabe J, Krishnaswamy A, et al. One-year outcomes of mitral valve-in-valve using the SAPIEN 3 transcatheter heart valve. *JAMA Cardiol.* (2020) 5:1245–52. doi: 10.1001/jamacardio.2020.2974

2. D'Onofrio A, Zucchetta F, Gerosa G. Simultaneous transapical aortic and mitral valve-in-valve implantation for double prostheses dysfunction: case report and technical insights. *Catheter Cardiovasc Interv.* (2014) 84:509–12. doi: 10.1002/ccd.25498

3. Caus T, Rouvière P, Collart F, Mouly-Bandini A, Montiès J, Mesana T. Late results of double-valve replacement with biologic or mechanical prostheses. *Ann Thorac Surg.* (2001) 71:S261–4. doi: 10.1016/s0003-4975(01)02499-7

4. Liu K, Shen J, Wu K, Meng F, Wang S, Zheng S, et al. Transapical mitral valve-in-valve implantation for failed bioprosthetic valve using the J-valve system with locator device: early and mid-term outcomes. *Ann Transl Med.* (2022) 10:21. doi: 10.21037/atm-21-6513

5. Bauernschmitt R, Bauer S, Liewald C, Emini R, Oechsner W, Beer M, et al. First successful transcatheter double valve replacement from a transapical access and nine-month follow-up. *EuroIntervention.* (2017) 12:1645–8. doi: 10.4244/EIJ-D-16-00896

6. Savoj J, Iftikhar S, Burstein S, Hu P. Transcatheter double valve-in-valve replacement of aortic and mitral bioprosthetic valves. *Cardiol Res.* (2019) 10:193–8. doi: 10.14740/cr863

7. Agarwal V, Kaple R, Mehta H, Singh P, Bapat V. Current state of transcatheter mitral valve implantation in bioprosthetic mitral valve and in mitral ring as a treatment approach for failed mitral prosthesis. *Ann Cardiothorac Surg.* (2021) 10:585–604. doi: 10.21037/acs-2021-tviv-80

frontiers | Frontiers in Surgery

TYPE Case Report
PUBLISHED 06 January 2023
DOI 10.3389/fsurg.2022.1008444

OPEN ACCESS

EDITED BY
Hendrik Tevaearai Stahel,
Bern University Hospital, Switzerland

REVIEWED BY
Bineesh Radhakrishnan,
Sree Chitra Tirunal Institute for Medical Sciences and Technology (SCTIMST), India
Maruti Haranal,
U N Mehta Institute of Cardiology and Research, India

*CORRESPONDENCE
Yiming Ni
1183020@zju.edu.cn
Junnan Zheng
zhengjunnan@zju.edu.cn

†These authors have contributed equally to this work

SPECIALTY SECTION
This article was submitted to Heart Surgery, a section of the journal Frontiers in Surgery

RECEIVED 31 July 2022
ACCEPTED 17 October 2022
PUBLISHED 06 January 2023

CITATION
Guo L, Yang Q, Han Y, Zhao H, Chen L, Zheng J and Ni Y (2023) Case Report: Using Medtronic AP360 mechanical prosthesis in mitral valve replacement for patients with mitral insufficiency after primum atrial septal defect repair to reduce left ventricular outflow tract obstruction risk.
Front. Surg. 9:1008444.
doi: 10.3389/fsurg.2022.1008444

Case Report: Using Medtronic AP360 mechanical prosthesis in mitral valve replacement for patients with mitral insufficiency after primum atrial septal defect repair to reduce left ventricular outflow tract obstruction risk

Lei Guo†, Qiqi Yang†, Yu Han, Haige Zhao, Liangwei Chen, Junnan Zheng* and Yiming Ni*

Department of Cardiovascular Surgery, The First Affiliated Hospital, College of Medicine, Zhejiang University, Hangzhou, China

Background: Atrial septal defect is one of the most common congenital heart diseases in adults. Primum atrial septal defect (PASD) accounts for 4%–5% of congenital heart defects. Patients with PASD frequently suffer mitral insufficiency (MI), and thus, mitral valvuloplasty (MVP) or mitral valve replacement (MVR) is often required at the time of PASD repair. Unfortunately, recurrent unrepairable severe mitral regurgitation can develop in many patients undergoing PASD repair plus MVP in either short- or long-term after the repair surgery, requiring a re-do MVR. In those patients, the risk of left ventricular outflow tract obstruction (LVOTO) has increased.

Case presentation: We present five such cases, ranging in age from 24 to 47 years, who had a PASD repair plus MVP or MVR for 14–40 years while suffering moderate to severe mitral regurgitation. Using Medtronic AP360 mechanical mitral prostheses, only one patient experienced mild LVOTO.

Conclusions: The use of Medtronic AP360 mechanical mitral prostheses to perform MVR in patients with MI who had a history of PASD repair can potentially reduce the risk of LVOTO. Long-term follow-up is required to further confirm this clinical benefit associated with AP360 implantation in patients with PASD.

KEYWORDS

PASD repair, MVR, LVOTO, congenital heart disease, case report

Introduction

Atrial septal defect (ASD) is one of the most common congenital heart diseases in adults. Primum atrial septal defect (PASD), also known as endocardial cushion defect or partial atrioventricular (AV) septal defect, accounts for 4%–5% of congenital heart defects (1, 2). PASD is defined as a defect at the base of the interatrial septum caused

Abbreviations
AV, atrioventricular; LA, left atrium; LV, left ventricle; LVOT, left ventricular outflow tract; LVOTO, left ventricular outflow tract obstruction; MI, mitral insufficiency; MVP, mitral valvuloplasty; MVR, mitral valve replacement; PASD, Primum atrial septal defect.

by failure of the primum septum to fuse with the endocardial cushions. PASD is usually associated with defects in AV valves, especially in the anterior mitral valve leaflet, and thus, patients with PASD are mostly complicated with mitral insufficiency (MI) requiring mitral valvuloplasty (MVP) or mitral valve replacement (MVR) at the time of PASD repair. Also, recurrent severe mitral regurgitation is observed in many patients undergoing PASD repair plus MVP in either short- or long-term after the repair surgery, requiring a reoperation (3). An MVR is often required in these patients with unrepairable MI. Nevertheless, left ventricular outflow tract obstruction (LVOTO) often occurred after PASD repair in these patients, with or without MVR, leading to dyspnea, coronary insufficiency, congestive heart failure, and even death (4). Here, we present five cases of successful treatment of MI in patients with PASD repair history using Medtronic AP360 mechanical prostheses.

Case report

Case 1

A 34-year-old female was admitted to our hospital because of chest pain complaint for 2 days. She had a PASD repair followed by an MVR 5 months after the PASD repair because of MI 25 years ago. Her echocardiography showed a peak left ventricular outflow tract (LVOT) pressure gradient of 109 mmHg, left ventricular outflow peak velocity of 5.23 m/s, minimum LVOT diameter in anteroposterior dimension of 7 mm, and the thickness of muscular part of interventricular septum of 14–16 mm, causing severe LVOTO (**Figure 1A**). The patient underwent MVR and LVOT repair *via* median sternotomy. Intraoperative examination revealed that part of the sewing cuff of the previously implanted mitral prosthesis was covered with hyperplastic annulus fibrosus tissue, which protruded from the mitral annulus underneath the mechanical valve into the left ventricular outflow tract (**Figure 1B**) and that one prosthetic valve lobe failed to open completely. Thus, the hyperplastic fibrous ring on the prosthetic valve and the thickened endocardium of the ventricular septum resulted in a stenosis ring. We implanted a 22# AP360 mechanical prosthesis (Medtronic, Inc., Minneapolis, MN, USA) to replace the previous prosthetic valve. The patient's postoperative echocardiography showed that the newly implanted mechanical valve worked well without residual LVOTO.

Case 2

Patient 2 was a 24-year-old female. She was hospitalized because of a 1-month history of palpitation, accompanied by occasional chest tightness and shortness of breath. She had PASD repair plus MVP 14 years ago. Her echocardiography at the hospital admission showed moderate to severe MI and anterior mitral valve leaflet cleft. The mitral valve was unrepairable and a 24# AP360 mechanical prosthesis implantation was performed. Mild postoperative LVOT stenosis was observed: Her postoperative echocardiography confirmed that the implanted prosthetic valve performed well and showed that her peak LVOT pressure gradient was 40 mmHg and minimum LVOT diameter in anteroposterior dimension was 8.9 mm.

Cases 3–5

Patients 3–5 were aged from 29 to 47 years and hospitalized because of MI. They had PASD repair plus MVP 15–40 years ago. The existing mitral valve was beyond repair, and thus,

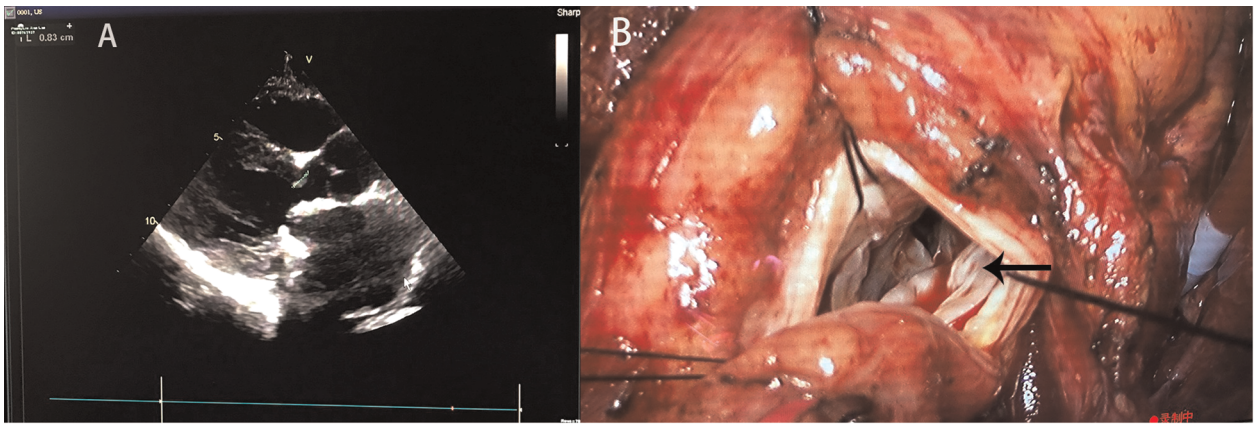

FIGURE 1
(A) Preoperative echocardiography showed and (B) intraoperative findings of Case 1. The black arrow indicates the protruding mitral annulus tissue.

TABLE 1 Clinical data of five patients.

Case no.	Gender	Age	Previous surgery	Preoperative MI	Interventricular septal thickness (mm)	Preoperative gradient of LVOT (mmHg)	Preoperative peak velocity of LVOT (m/s)	Prosthesis implantation and suturing technique	Postoperative LVOTO
1	Female	34	PASD repair, MVR	Mild	14–16	109	5.23	22# AP360, non-everting suture	None
2	Female	23	PASD repair	Severe	8	<40	<3.0	24# AP360, everting suture	Mild (peak velocity 3.2 m/s, gradient 40 mmHg)
3	Male	57	PASD repair	Severe	9	<40	<3.0	24# AP360, everting suture	None
4	Female	29	PASD repair	Moderate to severe	10	<40	<3.0	24# AP360, everting suture	None
5	Female	45	PASD repair	Severe	9	<40	<3.0	26# AP360, everting suture	None

MI, mitral incompetence; LVOT, left ventricular outflow tract; LVOTO, left ventricular outflow tract obstruction; PASD, partial atrial septal defect.

MVR was performed on the patients. Medtronic AP360 mechanical prostheses of proper sizes were implanted. All three patients recovered uneventfully.

All patients underwent surgery *via* regular cardiopulmonary bypass through median sternotomy or right thoracotomy. Standard prophylactic antibiotics with intravenous second-generation cephalosporin in the right dose were given to patients with AP360 or other prostheses. After 1 year of follow-up, all five patients were still alive and in NYHA function class 1 or 2 with no major complications. Echocardiography showed no apparent abnormality (**Table 1**).

Discussion

LVOTO, which has an incidence rate of up to 6%, is one of the most common complications in patients undergoing PASD repair (5, 6). In this case series, we reported five patients with previous PASD repair history, who underwent MVR for MI in our center. All of them were implanted with a Medtronic AP360 mechanical mitral valve including one re-MVR, and only one patient developed mild postoperative LVOTO.

We used AP360 valves in these five patients because we believe that the design of AP360 could reduce the risk of LVOTO. In normal anatomy, LVOT is only a few millimeters long and the aorta is "wedged" between the mitral and tricuspid valves. However, in patients with PASD, the aortic valve is anterior and rightward but is not positioned between the two normal AV valves, which consequently changes the anteroposterior dimension of the LVOT. The should-be position of the aortic root forms an extra length of LVOT, which is absent in the heart with normal anatomy. Moreover, the deficiency of the septum makes a convexity towards the ventricular side, narrowing the LVOT. These anatomic abnormalities lead to a narrow and elongated LVOT with an abnormal outlet angle, which is described classically as the "goose neck" deformity in angiography (6). Because of the anatomic characteristics of PASD as mentioned above, performing an MVR on a PASD patient is risky. An intra-annularly placed prosthetic valve may even worsen LVOTO (7, 8).

Medtronic AP360 mechanical prosthesis has unique advantages. Thanks to its special design which looks like an inverted ATS mechanical prosthesis, it locates mostly on the atrial side (**Figure 2B**). Combined with supra-annular placement, the AP360 prosthesis can be lifted by several millimeters and thus reduce the influence on the LVOT to the minimum. While intra-annular placement makes the main part of a prosthetic valve, such as ATS mechanical prosthesis, locate on the ventricular side, narrowing the LVOT even further (**Figure 2A**).

Besides, a prosthetic valve with pannus and hyperplastic annulus fibrous tissue can partially block the LVOT and thus increase the risk of LVOTO. In Case 1 of this report, we found that part of the sewing cuff of the previously implanted prosthetic valve was covered with hyperplastic annulus fibrous tissue protruding into the LVOT. The sewing cuff of the AP360 mechanical prosthesis, which is not in the same horizontal plane as the prosthetic valve's opening and different from other prosthetic valves in terms of positioning, can avoid hyperplastic annulus fibrous tissue formation. Thus, the potential risk of LVOTO associated with AP360 prosthesis implantation can be reduced.

Notably, the Carbomedics mechanical mitral prosthesis can be squeezed by the scarred annulus and thus sink into the ventricular side (normally pushed to the atrial side due to pressure difference) and worsen LVOTO because of its flexible and longitudinal symmetrical sewing cuff. Although other types of mechanical valves with a similar design as the ATS prosthetic valves maybe not be as bad as the Carbomedics valves in terms of the risk of LVOTO, could still sink to the

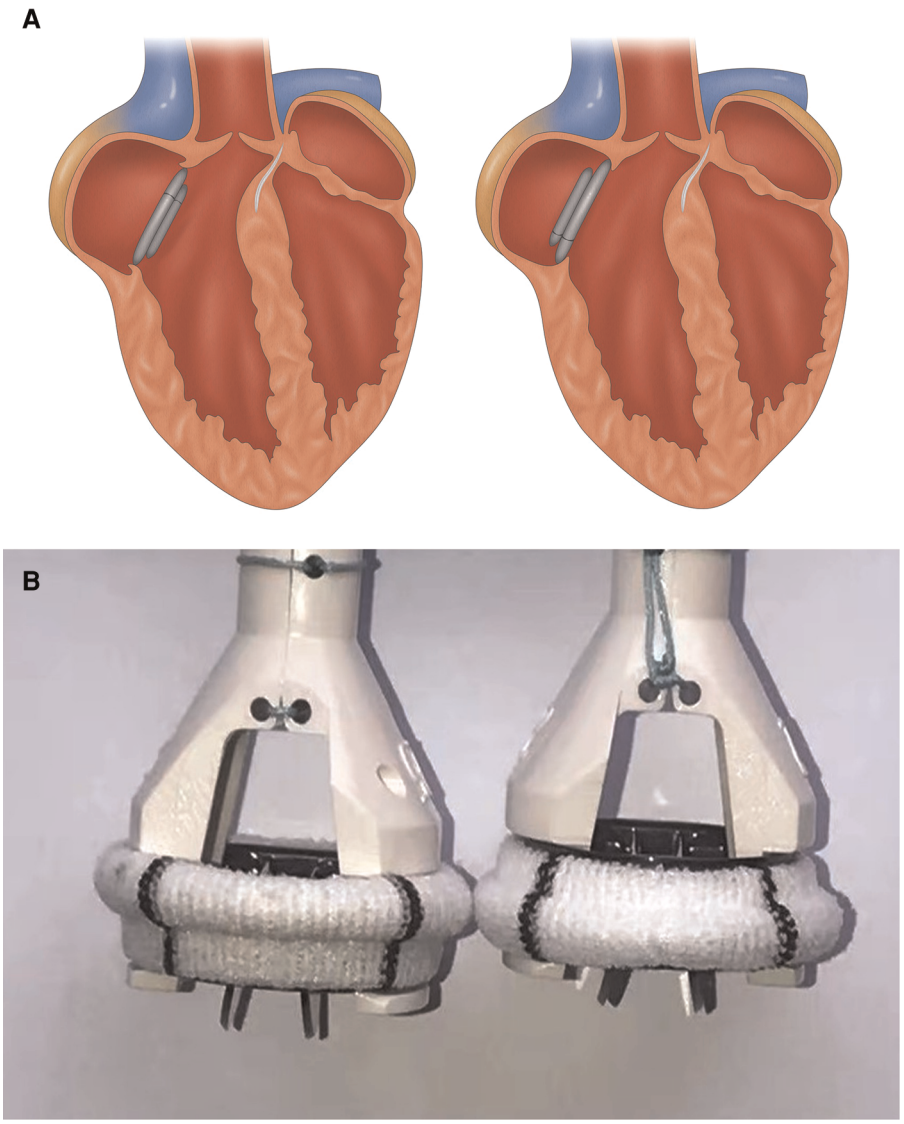

FIGURE 2
(**A**) Cartoon showing an implanted ATS mechanical mitral valve (left) and AP360 (right) after MVR, and (**B**) photos of an ATS mechanical mitral valve (left) and AP360 (right). Panel **A** shows that after the implantation, ATS valve will subside more substantially into the LVOT than an AP360, resulting in a higher risk of LVOTO. Panel **B** shows that with the sewing cuff in the same plane, the ATS is approximately 3 mm lower than the AP360. MVR, mitral valve replacement; LVOT, left ventricular outflow tract; LVOTO, left ventricular outflow tract obstruction.

LV to some degree. Implantation of Medtronic AP360 prosthesis using a non-everting suture can lift the prosthesis to the left atrium (LA) and avoid this situation.

We had encountered a case showing Carbomedics mitral valve implantation associated with LVOTO. A 40-year-old female was diagnosed with primum ASD, anterior mitral valve leaflet cleft, and moderate tricuspid regurgitation. She underwent tricuspid valvuloplasty and PASD repair. However, her mitral valve was beyond repair and thus a 27# Carbomedics mechanical mitral valve was then implanted. Her postoperative TEE showed the well-performed implanted prosthetic mitral valve, a peak LVOT pressure gradient of 34 mmHg, and left ventricular outflow peak velocity of 2.9 m/s. Her postoperative 3-month follow-up echocardiography showed moderate LVOT stenosis with a peak LVOT pressure gradient of 73 mmHg, left ventricular outflow peak velocity of 4.2 m/s, minimum LVOT diameter in an anteroposterior dimension of 13 mm, and an interventricular septum thickness of 10 mm. Postoperative 18-month follow-up echocardiography showed severe LVOT stenosis with a peak LVOT pressure gradient of 92 mmHg, left ventricular outflow peak velocity of 4.8 m/s, minimum LVOT diameter in an

TABLE 2 Mitral prosthesis and LVOT dimension in re-do MVR patients.

Types of mitral prostheses	Pre-surgery LVOT dimension (mm)	Post-surgery LVOT dimension (mm)	*P*-value	Pre-surgery max LVOT gradients (mmHg)	Post-surgery max LVOT gradients (mmHg)	*P*-value
Medtronic ATS ($n = 11$)	18.46 ± 1.56	18.00 ± 3.22	NS	10.75 ± 5.76	9.93 ± 4.37	NS
Medtronic AP360 ($n = 5$)	15.41 ± 3.43	17.68 ± 2.08	<0.001	61 ± 53.98	19.28 ± 10.15	<0.001
Carbomedics ($n = 9$)	17.67 ± 1.66	17.22 ± 1.79	NS	5.76 ± 3.64	6.31 ± 1.24	NS
St. Jude ($n = 12$)	17.50 ± 1.57	17.42 ± 1.52	0.018	5.38 ± 2.08	5.18 ± 2.33	NS

LVOT, left ventricular outflow tract; NS, not significant; MVR, mitral valve replacement.

anteroposterior dimension of 6.6 mm and an interventricular septum thickness of 12 mm. The patient refused a re-MVR. Similarly, the Mayo Clinic had reported a case of acute LVOTO after Carbomedics MVR (9), and they used a non-everting suture to solve this problem, which coincided with us on this point.

Actually, LVOTO was more common in patients who had to have their MVR re-done. We compared the difference in LVOT dimension and LVOT gradients of patients who underwent re-do MVR for different reasons with various mechanical mitral prostheses, as shown in Table 2. For St. Jude, Carbomedics and ATS mitral valve, there is no significant change in LVOT dimension and max LVOT gradients between pre- and post-surgery, while for AP360 group, the LVOT dimension of post-surgery is larger than pre-surgery and the max LVOT gradients is significantly reduced after surgery. The sample capacity was not large enough and the fact that a part of the patients of the AP360 group was already complicated with LVOTO before surgery might partially contribute to the result. However, according to our experience, we still believe choosing an AP360 prosthesis with a proper size matching the patient's anatomic structure is critical for good clinical outcomes.

On the other hand, an oversized AP360 may cause valve dysfunction. One of the lobes of an oversized prosthesis could be blocked by the thickened interventricular septum, leading to valve dysfunction. Aggressive implantation of an oversized prosthetic valve to avoid mitral prosthesis-patient mismatch, which remains to be controversial regarding the patient outcome, thus is not recommended (10).

Some pediatric cardiac surgeons suggested that the chimney technique could be used to avoid LVOTO in young patients undergoing MVR (11). The Chimney technique is to suture a several-millimeter-long tubular dacron graft to the sewing cuff of a prosthetic valve and then suture the graft to the native mitral annulus, forming a composite graft floating in the LA like a "chimney". Although the chimney technique showed promising LVOTO prevention in children, the long-term effect is still unknown in patients with PASD.

Conclusion

Usage of Medtronic AP360 mechanical mitral prostheses to perform MVR in patients with MI who had a PASD repair history can potentially reduce the risk of LVOTO. Long-term follow-up is required to further confirm this clinical benefit associated with AP360 implantation in patients with PASD.

Data availability statement

The original contributions presented in the study are included in the article/Supplementary Material, further inquiries can be directed to the corresponding author/s.

Ethics statement

The studies involving human participants were reviewed and approved by the Clinical Research Ethics Committee of the First Affiliated Hospital, College of Medicine, Zhejiang University. Written informed consent of clinical detail and image publication was obtained from the patient.

Author contributions

LG and QY drafted the original manuscript. YN and LG participated in the treatment. YN, HZ, and JZ revised the manuscript. All authors contributed to the article and approved the submitted version.

Funding

This work was supported by (1) the Natural Science Foundation of Zhejiang Province, Zhejiang, China (Grant No. LY20H020003); (2) Medicine and Health Science and Technology Plan Projects of Zhejiang Province, Zhejiang China (Grant No. 2019KY377); (3) the Natural Science Foundation of Zhejiang Province, Zhejiang, China (Grant No. LQ20H020004); and (4) Medicine and Health

Science and Technology Plan Projects of Zhejiang Province, Zhejiang China (Grant No. 2020KY120).

Conflict of interest

The authors declare that the research was conducted in the absence of any commercial or financial relationships that could be construed as a potential conflict of interest.

Publisher's note

References

1. Reller MD, Strickland MJ, Riehle-Colarusso T, Mahle WT, Correa A. Prevalence of congenital heart defects in metropolitan Atlanta, 1998–2005. *J Pediatr*. (2008) 153(6):807–13. doi: 10.1016/j.jpeds.2008.05.059

2. Hoffman JI, Kaplan S. The incidence of congenital heart disease. *J Am Coll Cardiol*. (2002) 39(12):1890–900. doi: 10.1016/S0735-1097(02)01886-7

3. Patlolla SH, Dearani JA, Connolly HM, Warnes CA, Lahr BD, Schaff HV, et al. Repair of partial atrioventricular septal defects in adults: a single center experience. *Semin Thorac Cardiovasc Surg*. (2021) 33(2):469–78. doi: 10.1053/j.semtcvs.2020.08.009

4. Stulak JM, Burkhart HM, Dearani JA, Cetta F, Barnes RD, Connolly HM, et al. Reoperations after repair of partial atrioventricular septal defect: a 45-year single-center experience. *Ann Thorac Surg*. (2010) 89(5):1352–59. doi: 10.1016/j.athoracsur.2010.01.018

5. Gurbuz AT, Novick WM, Pierce CA, Watson DC. Left ventricular outflow tract obstruction after partial atrioventricular septal defect repair. *Ann Thorac Surg*. (1999) 68(5):1723–6. doi: 10.1016/S0003-4975(99)01074-7

6. Overman DM. Reoperation for left ventricular outflow tract obstruction after repair of atrioventricular septal. *Semin Thorac Cardiovasc Surg Pediatr Card Surg Annu*. (2014) 17(1):43–7. doi: 10.1053/j.pcsu.2014.01.008

7. Jones A, Livesey S. A novel case of late left ventricular outflow tract obstruction post mitral valve surgery. *J Surg Case Rep*. (2019) 2019(1):rjy357. doi: 10.1093/jscr/rjy357

8. Gallo P, Formigari R, Hokayem NJ, D'Offizi F, D'Alessandro Francalanci P, et al. Left ventricular outflow tract obstruction in atrioventricular septal defects: a pathologic and morphometric evaluation. *Clin Cardiol*. (1991) 14(6):513–21. doi: 10.1002/clc.4960140611

9. Alsidawi S, Joyce DL, Malouf JF, Nkomo VT. Acute LVOT obstruction with a carbomedics mechanical valve prosthesis. *J Card Surg*. (2016) 31(6):376–9. doi: 10.1111/jocs.12749

10. Akuffu AM, Zhao H, Zheng J, Ni Y. Prosthesis-patient mismatch after mitral valve replacement: a single-centered retrospective analysis in East China. *J Cardiothorac Surg*. (2018) 13(1):100. doi: 10.1186/s13019-018-0788-4

11. Gonzalez RA, Aroca Á, Polo L, Rey J, Villagrá F. Chimney technique for mitral valve replacement in children. *Ann Thorac Surg*. (2013) 96(5):1885–7. doi: 10.1016/j.athoracsur.2013.04.092

frontiers | Frontiers in Surgery

TYPE Case Report
PUBLISHED 11 January 2023
DOI 10.3389/fsurg.2022.1102742

OPEN ACCESS

EDITED BY
Hendrik Tevaearai Stahel,
Bern University Hospital, Switzerland

REVIEWED BY
Anshuman Darbari,
All India Institute of Medical Sciences, India
Daniele Linardi,
University of Verona, Italy

*CORRESPONDENCE
Jijia Liu
✉ mcliujijia@csu.edu.cn

SPECIALTY SECTION
This article was submitted to Heart Surgery, a section of the journal Frontiers in Surgery

RECEIVED 19 November 2022
ACCEPTED 19 December 2022
PUBLISHED 11 January 2023

CITATION
Gong K, Yang Y, Shen Y, Liu H, Xie L and Liu J (2023) Successful management of a rare case of juvenile giant right ventricular myxoma. Front. Surg. 9:1102742. doi: 10.3389/fsurg.2022.1102742

Successful management of a rare case of juvenile giant right ventricular myxoma

Ke Gong[1], Yifeng Yang[1], Yadan Shen[1,2], Haidan Liu[1], Li Xie[1] and Jijia Liu[1]*

[1]Department of Cardiovascular Surgery, The Second Xiangya Hospital of Central South University, Central South University, Changsha, China, [2]Extracorporeal Life Support Center of Cardiovascular Surgery, The Second Xiangya Hospital of Central South University, Central South University, Changsha, China

Primary cardiac tumors are extremely uncommon in young children and infants. Cardiac myxoma are typically found in the atria, predominately in the left atrium, with relatively few found on the right side, such as in the right ventricle or pulmonary artery. Numerous significant complications, including sudden death, can result from obstruction of the main pulmonary artery trunk and right ventricular outflow tract. Here, we describe the case of a 14-year-old Chinese girl diagnosed with a right ventricular myxoma located in the right ventricle and extended into the main pulmonary trunk. Complete resection of the myxoma and histological confirmation were performed.

KEYWORDS
primary cardiac tumors, right ventricle, diagnosis, treatment, surgery

Introduction

Myxomas occur in all age groups, most commonly between the ages of 30 and 60, and are predominantly found in females. Rhabdomyomas and teratomas are the most common tumors found in children, while myxomas and fibroids are less common. They are most commonly found in the left atrium. The right atrium (RA) is the second most frequent place where myxomas arise, constituting about 7%–12% of cases. Only a few cases of myxoma found in the right ventricle have been documented (1–4). The majority of medical professionals advise early surgical resection to lower mortality brought on by complications, such obstruction of the heart's inflow or outflow system (5). Here, we present a case of a primary cardiac myxoma in a child that had protruded into the pulmonary trunk from the right ventricle (RV).

Case report

This study obtained the informed consent of the patients and their families for publication. Due to chest congestion and edema, a 14-year-old girl with nephrotic syndrome who had been identified in a smaller district hospital in China was sent to our division. Her blood pressure was 109/80 mmHg at the time of admission, and her pulse rate was 107 beats per minute. Physical examination revealed face and ankle edema as well as a grade 4/6 systolic ejection murmur at the left upper sternal border.

Transthoracic echocardiography revealed a significant 70 × 30 mm RV mass which protruded into the right ventricular outflow tract (RVOT) and the pulmonary trunk. The pressure gradient from the pulmonary artery to the RV was 64 mmHg (**Figure 1A**). There was also enlargement of the RV and right axis deviation along with sinus tachycardia. A filling deficit in the RV, pulmonary trunk, and right pulmonary artery was discovered by computed tomography (CT) (**Figures 1C,D**).

She underwent a sternotomy and cardiopulmonary bypass creation by aortic and bicaval cannulation under general anesthesia. She had her RA and RVOT opened. The myxoma was attached to the membranous portion of interventricular septum and had grown into the main pulmonary artery and the right pulmonary artery. The mass was entirely eliminated (**Figure 2**). According to pathological findings, there were two pieces of tumor tissue totaling 5 × 4 × 2 cm, the majority of which was mucus. It appeared to be a myxoma under a microscope, with slightly larger individual nuclei. CD34 (vascular+), NSE(−), SMA(+), CK(−), CD68(+), MC(−), CR (+), Desmin(−), CEA(−), EMA (1), and F8(+) were immunohistochemically positive. She was discharged 7 days after surgery and the recovery time was uncomplicated. Following surgery, echocardiography showed an unobstructed RVOT (**Figure 1B**). Seven-year postoperative follow-up showed no recurrence of the patient's tumor. The entire process of disease development is described in **Table 1**.

Discussion

Up to 75% of myxomas are found in the left atrium. Right-sided myxomas are uncommon (15%–20%), and RV (3%–4%) or pulmonary artery myxomas are exceedingly uncommon (6). Syncope, pulmonary embolism, chest congestion, and sudden death are complications that can result from obstruction of the outflow of blood from the RV (2, 7).

Myxomas are uncommon in children despite being the most frequent primary heart tumor. A study reported that 8 children with a clinical diagnosis of cardiac tumor underwent surgery between 1986 and 2003. Surgical pathology only revealed myxomas in 2 patients (25%) (8). In another study, 56 children had primary heart tumors. Of those, 6 children had fibrosarcoma and 44 children had rhabdomyosarcoma. No myxomas were discovered (9). Thus, pediatric cardiac myxomas are quite uncommon. Although right ventricular myxomas in children have been documented in the past,

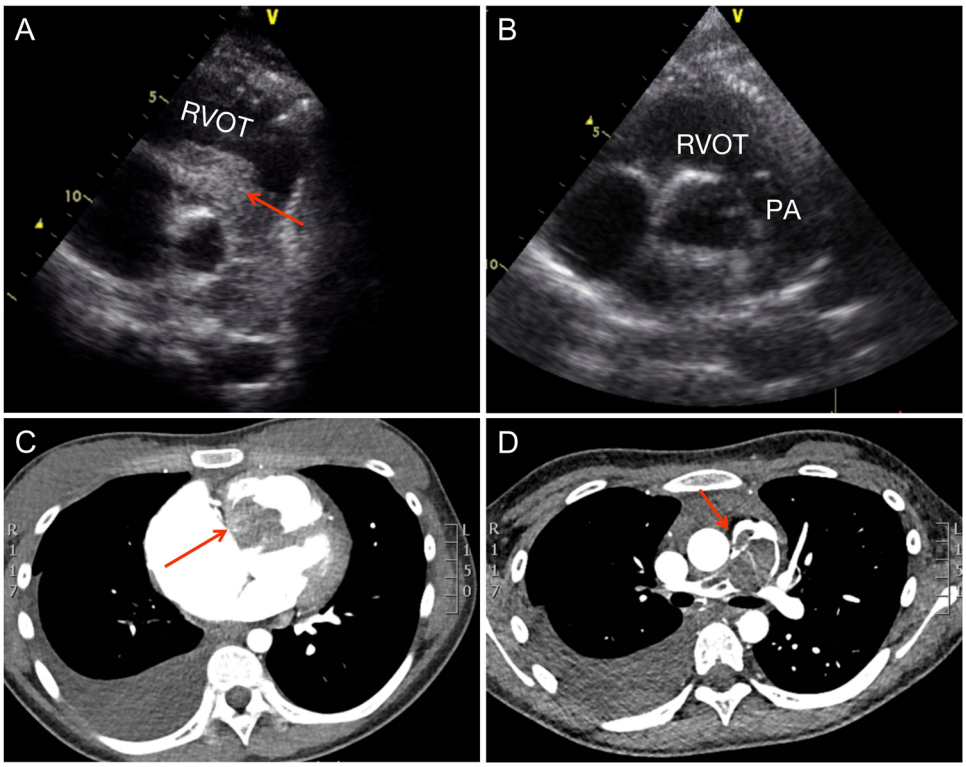

FIGURE 1
Preoperative and postoperative examination. (**A**) Preoperative parasternal short-axis view at the level of the aortic valve showing the obstructed right ventricular outflow tract and pulmonary trunk. (**B**) Postoperative parasternal short-axis view at the level of the aortic valve showing the unobstructed right ventricular outflow tract and pulmonary trunk. (**C**) Computed tomography reveals the right ventricular outflow tract. (**D**) Computed tomography reveals the pulmonary trunk and right pulmonary artery. RVOT, right ventricular outflow tract; PA, pulmonary artery.

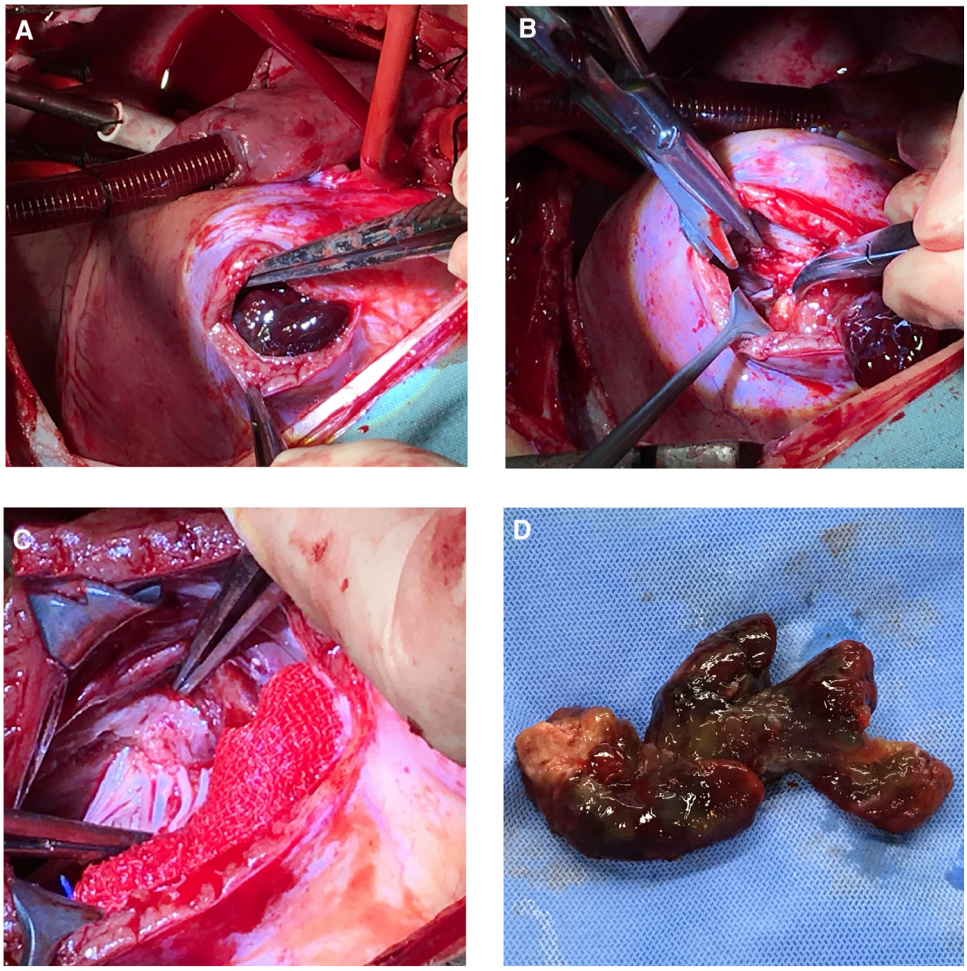

FIGURE 2
Surgery pictures. Operative procedures. (**A**) Right ventricular outflow tract incision was made to expose the tumor. (**B**) and (**C**) The tumor root which attached to the membranous portion of interventricular septum was surgically removed. (**D**) The entire tumor.

pediatric cases of enormous right ventricular mucinous tumors that extend into the pulmonary artery are extremely rare. Patients of this type are at a significant risk for sudden death and pulmonary embolism.

It is especially useful for the diagnosis and treatment of patients to properly represent the size, quantity, and attachments of tumors. Consequently, it is crucial to appropriately describe cardiac tumor using imaging. CT, MRI and echocardiography are frequently used to assess cardiac tumor, according to the guidelines. The location, size, form, attachment points, and motion features of mucinous tumors can be determined *via* transthoracic echocardiography and, if required, transesophageal access. CT provides a better assessment of tumor extent, including invasion of adjacent vessels and pulmonary metastases, than echocardiography. In addition, CT is capable of directly imaging tumorigenic pulmonary emboli and can also be used to assess calcification (10). MRI can assess myocardial infiltration, pericardial involvement, and/or extracardiac extension. MRI overcomes the usual limitations of echocardiography and can more accurately assess changes in cardiac function. The use of intravenous contrast agents has improved tumor characterization and delineation of tumor boundaries. MRI can also differentiate tumors from other non-tumor masses (11–13). In our case, the patient did not undergo the MRI, because MRI is still a relatively expensive examination. The financial burden on the patient is why this examination was not performed. Although not used in our report, MRI is still important as an adjunct to diagnose tumors and determine the type of tumor.

In our case, the symptoms of chest tightness, facial edema, and lower extremity edema were so first diagnosed as nephrotic syndrome. This may be due to a possible lack of cardiac auscultation. Therefore, in suspicious cases, a brief auscultation and routine imaging should be performed at the regional hospital before the patient is referred to a higher

10.3389/fsurg.2022.1102742

TABLE 1 Timeline. The process of the patient's disease progression and treatment.

Timeline	3 months before hospitalization	14 days before hospitalization	3 days before hospitalization	Hospitalization	Day 2 of hospitalization	Day 4 of hospitalization	5:00 am on the day 5 of hospitalization	9:00 am on the day 5 of hospitalization	Day 11 after surgery	Follow-up review
Process	Finding symptoms	Hospitalization in other hospitals, diagnosis of nephrotic syndrome	Hyperechoic findings on heart ultrasound at other hospitals, pending confirmation	Transferred to our hospital pediatric department, blood test	Echocardiography	CT	Transferred to our cardiovascular surgery department	Surgery	Discharged from hospital	Annually

level hospital. This is important because delays in diagnosis and treatment can lead to complications and, in severe cases, death.

Since no medications have been developed to diminish or stop the growth of myxomas, surgical excision is the only effective treatment for them in any heart cavity. The surgical plan includes complete removal of the tumor while restoring any tumor-affected valves that may be present. Vigorous palpation and other cardiac manipulation should be avoided until extracorporeal circulation is started since the threat of tumor fragmentation and embolization remains high. Asymptomatic myxoma patients have also undergone surgery with positive outcomes and no postoperative fatalities (14, 15). Recurrence has been observed in approximately 5% of patients months or years after surgery. On the surgical approach, some surgeons choose either the RA or RVOT approach. We chose both the RA and RVOT approach because the root of the patient's tumor was located in the membranous portion of interventricular septum and entered the pulmonary artery along the RVOT. Therefore, we believe that a simple right atrial incision is not sufficient to remove the tumor cleanly, so we choose a dual approach for an incision. After the operation, the child did very well and was almost back to normal upon discharge from the hospital. Rarely, a RV myxoma will block the RVOT in children (16). However, immediate and thorough surgical resection should be performed to prevent outflow tract occlusion, which could cause rapid mortality.

Data availability statement

The original contributions presented in the study are included in the article/Supplementary Material, further inquiries can be directed to the corresponding author/s.

Ethics statement

The studies involving human participants were reviewed and approved by Ethics Committee of the Second Xiangya Hospital of Central South University. Written informed consent to participate in this study was provided by the participants' legal guardian/next of kin. Written informed consent was obtained from the individual(s), and minor(s)' legal guardian/next of kin, for the publication of any potentially identifiable images or data included in this article.

Author contributions

KG, YDS, HDL, LX and JJL: contributed to conception and design of the study. KG: wrote the first draft of the manuscript.

KG, YFY and JJL: wrote sections of the manuscript. All authors contributed to the article and approved the submitted version.

Conflict of interest

The authors declare that the research was conducted in the absence of any commercial or financial relationships that could be construed as a potential conflict of interest.

Publisher's note

References

1. Shah IK, Dearani JA, Daly RC, Suri RM, Park SJ, Joyce LD, et al. Cardiac myxomas: a 50-year experience with resection and analysis of risk factors for recurrence. *Ann Thorac Surg*. (2015) 100(2):495–500. doi: 10.1016/j.athoracsur.2015.03.007

2. Karagoz A, Keskin B, Karaduman A, Tanyeri S, Adademir T. Multidisciplinary approach to right ventricular myxoma. *Braz J Cardiovasc Surg*. (2021) 36(2):257–60. doi: 10.21470/1678-9741-2020-0177

3. Kaulitz R, Haen S, Sieverding L. Neonatal aortic arch obstruction due to pedunculated left ventricular foetal myxoma. *Cardiol Young*. (2015) 25 (7):1393–5. doi: 10.1017/S1047951114001929

4. Li Y, Yang W, Liao S, Zuo H, Liu M. Cardiac myxomas as great imitators: a rare case series and review of the literature. *Heart Lung*. (2022) 52:182–9. doi: 10.1016/j.hrtlng.2022.01.010

5. Samanidis G, Khoury M, Balanika M, Perrea DN. Current challenges in the diagnosis and treatment of cardiac myxoma. *Kardiol Pol*. (2020) 78(4):269–77. doi: 10.33963/KP.15254

6. Mittle S, Makaryus AN, Boutis L, Hartman A, Rosman D, Kort S. Right-sided myxomas. *J Am Soc Echocardiogr*. (2005) 18(6):695. doi: 10.1016/j.echo.2005.03.007

7. Lu C, Yang P, Hu J. Giant right ventricular myxoma presenting as right heart failure with systemic congestion: a rare case report. *BMC Surg*. (2021) 21(1):64. doi: 10.1186/s12893-020-00977-4

8. Padalino MA, Basso C, Milanesi O, Vida VL, Moreolo GS, Thiene G, et al. Surgically treated primary cardiac tumors in early infancy and childhood. *J Thorac Cardiovasc Surg*. (2005) 129(6):1358–63. doi: 10.1016/j.jtcvs.2004.10.020

9. Beghetti M, Gow RM, Haney I, Mawson J, Williams WG, Freedom RM. Pediatric primary benign cardiac tumors: a 15-year review. *Am Heart J*. (1997) 134(6):1107–14. doi: 10.1016/S0002-8703(97)70032-2

10. Ekmektzoglou KA, Samelis GF, Xanthos T. Heart and tumors: location, metastasis, clinical manifestations, diagnostic approaches and therapeutic considerations. *J Cardiovasc Med*. (2008) 9(8):769–77. doi: 10.2459/JCM.0b013e3282f88e49

11. Lyon AR, Lopez-Fernandez T, Couch LS, Asteggiano R, Aznar MC, Bergler-Klein J, et al. 2022 ESC guidelines on cardio-oncology developed in collaboration with the European hematology association (EHA), the European society for therapeutic radiology and oncology (ESTRO) and the international cardio-oncology society (IC-OS). *Eur Heart J*. (2022) 43(41):4229–361. doi: 10.1093/eurheartj/ehac244

12. Poterucha TJ, Kochav J, O'Connor DS, Rosner GF. Cardiac tumors: clinical presentation, diagnosis, and management. *Curr Treat Options Oncol*. (2019) 20 (8):66. doi: 10.1007/s11864-019-0662-1

13. Luna A, Ribes R, Caro P, Vida J, Erasmus JJ. Evaluation of cardiac tumors with magnetic resonance imaging. *Eur Radiol*. (2005) 15(7):1446–55. doi: 10.1007/s00330-004-2603-y

14. Pinede L, Duhaut P, Loire R. Clinical presentation of left atrial cardiac myxoma. A series of 112 consecutive cases. *Medicine*. (2001) 80(3):159–72. doi: 10.1097/00005792-200105000-00002

15. Tetera W, Wilk A, Krol W, Braksator W. Asymptomatic left atrial myxoma. *J Cardiovasc Echogr*. (2022) 32(2):116–8. doi: 10.4103/jcecho.jcecho_70_21

16. Delmo Walter EM, Javier MF, Sander F, Hartmann B, Ekkernkamp A, Hetzer R. Primary cardiac tumors in infants and children: surgical strategy and long-term outcome. *Ann Thorac Surg*. (2016) 102(6):2062–9. doi: 10.1016/j.athoracsur.2016.04.057

frontiers | Frontiers in Cardiovascular Medicine

TYPE Case Report
PUBLISHED 18 January 2023
DOI 10.3389/fcvm.2022.1096973

OPEN ACCESS

EDITED BY
Hendrik Tevaearai Stahel,
Bern University Hospital, Switzerland

REVIEWED BY
Gabor Szeplaki,
Mater Private Hospital, Ireland
Alberto Guido Pozzoli,
Ospedale Regionale di Lugano, Switzerland
Michael Hofmann,
University of Zurich, Switzerland

*CORRESPONDENCE
Jian Liu
✉ Jameslau1984@sina.com
Peijian Wei
✉ pjwei14@163.com
Huiming Guo
✉ guohuiming@gdph.org.cn

†These authors have contributed equally to this work

SPECIALTY SECTION
This article was submitted to Heart Surgery, a section of the journal Frontiers in Cardiovascular Medicine

RECEIVED 13 November 2022
ACCEPTED 30 December 2022
PUBLISHED 18 January 2023

CITATION
Liu H, Tan T, Qiu H, Chen J, Liu J, Wei P and Guo H (2023) Case report: Thoracoscopic ablation for a patient with atrial fibrillation and persistent left superior vena cava.
Front. Cardiovasc. Med. 9:1096973.
doi: 10.3389/fcvm.2022.1096973

Case report: Thoracoscopic ablation for a patient with atrial fibrillation and persistent left superior vena cava

Haozhong Liu[1,2,3†], Tong Tan[1,2,3†], Hailong Qiu[2,3], Jimei Chen[2,3], Jian Liu[2,3*], Peijian Wei[2,3*] and Huiming Guo[2,3*]

[1]Shantou University Medical College, Shantou, China, [2]Department of Cardiovascular Surgery, Guangdong Cardiovascular Institute, Guangdong Provincial People's Hospital (Guangdong Academy of Medical Sciences), Southern Medical University, Guangzhou, China, [3]Guangdong Provincial Key Laboratory of South China Structural Heart Disease, Guangzhou, China

Persistent left superior vena cava (PLSVC) is a relatively rare congenital anomaly in the general population. It plays an important role in initiating and maintaining atrial fibrillation (AF) in some patients. Radiofrequency catheter ablation is the major treatment for patients with AF and PLSVC in most publications. Here, we reported a case of thoracoscopic ablation for a patient with atrial fibrillation and persistent left superior vena cava. After preprocedural simulation using virtual reality, we successfully completed box-lesion, ablation line from superior vena cava to inferior vena cava, left atrial appendage (LAA) excision, and PLSVC ablation. It provides a new perspective on surgical treatment for patients with AF and PLSVC.

KEYWORDS

persistent left superior vena cava, atrial fibrillation, surgical ablation, thoracoscopic surgery, virtual reality

Introduction

During fetal development, the failure of obliteration of the left anterior cardinal vein and the left Cuvier's canal of the left superior vena cava in time would result in their continued existence after birth and the formation of PLSVC (1). Meanwhile, PLSVC has been previously reported to be a potential arrhythmogenic source of trigger or driver of AF (2, 3). Meanwhile, AF is associated with a five-fold risk of stroke (4). It has been reported that both surgical and catheter ablation of AF with different energy sources and lesion types have promising clinical outcomes (5–7). In this paper, we reported a case of thoracoscopic ablation for a patient with AF and PLSVC.

Case presentation

A 61-year-old male patient was admitted to our hospital due to drug-refractory recurrent palpitations for 5 years. The electrocardiogram showed AF at 66 beats per minute. Echocardiography revealed the presence of PLSVC with an enlarged left atrium (57 mm) and right atrium (61 mm). Further computed tomography (CT) confirmed the identification of PLSVC (Figure 1A). Then three-dimensional reconstruction of cardiac structures was performed using the obtained CT images to visualize the anatomical features (Figure 1B). The PLSVC was shown to drain into the right atrium. Surgical ablation was required for this patient.

However, the surgical approach is hard to determine since LAA Resection may cause injury to the PLSVC. Therefore, a preprocedural simulation of thoracoscopic ablation using virtual reality was performed and it verified the feasibility of the thoracoscopic approach (Figure 1C). So, we decided to perform bilateral two-port thoracoscopic ablation for this patient. Written informed consent was obtained from the patient.

Details of the procedure have been reported previously (8). The lesion set was shown in Figure 2A. Then the procedure was begun on the right side after left single lung ventilation. The pericardium was incised 2 cm anterior to the parallel phrenic nerve and suspended to expose the right atrium and pulmonary vein. The oblique and transverse sinuses were bluntly dissected, and the right pulmonary vein was ablated six times by inserting the AtriCure bipolar isolator (AtriCure. Inc., Ohio, USA) through the right inferior pulmonary vein. Subsequently, the AtriCure bipolar ablation pen was used to complete the ablation of the left roof line and floor line, the superior vena cava to the inferior vena cava line, and the coronary sinus. In the same manner, the thoracic cavity was entered from the left side except the assistant port was set third intercostal space. The left atrial appendage was completely resected with a stapler (Figure 2B). By steering clear of the PLSVC, the AtriCure bipolar isolator was inserted through the left inferior pulmonary vein, and the left pulmonary vein was then ablated six times (Figure 2C). The PLSVC was also carefully clamped and ablated in the case of blood pressure stabilization. The intraoperative electrocardiogram revealed sinus rhythm. At the 12-month follow-up, the electrocardiogram showed sinus and rhythmic rhythm. No major adverse events (bleeding and thromboembolic events) were reported.

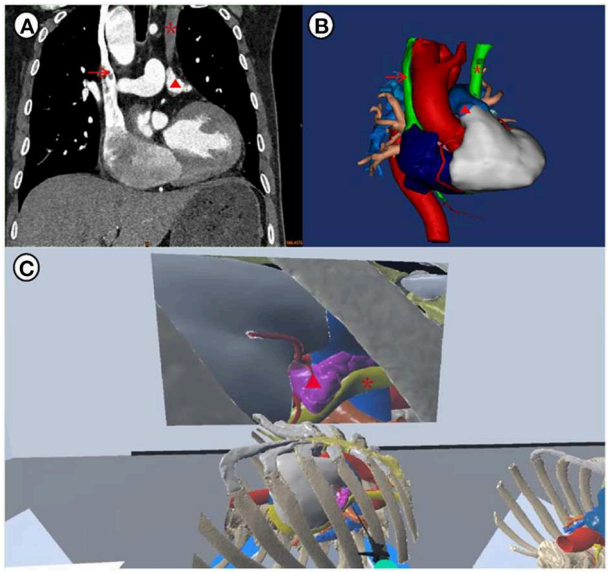

FIGURE 1
Preprocedural planning and simulation: **(A)** anatomical identification of PLSVC by CT; **(B)** three-dimensional reconstruction of the cardiac structures; **(C)** detection of the PLSVC and simulation of the thoracoscopic ablation using virtual reality tools. Surgeons' views can be obtained on this platform, and the 3D model can be zoomed in or out in a 360-degree version. The red triangle indicates left atrial appendage, the red arrow indicates right superior vena cava and the red asterisk indicates PLSVC.

Discussion

PLSVC is a relatively rare congenital anomaly, but it is one of the most common systemic venous anomalies in the thoracic cavity and has been reported to occur in 0.3–2% of the otherwise normal population and up to 10% of patients with congenital heart disease (9, 10). The current literature suggests that it is an incidental finding that often occurs with central venous catheters through the internal jugular vein or the subclavian vein. There are four anatomic types of PLSVC: PLSVC with atresia of the right superior vena cava (type 1); PLSVC draining into the right atrium with (type 2A) or without (type 2B) an anastomosis with right superior vena cava; and PLSVC draining into the left atrium (type 3) (11). Type 1 and 2 PLSVC have a higher frequency, which therein passes through the coronary sinus into the right atrium and therefore do not have significant hemodynamic consequences and in most cases manifest asymptomatically (12). However, PLSVC may be the arrhythmic source of persistent AF (2, 3), which is reasonable to apply surgical, catheter, or hybrid ablation (13). In this case, the patient preferred a minimally invasive surgical approach. Most AF patients with PLSVC were reported to undergo radiofrequency ablation, but data were limited and the long-term outcomes of freedom from AF were awaiting. During the thoracoscopic surgery, we were also allowed to perform left atrial appendage excision, which would further decrease the further adverse events like stroke. Besides, PLSVC can distort the normal anatomy of the atrium, leading to a higher risk of procedure complications, such as bleeding, and cardiac tamponade (3). On the contrary, thoracoscopic ablation offered a wide field of cardiac structures. Overall, surgical ablation through a double port thoracoscopic approach might be a more efficient and safer strategy for AF patients with PLSVC.

In this case of thoracoscopic ablation for a patient with AF and PLSVC, better visualization and surgical simulation were achieved by three-dimensional reconstruction and virtual reality technique. However, the first dilemma was the feasibility of thoracoscopic surgical ablation. The PLSVC sterically blocked our insulator from reaching the pulmonary veins. By measuring the diameter of the PLSVC and observing its relationship with surrounding structures, the diagnosis of a type 2B PLSVC was reconfirmed, and we concluded that the PLSVC could be bypassed without incisional enlargement or cardiopulmonary bypass. During the surgical simulation, we assumed the operation hole was set at the 4th rib, and the virtual visual field of thoracoscopy showed that both the PLSVC and the left atrial appendage were exposed within the operating range. Lu et al. (14) had a similar experience of deciding on a treatment strategy by using the 3D acquisition technique to understand the vascular anatomy of the PLSVC.

In addition, when clamping the PLSVC for ablation, the venous volume return to the heart might suddenly decrease, leading to a dipping in blood pressure. In such cases, cooperation between the surgeon and the anesthetist is required. The PLSVC should be relieved till to the hemodynamics return stable. Volume management and vasoactive agents were required when necessary. To achieve PLSVC ablation, we preferred performing more times instead of each long-time scale. There might be an extremely rare condition which only the PLSVC is complicated by atrial fibrillation while the right

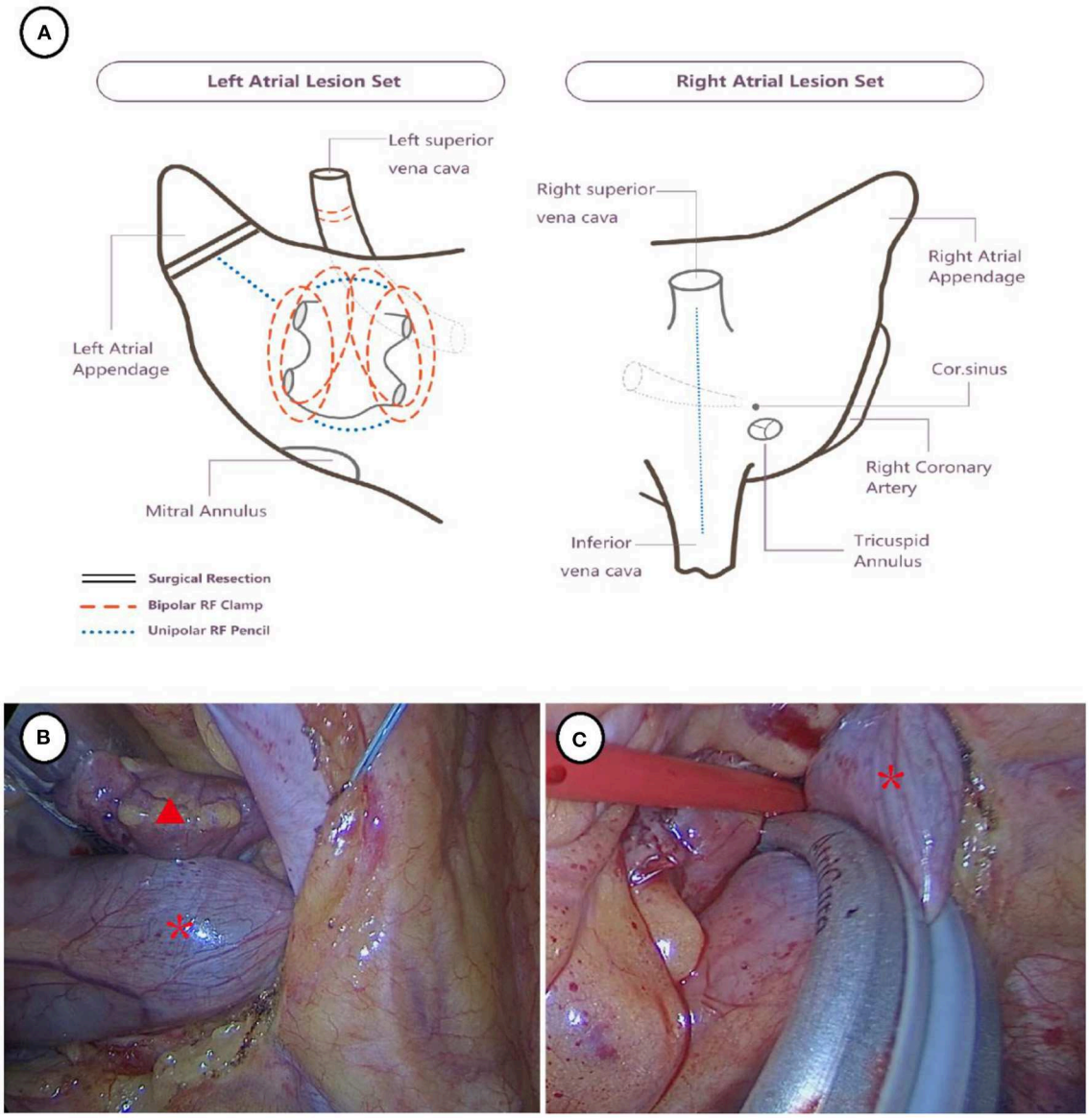

FIGURE 2
Surgical strategy **(A)** and thoracoscopic view of left atrial appendage excision and ablation of PLSVC **(B, C)**. The red triangle indicates left atrial appendage and the red asterisk indicates PLSVC.

superior vena cava (RSVC) is absent. In such a scenario, decision to ablate the LSVC depends on the adjacent structures and the diameter of the left superior cavity. On the one hand, if the cavity of LSVC is too small, it should not be ablated because the risk of LSVC stenosis is too high. On the contrary, if the lumen of LSVC was large enough and easy to separate from adjacent tissue, we thought it would be reasonable to perform ablation.

In this case, we confirmed that thoracoscopic ablation can be a feasible surgical option for patients with AF and PLSVC.

Data availability statement

The original contributions presented in the study are included in the article/supplementary material, further inquiries can be directed to the corresponding authors.

Ethics statement

The studies involving human participants were reviewed and approved by Ethics Committee of Guangdong Provincial People's Hospital, Guangdong Academy of Medical Sciences. The patients/participants provided their written informed consent to participate in this study. Written informed consent was obtained from the individual(s) for the publication of any potentially identifiable images or data included in this article.

Author contributions

HL and TT contributed to the study design and manuscript drafting. HQ contributed to data acquisition. JC, PW, and HG contributed greatly to the revision of the manuscript. JL approved the

submission of the final version. All authors contributed to the article and approved the submitted version.

Funding

This study was supported by grants from the Cardiovascular Special Project of Guangdong Provincial People's Hospital (2020XXG010); Guangdong Provincial Clinical Research Center for Cardiovascular disease (2020B1111170011); and Science and Technology Program of Guangzhou (202201010768). This article is also supported by Guangdong special funds for science and technology innovation strategy, China (Stability support for scientific research institutions affiliated to Guangdong Province-GDCI 2021).

Conflict of interest

The authors declare that the research was conducted in the absence of any commercial or financial relationships that could be construed as a potential conflict of interest.

Publisher's note

References

1. Batouty NM, Sobh DM, Gadelhak B, Sobh HM, Mahmoud W, Tawfik AM. Left superior vena cava: cross-sectional imaging overview. *Radiol Med.* (2020) 125:237–46. doi: 10.1007/s11547-019-01114-9

2. Wissner E, Tilz R, Konstantinidou M, Metzner A, Schmidt B, Chun KR, et al. Catheter ablation of atrial fibrillation in patients with persistent left superior vena cava is associated with major intraprocedural complications. *Heart Rhythm.* (2010) 7:1755–60. doi: 10.1016/j.hrthm.2010.08.005

3. Kim YG, Han S, Choi JI, Lee KN, Baek YS, Uhm JS, et al. Impact of persistent left superior vena cava on radiofrequency catheter ablation in patients with atrial fibrillation. *Europace.* (2019) 21:1824–32. doi: 10.1093/europace/euz254

4. Zimetbaum P. Atrial fibrillation. *Ann Intern Med* (2017) 166:ITC33-ITC48. doi: 10.7326/AITC201703070

5. Krul SP, Driessen AH, Zwinderman AH, van Boven WJ, Wilde AA, de Bakker JM, et al. Navigating the mini-maze: systematic review of the first results and progress of minimally-invasive surgery in the treatment of atrial fibrillation. *Int J Cardiol.* (2013) 166:132–40. doi: 10.1016/j.ijcard.2011.10.011

6. Pison L, Gelsomino S, Luca F, Parise O, Maessen JG, Crijns HJ, et al. Effectiveness and safety of simultaneous hybrid thoracoscopic and endocardial catheter ablation of lone atrial fibrillation. *Ann Cardiothorac Surg.* (2014) 3:38–44. doi: 10.3978/j.issn.2225-319X.2013.12.10

7. Je HG, Shuman DJ, Ad N. A systematic review of minimally invasive surgical treatment for atrial fibrillation: a comparison of the Cox-Maze procedure, beating-heart epicardial ablation, and the hybrid procedure on safety and efficacy. *Eur J Cardiothorac Surg.* (2015) 48:531–40. doi: 10.1093/ejcts/ezu536

8. Chen Z, Ke Y, Xie X, Huang J, Zeng Q, Guo H, et al. Beating-heart totally endoscopic tricuspid valvuloplasty in reoperative cardiac surgery. *Ann Thorac Surg.* (2019) 107:e79–82. doi: 10.1016/j.athoracsur.2018.07.013

9. Kochav J. *Persistent Left Superior Vena Cava.* (2018). Berlin, Germany: Springer International Publishing.

10. Perles Z, Nir A, Gavri S, Golender J, Tashma A, Ergaz Z, et al. Prevalence of persistent superior vena cava and association with congenital heart anomalies. *Am J Cardiol.* (2013) 112:1214–8. doi: 10.1016/j.amjcard.2013.05.079

11. Soward A. ten Cate F, Fioretti P, Roelandt J, Serruys PW. An elusive persistent left superior vena cava draining into left atrium. *Cardiology.* (1986) 73:368–71. doi: 10.1159/000174030

12. Robledo GC, Palafox LEG, Hernández MYJ, Paez YAC, César MG, Flores KLH, et al. Tricuspid atresia with persistent left superior vena cava and pulmonary arterial hypertension. *Case Report Curr Probl Cardiol.* (2022) 47:100837. doi: 10.1016/j.cpcardiol.2021.100837

13. Calkins H, Hindricks G, Cappato R, Kim YH, Saad EB, Aguinaga L, et al. 2017 HRS/EHRA/ECAS/APHRS/SOLAECE expert consensus statement on catheter and surgical ablation of atrial fibrillation: executive summary. *Heart Rhythm.* (2017) 14:e445–e94. doi: 10.1016/j.hrthm.2017.07.009

14. Lu H, Wang H, Huo X, Li G. Case report of double superior vena cava and double odd vein with hypoplastic left brachiocephalic vein. *J Int Med Res.* (2022) 50:3000605221119655. doi: 10.1177/03000605221119655

frontiers | Frontiers in Cardiovascular Medicine

TYPE Case Report
PUBLISHED 23 February 2023
DOI 10.3389/fcvm.2023.1091303

OPEN ACCESS

EDITED BY
Hendrik Tevaearai Stahel,
University Hospital of Bern, Switzerland

REVIEWED BY
Guillaume Goudot,
Institut National de la Santé et de la Recherche Médicale (INSERM), France
Hong Qian,
Sichuan University,
China

*CORRESPONDENCE
Zhiping Wang
✉ wangzhip12345@aliyun.com
Guanhua Li
✉ dr.liguanhua@hotmail.com

†These authors have contributed equally to this work

SPECIALTY SECTION
This article was submitted to Heart Surgery, a section of the journal Frontiers in Cardiovascular Medicine

RECEIVED 06 November 2022
ACCEPTED 01 February 2023
PUBLISHED 23 February 2023

CITATION
Li G, Chen Y, Wang H, Liu Y, Liu H, Sun H and Wang Z (2023) Case report: Surgical strategies of a giant thrombus from the ascending aorta to the arch.
Front. Cardiovasc. Med. 10:1091303.
doi: 10.3389/fcvm.2023.1091303

Case report: Surgical strategies of a giant thrombus from the ascending aorta to the arch

Guanhua Li[1*†], Yingzhen Chen[2†], Haikuo Wang[3†], Yanping Liu[4†], Hangyu Liu[1], He Sun[1] and Zhiping Wang[1*]

[1]Department of Cardiovascular Surgery, Sun Yat-sen Memorial Hospital, Sun Yat-sen University, Guangzhou, Guangdong, China, [2]Department of Anesthesiology, Sun Yat-sen Memorial Hospital, Sun Yat-sen University, Guangzhou, Guangdong, China, [3]Department of Hepatobiliary Surgery, Sun Yat-sen Memorial Hospital, Sun Yat-sen University, Guangzhou, Guangdong, China, [4]Department of Pathology, Sun Yat-sen Memorial Hospital, Sun Yat-sen University, Guangzhou, Guangdong, China

Large mural thrombi in the relatively normal ascending aorta are extremely uncommon conditions that may lead to major adverse cardiovascular events due to new embolism. Because of their changeable variations, the management of these unstable thrombi is challenging and controversial. The size, morphology, location, embolic involvement, and patients' conditions are all crucial for therapeutic decision-making. Treatment options include anticoagulation, thrombolysis, surgical thrombectomy, and endovascular stenting. Therefore, surgical strategies should be highly individualized. Herein, we present a rare case of a huge thrombus from the ascending aorta to the arch in a 43-year-old man. Considering the high risks of catastrophic embolic events, surgical removal of the aortic mass, thromboendarterectomy, and reconstruction of the arterial wall were performed with a satisfactory outcome. This report illustrates our experience of surgical strategies and perioperative treatments for this challenging case, and contemporary surgical management for mural thrombi in the ascending aorta was also thoroughly discussed.

KEYWORDS

thrombus, ascending aorta, aortic arch, surgical strategies, deep hypothermic circulatory arrest

Introduction

Non-atherosclerotic and non-aneurysmal thrombi located in the ascending aorta are scarce since the high-speed flow environment would have suppressed thrombotic formation (1). It has the possibility of catastrophic complications due to secondary embolism, including stroke, myocardial infarction (2), and peripheral embolism (3, 4). The treatment for thrombi in the normal ascending aorta is challenging and should be in an individualized manner (5). Herein, we present a rare case of a huge thrombus from the ascending aorta to the arch, which was surgically removed with a satisfactory outcome.

Case presentation

A 43-year-old man with a history of stroke was referred to our department due to a giant mass located in the aorta found incidentally in a local hospital. The patient presented with slurred speech and paralysis of the right limb. No histories of atherosclerosis, coronary artery

diseases, hypertension, and trauma were noted. No symptoms of coronary ischemia or thrombosis of the extremities were found. The patient was a non-smoker and was healthy previously with no medications. The contrast-enhanced computer tomography of the whole aorta revealed a low-density lesion without enhancement from the ascending aorta to the arch and ruled out the possibility of malignancy (Figures 1A,B). The results of positron-emission tomography, tumor biomarkers, inflammatory biomarkers, and clotting tests were also normal (Table 1). The biological hemostasis tests, including mutation detection for factor II and factor V, levels of antithrombin III, protein C, protein S, and anti-phospholipid antibodies were within normal ranges. The coronavirus disease 2019 (COVID-19) test was negative. Atrial fibrillation was not detected in the electrocardiogram, and normal cardiac function was found in ultrasonography, without the presence of an intraventricular thrombus, cardiac tumor, patent foramen ovale, and concomitant deep vein thrombosis. Considering the risks for secondary embolic events and myocardial infarction of the floating mass, surgery involving the removal of the aortic mass and thromboendarterectomy was indicated. However, a large infarct area in the left cerebral hemisphere with scattered hemorrhagic lesions was observed on admission by the cerebral computed tomography, and surgery was therefore postponed for 3 weeks (Supplementary Figure S1).

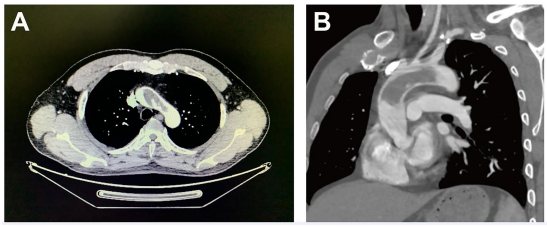

FIGURE 1
Computer tomography images (cross-section for Panel **A** and longitudinal-section for Panel **B**) of a giant floating thrombus from the ascending aorta to the arch.

TABLE 1 Clinical characteristics of the patient on admission.

Clinical characteristics	
Age	43
Gender	Male
BMI	25.1 kg/m^2
Red blood cell	4.56*10^12/L
Hemoglobin	146 g/L
White blood cell	7.38*10^9/L
Proportion of neutrophils	54.5%
Platelet	157*10^9/L
PTINT	0.96
PT	11.4S
D-dimer	0.98 mg/l FEU↑
TNF	0.50 pg./mL
Interferon	0.43 pg./mL
Interleukin 6	0.78 pg./mL
cTnT	6.1 pg./mL
NT-proBNP	18.3 pg./mL
ESR	7.0 mm/h
rheumatoid factors	<11.3
Antistreptolysin O	68.5 IU/mL
Triglycerides	1.70 mmol/L
Albumin	41.9 g/L
Total cholesterol	4.19 mmol/L
HDL cholesterol	0.68 mmol/L
LDL cholesterol	2.62 mmol/L

PTINT, Prothrombin international ratio; PT, Prothrombin time; TNF, tumor necrosis factor; ESR, Erythrocyte sedimentation rate.

At 3 weeks after admission, surgery was performed *via* median sternotomy, with all supra-aortic branches mobilized. The femoral artery was used to perfuse the body, while the brachiocephalic artery and the left common carotid artery were cannulated for bilateral cerebral perfusion (Figure 2A). With a venous cannula placed in the right atrium, the cardiopulmonary bypass was established in a pulsatile fashion (6). Cooling to 26°C, the cardiac rhythm turned to ventricular fibrillation. To avoid secondary embolism, all supra-aortic branches were clamped with the circuit flow decreased to 10%. We removed the floating mass *via* aortotomy without aortic cross-clamping, which was 9*4 cm in size and was attached to the wall of the ascending aorta (Figures 2B,C). The cardioplegic solution was delivered through the coronary ostia, and the heart was arrested successfully. The ascending aorta was clamped subsequently, and the rewarming process was started. The site of attachment was further excised, and the wall of the ascending aorta was reconstructed using a bovine pericardial patch measuring 5*5 cm in size (Figure 2D). Pathological examination confirmed that the red-yellow mass was a thrombus (Figure 2E). The presence of fibrosis and infiltration of neutrophils suggested that the thrombus was formed several months ago (7). Neither atherosclerotic plaque nor endothelial injury was seen in the thrombus-aortic wall attachment zone (Supplementary Figure S2). Postoperative hemodynamics went smoothly, without the usage of inotropes. Glucocorticoids and antibiotics were prophylactically administered for 5 days postoperatively. With long-term anticoagulants administered, the patient was discharged 12 days after surgery. The patient returned to a local rehabilitation hospital for stroke recovery. The movement and mobility of the body are now greatly improved, with normal flexibility for speech after 6 months of follow-up.

Discussion and conclusion

Non-atherosclerotic and non-aneurysmal thrombi in the ascending aorta are scarce due to the high-speed flow environment (1). In the present case, the etiology of this giant thrombus raises our great concerns. The arterial wall implant site and the peduncle of the thrombus were carefully examined, while histopathology revealed no evidence of atherosclerosis and other lesions. We also observed sporadic lymphocytic infiltration and fibrotic transformation in the mass, suggesting that the thrombus was formed for months. Amid the COVID-19 pandemic, the cytokine storm and hypoxemia caused

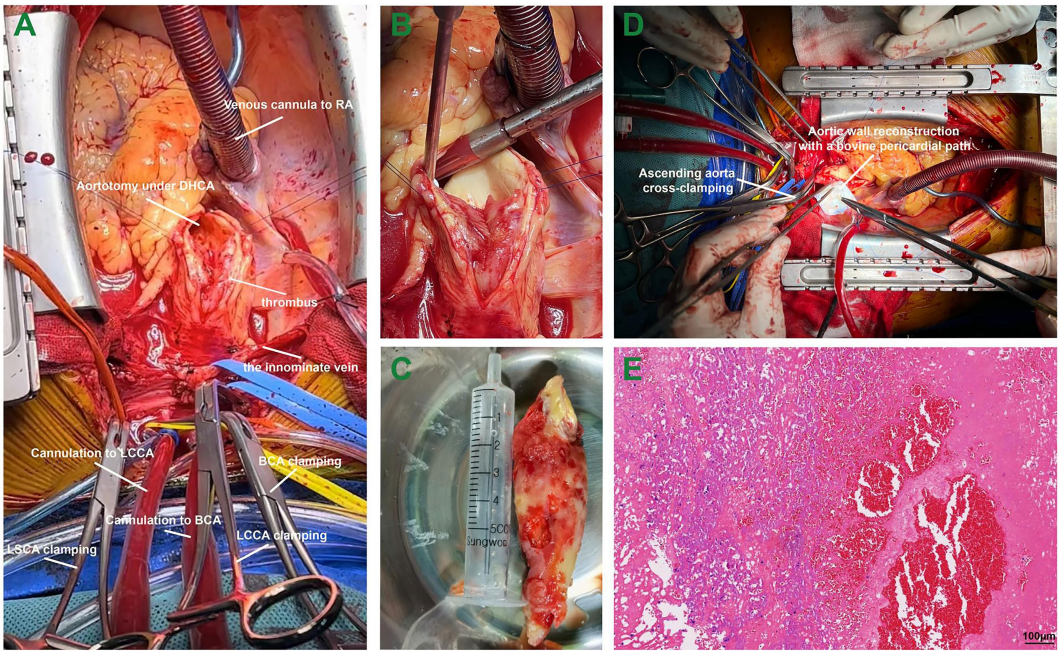

FIGURE 2
The surgical procedure in a patient with a giant thrombus from the ascending aorta to the arch. Panel **A**, the cannulation strategies for bilateral cerebral perfusion; Panel **B**, the giant floating thrombus attached to the aortic wall of the ascending aorta; Panel **C**, the giant thrombus measuring 9*4cm in size; Panel **D**, the aortic wall reconstruction using a bovine pericardial patch; and Panel **E**, pathological evaluation of the thrombus in hematoxylin and eosin staining. Abbreviations: RA, right atrium; DHCA, deep hypothermic circulatory arrest; BCA, brachiocephalic artery; LCCA, left common carotid artery; LSCA, left subclavian artery.

by COVID-19 may increase the risk for arterial thrombosis (8), and a recent study also revealed that COVID-19 might attack the vascular endothelium, resulting in endothelial injury (9). However, the test for COVID-19 was negative in this patient. The mechanism of thrombosis, in this case, is still unclear; however, regional weakness and inflammation of the endothelium may contribute to thrombosis.

Before considering surgical interventions, it is crucial to exclude some conditions such as malignancy, vasculitis, and hypercoagulation (10); hence, results of positron-emission tomography, tumor biomarkers, inflammatory biomarkers, and clotting tests must be obtained before decision-making. Verma et al. (5) classified mural thrombi of the aorta into four types (type I: the ascending aorta and the arch until the left subclavian artery origin; type II: the descending thoracic aorta up to the celiac artery; type III: between the celiac artery and the most distal renal artery; and type IV: between the lowest renal artery and the aortic bifurcation) based on the location. Type I thrombi, as this case presented, are the least common. According to morphology, aortic thrombi could be sessile, pedunculated, or occlusive. Karalis et al. (11) reported that much more embolic events occur in the pedunculated thrombi as compared to other thrombi with non-floating features. A systematic review comparing anticoagulation only and surgical treatment for aortic mural thrombus reported that the recurrence rate and complication rate are significantly lower in patients who were surgically managed (12).

Currently, there are no guidelines or therapeutic consensus on the management of aortic thrombi (13). Therapeutic options include anticoagulant medications, thrombolysis, surgical thrombectomy, endovascular stenting, and balloon embolectomy, which should be used in an individualized manner based on size, location, morphology, and involvement (5). For typically type I thrombi, especially those with pedunculated or floating features, which have higher risks for embolic events, surgical thrombectomy on cardiopulmonary bypass should be indicated. If supra-aortic branches were involved, embolectomy or supra-aortic debranching procedure with stent implantation should be considered (5). Arterial cannulation strategies for cardiopulmonary bypass in type I thrombi should also be individualized to ensure the best visceral or cerebral perfusion and the lowest risks for exfoliation of the thrombus. Sites for cannulation include the femoral artery, axillary artery, and other supra-aortic branches.

Considering the relatively large size, floating characteristics, and the previous history of embolic events in this case, surgical removal of the thrombus and aortic wall reconstruction were performed under cardiopulmonary bypass with deep hypothermic circulatory arrest. It is noteworthy that circulatory arrested should be used if possible clamping sites were unavailable because of thrombotic involvement. Bilateral cerebral perfusion was achieved by dual cannulation of supra-aortic branches, while the retrograde flow of femoral cannulation not only perfused the body but also prevented secondary distal embolism caused by small thrombotic fragments.

It is recommended that the site of thrombus implantation should be surgically excised or replaced to prevent occurrence (7). We used a bovine pericardial patch to reconstruct the arterial wall in this case; however, segmental aortic replacement should be indicated in those sessile thrombi with larger attachment sites. Long-term aspirin was

administered postoperatively to avoid recurrence owing to the possible residual thrombus (14). In brief, although guidelines or consensus on the treatments for thrombi located in the ascending aorta and the arch, surgical removal is strongly recommended in those pedunculated or floating thrombi that carry higher risks for secondary embolic events.

Data availability statement

The raw data supporting the conclusions of this article will be made available by the authors, without undue reservation.

Ethics statement

The studies involving human participants were reviewed and approved by the Ethics Committee of Sun Yat-sen Memorial Hospital. The patients/participants provided their written informed consent to participate in this study. Written informed consent was obtained for the publication of this case report.

Author contributions

GL and HW prepared and wrote the manuscript. YC and YL prepared surgical and pathological figures. HL and HS collected and analyzed the patient's data. ZW reviewed and revised the manuscript. All authors have read and approved the manuscript and agreed to be accountable for the content of the manuscript.

Funding

This study was supported by grants from the Medical Scientific Research Foundation of Guangdong Province of China (grant no. A2021433) and Guangdong Basic and Applied Basic Research Foundation (grant no. 2021A1515010280 and 2022A1515012170).

Conflict of interest

The authors declare that the research was conducted in the absence of any commercial or financial relationships that could be construed as a potential conflict of interest.

Publisher's note

All claims expressed in this article are solely those of the authors and do not necessarily represent those of their affiliated organizations, or those of the publisher, the editors and the reviewers. Any product that may be evaluated in this article, or claim that may be made by its manufacturer, is not guaranteed or endorsed by the publisher.

Supplementary material

The Supplementary material for this article can be found online at: https://www.frontiersin.org/articles/10.3389/fcvm.2023.1091303/full#supplementary-material

References

1. Yagyu, T, Naito, M, Kumada, M, and Nakagawa, T. Aortic mural thrombus in the non-atherosclerotic aorta of patients with multiple hypercoagulable factors. *Internal Med.* (2019) 58:381–5. doi: 10.2169/internalmedicine.0691-17

2. Ozaki, N, Yuji, D, Sato, M, Inoue, K, and Wakita, N. A floating thrombus in the ascending aorta complicated by acute myocardial infarction. *Gen Thorac Cardiovasc Surg.* (2017) 65:213–5. doi: 10.1007/s11748-015-0619-7

3. Gueldich, M, Piscitelli, M, Derbel, H, Boughanmi, K, Bergoend, E, Chanai, N, et al. Floating thrombus in the ascending aorta revealed by peripheral arterial embolism. *Interact Cardiovasc Thorac Surg.* (2020) 30:762–4. doi: 10.1093/icvts/ivaa017

4. Labsaili, H, Bouaggad, A, Alami, AA, Rama, A, and Leprince, P. Surgical treatment of a floating thrombus of the ascending aorta causing repeated arterial embolisms. *Ann Vasc Surg.* (2015) 29:1021.e5–7. doi: 10.1016/j.avsg.2015.01.027

5. Verma, H, Meda, N, Vora, S, George, RK, and Tripathi, RK. Contemporary management of symptomatic primary aortic mural thrombus. *J Vasc Surg.* (2014) 60:1524–34. doi: 10.1016/j.jvs.2014.08.057

6. Li, G, Jiang, W, Zhang, Y, Zhang, X, Chen, J, Zhuang, J, et al. The outcome of pediatric patients undergoing congenital cardiac surgery under pulsatile cardiopulmonary bypass in different frequencies. *Ther Clin Risk Manag.* (2018) 14:1553–61. doi: 10.2147/TCRM.S170642

7. Akhmerov, A, and Ramzy, D. Left atrial thrombus. *N Engl J Med.* (2022) 387:e8. doi: 10.1056/NEJMicm2117229

8. Goudot, G, Amrane, M, El Ayoubi, R, Bel, A, Gendron, N, Khider, L, et al. Thrombus of the aorta and SARS-CoV-2 infection: cause or trigger? *Front Cardiovasc Med.* (2021) 8:700292. doi: 10.3389/fcvm.2021.700292

9. Azouz, E, Yang, S, Monnier-Cholley, L, and Arrivé, L. Systemic arterial thrombosis and acute mesenteric ischemia in a patient with COVID-19. *Intensive Care Med.* (2020) 46:1464–5. doi: 10.1007/s00134-020-06079-2

10. Dai, X, Ni, C, Luo, W, Miao, S, and Ma, L. Large mural thrombus in the non-aneurysmal and non-atherosclerotic ascending aorta: a case report. *J Cardiothorac Surg.* (2021) 16:200. doi: 10.1186/s13019-021-01585-w

11. Karalis, DG, Chandrasekaran, K, Victor, MF, Ross, JJ Jr, and Mintz, GS. Recognition and embolic potential of intraaortic atherosclerotic debris. *J Am Coll Cardiol.* (1991) 17:73–8. doi: 10.1016/0735-1097(91)90706-F

12. Fayad, ZY, Semaan, E, Fahoum, B, Briggs, M, Tortolani, A, and D'Ayala, M. Aortic mural thrombus in the normal or minimally atherosclerotic aorta. *Ann Vasc Surg.* (2013) 27:282–90. doi: 10.1016/j.avsg.2012.03.011

13. Neves, NM, Coelho, SC, Marto, NF, and Horta, AB. Ascending aortic thrombus with peripheral embolization. *Cureus.* (2022) 14:e28766. doi: 10.7759/cureus.28766

14. Weiss, S, Bühlmann, R, von Allmen, RS, Makaloski, V, Carrel, TP, Schmidli, J, et al. Management of floating thrombus in the aortic arch. *J Thorac Cardiovasc Surg.* (2016) 152:810–7. doi: 10.1016/j.jtcvs.2016.03.078

frontiers | Frontiers in Cardiovascular Medicine

TYPE Case Report
PUBLISHED 06 March 2023
DOI 10.3389/fcvm.2023.1124181

OPEN ACCESS

EDITED BY
Hendrik Tevaearai Stahel,
University Hospital of Bern, Switzerland

REVIEWED BY
Erik Beckmann,
Hannover Medical School, Germany
Vito Domenico Bruno,
University of Bristol, United Kingdom

*CORRESPONDENCE
Santiago Besa
✉ sbesa@uc.cl

SPECIALTY SECTION
This article was submitted to Aortic Surgery and Endovascular Repair, a section of the journal Frontiers in Cardiovascular Medicine

RECEIVED 14 December 2022
ACCEPTED 14 February 2023
PUBLISHED 06 March 2023

CITATION
Besa S, Castelli F, Garrido-Olivares L, González R, Marine L and Becker P (2023) Case report: Multi-site perfusion strategy for type A acute aortic dissection complicated with cerebral malperfusion.
Front. Cardiovasc. Med. 10:1124181.
doi: 10.3389/fcvm.2023.1124181

Case report: Multi-site perfusion strategy for type A acute aortic dissection complicated with cerebral malperfusion

Santiago Besa[1]*, Fiorenza Castelli[2], Luis Garrido-Olivares[1], Rodrigo González[1], Leopoldo Marine[3] and Pedro Becker[1]

[1]Division of Surgery, Department of Cardiovascular Surgery, Pontificia Universidad Católica de Chile, Santiago, Chile, [2]Medical School, Pontificia Universidad Católica de Chile, Santiago, Chile, [3]Division of Surgery, Department of Vascular Surgery, Pontificia Universidad Católica de Chile, Santiago, Chile

Acute type A dissection presenting with cerebral malperfusion has high morbidity and mortality. Given the complexity of underlying vascular involvement, it is a challenging clinical scenario. Many of these patients are not deemed surgical candidates. If surgery is considered, it often requires complex aortic arch and neck vessel reconstruction. We present a 48-year-old male with an acute type A aortic dissection that presented with paraplegia and decreased level of consciousness. A Computed Tomography showed occlusion of both common carotid arteries. He was successfully treated with a multi-site perfusion strategy and a Hybrid Frozen Elephant Trunk graft to achieve fast restoration of the cerebral circulation and minimize brain ischemia and permanent neurological damage. From this case, we learn that aggressive arch and neck vessel reconstruction supported by multi-site perfusion could help improve mortality and neurological outcomes in selected patients.

KEYWORDS

aortic arch surgery, aortic dissection, cerebral malperfusion, Frozen Elephant Trunk (FET), case report

Introduction

Early mortality and morbidity after surgical treatment for acute type A aortic dissection (TAAD) have remained high over the last decades ranging between 10 and 30% (1). The patient's preoperative status remains the main predictor for outcomes after the surgery. Especially important is the presence of end-organ malperfusion, which is present in approximately one-third of patients (2). Cerebral malperfusion (CM) is the second most frequent form of malperfusion after the coronary arteries, and it is present in 5.2–13.1% of TAAD cases (3). A significant surgical dilemma is the treatment of TAAD patients with preoperative CM secondary to the involvement of supra-aortic branches, given its high mortality and risk for permanent neurological dysfunction.

The increasing availability of Hybrid Frozen Elephant Trunk (FET) prosthesis to address arch pathology, such as the Thoraflex (Terumo, FL, USA), gives a new perspective to treating TAAD involving the arch. Together with an aggressive and tailored cannulation strategy, they can help us treat this complex group of patients and achieve good outcomes (4).

We present a case of a TAAD involving all supra-aortic branches with severe neurological dysfunction where a multi-site perfusion strategy was used to perform emergent Thoraflex FET implantation. Fast and multi-site restoration of cerebral blood flow by this approach allowed to shorten brain ischemia time and minimize permanent neurological damage.

Case report

A 48-year-old male with no known medical history and no family history of aortic disease or connective tissue disorders was admitted to a secondary Regional Hospital due to paresis of the lower right extremity. CT scan showed a TAAD starting at the proximal aortic arch and extending to the left internal iliac artery. All three supra-aortic vessels were compromised, with occlusion of both carotid arteries. The patient was transferred to our center for emergent surgery. The patient arrived at our center (1.5-h flight) in a deep stupor (Glasgow coma scale of 8) and with right hemiparesis (MRC strength scale of 1). A repeated CT showed a complete occlusion and thrombosis of the right common and internal carotid artery. The left common carotid artery was also occluded and thrombosed, showing recovered flow just before the bifurcation (Figure 1). The left subclavian artery was dissected, with involvement of the vertebral artery origin. There were no signs of consolidated cerebral infarction on CT. A GERAADA score (5) of 28.7% mortality at 30-day was calculated. Although its neurological prognosis was uncertain, there were no categorical elements of poor prognosis if cerebral circulation was restored. For this reason, we decided to proceed with emergency surgery.

Bilateral radial and left femoral arterial lines were installed. Bilateral near-infrared spectroscopy (NIRS) was used. An incision from the left neck through the xiphoid was made. While the median sternotomy was performed, we controlled the left common, internal, and external carotid artery. The aorta was dissected from a short segment proximal to the innominate trunk, with a normal aspect of the root. All the supra-aortic vessels were compromised. There was no innominate vein, with a persistent left vena cava. We rapidly cannulated the left internal carotid artery with a 10-french pediatric aortic cannula to ensure cerebral perfusion. This cannula was perfused independently of the systemic line at 10 ml/kg throughout the procedure. We cannulated the ascending aorta in the uninvolved segment. Cardiopulmonary bypass (CPB) was initiated, inducing hypothermia to 24 °C. To achieve the best cerebral perfusion through the surgery, we decided to secure perfusion through the posterior territories by perfusing both subclavian arteries. The right subclavian artery was directly cannulated with a 12-french pediatric aortic cannula. The left subclavian artery was compromised in the observed segment, so we made a left sub-clavicular incision, and a Dracon graft was anastomosed in a terminal-lateral fashion. For the subclavian branches, we obtained flow from the systemic cannula (Figure 2).

The NIRS became adequate and symmetrical soon after CPB was initiated. We completed the dissection and control of all supra-aortic vessels. The left carotid artery and left subclavian artery were ligated at their origin. A guidewire from the right femoral artery was advanced through the true lumen with TEE support. We began systemic arrest. For this, an aortic clamp was installed distal to the aortic cannula, thereby maintaining pressure-regulated cardiac perfusion. In addition, we maintained the perfusion through the left carotid and both subclavian lines. The ascending aorta was opened, observing an intimal tear proximal to the innominate trunk. There was no retrograde flow through the right carotid artery. The arch was resected up to zone 2. A 30 × 32 × 100 mm Thoraflex hybrid prosthesis was deployed through the previously advanced guidewire and was anastomosed to the distal arch. The circulatory arrest was ended by starting the perfusion through the lateral branch of the Thoraflex graft. We then arrested the heart for a brief period to perform the proximal aorto-graft anastomosis in the mid-portion of the ascending aorta, after which the aortic cross-clamp time was completed. We continued with the supra-aortic vessel's anastomosis. The left subclavian graft was tunneled through the second intercostal space and anastomosed to its corresponding branch. The left carotid anastomosis was performed at the level of the carotid bifurcation (Figure 2).

Finally, we confirmed no retrograde flow in the right carotid artery, even after a Fogarty catheter was advanced. We excluded the right carotid, which was ligated, and performed the last branch anastomosis to the right subclavian artery. Once 36°C was reached, we weaned the patient off CPB without further incidents. The cross-clamp time was 21 mins and the systemic arrest time with antegrade cerebral perfusion was 28 mins.

On day 0, the patient had a cardiac arrest with ventricular fibrillation that required three shocks of defibrillation and recovered after 7 mins of resuscitation. An amiodarone infusion was started with no further events. He was weaned off vasoactive support on day 2. A head CT on day 2 showed small acute-subacute ischemic lesions on the left frontoparietal white matter. Weaning from mechanical ventilation was difficult because of severe delirium, requiring a tracheostomy on day 7. A new head CT on day 8 showed a new right cortico-subcortical frontal subacute infarction. He continue to improve clinically from a neurologic perspective, underwent neurological rehabilitation, and recovered complete mobility of his right side with minimum impairment (MRC strength scale of 4). He was decannulated from his tracheostomy on day 20. The patient was discharged on postoperative day 30 in good general condition.

Comment

Despite surgical technical advances, operative mortality for TAAD remains high. There is a wide variety of presentations, and the preoperative status is still one of the main factors in predicting operative mortality after surgical repair. In particular, neurological deficits resulting from CM have been reported as a sign of poor prognosis (6). However, the optimal management for patients with CM is unclear. The last report of the International Registry of Acute Aortic Dissections in 2019 reported an incidence of CM in TAAD of 15.1% with an operative mortality of 25.7% (7). The mortality reported is encouraging in this highly complex clinical scenario but must be carefully interpreted. The reported case presents a highly tailored approach and highlights the importance of pre-surgical evaluation and assessment for cannulation sites and perfusion strategies.

There are many surgical techniques to cannulate patients with TAAD complicated by CM, most based on retrospective series or expert opinions. Still, there is no "one fits all" type of cannulation. Carotid artery cannulation has been advocated as a safe cannulation method for aortic surgery, mainly by P. Urbansky (8). The main advantages are that it is easy and fast (suitable for emergencies), offers adequate arterial return, and offers the possibility of early establishment of cerebral perfusion without interruption. It is an

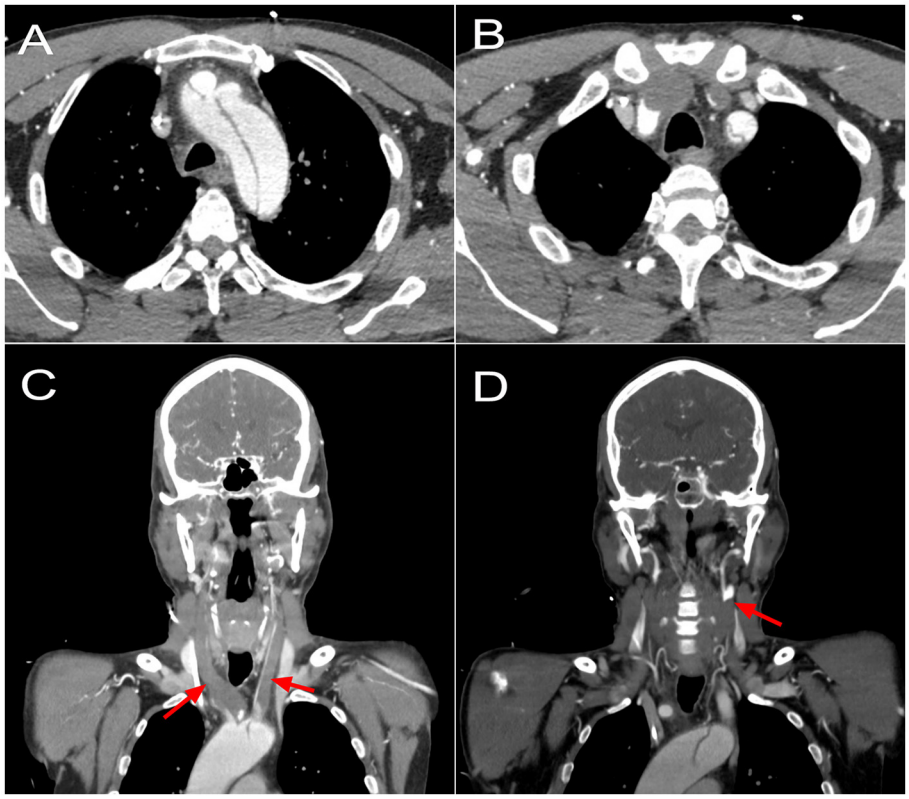

FIGURE 1
Preoperative CT scan showing **(A)** an acute type A dissection compromising the aortic arch and origin of supra-artic vessels. **(B)** A complete occlusion of the brachiocephalic trunk, with reperfusion of the right subclavian artery; a complete occlusion of the left common carotid artery; a dissected left subclavian artery. **(C)** A coronal reconstruction showing complete occlusion of both common carotid arteries since origin at the aortic arch (arrows). **(D)** A coronal reconstruction showing reperfusion at the level of the left carotid bifurcation (arrow).

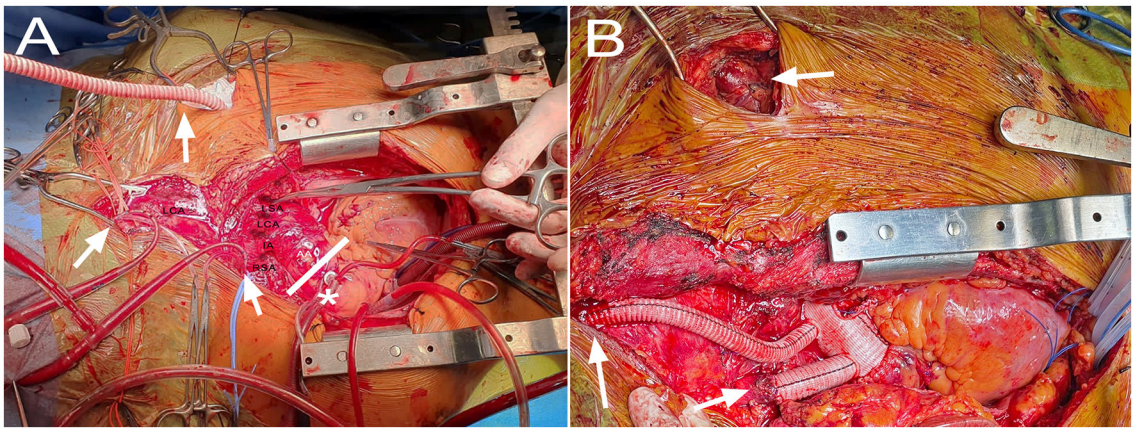

FIGURE 2
Intraoperative images showing **(A)** perfusion setup with direct ascending aorta (AA) cannulation in the uncompromised segment (*), pediatric cannulas to the right subclavian (RSA) and left internal carotid arteries, and Dacron graft to the left subclavian artery (arrows). The white lines depict the cross-clamp site to allow for cardiac perfusion through the aortic cannula. The innominate artery (IA), left carotid artery (LCA) and left subclavian artery (LSA) are also appreciated. **(B)** The final result with the Thoraflex deployed, and its branches anastomosed to the right subclavian artery, left carotid bifurcation, and left subclavian artery (arrows).

excellent alternative to the most frequently used axillar cannulation strategy, given that the innominate artery is frequently involved in dissection, possibly making it unsuitable for cannulation.

The present case was challenging because of the involvement of both common carotid arteries. Therefore, unconventional cannulation was done by cannulating the left internal carotid

artery with a pediatric aortic cannula. Moreover, given the extensive preoperative compromise of anterior cerebral circulation, we decided to secure perfusion through the posterior territories by perfusing both subclavian arteries, achieving similar 4-site perfusion as proposed by Tsagakis et al. (4).

This case also shows that minimizing aortic cross-clamp time by maintaining isolated cardiac perfusion is possible in specific scenarios. Reducing cardiac ischemia time to a minimum is essential for a good cardiac outcome, and non-cardioplegic continuous myocardial perfusion has been shown to have lower cardiac mortality, lower rate of bleeding complications, and more effective myocardial protection (9).

The Hybrid FET technique offers an innovative approach to complex aortic arch repair operations and has revolutionized this field of surgery. The use of Thoraflex presents some advantages over other FET devices without supra-aortic branches, simplifying the reconstruction and minimizing surgical time.

In conclusion, the use of multi-site perfusion strategies and Hybrid FET grafts could be considered to treat patients presenting with TAAD and CM to minimize brain ischemia time, and facilitate the aortic arch reconstruction and cerebral blood flow restoration.

Data availability statement

The original contributions presented in the study are included in the article/supplementary material, further inquiries can be directed to the corresponding author.

Ethics statement

Written informed consent was obtained from the participant/patient(s) for the publication of this case report. Written informed consent was obtained from the individual(s) for the publication of any potentially identifiable images or data included in this article.

Author contributions

SB, FC, and LG-O wrote the main manuscript. SB, RG, PB, and LM planned and performed the procedure. All authors reviewed the manuscript.

Conflict of interest

The authors declare that the research was conducted in the absence of any commercial or financial relationships that could be construed as a potential conflict of interest.

Publisher's note

All claims expressed in this article are solely those of the authors and do not necessarily represent those of their affiliated organizations, or those of the publisher, the editors and the reviewers. Any product that may be evaluated in this article, or claim that may be made by its manufacturer, is not guaranteed or endorsed by the publisher.

References

1. Rylski B, Urbanski PP, Siepe M, Beyersdorf F, Bachet J, Gleason TG,et al. Operative techniques in patients with type A dissection complicated by cerebral malperfusion. *Eur J Cardiothorac Surg.* (2014) 46:156–66. doi: 10.1093/ejcts/ezu251

2. Olsson C, Hillebrant CG, Liska J, Lockowandt U, Eriksson P, Franco-Cereceda A. Mortality in acute type A aortic dissection: validation of the Penn classification. *Ann Thorac Surg.* (2011) 92:1376–82. doi: 10.1016/j.athoracsur.2011.05.011

3. Norton EL, Khaja MS, Williams DM, Yang B. Type A aortic dissection complicated by malperfusion syndrome. *Curr Opin Cardiol.* (2019) 34:610–5. doi: 10.1097/HCO.0000000000000667

4. Tsagakis K, Osswald A, Weymann A, Demircioglu A, Schmack B, Wendt D et al. The frozen elephant trunk technique: impact of proximalization and the four-sites perfusion technique. *Eur J Cardiothorac Surg.* (2022) 61:195–203. doi: 10.1093/ejcts/ezab295

5. Czerny M, Siepe M, Beyersdorf F, Feisst M, Gabel M, Pilz M et al. Prediction of mortality rate in acute type A dissection: the German Registry for Acute Type A Aortic Dissection score. *Eur J Cardiothorac Surg.* (2020) 58:700–6. doi: 10.1093/ejcts/ezaa156

6. Di Eusanio M, Patel HJ, Nienaber CA, Montgomery DM, Korach A, Sundt TM, et al. Patients with type A acute aortic dissection presenting with major brain injury: should we operate on them? *J Thorac Cardiovasc Surg.* (2013) 145:S213–21. doi: 10.1016/j.jtcvs.2012.11.054

7. Sultan I, Bianco V, Patel HJ, Arnaoutakis GJ, Di Eusanio M, Chen EP, et al. Surgery for type A aortic dissection in patients with cerebral malperfusion: results from the international registry of acute aortic dissection. *J Thorac Cardiovasc Surg.* (2021) 161:1713–20. doi: 10.1016/j.jtcvs.2019.11.003

8. Urbanski PP, Lenos A, Lindemann Y, Weigang E, Zacher M, Diegeler A. Carotid artery cannulation in aortic surgery. *J Thorac Cardiovasc Surg.* (2006) 132:1398–403. doi: 10.1016/j.jtcvs.2006.07.024

9. Martens A, Koigeldiyev N, Beckmann E, Fleissner F, Kaufeld T, Krueger H, et al. Do not leave the heart arrested: Non-cardioplegic continuous myocardial perfusion during complex aortic arch repair improves cardiac outcome. *Eur J Cardiothorac Surg.* (2016) 49:141–8. doi: 10.1093/ejcts/ezv009

frontiers | Frontiers in Cardiovascular Medicine

TYPE Case Report
PUBLISHED 08 March 2023
DOI 10.3389/fcvm.2023.1071111

OPEN ACCESS

EDITED BY
Shahzad Raja,
Harefield Hospital, United Kingdom

REVIEWED BY
Arda Özyüksel,
Biruni University, Türkiye
Simone Speggiorin,
East Midlands Congenital Heart Centre, United Kingdom

*CORRESPONDENCE
Qi An
✉ anqi@scu.edu.cn

†These authors have contributed equally to this work and share first authorship

SPECIALTY SECTION
This article was submitted to Heart Surgery, a section of the journal Frontiers in Cardiovascular Medicine

RECEIVED 15 October 2022
ACCEPTED 20 February 2023
PUBLISHED 08 March 2023

CITATION
Li T, Ling Y, Xiong Z and An Q (2023) Case report: Reconstruction of the long-gap unilateral absence of right pulmonary artery with contralateral pulmonary artery flap and autologous pericardial graft.
Front. Cardiovasc. Med. 10:1071111.
doi: 10.3389/fcvm.2023.1071111

Case report: Reconstruction of the long-gap unilateral absence of right pulmonary artery with contralateral pulmonary artery flap and autologous pericardial graft

Tiange Li†, Yunfei Ling†, Ziqing Xiong and Qi An*

Department of Cardiovascular Surgery, West China Hospital of Sichuan University, Chengdu, China

Unilateral absence of pulmonary artery (UAPA) is a rare type of congenital abnormality that may coexist with other congenital abnormalities or present as an isolated lesion, the latter form can be asymptomatic. Surgical procedure is usually carried out when UAPA was diagnosed with significant symptoms, and the aim of surgery is to restore the pulmonary flow distribution. The right-side UAPA is a considerable challenge for surgeons to process surgery, however, technical description of this type of UAPA are limited. Here we described a rare case of a two-month girl with absence of right pulmonary artery, we presented a technique that reconstructs this long-gap UAPA with contralateral pulmonary artery flap and autologous pericardial graft.

KEYWORDS

unilateral absence of pulmonary artery (UAPA), congenital heart defects, cardiovascular surgery, reconstruction of pulmonary artery, surgical techinque

Introduction

Unilateral absence of the intrapericardial pulmonary artery (UAPA) is a rare congenital anomaly arising from proximal pulmonary arterial obstruction with the closure of the ductus arteriosus. Due to difficult diagnosis and mild early symptoms, the exact prevalence remains unknown, though the reported prevalence of isolated UAPA without associated cardiac anomalies ranged from 1 in 200,000 to 1 in 300,000 adults (1, 2). The primary treatment goal is to restore the pulmonary flow distribution as close to normal as possible, which can be achieved through surgical continuity. Previous studies have provided various surgical designs to correct UAPA, such as direct anastomosis of the affected pulmonary artery (PA) to the main pulmonary artery (MPA), reconstructing PA with autologous pericardial roll, pulmonary artery or prosthetic materials, creating a systemic-to-PA shunt, repairing absent PA with a contralateral PA autograft segment interposition, using an in-situ pedicle of transverse sinus pericardium as a base for a conduit to reconstruct PA and so on (3–7). The right-sided UAPA, however, poses a significantly greater surgical challenge compared to the left-sided UAPA due to the relatively long distance between the right pulmonary artery (RPA) and the MPA. Currently, technical descriptions of absent RPA reconstruction are limited. Here, we describe our technique of modified PA flap angioplasty used to reconstruct the right-sided UAPA with long-gap discontinuity

that permits tension-free anastomoses while also potentially mitigating the risk of long-term stenoses.

Case presentation

Our patient was a 2-month-old girl first presented with convulsion due to pneumonia at 4 days old. No obvious cardiac abnormality was discovered upon initial physical examination. Echocardiography at the time suggested the absence of RPA, a patent ductus arteriosus, a patent foramen ovale and pulmonary hypertension. She was then transferred to our institution for further treatments. Preoperative computer tomography angiography (CTA) and three-dimensional reconstruction revealed the absence of intrapericardial RPA, of which the diameter of distal RPA at hilus is normal. The diameters of MPA and left pulmonary artery (LPA) was 8.3 mm and 5.1 mm respectively (with z-scores of −1.25 and −0.83 respectively). The gap between the RPA at the hilum and MPA was estimated to be 18.5 mm (**Figure 1A**). We further performed cardiac catheterization for diagnostic purposes, which further revealed that blood supply of upper RPA comes from right subclavian artery, while inferior RPA was supplied by left subclavian artery through long collateral vessels (**Figures 1B,D**). Systolic/diastolic pressure of the ascending aorta (AAo), superior vena cava (SVC), MPA and RPA were 64/29 mmHg, 20/7 mmHg, 51/25 mmHg and 20/10 mmHg respectively.

After careful evaluation, the diagnosis of UAPA was confirmed, and the operation was electively performed on the patient. After median sternotomy, the pericardium was harvested and treated with glutaraldehyde solution for five minutes. The origin of the right ductus was visualized after the innominate artery mobilization. The distal RPA was located posterior and medial to the SVC. Bilateral branch PAs were completely dissected beyond the lobar division to facilitate a tension-free PA anastomosis. The AAo was also mobilized sufficiently to create adequate space for the neo-RPA. Cardiopulmonary bypass was established *via* AAo and bicaval cannulation. The operation was performed under mild hypothermia (34°C) with a beating heart. After transecting the left ductus, an extension flap was created using the anterior wall of MPA and LPA with the base of the flap located along the right lateral aspect of the MPA and slightly inferior to the level of the proximal LPA

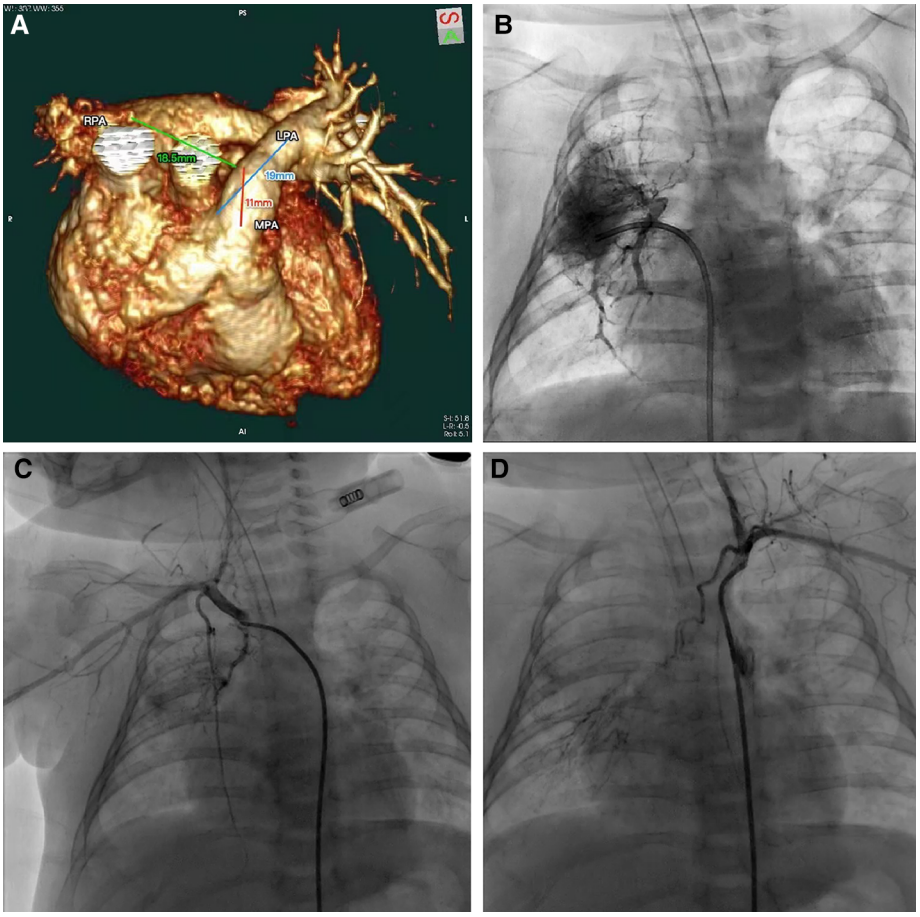

FIGURE 1
(A) CTA and three-dimensional reconstruction revealed the absence of intrapericardial right pulmonary artery. (B–D) Cardiac catheterization revealed blood supply of upper right pulmonary artery comes from right subclavian artery and inferior right pulmonary artery was supplied by left subclavian artery.

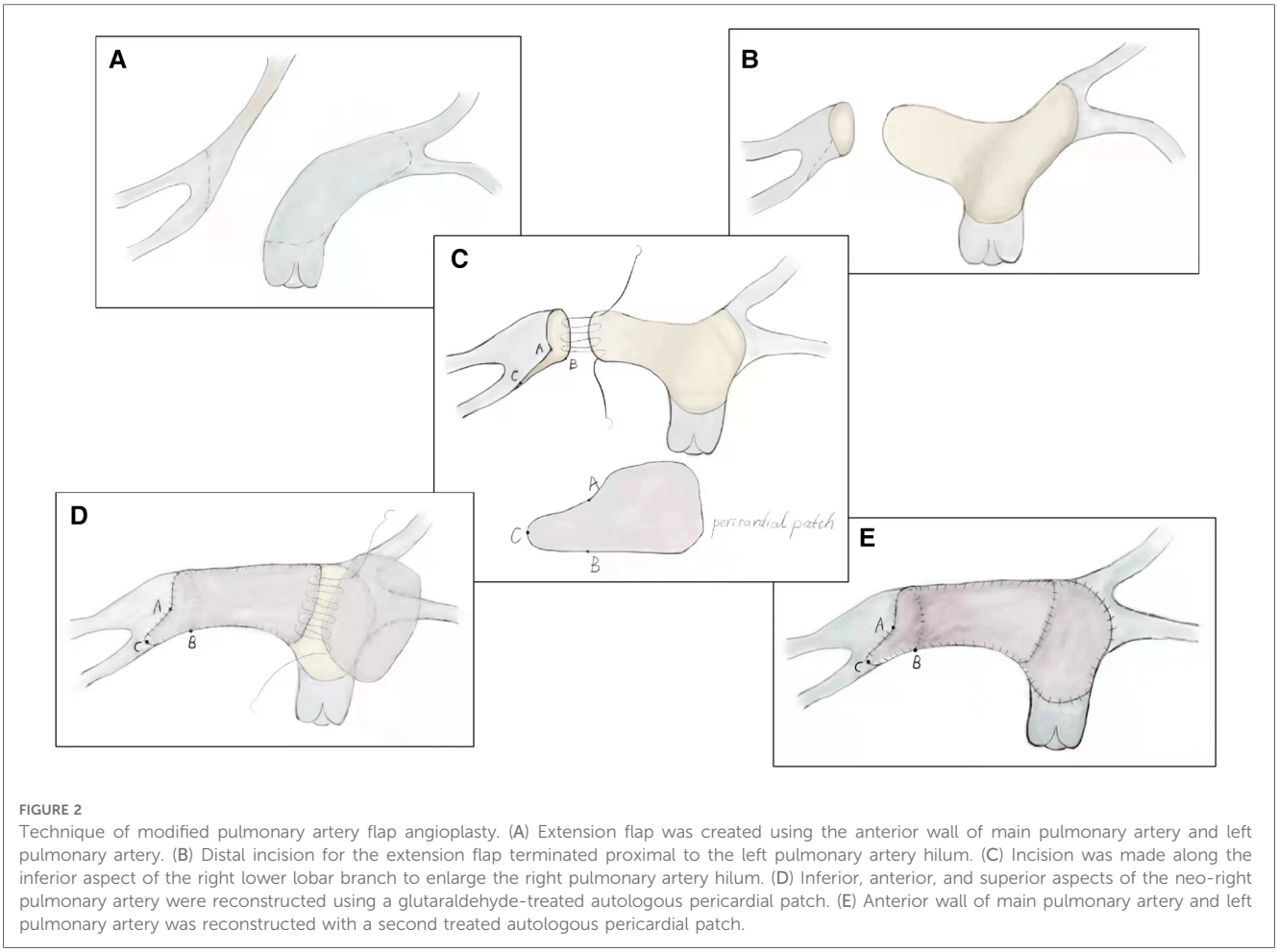

FIGURE 2
Technique of modified pulmonary artery flap angioplasty. (A) Extension flap was created using the anterior wall of main pulmonary artery and left pulmonary artery. (B) Distal incision for the extension flap terminated proximal to the left pulmonary artery hilum. (C) Incision was made along the inferior aspect of the right lower lobar branch to enlarge the right pulmonary artery hilum. (D) Inferior, anterior, and superior aspects of the neo-right pulmonary artery were reconstructed using a glutaraldehyde-treated autologous pericardial patch. (E) Anterior wall of main pulmonary artery and left pulmonary artery was reconstructed with a second treated autologous pericardial patch.

(Figure 2A). Care was taken to leave a 5 mm margin of MPA tissue above the sinotubular junction to preserve pulmonary valve function. The distal incision for the extension flap terminated just proximal to the LPA hilum (Figures 2B; 3A). The RPA was then harvested and ductal tissue was completely resected. The RPA was controlled distally with vessel loops on the lobar branches. Exposure was obtained by retracting the vessel loops distally. An incision was made along the inferior aspect of the right lower lobar branch to enlarge the RPA hilum (Figures 2C, 3B). The PA flap was then sutured to the distal segment of the opened RPA to construct the posterior aspect of the neo-RPA using running 7-0 polypropylene sutures (Prolene, Ethicon Inc, USA) (Figure 2C). The inferior, anterior, and superior aspects of the neo-RPA were reconstructed using a glutaraldehyde-treated autologous pericardial patch with a tongue extending into the right lower lobe according to the orientation of the vessel (Figures 2D, 3C). Running 8-0 polypropylene sutures were used for this portion of the PA angioplasty. After completion of the RPA reconstruction, the anterior wall of MPA and LPA was reconstructed with a second treated autologous pericardial patch (Figures 2E, 3D. After finishing the procedure, we successfully reconstructed the PA with satisfactory morphology and diameters (Figure 4). The patient recovered from the surgery uneventfully. Postoperative echocardiography demonstrated no residual vascular shunt and laminar flow in RPA. Postoperative CTA after 1 month revealed normal PA branching patterns and diameter. The patient remains asymptomatic and well upon last follow-up.

It is worth noting that the same surgery was performed on another 3-month-old boy with RPA absence at our institution. The patient also fully recovered from the surgery and showed satisfactory examination results during follow-up.

Discussion

UAPA is a rare type of congenital abnormality that may coexist with other congenital abnormalities or present as an isolated lesion, the latter form can be asymptomatic (8). RPA absence is more common than LPA absence, and the latter is more frequently associated with fatal cardiovascular abnormalities (4). Those who have only isolated UAPA may present no symptom and can remain asymptomatic into adulthood. It is proposed that UAPA may arise from the persistent connection between the intrapulmonary PA and the distal sixth aortic arch, in addition to the

10.3389/fcvm.2023.1071111

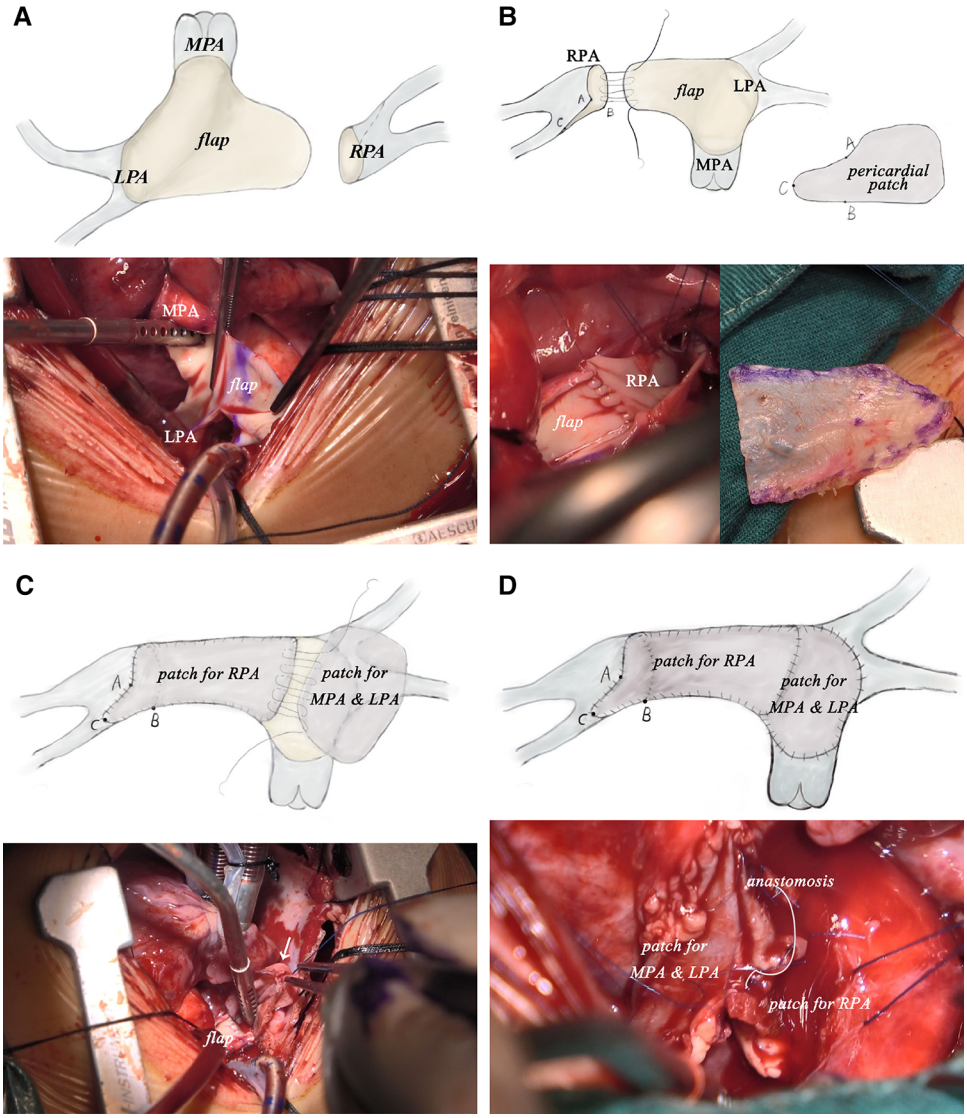

FIGURE 3
Intraoperative pictures of modified pulmonary artery flap angioplasty corresponding to procedure diagram. (LPA, left pulmonary artery; MPA, main pulmonary artery; RPA, right pulmonary artery.

involution of the proximal sixth aortic arch during embryonic development (8).

Diagnosis of UAPA is made upon the basis of a comprehensive medical history, careful physical examination and multi-modality imaging. Most UAPA patients in infancy present with symptoms of pulmonary hypertension or congestive heart failure, while adult patients may mainly complain about exertional dyspnea, recurrent pulmonary infections, haemoptysis and increased exercise intolerance (8). Multi-modality imaging is necessary to establish a UAPA diagnosis, since most imaging features of UAPA are non-specific, whereas angiography remains the gold standard. Although reports on efficacy and benefits of pulmonary vasodilators have been made in UAPA patients, surgery remains the most effective treatment that harbor the potential of curing the abnormality (5).

Previous studies have demonstrated that aggressive early one-stage surgical correction was associated with greater preservation of lung vasculature and improved restoration of pulmonary perfusion (9). El-Hattab et al. have introduced the MPA flap for semi-autologous repair of right-sided UAPA (4); however, this technique has been utilized primarily for left-sided UAPA reconstruction. By comparison, absent RPAs were most commonly reconstructed using a tubular graft, which must be replaced to a size commensurate with the patient's somatic growth (6). Additionally, the proximal incision for the flap should terminate several millimeters above the sinotubular junction to preserve the structural integrity of the pulmonary valve, which may be a particularly important consideration in younger infants. These limitations highlight the inadequacy of using the MPA anterior wall to establish a tension-free reconstruction of the RPA given the

10.3389/fcvm.2023.1071111

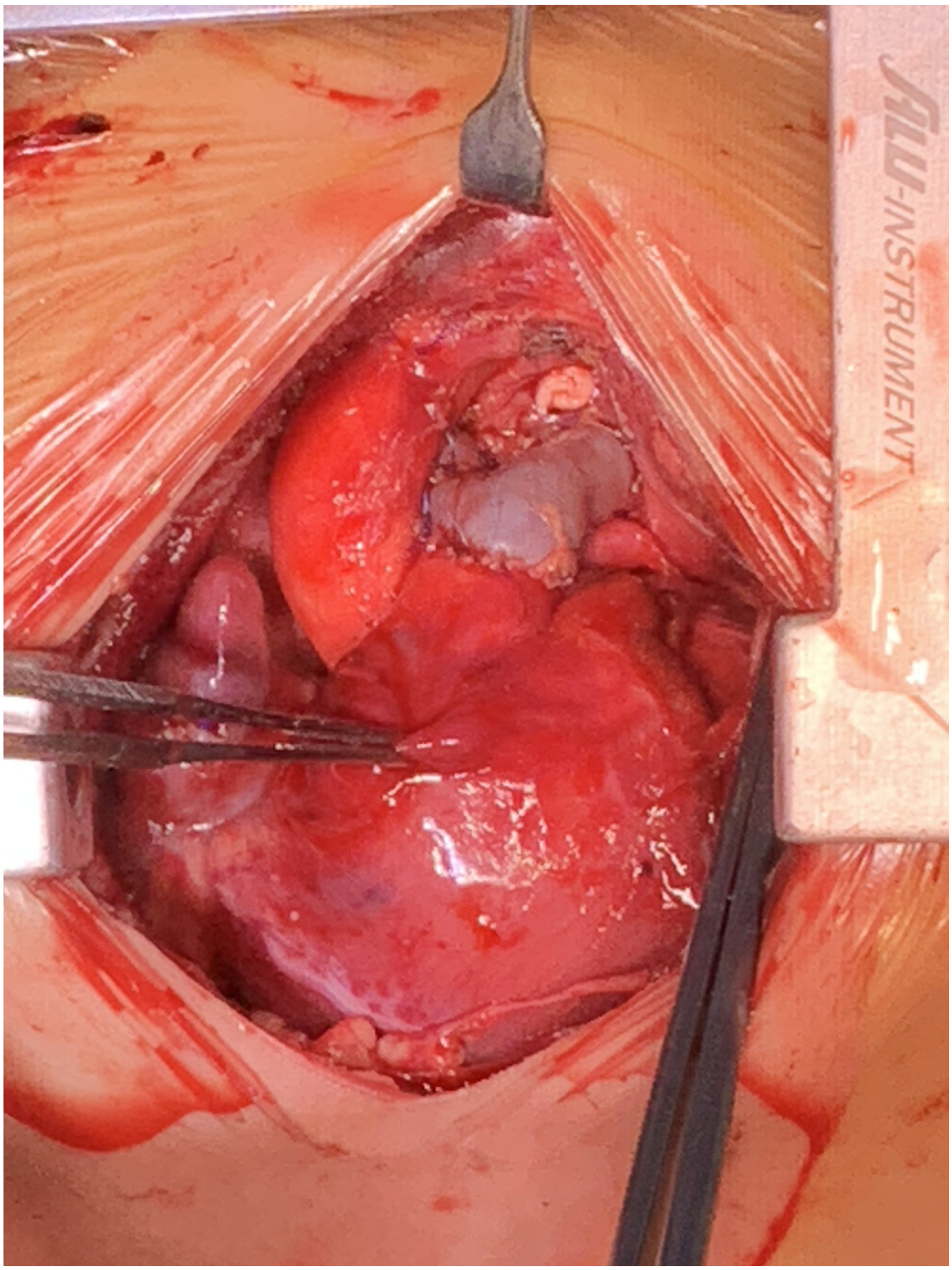

FIGURE 4
Surgery eventually reconstructed the pulmonary artery with satisfactory morphology and diameters.

latter's discontinuity over a significant distance. Furthermore, in patients with right-sided UAPA, the LPA receives all pulmonary blood flow, which promotes progressive vascular remodeling through elongation and dilatation. Our modified MPA flap angioplasty technique takes advantage of this phenomenon by incorporating the anterior wall of both MPA and LPA into the posterior aspect of the neo-MPA and RPA anastomosis to maximize the extent of autologous tissue used to bridge the gap while simultaneously minimizing anastomotic tension. The anterior wall of the LPA can be easily reconstructed with a separate pericardial patch with excellent geometry after RPA reconstruction.

Conclusion

Right-sided UAPA with long-gap discontinuity was traditionally considered as one of the most challenging congenital heart malformations for surgeons. We developed a novel technique using MPA and contralateral PA flap combined with fresh autologous pericardium patch for UAPA reconstruction. Short-term postoperative results of two infants with absent RPA were excellent and showed no sign of PA narrowing or pulmonary hypertension. However, growth potential and possibility of stenosis need to be further observed through long-term follow-up.

Data availability statement

The original contributions presented in the study are included in the article/**Supplementary Material**, further inquiries can be directed to the corresponding author/s.

Ethics statement

Written informed consent was obtained from the minor(s)' legal guardian/next of kin for the publication of any potentially identifiable images or data included in this article. Written informed consent was obtained from the participant/patient(s) for the publication of this case report.

Author contributions

ZX and TL wrote this manuscript. ZX collected raw data and patient information. TL was responsible for figures. YL and QA completed the surgery and revised the manuscript. YL modified sentences and grammar. All authors contributed to the article and approved the submitted version.

Funding

This article was funded by 1·3·5 project for disciplines of excellence–Clinical Research Incubation Project, West China Hospital, Sichuan University (No. ZYJC21064)

Acknowledgments

We thank the patient and her parents for providing her information for this case report.

Conflict of interest

The authors declare that the research was conducted in the absence of any commercial or financial relationships that could be construed as a potential conflict of interest.

Publisher's note

Supplementary material

The Supplementary Material for this article can be found online at: https://www.frontiersin.org/articles/10.3389/fcvm.2023.1071111/full#supplementary-material.

References

1. Bouros D, Pare P, Panagou P, Tsintiris K, Siafakas N. The varied manifestation of pulmonary artery agenesis in adulthood. *Chest*. (1995) 108:670–6. doi: 10.1378/chest.108.3.670

2. Kadir IS, Thekudan J, Dheodar A, Jones MT, Carroll KB. Congenital unilateral pulmonary artery agenesis and aspergilloma. *Ann Thorac Surg*. (2002) 74:2169–71. doi: 10.1016/s0003-4975(02)03979-6

3. Bilal MS, Yildirim O, Avsar M, Ozyuksel A. Repair of unilateral absence of right pulmonary artery with contralateral pulmonary artery autograft interposition in an infant. *Ann Thorac Surg*. (2015) 99:1467–9. doi: 10.1016/j.athoracsur.2014.12.036

4. El-Hattab AY, Calcaterra D, Parekh KR, Rossi NP, Davis JE, Turek JW. Semiautologous repair for congenital discontinuous right pulmonary artery. *Ann Thorac Surg*. (2013) 96:2230–1. doi: 10.1016/j.athoracsur.2013.02.057

5. Horinouchi K, Ueno K, Nakae K, Kawamura J, Kawano Y. Successful treatment of pulmonary hypertension with unilateral absent pulmonary artery. *Pediatr Int*. (2020) 62:1117–8. doi: 10.1111/ped.14262

6. Li W, Ma L, Xia S, Zou M, Chen W, Chen X. Early single-stage surgical revascularization of pulmonary artery in unilateral absence of a pulmonary artery. *J Cardiothorac Surg*. (2021) 16:80. doi: 10.1186/s13019-021-01481-3

7. Pourmoghadam KK, Schwartz MC, DeCampli WM, O'Brien MC. Novel approach to construct absent intrapericardial branch pulmonary arteries. *Ann Thorac Surg*. (2015) 100:738–40. doi: 10.1016/j.athoracsur.2015.03.046

8. Kruzliak P, Syamasundar RP, Novak M, Pechanova O, Kovacova G. Unilateral absence of pulmonary artery: pathophysiology, symptoms, diagnosis and current treatment. *Arch Cardiovasc Dis*. (2013) 106:448–54. doi: 10.1016/j.acvd.2013.05.004

9. Kim GB, Ban JE, Bae EJ, Noh CI, Kim WH, Lee JR, et al. Rehabilitation of pulmonary artery in congenital unilateral absence of intrapericardial pulmonary artery. *J Thorac Cardiovasc Surg*. (2011) 141:171–8. doi: 10.1016/j.jtcvs.2009.09.072

frontiers | Frontiers in Cardiovascular Medicine

TYPE Case Report
PUBLISHED 10 March 2023
DOI 10.3389/fcvm.2023.1081162

OPEN ACCESS

EDITED BY
Salah D. Qanadli,
Université de Lausanne, Switzerland

REVIEWED BY
Sandeep Sainathan,
University of Miami Health System,
United States
Krzysztof Bartus,
Jagiellonian University, Poland

*CORRESPONDENCE
Thierry Carrel
✉ thierry.carrel@gmail.com

†These authors have contributed equally to this work

SPECIALTY SECTION
This article was submitted to Heart Surgery, a section of the journal Frontiers in Cardiovascular Medicine

RECEIVED 26 October 2022
ACCEPTED 20 February 2023
PUBLISHED 10 March 2023

CITATION
Ouda A, Schürner AM, Schmiady MO, Jukema GN, Vogt PR and Carrel T (2023) Case report: Eighteen nails gun shots in the head, thorax and abdomen but still conscious at admission: A challenging patient for the cardiac surgeon!.
Front. Cardiovasc. Med. 10:1081162.
doi: 10.3389/fcvm.2023.1081162

Case report: Eighteen nails gun shots in the head, thorax and abdomen but still conscious at admission: A challenging patient for the cardiac surgeon!

Ahmed Ouda[1†], Anna Maria Schürner[2†], Martin Oliver Schmiady[1], Gerrolt Nico Jukema[3], Paul Robert Vogt[1] and Thierry Carrel[1*]

[1]Department of Cardiac Surgery, University Hospital, Zurich, Switzerland, [2]Institute of Anesthesiology, University Hospital, Zurich, Switzerland, [3]Department of Trauma Surgery, University Hospital, Zurich, Switzerland

We report an unusual case of multiple penetrating cerebral, cardiac and abdominal injuries following a suicidal attempt using a nail gun. Successful treatment required several emergency procedures and resulted from a wise interdisciplinary management and timing of surgery.

KEYWORDS

penetrating cardiac trauma, head injury, cerebral bleeding, anticoagulation, surgical treatment

Case report

A 59-year-old male was admitted to the emergency department following a suicidal attempt using an automatic nail gun less than 1 h before. He presented with a Glasgow scale of 15 and was in a hemodynamically stable condition. Inspection revealed multiple nails penetrating the head, the neck, the thorax and the left upper abdomen (**Figure 1**). Total body computer tomography was performed (**Figure 2**) and demonstrated eighteen 7.5 cm long nails: two nails penetrated the skull, one from left paramedian and the other from right parietal causing a small subarachnoid and a thin subdural hematoma with a small amount of blood in both ventricles. One nail penetrated the neck at the level of the 7^{Th} cervical vertebra with the tip close to the left subclavian artery. Ten nails penetrated the left chest with the tips both in the right and left ventricle, some of them were shot through the interventricular septum. As expected, pericardial effusion was noticed but without signs of tamponade. Two nails penetrated the left chest: one superficially into the pectoralis muscle and the other one into the lingula lobe of the left lung. Finally, three nails entered the upper abdomen and perforated the stomach with a small amount of sub-diaphragmatic air. The patient was discussed at an interdisciplinary meeting including all concerned medical specialists to decide on the optimal sequence of surgical explorations.

The main concerns were the following:

- occurrence of cerebral bleeding following removal of the intracranial nails,
- pericardial tamponade if removal of the intracardiac nails would be delayed,
- need for full heparinization with the potential of delayed cerebral bleeding in case extracorporeal circulation would be required to allow safe cardiac repair.

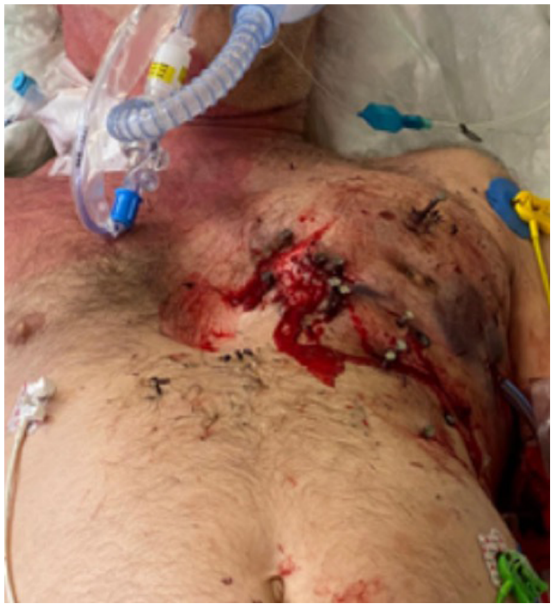

FIGURE 1
Multiple nail gunshots through the chest wall.

Finally, decision was taken to remove the nails from the skull first and to proceed thereafter with chest and especially cardiac exploration since the patient was in a hemodynamic stable condition. The procedure was performed in a multipurpose trauma operating room, in which immediate cardiac exploration would have been possible.

Following removal of the nails from the head, decision was made to observe the situation for a short interval. Cerebral CT-scan was repeated and showed a slight increase of the hematoma in the left frontal and right temporal regions (**Figure 3**). Since echocardiography did not show any increase of pericardial effusion, the patient was transferred to the intensive care unit and reassessed 2 and 4 h later. There, during careful removal of the clothes that had been transfixed by the nails, the patient's condition suddenly deteriorated very rapidly and echocardiography showed pericardial tamponade. Because of circulatory collapse, mechanical resuscitation would have been necessary but chest compression was not possible because of the nails still *in situ*. For this reason, emergency left thoracotomy was performed on the intensive care unit but adequate manual cardiac massage was not possible with the nails still *in situ*.

Opening the pericardium allowed immediate decompression of the tamponade. Following removal of the nails, quick inspection revealed seven myocardial lesions, some of them very close to the left anterior descending branch. Median sternotomy to improve exposure and allow better access to all injuries was performed: during that time, control of the most important myocardial injuries was performed with fingers and swabs. The lesions of the ventricular wall were closed using 2.0 polypropylene, while a diffuse epicardial venous bleeding was covered with a xeno-pericardial patch under which bio-glue (CryoLife Inc. GA, USA) was injected (**Figure 4**). Despite sufficient hemostasis within the chest, the patient remained unstable. Median laparotomy was performed to exclude intra-abdominal bleeding; this allowed removal of the last two nails that

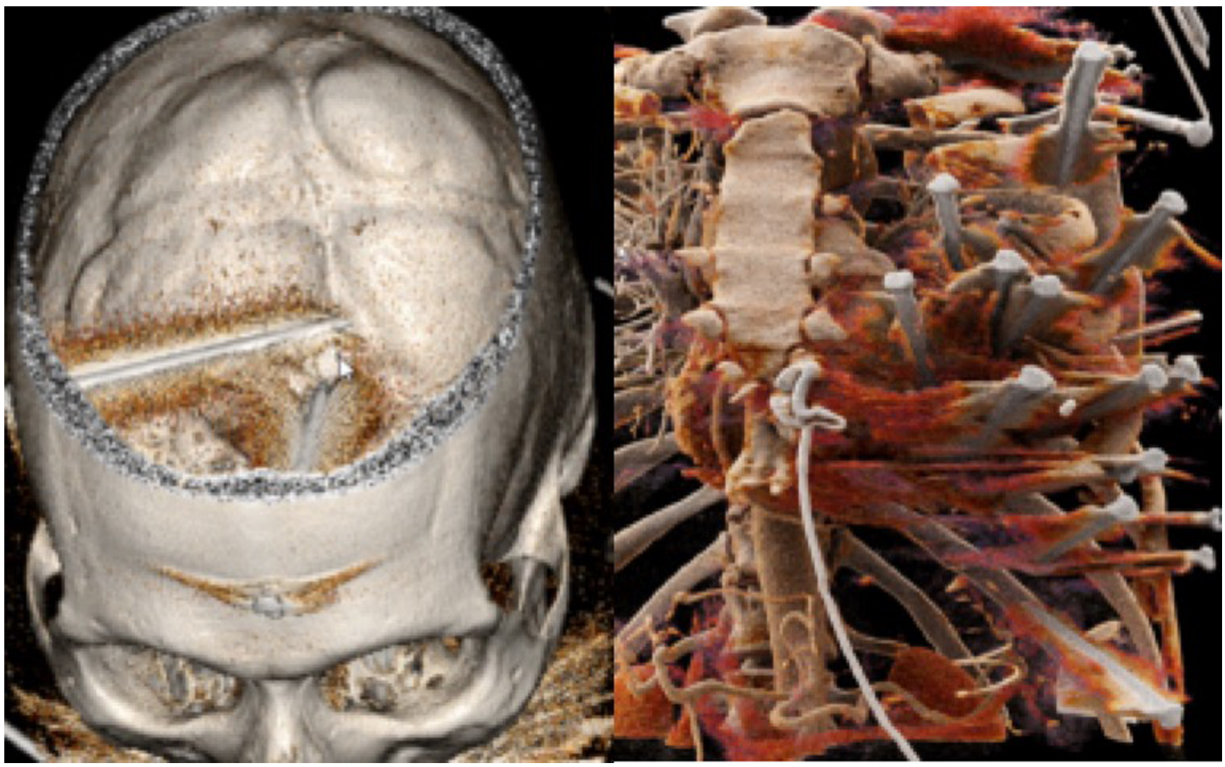

FIGURE 2
3d reconstruction of the CT-scan showing nails in the head (left) and those penetrating into the heart, the left lung and the stomach (right).

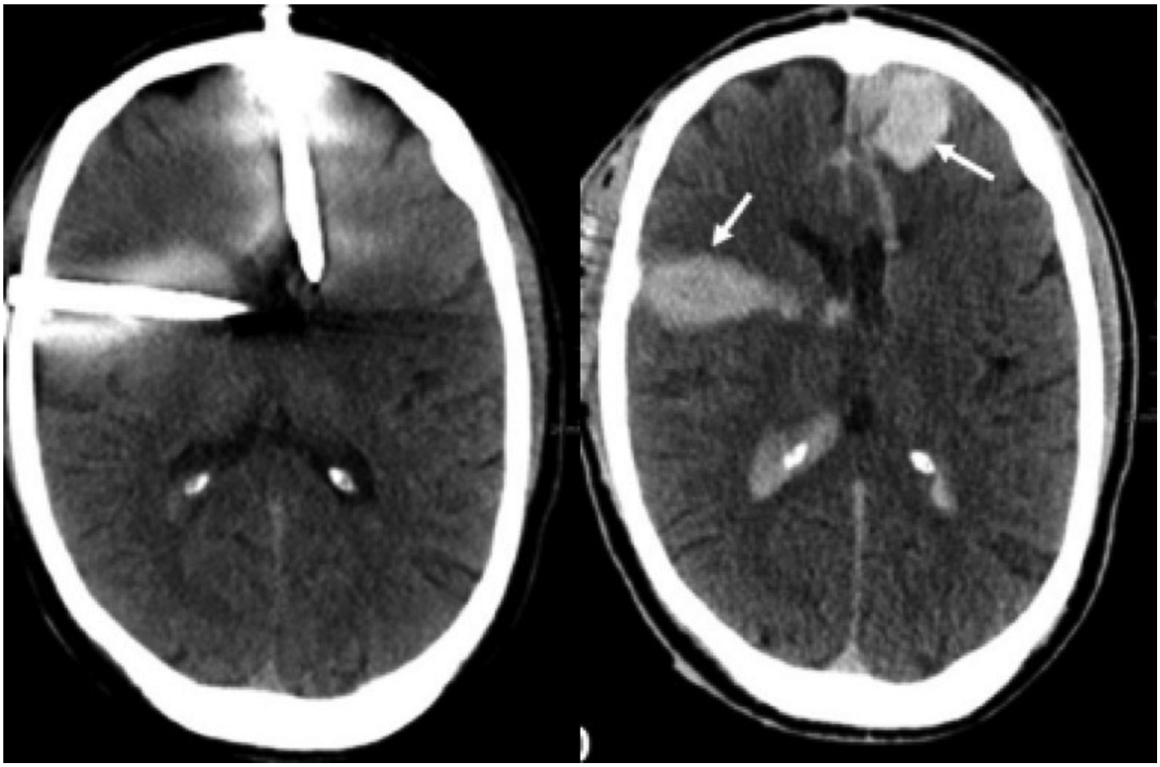

FIGURE 3
Cranial CT-scan before removal of the nails from the skull (left) with discrete bleeding and after removal with a progressive hematoma (arrow) (right).

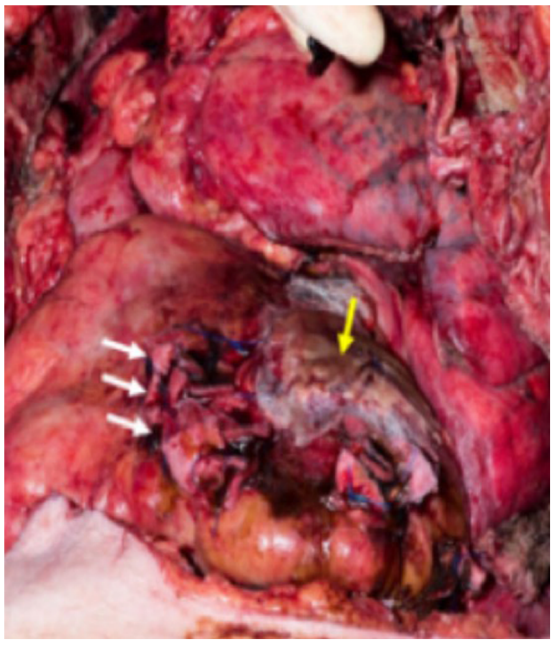

FIGURE 4
Intraoperative picture during repair of the right ventricular lesions (white arrows) and pericardial patch covering the left ventricular lesion (yellow arrow).

had perforated the stomach. These injuries were sutured with 4.0 Polydiaxone. The patient received 6 units of red blood cells.

Because of the contaminated operative field and semi-sterile operative conditions, the sternotomy wound was covered with a vacuum-dressing and delayed chest closure was performed five days later. Antibiotic regime consisted in cephalosporine until the chest was closed and vancocin for 48 h. The patient required prolonged ventilation and tracheotomy for weaning from ventilator. He was discharged on postoperative day 28, with full recovered motoric and cognitive functions.

The pre-discharge echocardiography showed normal biventricular function without valvular lesion or intracardiac shunts. Cardiac CT-scan showed patent coronary arteries (**Figure 5**).

Comment

Combined penetrating cerebral and cardiac injuries constitute a particular challenge for decision-making regarding the optimal sequence of surgical explorations (1, 2). Especially patients who may need cardiopulmonary bypass and full heparinization have to be considered very carefully in presence of concomitant cerebral and/or abdominal injuries. In case of polytrauma and unstable hemodynamics, the lesion with the highest blood loss

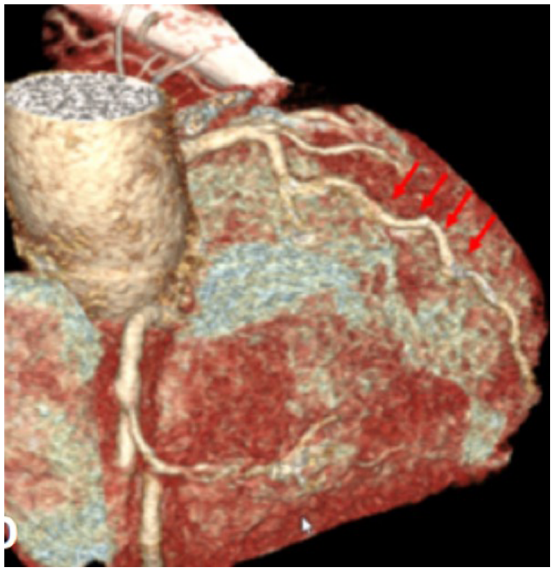

FIGURE 5
Postoperative CT scan showing the patent left anterior descending artery (red arrows).

has to be treated first. Whenever possible, repair of cardiac injuries should be attempted without cardiopulmonary bypass to avoid full heparinization in a situation with multiple injuries. Adenosine administration to decrease pulse rate and blood pressure may be helpful (3). When this is not possible, heparinization should be quickly reversed by protamine in a 1 : 1 dosage to minimize the bleeding risk. Since simple algorithms for such situations are not available, multi-disciplinary evaluation of each individual case is of utmost importance to balance advantages and disadvantages of the different operative sequences.

In this case, the decision to proceed with cerebral extraction of the nails first and delay explorative thoracotomy was suboptimal since it led to an emergency situation on the intensive care unit and cardiac massage was not possible until the nails were removed. Nevertheless, the situation could be controlled and the final control of all cardiac injuries was realized through sternotomy.

In addition, postponing the removal of the intra-cranial nails would probably have avoided the progression of cerebral bleeding. Extraction could have been performed after optimization of the coagulation.

The choice of the optimal access to the heart was also an important aspect in this patient. Although median sternotomy is usually suitable for a single penetrating injury, it was thought inappropriate in this case because the nails *in situ* would have made spreading of the sternum impossible before removal of the nails.

Fortunately, the nails could be removed and the myocardial lesions successfully treated without the need for extracorporeal circulation. If this would not have been possible either ECMO or CPB with coated tubes would have been attractive options to avoid full heparinization. Despite all challenges encountered, this case ended successfully without wound infection despite the hardly sterile operative conditions and the patient could be discharge at home with a psychiatric supervision.

Data availability statement

The raw data supporting the conclusions of this article will be made available by the authors, without undue reservation.

Ethics statement

Informed consent could not be obtained before treatment because of the emergency condition but the patient signed the institutional consent for anonymous use of patient's data for scientific purposes. Since the patient was further treated in a psychiatric institution, we received the permission of the brother (document signed by U.F.), as his legal representative, to re-use the full material in an anonymized form, including: clinical details of the hospital chart, pre-, intra- and post-operative pictures, and intraoperative video. As soon as the patient recovered, he was informed by the brother and gave his approval too (document signed by F. F.). Written informed consent was obtained from the patient and from his relatives for the publication of this case report.

Author contributions

AO, MOS, TC contributed to conception and design of the study. AO, AMS, GJ organized the database. AO and AMS wrote the first draft of the manuscript. TC and PRV wrote sections of the manuscript and made substantial contributions to the final version of the manuscript. All authors contributed to the article and approved the submitted version.

Conflict of interest

The authors declare that the research was conducted in the absence of any commercial or financial relationships that could be construed as a potential conflict of interest.

Publisher's note

All claims expressed in this article are solely those of the authors and do not necessarily represent those of their affiliated organizations, or those of the publisher, the editors and the reviewers. Any product that may be evaluated in this article, or claim that may be made by its manufacturer, is not guaranteed or endorsed by the publisher.

References

1. Ye CN, Lin MC, Huang CL. Double penetration wound: a nail gun injury involving the head and the heart. *Radiol Case Rep*. (2020) 15:334–8. doi: 10.1016/j.radcr.2019.11.021

2. Fang X, Yu C, He F. The self-inflicted multiple organs injury with nail gun. *Heart Surg Forum*. (2021) 24:E1049–51. doi: 10.1532/hsf.4201

3. Rupprecht H, Ghidau M. Penetrating nail gun injury of the heart managed by adenosine-induced asystole in the absence of heart-lung machine. *Tex Heart Inst J*. (2014) 41:429–32. doi: 10.14503/THIJ-13-3405

frontiers | Frontiers in Cardiovascular Medicine

TYPE Case Report
PUBLISHED 12 April 2023
DOI 10.3389/fcvm.2023.1101750

OPEN ACCESS

EDITED BY
Bernhard Winkler
Vienna Health Association, Australia

REVIEWED BY
Salah Said,
Ziekenhuis Groep Twente, Netherlands
Stephan Stöbe,
Leipzig University, Germany

*CORRESPONDENCE
Qiang Huo
✉ hqxjheart@sohu.com

†These authors have contributed equally to this work

SPECIALTY SECTION
This article was submitted to Heart Surgery, a section of the journal Frontiers in Cardiovascular Medicine

RECEIVED 18 November 2022
ACCEPTED 13 March 2023
PUBLISHED 12 April 2023

CITATION
Zhang W, Maimaitiaili A, Xing Y, Yan F and Huo Q (2023) Case report: Surgical repair for left main coronary artery to right atrium fistula with endocarditis.
Front. Cardiovasc. Med. 10:1101750.
doi: 10.3389/fcvm.2023.1101750

Case report: Surgical repair for left main coronary artery to right atrium fistula with endocarditis

Weimin Zhang[1†], Abdunabi Maimaitiaili[1†], Yan Xing[2], Fei Yan[1] and Qiang Huo[1*]

[1]Department of Cardiac Surgery, The First Affiliated Hospital of Xinjiang Medical University, Urumqi, China, [2]Imaging Center, The First Affiliated Hospital of Xinjiang Medical University, Urumqi, China

Coronary artery fistula (CAF) is a rare coronary anomaly defined as a communication between coronary artery and other heart chambers or vascular structures. In this case report, a 32-year-old woman with a giant left main coronary artery to the right atrium fistula with endocarditis was presented. CAF was diagnosed by transthoracic echocardiography and subsequently confirmed by cardiac computerized tomographic and coronary angiography. The patient received antibiotic treatment for infective endocarditis for 6 weeks preoperatively. The fistula was successfully treated with surgical repair. The patient is well now after 18 months of follow-up.

KEYWORDS

coronary artery fistula, heart failure, echocardiography, computed tomography, surgery

Introduction

Coronary artery fistula (CAF) is a rare coronary artery anomaly that originates from the coronary artery and drains into any cardiac chamber and great vessel. The estimated prevalence of CAF is about 0.002% in the general population and 0.2% in patients undergoing coronary angiography (1). Most CAFs originate from the right coronary artery (55%), the left anterior descending artery (35%), and both coronary arteries (5%) (2). The involvement of the left main coronary artery (LMCA) accounts for only 0.7% of CAFs (3). Endocarditis of CAFs in the cardiac chambers is extremely rare (4). Here, a case of a giant CAF connecting the LMCA to the right atrium (RA) with endocarditis was presented.

Case report

A 32-year-old Chinese woman presented with a 1-year history of chest tightness and chest pain after exertion and intermittent fever lasting for 1 month. Cardiac examination revealed continuous murmur at the right parasternal border. Laboratory findings were as follows: leucocytes, 10.15 × 109/L; hemoglobin, 86 g/L; C-reactive protein, 27.3 mg/L; IL-6, 31.56 pg/mL; erythrocyte sedimentation rate, 62 mm/h. Myocardial biomarkers were within normal range. Blood cultures taken at admission grew *Streptococcus sanguinis*. Electrocardiography displayed a sinus rhythm. Chest x-ray showed gross cardiomegaly (**Figure 1A**). Transthoracic echocardiography (TTE) showed that a giant fistula structure between the left coronary sinus (CS) and the RA, and the LMCA diameter was 19 mm (**Figure 1B**). The opening of the fistula in the RA was adjacent to the CS (**Figure 1C**), with a diameter of 6 mm. Blood initially passes from the high-pressure aorta to the RA,

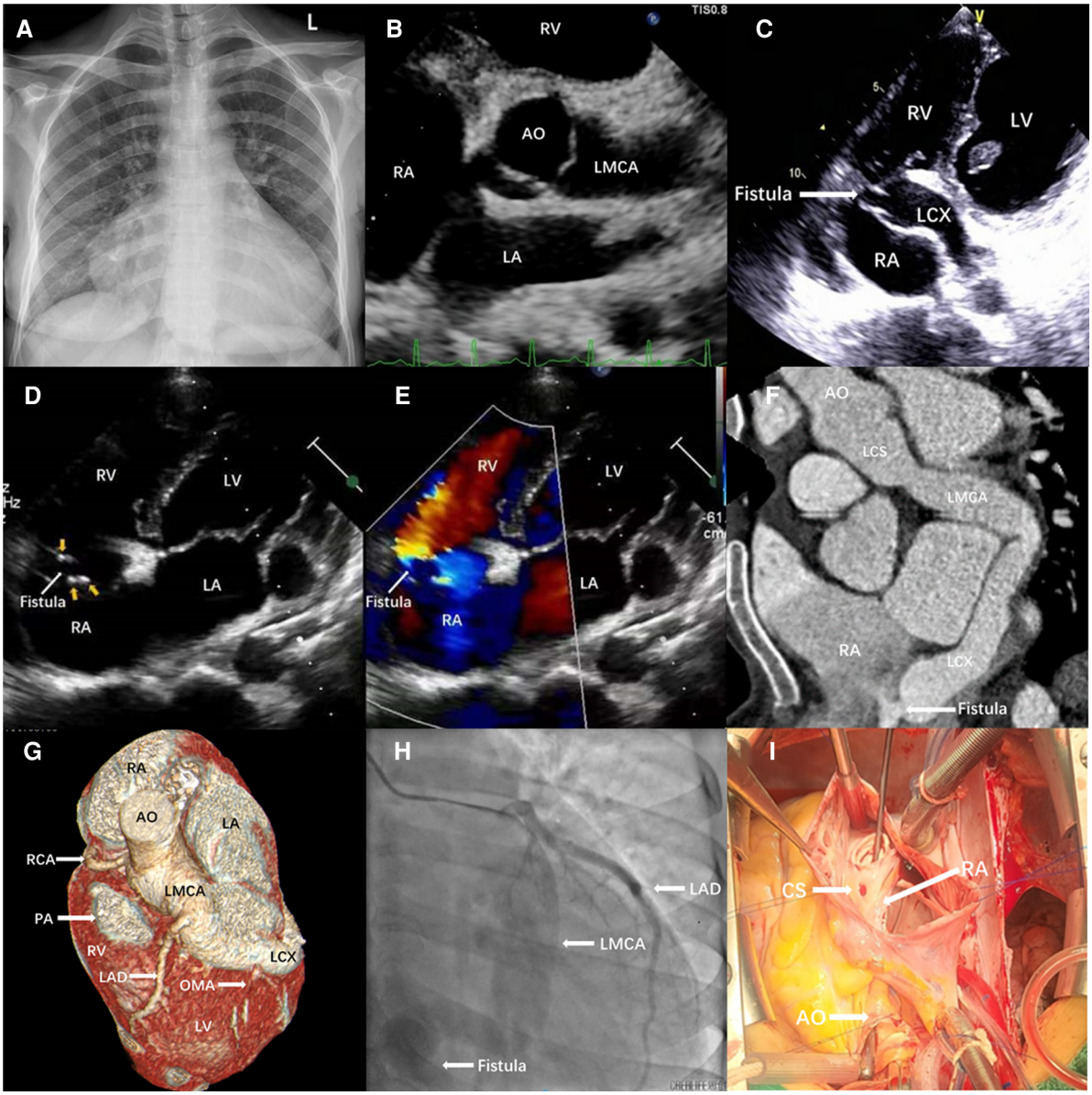

FIGURE 1
(A) Chest x-ray showed gross cardiomegaly. (B–E) Transthoracic echocardiography. (B) The parasternal short-axis image showed a large fistula, originating in LMCA. (C) Modified four-chamber view showed the fistula drained from LMCA into RA, adjacent to the coronary sinus. (D) A continuous systolic–diastolic flow inside the structure at color Doppler, which was confirmed at continuous wave Doppler directed from the LMCA toward RA. (E) Cardiac vegetations were found on the orifice of the fistula in the RA. Computed tomography angiography (F,G) and coronary angiography (H). A large fistula originating from LMCA and entering into RA was shown, and the LAD and OM arteries originate directly from LMCA (G,H). (I) Intraoperative findings. An abnormal vascular channel between left aortic sinus and RA (probe) was observed. AO, aorta; CS, coronary sinus; LA, left atrium; LAD, left anterior descending coronary artery; LMCA, left main coronary artery; LCX, left circumflex coronary artery; LV, left ventricle; OMA, oblique marginal artery; PA, pulmonary artery; RA, right atrium; RCA, right coronary artery; RV, right ventricle.

thereby leading to left-to-right shunt (Figure 1D). In addition, cardiac vegetations were found on the orifice of the fistula in the RA (Figure 1E). Few tiny calcified nodules were found at the aortic and mitral valves.

Cardiac computerized tomography showed obvious dilatation in the left CS and LMCA. LMCA originated from the left CS and coursed along the coronary sulcus to form the dilated left circumflex artery (LCX) (Figure 1F). The volume-rendered image demonstrates the fistulous communication to the LMCA and the RA (Figure 1G). Meanwhile, the left anterior descending artery (LAD) and the oblique marginal artery (OMA) originated from the LMCA. The proximal diameter of the LMCA was 20 mm. The LCX narrowed at the right atrial posterior wall and drained into the RA adjacent to the opening of the CS. Coronary angiography showed a very large CAF originating from the left CS and terminating directly into the RA (Figure 1H). LAD and OMA originated separately from LMCA, whereas the right coronary artery (RCA) was normal.

The patient received antibiotic treatment for infective endocarditis for 6 weeks in and out of hospital, as follows: Penicillin G (200,000 U/day i.v. four doses, for 2 weeks), but the patient remained intermittently feverish, necessitating the change to vancomycin (30 mg/kg/day i.v. two doses, for 4 weeks) based on the drug sensitivity test results. The patient was referred for surgical repair. The CAF was identified (**Figure 1I**), with complete resection vegetations on the orifice of the fistula in the RA. Fistula repair was performed with a Dacron patch inside the RA. During intraoperative exploration, no vegetations were found at the mitral or aortic valves. The patient tolerated the procedure well without complication. She uneventfully recovered following the operation. Postoperatively, she received intravenous antibiotics for 6 weeks. Antiplatelet therapy was recommended for 6 months. At 18 months follow-up, the patient was asymptomatic without complications.

Discussion

CAF is a rare abnormal vascular connection between a coronary artery and any heart cavity or vessel. The most common sites of drainage are low-pressure structures, such as the right ventricle, RA, and pulmonary artery (5). LMCA aneurysm combined with LMCA fistulous connection to the RA is an extremely rare finding.

Most patients with CAF do not demonstrate any symptoms throughout their lives due to their small and insignificant left-to-right shunts. CAFs have different symptoms on the basis of their size and shunt flow (6). They may cause angina pectoris from myocardial ischemia due to coronary steal phenomenon, exertional dyspnea, syncope, and palpitations. The most important and dangerous complications of CAF include congestive heart failure, myocardial ischemia, thrombosis and embolism, pulmonary hypertension, aneurysm rupture, and endocarditis (7).

Echocardiography, CT, MRI, and coronary angiography are useful diagnostic modalities (8). In particular, CT has become an important noninvasive method for coronary artery anomalies, and it could clearly diagnose different types of CAF (9). CT angiography could clearly display the specific location, size, and morphology of the fistula, enabling surgeons to better understand the possible anatomical complexity of the CAF before surgery. Coronary angiography remains the gold standard in diagnosing CAF. It is used to determine the size, number, and anatomical characteristics of the fistulous tract, but it is expensive and invasive. In this case, multimodality imaging was used for diagnosis and procedural planning for CAF.

The patient had chest tightness and chest pain after exertion for 1 year. She also presented with intermittent fever of unknown origin for 1 month. Cardiac examination revealed a heart murmur, and blood cultures grew *S. sanguinis*. TTE found multiple vegetations in the heart. The patient was diagnosed with infective endocarditis on the basis of the modified Duke criteria and the ESC guidelines improvement from 2015 (10).

Symptomatic and asymptomatic patients at risk of complications in the future are recommended to receive treatment (2). No standardized treatment is currently available for CAF. The surgeon must decide the method of operation in accordance with the patient's condition and the type of CAF. The treatments include ligation, surgical patch closure, bypass graft, and transcatheter closure (11). This case underwent successful surgical repair after systematic anti-infection treatment.

In conclusion, infective endocarditis is an extremely rare but life-threatening complication of CAF. The 1-year mortality rate of infective endocarditis was around 30% in different series (12). The mortality rates could be reduced by strictly adhering to a standard therapeutic protocol.

Data availability statement

The original contributions presented in the study are included in the article/supplementary material, further inquiries can be directed to the corresponding author.

Ethics statement

The studies involving human participants were reviewed and approved by the ethics committee of The First Affiliated Hospital of Xinjiang Medical University. The participant provided her written informed consent to participate in this study. Written informed consent was obtained from the individual(s) for the publication of any potentially identifiable images or data included in this article.

Author contributions

WZ and AM contributed to the data collection and drafting of the article. YX contributed to imaging diagnosis by CT. FY gave some suggestions. QH was involved revised the paper. All authors contributed to the article and approved the submitted version.

Funding

The study was supported by the Xinjiang Uyghur Autonomous Region Science and Technology Support Project Plan (grant no. 2020E0283).

Conflict of interest

The authors declare that the research was conducted in the absence of any commercial or financial relationships that could be construed as a potential conflict of interest.

Publisher's note

References

1. Gillebert C, Van Hoof R, Van de Werf F, Piessens J, De Geest H. Coronary artery fistulas in an adult population. *Eur Heart J*. (1986) 7(5):437–43. doi: 10.1093/oxfordjournals.eurheartj.a062086

2. Gowda RM, Vasavada BC, Khan IA. Coronary artery fistulas: clinical and therapeutic considerations. *Int J Cardiol*. (2006) 107(1):7–10. doi: 10.1016/j.ijcard.2005.01.067

3. Dodge-Khatami A, Mavroudis C, Backer CL. Congenital heart surgery nomenclature and database project: anomalies of the coronary arteries. *Ann Thorac Surg*. (2000) 69(4 Suppl):S270–97. doi: 10.1016/S0003-4975(99)01248-5

4. Wang F, Cranston-D'Amato H, Pearson A. Coronary artery fistula-associated endocarditis: report of two cases and a review of the literature. *Echocardiography*. (2015) 32(12):1868–72. doi: 10.1111/echo.13041

5. Yun G, Nam TH, Chun EJ. Coronary artery fistulas: pathophysiology, imaging findings, and management. *Radiographics*. (2018) 38(3):688–703. doi: 10.1148/rg.2018170158

6. Challoumas D, Pericleous A, Dimitrakaki IA, Danelatos C, Dimitrakakis G. Coronary arteriovenous fistulae: a review. *Int J Angiol*. (2014) 23(1):1–10. doi: 10.1055/s-0033-1349162

7. Shiga Y, Tsuchiya Y, Yahiro E, Kodama S, Kotaki Y, Shimoji E, et al. Left main coronary trunk connecting into right atrium with an aneurysmal coronary artery fistula. *Int J Cardiol*. (2008) 123(2):e28–30. doi: 10.1016/j.ijcard.2006.11.108

8. Goo HW. Imaging findings of coronary artery fistula in children: a pictorial review. *Korean J Radiol*. (2021) 22(12):2062–72. doi: 10.3348/kjr.2021.0336

9. Zhang P, Cai G, Chen J, Wang Y, Duan S. Echocardiography and 64-multislice computed tomography angiography in diagnosing coronary artery fistula. *J Formos Med Assoc*. (2010) 109(12):907–12. doi: 10.1016/S0929-6646(10)60138-6

10. Habib G, Lancellotti P, Antunes MJ, Bongiorni MG, Casalta JP, Del Zotti F, et al. 2015 ESC guidelines for the management of infective endocarditis: the task force for the management of infective endocarditis of the European Society of Cardiology (ESC). Endorsed by European Association for Cardio-Thoracic Surgery (EACTS), the European Association of Nuclear Medicine (EANM). *Eur Heart J*. (2015) 36(44):3075–128. doi: 10.1093/eurheartj/ehv319

11. Mangukia CV. Coronary artery fistula. *Ann Thorac Surg*. (2012) 93(6):2084–92. doi: 10.1016/j.athoracsur.2012.01.114

12. Netzer RO, Zollinger E, Seiler C, Cerny A. Infective endocarditis: clinical spectrum, presentation and outcome. An analysis of 212 cases 1980–1995. *Heart*. (2000) 84(1):25–30. doi: 10.1136/heart.84.1.25

frontiers | Frontiers in Cardiovascular Medicine

TYPE Case Report
PUBLISHED 31 July 2023
DOI 10.3389/fcvm.2023.1085755

OPEN ACCESS

EDITED BY
Antonio Miceli,
Istituto Clinico Sant'Ambrogio, Italy

REVIEWED BY
Bleri Celmeta,
IRCCS Ospedale Galeazzi Sant'Ambrogio, Italy
Robert Jeenchen Chen,
Stanford University, United States

*CORRESPONDENCE
Hui Li
lihuiyjs201601@csu.edu.cn

RECEIVED 31 October 2022
ACCEPTED 03 July 2023
PUBLISHED 31 July 2023

CITATION
Zhao Y, Mi C, Xie J and Li H (2023) Case report: Intraoperative reversal of flow through an atrial septal defect presenting as hypoxemia during off-pump coronary artery bypass grafting. Front. Cardiovasc. Med. 10:1085755. doi: 10.3389/fcvm.2023.1085755

Case report: Intraoperative reversal of flow through an atrial septal defect presenting as hypoxemia during off-pump coronary artery bypass grafting

Yun Zhao[1], Chaorui Mi[1], Juan Xie[2] and Hui Li[1]*

[1]Department of Anesthesiology, The Second Xiangya Hospital, Central South University, Changsha, China, [2]Department of Academic Affairs, The Second Xiangya Hospital, Central South University, Changsha, China

The co-existence of atrial septal defect and coronary artery disease in a patient is rare in clinical practice. In the combined surgery of off-pump coronary artery bypass grafting and atrial septal defect closure, the unusual cardiac positions may affect the direction of blood shunting between the atriums, leading to more complex hemodynamic changes. Here, we report a case of a 67-year-old female who underwent refractory hypoxemia related to heart position in such a combined operation.

KEYWORDS

off-pump coronary artery bypass grafting, atrial septal defect, end-tidal carbon dioxide partial pressure, reversal of shunt flow, hypoxemia

1. Introduction

Coronary artery disease (CAD) is the major cause of mortality and morbidity worldwide (1). In adults, atrial septal defect (ASD) is the most prevalent congenital heart defect (2). In clinical practice, it may occasionally be encountered that these two common diseases are present together in one patient. Previous studies have shown that off-pump coronary artery bypass graft (OPCABG) with intraoperative device closure of ASD is a viable option for some select patients (3). However, in such combined surgery, the unusual cardiac positions of OPCABG may affect the shunt direction of ASD, leading to more complex hemodynamic changes, which have not been reported so far. In this report, we provide the first description of refractory hypoxemia caused by shunt reversal in a patient with ASD undergoing off-pump cardiac surgery.

2. Case description

A 67-year-old woman with a history of hypertension and type 2 diabetes mellitus presented to us with symptoms of unstable angina and exertional dyspnea (NYHA class III). Cardiac catheterization revealed triple-vessel disease, including a 60% stenosis of the left main artery, an 85%–90% stenosis of the left anterior descending artery, an 80% stenosis of the diagonal artery, a 90% stenosis of the circumflex artery, and a 60%–90% stenosis of the right coronary artery. Echocardiography was performed, which showed an ASD measuring about 13 mm and unidirectional blood shunting from the left to the right atrium. Due to volume overload, the right ventricle and right atrium dilated, and the mean pulmonary arterial pressure (MPAP) was 28 mmHg. In addition, there was moderate mitral

regurgitation as well as mild tricuspid regurgitation. The ejection fraction (EF) was 62%. All other values were within acceptable limits. Considering the comorbidities associated with cardiopulmonary bypass (CPB) and the fact that the ASD was deemed suitable for closure with a percutaneous device, the patient was scheduled for OPCABG and ASD device closure.

Anesthesia was routinely induced with midazolam, sufentanil, and etomidate and maintained with propofol, remifentanil, and cis-atracurium. Then, we performed a right internal jugular vein puncture, and the patient's baseline central venous pressure (CVP) was measured to be about 10 cmH_2O. The plan is to graft the left internal mammary artery to the left anterior descending artery and anastomose the saphenous venous to the diagonal, circumflex, and posterior descending branches with the heart beating. The heart was displaced and stabilized during the procedure to expose the target vessel. When the heart was lifted for posterior descending branch distal anastomosis, CVP rose to 20 cmH_2O, systolic blood pressure (SBP) fell to 79 mmHg, and the heart rate slightly increased. At the same time, the blood oxygen saturation level (SpO_2) slowly declined from 99% to 91%. We immediately increased the fraction of inspiratory oxygen (FiO_2) from 60% to 100%, and no problems with the airway, ventilation, or breathing sounds of the patient were reported. However, the SpO_2 was decreasing even faster, reaching a minimum of 69%. Meanwhile, the end-tidal carbon dioxide partial pressure ($PetCO_2$) was unmeasurable by the ventilator. To confirm the SpO_2 and $PetCO_2$, an arterial blood gas analysis was performed, which showed a PaO_2 level of 40 mmHg and a $PaCO_2$ level of 26 mmHg. During this process, a single intravenous injection of 4 μg of norepinephrine could increase BP to above 90 mmHg, and SpO_2 could also be improved but soon dropped again. In consideration of the altered cardiac anatomy and the elevated right atrial pressure, we assumed there was a shunt reversal with flow from the right atrium into the left and informed the surgical team at once. When the position of the heart was restored to normal, SpO_2 rapidly went back to 100%, and BP also came back to normal (**Figure 1**). After coronary revascularization, the ASD was closed with a 16 mm septal occluder under the guidance of transesophageal echocardiography (TEE) in the operating room. The hemodynamics were stable without significant fluctuations during this period. The patient was then taken to the cardiac intensive care unit after the chest was closed. She was successfully extubated on the first day after surgery. According to the postoperative transthoracic echocardiography, the device was in a stable position with no residual shunt. The recovery was uneventful, and the patient was discharged home 7 days later.

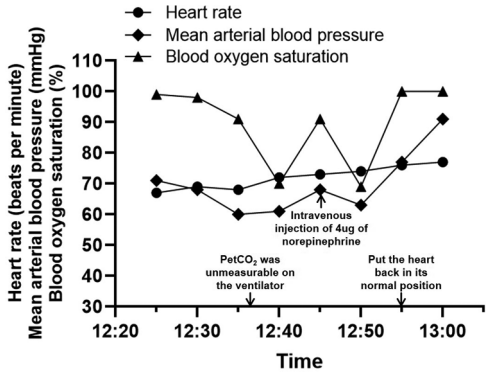

FIGURE 1
Anesthesia record.

3. Discussion

ASD is a common non-cyanotic congenital heart defect with a protracted period of asymptomatic development, which accounts for 30% to 40% of heart defects identified in patients over the age of 40 years. Moreover, CAD is the most prevalent acquired heart disease. However, the co-existence of ASD and CAD in a patient is rare in clinical practice. Traditionally, CABG and ASD closure are performed using CPB. With the help of CPB machines, cardiac arrest could provide a clean surgical field of view, allowing the surgeon to perform fine coronary anastomoses. On the other hand, CPB can cause some complications, and ASD trans-atrial closure is more damaging to the heart. Recent studies have demonstrated that device closure of ASD during OPCABG could be a safe and effective alternative technique for some selected patients (4). It can prevent CPB-related injury. For elderly patients, the damage is smaller, the recovery is faster, and the prognosis is better. However, a beating heart can make surgery more difficult and reduce the fineness of surgical operations. In our hospital, OPCABG is routinely preferred because it can avoid CPB-related complications and reduce reperfusion injury. It has also been suggested that while performing the combined procedures, it may be preferable to treat CAD first and then close the ASD because coronary revascularization is expected to enhance ventricular contractility (5) and may affect the occluder position. However, some special hemodynamic changes may occur due to the unusual cardiac positions and the presence of ASD during OPCABG, which have not been reported yet.

In our case, to access the posterior descending branch, the heart had to be elevated and rotated during the procedure. We believed that this unusual position caused a shunt reversal in ASD. On the one hand, blood shunted from right to left through the ASD entered the systemic circulation without being oxygenated by the lungs. On the other hand, the reduced blood flow into the pulmonary circulation led to a reduction in the amount of blood oxygenated through the lungs and an imbalance in V/Q. Both of these reasons led to a decrease in the proportion of oxygenated hemoglobin in the body, resulting in a fall in systemic desaturation. We also observed a peculiar phenomenon—the $PetCO_2$ on the ventilator was undetectable, while the $PaCO_2$ level in arterial blood gas remained at 26 mmHg. Alveolar ventilation, peripheral CO_2 production, and pulmonary blood flow all affect $PetCO_2$ levels. Since the first two factors are constant during general anesthesia, $PetCO_2$ is primarily influenced by pulmonary blood flow. Saleh and Pullan noted that as the heart was elevated to expose the target vessels

in OPCABG, $PetCO_2$ almost instantly dropped to the low 20 mmHg range and then stabilized or trended back to pre-displacement levels (6). It is consistent with our usual experience. However in this case, $PetCO_2$ fell to such a low level that even the ventilator could no longer measure it. It is likely that ASD was also involved in this process. The increased right atrial pressure may have provoked a shunt reversal from the right atrium to the left, leading to a further decrease in pulmonary blood flow and increasing the chance of hemoglobin desaturation.

In addition, previous studies have demonstrated that the Pa-ET CO_2 can be increased both in cyanotic and non-cyanotic congenital heart diseases. Among them, the cyanotic patients have the highest Pa-ET CO_2 with a mean of approximately 15 mmHg and a maximum of approximately 20 mmHg (7). In this case, although the patient's preoperative echocardiography showed a unidirectional left-to-right shunt through the ASD, the Pa-ET CO_2 transiently reached over 20 mmHg during the operation, which meant that a similar shunt direction to cyanotic heart disease may have occurred. This was further evidence that a right-to-left shunt may have existed at that time.

Intraoperatively, the patient had a combination of hypotension in addition to hypoxemia. We believe that the reasons are as follows. During anastomosis of the posterior descending branch, the heart was elevated to a nearly vertical position, and part of the right ventricular free wall was pressed against the ventricular septum. The right ventricular wall was prone to deformation due to its thinness. In early diastole, the left ventricular septum moved toward the right ventricular free wall, further reducing the right ventricular size with a consequent reduction in diastolic return blood volume. In addition, due to the use of cardiac fixators, the systolic and diastolic function of the heart was limited, resulting in a decrease in cardiac output, a decrease in mean arterial pressure, and a compensatory increase in heart rate. For these reasons, hypotension is prone to occur during posterior descending branch anastomosis performed in OPCABG. In this case, because the patient also had an ASD, blood flow not passing through the lung bed may enter the left heart through the ASD during excessive cardiac torsion. However, due to the limitation of the diastolic and systolic function of the heart and the reduction of both return blood volume and cardiac output, systemic hypotension may still occur. Our treatment was to use vasoactive drugs and change the patient to a head-down position to maintain hemodynamic stability.

From this case, we have gained some experience in performing such combined procedures. Before the operation, the patient should be strictly screened for indications and contraindications, and the risk of possible complications should be carefully assessed. For patients with CAD combined with ASD, the advantages and disadvantages of cardiac arrest surgery should be fully considered according to the specific conditions, recognizing the unique benefits of CPB for these patients. If OPCABG and ASD device closure is performed, communication with the surgeon throughout the procedure is required to avoid excessive movement of the heart. When the shunt reversal occurs, intraoperative TEE can provide a fundamental diagnostic tool to detect interatrial shunts (8), which is useful in quickly diagnosing the problem. Furthermore, for this case, we focused on the change in $PetCO_2$. Previous work has shown that when there was a decreased cardiac output after repositioning the heart during OPCABG, the change in $PetCO_2$ preceded electrical instability and hemodynamics. This method has the benefits of simplicity, general availability, and a quick response time to cardiac output changes (6). If there is a sudden and persistent arterial desaturation during coronary revascularization and TEE or $PetCO_2$ indicates the shunt flow going from right to left through ASD, the surgical team must be notified at once and put the heart back in its natural position. Initiating CPB may be considered if desaturation remains severe even after repositioning the heart.

In conclusion, we have described a case of refractory hypoxemia in an OPCABG patient with ASD. For the first time, we report atrial blood flow reversal related to heart position in such combined surgery. When ventilatory causes can be ruled out, the sudden and persistent arterial desaturation associated with cardiac mobilization should be taken as an indication of a possible right-to-left shunt via ASD. The use of intraoperative TEE can be very helpful in confirming the presence of a reverse shunt. In addition, special attention should be paid to the changes in $PetCO_2$, which can provide a significant reference for rapid diagnosis.

Data availability statement

The original contributions presented in the study are included in the article, further inquiries can be directed to the corresponding author.

Ethics statement

Written informed consent was obtained from the individual(s) for the publication of any potentially identifiable images or data included in this article.

Author contributions

YZ wrote the manuscript. CM and JX contributed to the revision of the manuscript. HL performed critical revision of the manuscript and approved the final version to be published. All authors contributed to the article and approved the submitted version.

Funding

This study was supported by grants from the Natural Science Foundation of Hunan Province (No. 2022JJ80039) and the Science and Technology Program of Hunan Province (No. 2020SK53411).

Conflict of interest

The authors declare that the research was conducted in the absence of any commercial or financial relationships that could be construed as a potential conflict of interest.

Publisher's note

References

1. Weber C, Noels H. Atherosclerosis: current pathogenesis and therapeutic options. *Nat Med*. (2011) 17(11):1410–22. doi: 10.1038/nm.2538

2. Brida M, Chessa M, Celermajer D, Li W, Geva T, Khairy P, et al. Atrial septal defect in adulthood: a new paradigm for congenital heart disease. *Eur Heart J*. (2022) 43(28):2660–71. doi: 10.1093/eurheartj/ehab646

3. Cui YC, Hao XH, Huang FJ, Li JH, Lai YQ, Zhou QW. Coronary artery bypass grafting in adults with congenital heart disease. *J Card Surg*. (2010) 25(6):629–32. doi: 10.1111/j.1540-8191.2010.01110.x

4. Hao XH, Huang FJ, Wang SY, Zhang C, Zhang ZG, Lai YQ. Off-pump coronary artery bypass grafting with device closure of atrial septal defect. *Ann Thorac Surg*. (2010) 90(5):1727–9. doi: 10.1016/j.athoracsur.2009.12.044

5. Desabandhu V, Sulaiman S, Bastian C, Goyal KK. Combined percutaneous intervention of coronary artery disease and atrial septal defect. *IHJ Cardiovasc Case Rep CVCR*. (2018) 2(1):24–6. doi: 10.1016/j.ihjccr.2017.10.006

6. Saleh HZ, Pullan DM. Monitoring cardiac output trends with end-tidal carbon dioxide pressures in off-pump coronary bypass. *Ann Thorac Surg*. (2011) 91(5):e81–2. doi: 10.1016/j.athoracsur.2010.12.039

7. Choudhury M, Kiran U, Choudhary SK, Airan B. Arterial-to-end-tidal carbon dioxide tension difference in children with congenital heart disease. *J Cardiothorac Vasc Anesth*. (2006) 20(2):196–201. doi: 10.1053/j.jvca.2005.11.008

8. Falcucci OA, Kasirajan V, Green JA. Transesophageal echocardiographic and oxymetric evidence of intraoperative reversal of flow through a patent foramen ovale during an off-pump coronary artery bypass grafting. *J Clin Anesth*. (2005) 17(8):617–20. doi: 10.1016/j.jclinane.2005.01.010

Frontiers in
Cardiovascular Medicine

Innovations and improvements in cardiovascular treatment and practice

Focuses on research that challenges the status quo of cardiovascular care, or facilitates the translation of advances into new therapies and diagnostic tools.

Discover the latest Research Topics

See more →

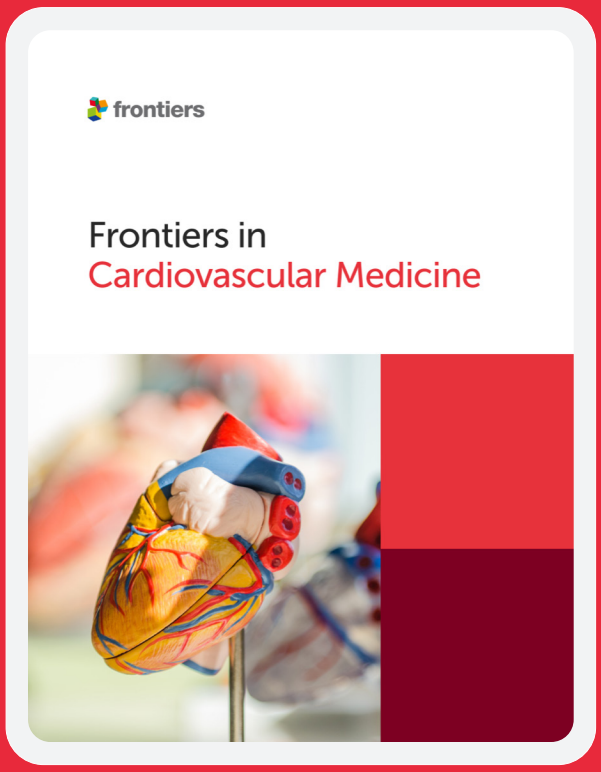

Frontiers

Avenue du Tribunal-Fédéral 34
1005 Lausanne, Switzerland
frontiersin.org

Contact us

+41 (0)21 510 17 00
frontiersin.org/about/contact